



Kent Academic Repository

Hanney, Oliver (2021) *Copper, Zinc and Silver Tetrafluoroborate Reactions with Acyclovir (ACV) Creating Novel Complexes*. Master of Science by Research (MScRes) thesis, University of Kent,.

Downloaded from

<https://kar.kent.ac.uk/86578/> The University of Kent's Academic Repository KAR

The version of record is available from

<https://doi.org/10.22024/UniKent/01.02.86578>

This document version

UNSPECIFIED

DOI for this version

Licence for this version

CC BY (Attribution)

Additional information

Versions of research works

Versions of Record

If this version is the version of record, it is the same as the published version available on the publisher's web site. Cite as the published version.

Author Accepted Manuscripts

If this document is identified as the Author Accepted Manuscript it is the version after peer review but before type setting, copy editing or publisher branding. Cite as Surname, Initial. (Year) 'Title of article'. To be published in *Title of Journal*, Volume and issue numbers [peer-reviewed accepted version]. Available at: DOI or URL (Accessed: date).

Enquiries

If you have questions about this document contact ResearchSupport@kent.ac.uk. Please include the URL of the record in KAR. If you believe that your, or a third party's rights have been compromised through this document please see our [Take Down policy](https://www.kent.ac.uk/guides/kar-the-kent-academic-repository#policies) (available from <https://www.kent.ac.uk/guides/kar-the-kent-academic-repository#policies>).

Copper, Zinc and Silver Tetrafluoroborate Reactions with Acyclovir (ACV) Creating Novel Complexes

Oliver Hanney

Abstract

This thesis seeks to develop insights into how the antiviral ligand (ACV) interacts with biologically and medically relevant metals so as to aid future treatments of various microbial and viral diseases. The study focuses on synthesis of novel polymorphic structures that possess unique bonding patterns not otherwise seen in the literature.

Specifically, nine single crystal structures have been obtained, derived from three different metal tetrafluoroborate salts: copper, zinc, silver. Both the copper and silver species were found to produce a range of polymorphic structures under different conditions; however, zinc produced only a single structure. These unique structures include a copper structure, $[\text{Cu}(\text{ACV})_2(\text{BF}_4)_2] \cdot \text{ACV} + 2\text{H}_2\text{O}$, that shows bonding between the counter ion (BF_4^-) and the metal centre. In addition, in the silver structure, $2[\text{Ag}(\text{ACV})] \cdot \text{SiF}_6 + 2\text{H}_2\text{O}$, a novel polymer was observed between silver and ACV.

The potential for these metal-ACV compounds to be used in the pharmaceutical field needs further exploration, and is beyond the scope of this Masters project. However, this work provides a structural insight that will assist these future studies.

Acknowledgements

A special thank you to Dr William Gee, for without his support, patience, knowledge and wisdom, this project would have ceased a long time ago. Also, my gratitude to the Gee Group, which was made up of some fantastic people with great ideas; their support was huge.

Additionally, I'd like to thank my family for putting up with my incessant chat of, and enthusiasm for, crystals.

Contents

Abstract.....	2
Acknowledgements.....	3
1.1. Introduction	10
1.2. Literature Analysis.....	14
1.3. Aims.....	27
2. Experimental.....	28
2.1. Synthesising Single Crystals of 1-9	28
2.1.1. General Method.....	28
2.1.2. Equipment and Chemicals	28
2.1.3. Copper Compounds 1-5	28
1: $[\text{Cu}(\text{ACV})_2(\text{H}_2\text{O})_3] \cdot 2\text{BF}_4$	30
2: $[\text{Cu}(\text{ACV})_2(\text{H}_2\text{O})_2(\text{OH})_2] \cdot \text{ACV} + 2\text{H}_2\text{O}$	31
3: $[\text{Cu}(\text{ACV})_4(\text{H}_2\text{O})] \cdot 2\text{BF}_4$	31
4: $[\text{Cu}(\text{ACV})_2(\text{H}_2\text{O})_2] \cdot 2\text{BF}_4$	32
5: $[\text{Cu}(\text{ACV})_2(\text{BF}_4)_2] \cdot \text{ACV} + 2\text{H}_2\text{O}$	32
2.1.4. Zinc Compound 6	33
6: $[\text{Zn}(\text{ACV})_4] \cdot \text{SiF}_6 + \text{H}_2\text{O}$	34
2.1.5. Silver Compounds 7-9	34
7: $2[\text{Ag}_2(\text{ACV})_3] \cdot 2\text{SiF}_6 + 3\text{H}_2\text{O}$	35
8: $2[\text{Ag}(\text{ACV})] \cdot \text{SiF}_6 + 2\text{H}_2\text{O}$	36
9: $2[\text{Ag}(\text{ACV})_2] \cdot \text{SiF}_6 + 2\text{H}_2\text{O}$	36

2.1.6. Scaling Up the synthesis of 1-9	37
2.2. Synthesising Powder Samples.....	38
2.2.1. General Method 1 – Evaporation	38
2.2.2. General Method 2 – Layering	38
2.3. Synthesis of 1 ($[\text{Cu}(\text{ACV})_2(\text{H}_2\text{O})_3] \cdot 2\text{BF}_4$)	38
2.4. Synthesis of 2 ($[\text{Cu}(\text{ACV})_2(\text{H}_2\text{O})_2(\text{OH})_2] \cdot \text{ACV} + 2\text{H}_2\text{O}$)	39
2.5. Synthesis of 3 ($[\text{Cu}(\text{ACV})_4(\text{H}_2\text{O})] \cdot 2\text{BF}_4$).....	39
2.6. Synthesis of 4 ($[\text{Cu}(\text{ACV})_2(\text{H}_2\text{O})_2] \cdot 2\text{BF}_4$).....	40
2.7. Synthesis of 5 ($[\text{Cu}(\text{ACV})_2(\text{BF}_4)_2] \cdot \text{ACV} + 2\text{H}_2\text{O}$).....	40
2.8. Synthesis of 6 ($[\text{Zn}(\text{ACV})_4] \cdot \text{SiF}_6 + \text{H}_2\text{O}$)	41
2.9. Synthesis of 7 ($2[\text{Ag}(\text{ACV})_3] \cdot \text{SiF}_6 + 3\text{H}_2\text{O}$).....	41
2.10. Synthesis of 8 ($2[\text{Ag}(\text{ACV})] \cdot \text{SiF}_6 + 2\text{H}_2\text{O}$).....	42
2.11. Synthesis of 9 ($2[\text{Ag}(\text{ACV})_2] \cdot \text{SiF}_6 + 2\text{H}_2\text{O}$).....	42
3. Results and Discussion	43
3.1. Acyclovir (ACV) (Ligand)	43
3.1.1. Bonding	44
3.1.2. Packing	45
3.1.3. Predicted Infrared Bands	46
3.2. Copper Complexes 1-5.....	48
3.2.1. 1 $[\text{Cu}(\text{ACV})_2(\text{H}_2\text{O})_3] \cdot 2(\text{BF}_4)$	48
3.2.2. Bond Angles	49
3.2.3. Bond Distances.....	51

3.2.4. Unit Cell, Intermolecular and Intramolecular Bonding.....	52
3.2.5. Scanning Electron Microscope Data	55
3.2.6. 2 [Cu(ACV) ₂ (H ₂ O) ₂ (OH) ₂]•ACV + 2H ₂ O	57
3.2.7. Bond Angles	58
3.2.8. Bond Distance	60
3.2.9. Unit Cell, Intermolecular and Intramolecular Bonding.....	61
3.2.10. Scanning Electron Microscope Data	64
3.2.11. 3 [Cu(ACV) ₄ H ₂ O]•2(BF ₄)	66
3.2.12. Bond Angles	67
3.2.13. Bond Distances.....	69
3.2.14. Unit Cell, Intermolecular and Intramolecular Bonding.....	70
3.2.15. Scanning Electron Microscope Data	74
3.2.16. 4 [Cu(ACV) ₂ (H ₂ O) ₂]•2BF ₄	75
3.2.17. Bond Angles	76
3.2.18. Bond Distance	78
3.2.19. Unit Cell, Intermolecular and Intramolecular Bonding.....	79
3.2.20. Scanning Electron Microscope Data	81
3.2.21. 5 [Cu(ACV) ₂ (BF ₄) ₂]•ACV + 2H ₂ O.....	83
3.2.22. Bond Angles	84
3.2.23. Bond Distances.....	85
3.2.24. Unit Cell, Intermolecular and Intramolecular Bonding.....	86
3.2.25. Scanning Electron Microscope Data	88

3.3. Zinc Complexes 6	89
3.3.1. 6 [Zn(ACV) ₄]•SiF ₆ + H ₂ O.....	89
3.3.2. Bond Angles	90
3.3.3. Bond Distances.....	91
3.3.4. Unit Cell, Intermolecular and Intramolecular Bonding.....	92
3.3.5. Scanning Electron Microscope Data	94
3.4. Silver Complexes 7-9.....	96
3.4.1. 7 2[Ag ₂ (ACV) ₃]•2SiF ₆ + 3H ₂ O	96
3.4.2. Bond Angles	97
3.4.3. Bond Distances.....	98
3.4.4. Unit Cell, Intermolecular and Intramolecular Bonding.....	99
3.4.5. Scanning Electron Microscope Data	102
3.4.6. 8 2[Ag(ACV)]•SiF ₆ + 2H ₂ O	103
3.4.7. Bond Angles	103
3.4.8. Bond Distances.....	104
3.4.9. Unit Cell, Intermolecular and Intramolecular Bonding.....	104
3.4.10. Scanning Electron Microscope Data	106
3.4.11. 9 2[Ag(ACV) ₂]•SiF ₆ + 2H ₂ O	108
3.4.12. Bond Angles	109
3.4.13. Bond Distances.....	110
3.4.14. Unit Cell, Intermolecular and Intramolecular Bonding.....	111
3.4.15. Scanning Electron Microscope Data	114

4.1. Conclusion.....	115
4.2. Future Work.....	118
Appendix A.....	123
Appendix B.....	128
Cu 1 Crystal Data.....	128
Cu 2 Crystal Data.....	128
Cu 3 Crystal Data.....	129
Cu 4 Crystal Data.....	130
Cu 5 Crystal Data.....	131
Zn 1 Crystal Data.....	131
Ag 1 Crystal Data.....	132
Ag 2 Crystal Data.....	133
Ag 3 Crystal Data.....	134
Appendix C.....	135
Crystal 1.....	135
Crystal 2.....	138
Crystal 3.....	141
Crystal 4.....	145
Crystal 5.....	147
Crystal 6.....	149
Crystal 7.....	154
Crystal 8.....	159

1.1. Introduction

Acyclovir (*Aciclovir* or ACV) is an antiviral placed on the essential medicine list by the World Health Organisation (WHO), [1], first discovered by the synthesis of marine sponge extracts in 1951, [2]. The extract found was the nucleoside deoxyguanosine (Figure 1), the precursor of acyclovir. Since its discovery, the acyclovir compound has been found to be an effective antiviral as a 'prodrug': a molecule that is very slightly or not at all pharmacologically active until it has metabolised with the virus' or host's system. Prior to the mainstream use of acyclovir as an antiviral, other nucleoside analogue antivirals were used, however, these proved to have a high cytotoxicity to them which did not impact the virus but placed the user in danger. However, within the second generation of nucleoside based antivirals, acyclovir proved not only to be safer for the patient, but was also extremely effective against the herpes virus (HSV-1) and infections caused by the varicella virus such as chicken pox and shingles, [3] leading to a future of marine sponge therapeutics, [4].

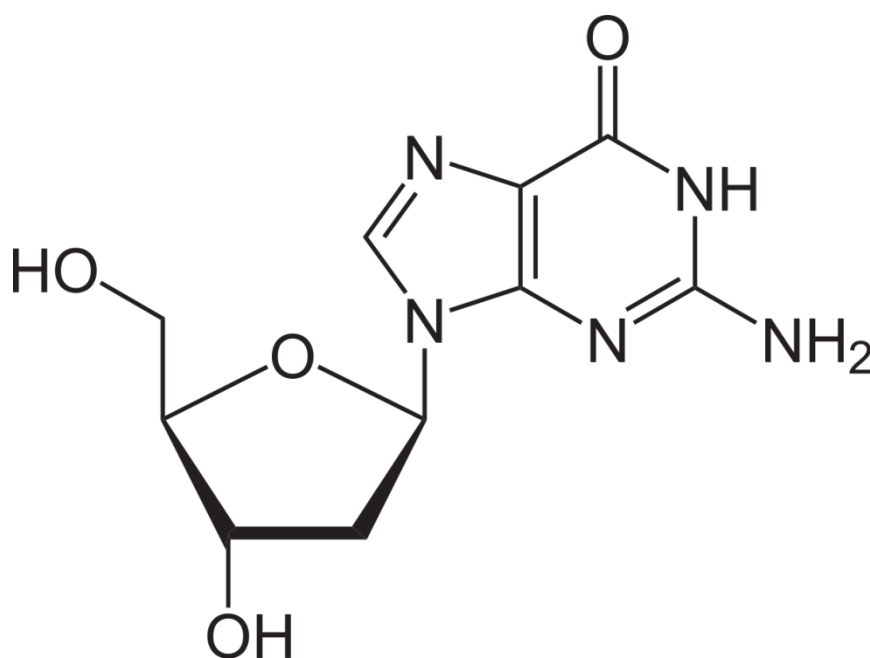


Figure 1 – the structure of a guanosine molecule.

As previously mentioned, ACV acts as a prodrug, only becoming pharmacologically active once it is metabolised within the user's system. The therapeutic breakdown of acyclovir is as a consequence of it being a nucleoside analogue. Key to its function is the absence of the deoxyribose group (Figure

2). ACV is phosphorylated by viral thymidine kinase until it is converted into ACV-TP. At this point it is able to be integrated into the virus' DNA strand, acting as a chain terminator, [5]. Whilst this does not cure the patient of the virus, it stops the replication of the virus which is crucial for its survival within the host. Due to the specific kinase, ACV only targets the virus DNA. It is processed by being phosphorylated which is only present in viral replication enzymes. In healthy host cell DNA, the ACV chain terminator is less effective compared to how it behaves in viral chain termination.

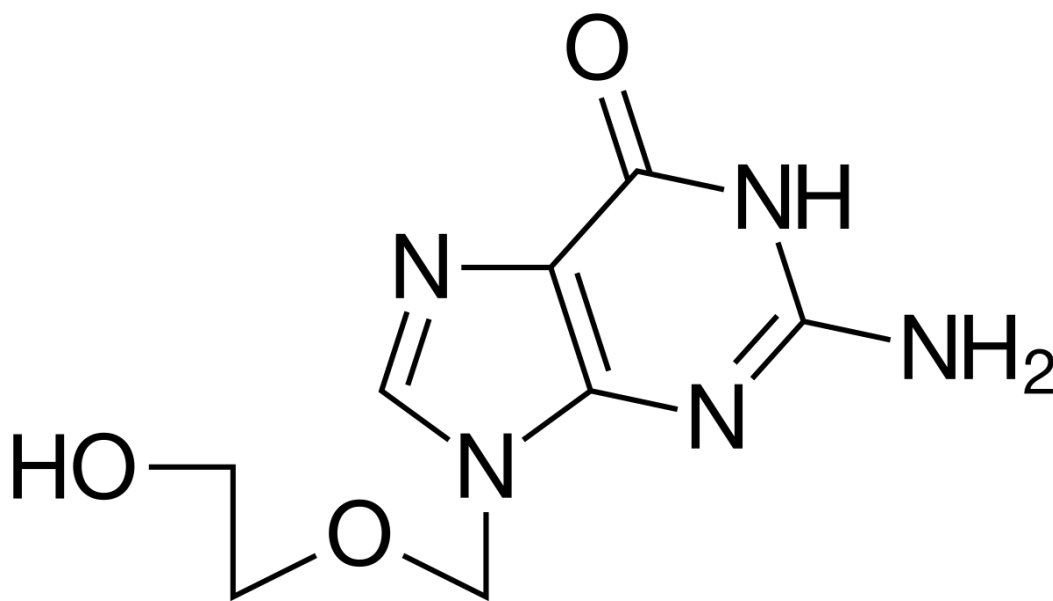


Figure 2 – the structure of an Acyclovir molecule.

Whilst the ACV only works when phosphorylated, it cannot be administered if the user is on other specific medication. An example of such medication would be chemotherapy and contrast agents (i.e. iohexol) due to the chemical components present; mutual inhibition of the chemical processes of both medications can occur due to the formation of other structures that could potentially be harmful [6]. Another example of contraindicative medications are those for the kidneys or medications that are heavily extracted and processed by the kidneys. These impair the effectiveness of ACV as well as place a potentially dangerous stress on the renal system [6]. ACV seems to have a high reactivity rate which is demonstrated by how it can interact with other medications and the biochemistry of the patient's body.

Intermolecular interactions that occur between acyclovir molecules creates ACV crystals. As mentioned before, ACV is a guanosine analogue and guanosine's precursor is guanine, the nucleobase essential for DNA replication, [7]. Guanine is able to form layers of binding molecules to form crystals through π - π bonding, [8] in nature. This is observed in some animals, such as insects, reptiles and fish, [9] which can reflect light at different energies to give the appearance of different colours. Acyclovir can also stack in layers of molecules bound together, however, this does not produce any colour change or light interaction when in solution or as solid crystals, [10]. Given the fact that ACV interacts both in vivo and with itself, the possibility for ACV to interact and bond with other biological components, such as metals naturally occurring in the body, is highly probable. As previously explored, some other medications do interact with ACV by potentially inhibiting or modifying the structure of ACV.

On the other hand, ACV is noted to have a very low solubility level, especially in water, [11]. This would suggest that ACV was not as reactive as previously believed, contradicting the observed drug-drug interactions that could occur when taking ACV alongside other medications. In addition to ACV's low solubility, is the issue of bioavailability once administered due to the variety of polymorphic structures ACV can exist as, [12]. Currently, to counteract this issue, higher doses are given or intravenous acyclovir is given to ensure that the user will receive enough of the correct acyclovir structure, [13]. To overcome these issues, the bioavailability of ACV would need to be improved, thus ensuring the correct bioactive polymorph of ACV arrives at the targeted virus' DNA by thymidine kinase within the patient's system. A potential means to achieve this would be to increase the solubility of ACV in aqueous environments without the need to sacrifice its neutral form. This would reduce the need for higher doses of ACV to be administered, due to a higher presence of the correct ACV structure in the solution, as previously discussed.

Overcoming these issues of ACV would provide patients with a greater variety of treatment options and pathways to pursue. With an ever-increasing move away from a 'one size fits all' approach to

the treatment and care of patients [14], improvements to, and variations of, this antiviral could be as simple as the addition of other elements to the structure. For example, a useful addition for some individuals could be biological metals and minerals that are necessary for healthy day-to-day living. It is highly probable that those requiring acyclovir drug therapy are unlikely to be in peak physical health and would likely benefit from such nutritional additions. For example, copper, which is essential for the production and efficiency of red blood cells, may be a useful addition to the ACV structure, in order to avoid a deficiency in copper that could potentially lead to anaemia, [15].

1.2. Literature Analysis

To gain an insight into metal-ACV complexes, an analysis of the previous methods and structures present in existing literature was conducted. Garcia-Raso and e. al. discuss different transition metals that have been synthesised with ACV using metal chlorides, [16]. Initially, this article demonstrates that metal-ACV complexes can be formed with metals, (nickel, cobalt, zinc, cadmium, and mercury) from their corresponding chloride salt. The salt and ACV are combined in an aqueous solution, stirred, and crystals were obtained after 2-3 days. This report illustrates that the solubility issue previously encountered with ACV in water can be overcome and coordination with metals centres was possible. In infrared (IR) spectroscopy, a shift in the significant C=O carbonyl group band on the purine ring suggests that, upon coordination to different metals, intramolecular interactions occur here. Compounds synthesised with nickel and cobalt both formed elongated centrosymmetric octahedral molecules with aqua ligands in the basal plane and ACV ligands in the axial positions (Figure 3). The oxygen atom from the carbonyl group forms an intramolecular hydrogen bond with the one of the aqua ligands.

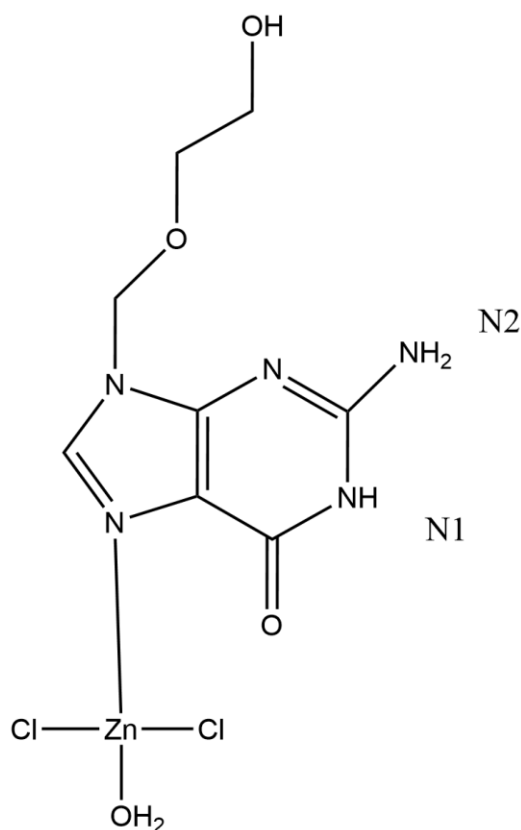


Figure 4 –a molecule structure of [Zn(ACV)Cl₂(H₂O)], one asymmetric unit.

Cadmium forms a distorted octahedral geometry complex with one ACV ligand in the basal plane with three chloride atom ligands, and another chloride atom in one of the axial planes. Another ACV ligand is found in the other axial position but is bonded by the hydroxyl (-OH) group at the end of the ACV tail (Figure 5). Such bonding by the hydroxyl (-OH) group was the first of its kind to be found in the literature reviewed. This forms an additional intramolecular bond between the carbonyl group of the purine ring which would increase the stability of the molecule overall. Similar to compound 3 ([Cu(ACV)₄(H₂O)]•2BF₄), the asymmetric unit would have three cadmium-ACV complex molecules in. However, they form a polymeric chain, linking through a (CdCl₂)_n bond leading to an infinite chain.

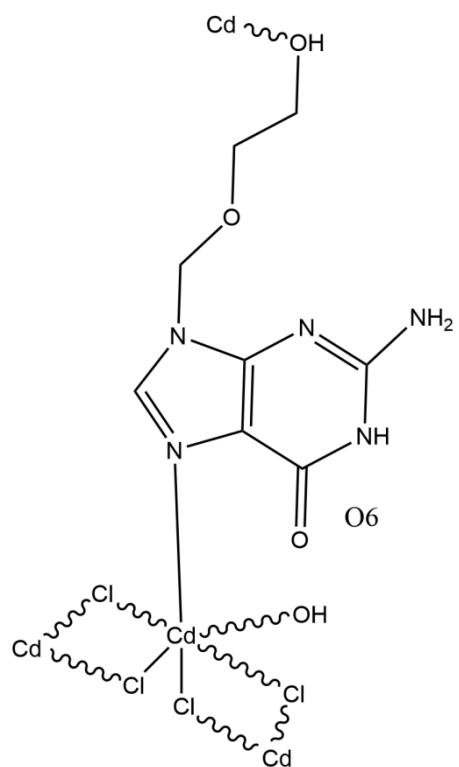


Figure 5 – a molecule structure of [Cd(ACV)Cl₂] \cdot H₂O, one asymmetric unit.

In a further investigation into this uncommon bonding, a change of solvent demonstrated that in water, the type of bonding for copper metal was considerably different to that of methanol, forming instead an octahedral geometric structure. Proton NMR spectroscopy was not able to differentiate between the ACV acting as a bidentate ligand (Figure 7) and an octahedral structure (Figure 6) with hexacoordination, meaning the true structural representation is uncertain.

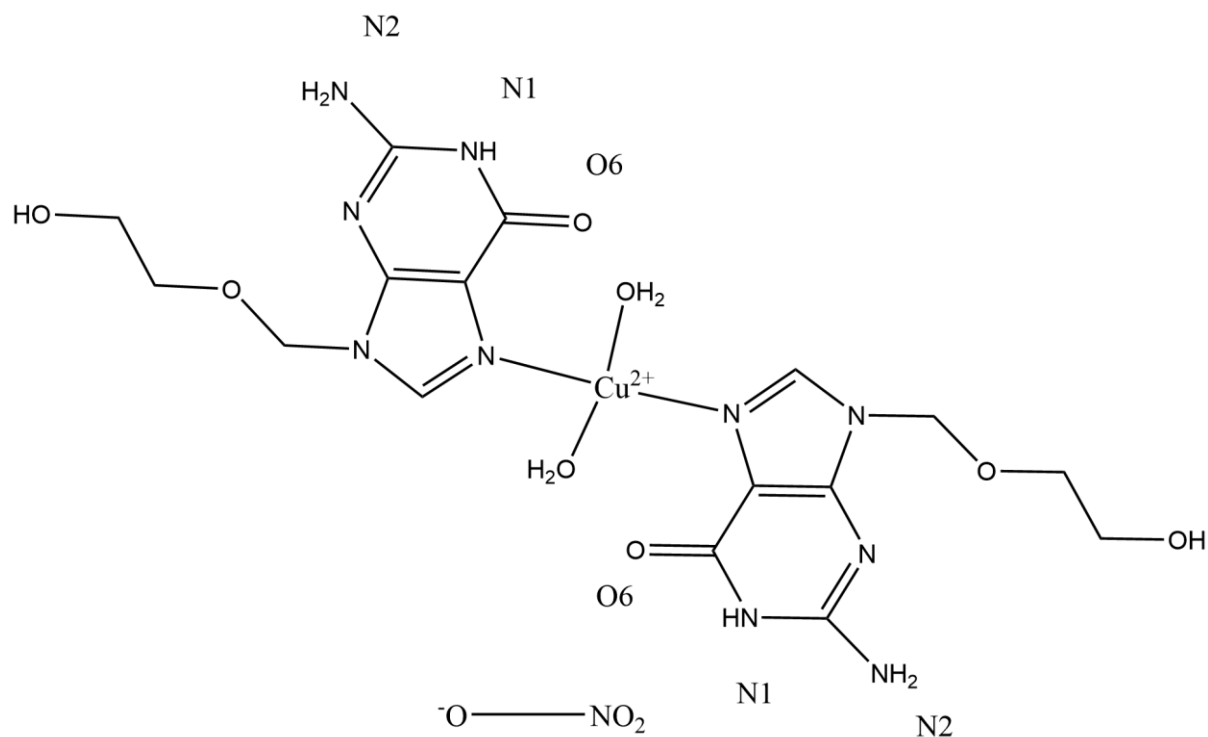


Figure 6 – a molecule structure of $[\text{Cu}(\text{ACV})_2(\text{H}_2\text{O})_2](\text{NO}_3)$, in a square planar geometric shape.

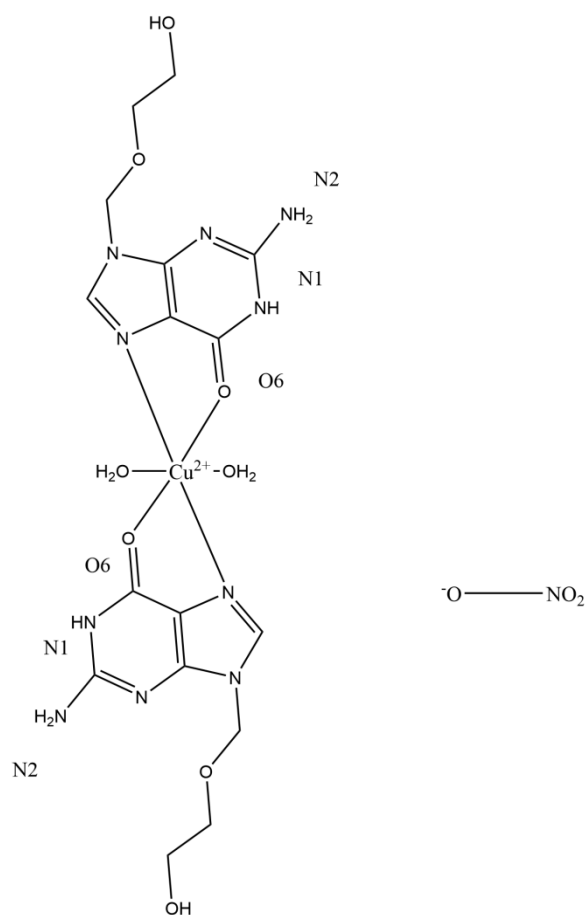


Figure 7 – a molecule structure of $[\text{Cu}(\text{ACV})_2(\text{H}_2\text{O})_2]$ in theoretical octahedral geometry

In the asymmetric unit of $[\text{Cu}(\text{ACV})_2(\text{H}_2\text{O})_2](\text{NO}_3)$, there are three molecules and their accompanying NO_3^- ions. Uniquely, the intermolecular hydrogen bonds form ribbons of the molecules, bonding at N2-N3 through N-H...N. N2 and N1 also use this type of bonding to the NO_3^- ions as well as through the hydroxyl terminal group of the ACV tail.

In addition to the analytical investigation, another approach to the complexes, is DNA binding in order to investigate the bioactivity and cytotoxicity of each of the metal-ACV complexes due to the presence of the antiviral nature of ACV. This approach was the focus of Avicioglu and Golcu's work, [17]. The metal salt used in this study was chloride salt ($\text{CuCl}_2 \cdot 2\text{H}_2\text{O}$, ZnCl_2 , $\text{FeCl}_3 \cdot 6\text{H}_2\text{O}$, K_2PtCl_4 , and $\text{RuCl}_2 \cdot 3\text{H}_2\text{O}$) which was placed in a methanol/water solution (1/5 v/v) under a pH buffer controlled environment. ACV, which had already been dissolved in methanol, was added to this solution. The ratios of ACV were essential for the different structures of metal and ACV ligands: $[\text{Cu}(\text{ACV})\text{Cl}_2]$, $[\text{Zn}(\text{ACV})\text{Cl}_2] \cdot 5\text{H}_2\text{O}$, and $[\text{Pt}(\text{ACV})\text{Cl}_2] \cdot 4\text{H}_2\text{O}$ were all 1:1 ratio (Figure 8); $[\text{Ru}(\text{ACV})_2\text{Cl}_2]\text{Cl} \cdot 3\text{H}_2\text{O}$ was in a 2:1 ratio (Figure 9); and $[\text{Fe}(\text{ACV})_3] \cdot 3\text{Cl}$ was in a 3:1 ratio (Figure 10).

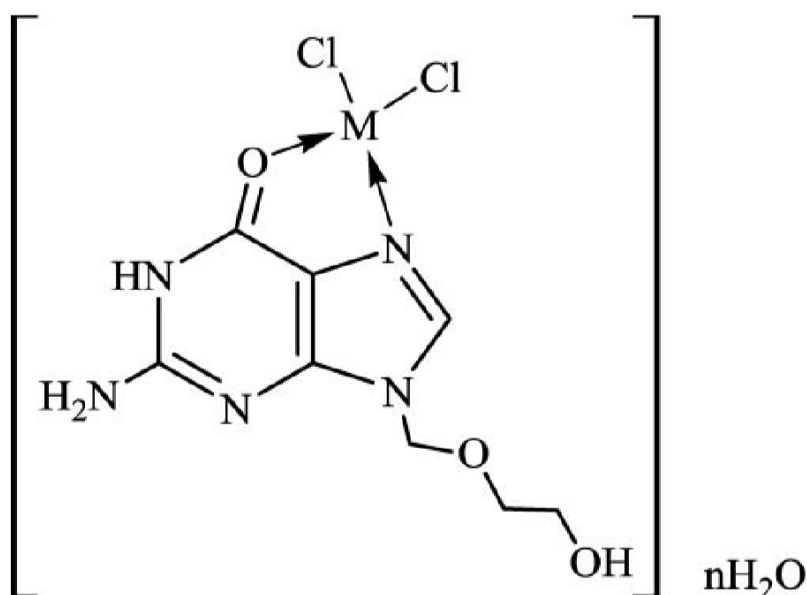


Figure 8 – the outline structure of the copper, zinc, and platinum structures, $[\text{M}(\text{ACV})\text{Cl}_2] \cdot n\text{H}_2\text{O}$, [17].

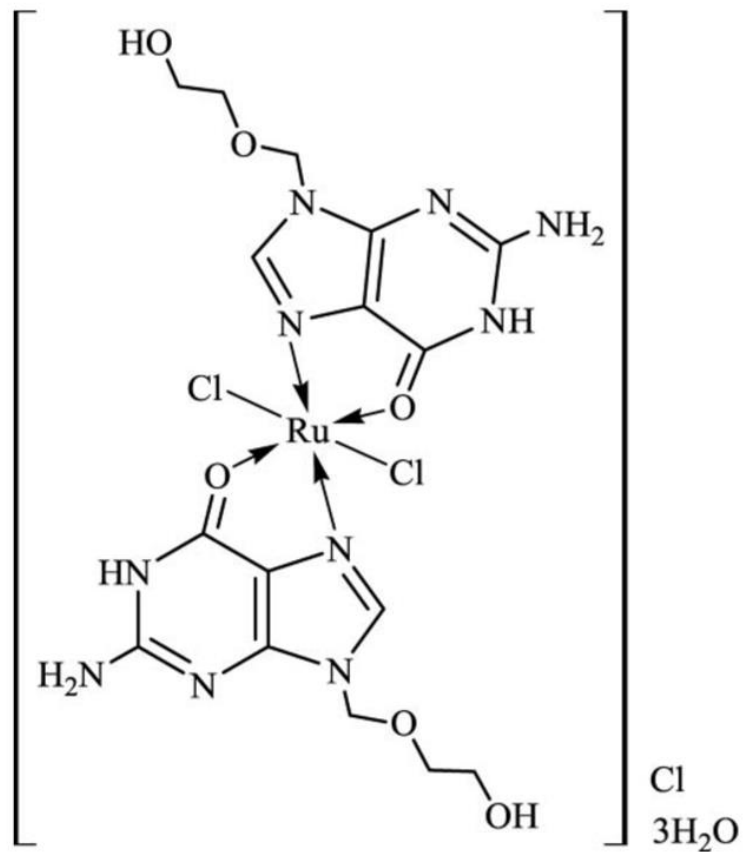


Figure 9 – One complex of $[Ru(ACV)_2Cl_2]Cl \cdot 3H_2O$, [17].

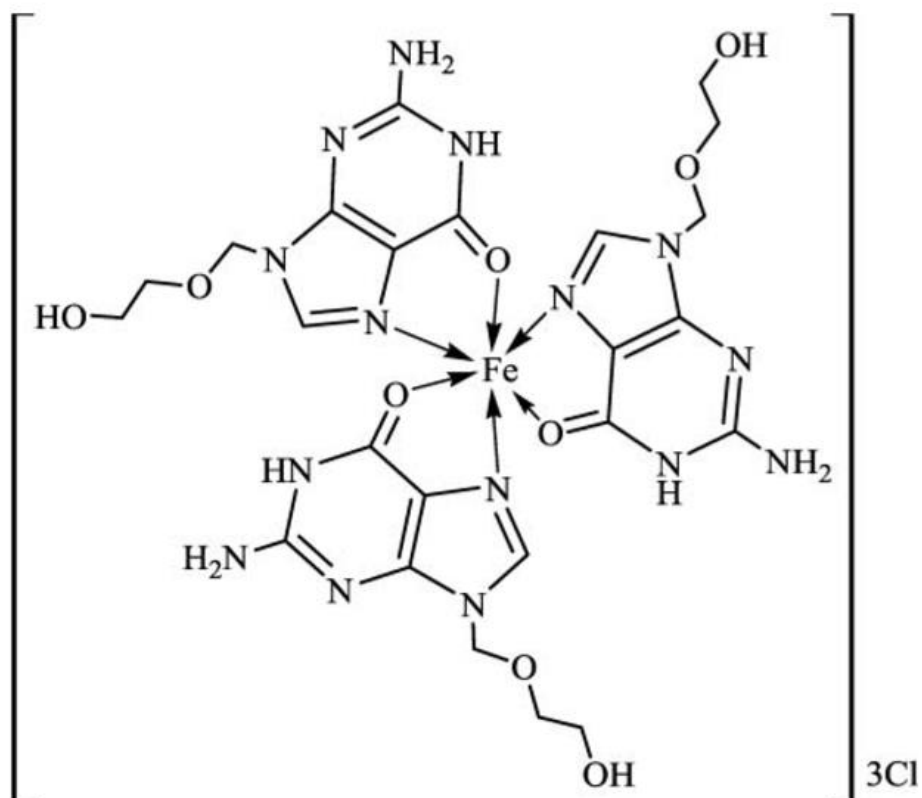


Figure 10 – One complex of $[\text{Fe}(\text{ACV})_3]3\text{Cl}$, [17].

Analytically, UV-Vis spectroscopy, IR spectroscopy, mass spectrometry, thermal analysis, and proton NMR spectroscopy all featured in these articles. The UV-Vis spectroscopy found that all complexes had a $d \rightarrow d^*$ transition between 437-492 nm except for the platinum and zinc compounds. All complexes had Metal \rightarrow Ligand charge transfer transitions and Ligand \rightarrow Metal charge transfer transitions, as well as $n \rightarrow \pi^*$ and $\pi \rightarrow \pi^*$ transitions. The conclusion of the geometry of the ruthenium and iron was that it formed octahedral structures, while platinum and copper formed square planar and zinc formed tetrahedral. IR spectroscopy found that all metal-ACV complexes' spectra were similar to that of the pure ACV spectrum with the exception of the C=O carbonyl group in each complex. The bonding of the carbonyl to the metal impacted the π bond interaction which gave a slightly altered IR reading. Thermal analysis found all complexes had 'absorbed and/or hydrated water molecules' present, except copper and iron [17]. Water coordinated to metal was found to have been eliminated in the range of 100-250°C and at 250-500°C the 'elimination of one, two or three coordinated chloride ions' [17] occurred leaving the metal-ACV species. Mass

spectroscopy found the molecular ions peaks and fragmentations expected in each compound. However, the proton NMR spectra had difficulty differentiating between the non-paramagnetic complexes, in particular the platinum and zinc compounds where there were only some small differences, leading to inconclusive data.

A key difference in Avicioglu and Golcu's study when compared to others was the incorporation of antimicrobial and antiviral tests. In the antimicrobial studies, each metal-ACV complex was introduced to certain strains of bacterium and fungi, and would be judged on the inhibition area size it created. It was found that only $[\text{Pt}(\text{ACV})\text{Cl}_2]\cdot 4\text{H}_2\text{O}$ showed a high effectiveness against two fungi microbials, but none of the bacteria samples. The antiviral study demonstrated that all compounds were effective against viruses. When diluted, all but iron still had effective cytotoxicity up to and including 1/1024 dilution rate; $[\text{Fe}(\text{ACV})_3]\cdot 3\text{Cl}$ was only effective up to and including 1/512 dilution rate.

All compounds synthesised in Avicioglu and Golcu's study showed a strong binding ability to DNA, being replaced with guanine ligands *in vivo*. The study acknowledges the potential for the use of Metal-Ligand compounds to be extended beyond antimicrobial or antiviral, such as biomarkers for medical investigations [17].

Another paper by Iztok Turel explores the possible complexes with ruthenium(III)-DMSO in solution, solid state and the biological characterisation of each with purine base derivatives, one of which is ACV, [18]. The initial synthesis was $[(\text{DMSO})_2\text{H}][\text{trans-RuCl}_4(\text{DMSO})_2]$ and ACV added to dried ethanol in a 2:1 ratio taking 14 days to obtain a small amount of orange needle like crystals which were suitable for single crystal XRD. These crystals were characterised as $[\text{mer-RuCl}_3(\text{ACV})(\text{DMSO})(\text{C}_2\text{H}_5\text{OH})]\cdot \text{C}_2\text{H}_5\text{OH}$ in an octahedral geometric structure (Figure 11). This compound is similar to a new anti-tumour metastasis inhibitor (NAMI) used currently as an anticancer drug, [19]. The hydrogen bond acceptor ($\text{C}_2\text{H}_5\text{OH}$) replacing one of the DMSO from the reactant precursor allows the bonding between ruthenium and the ACV ligand via N7. Methanol

(*[mer-RuCl₃(ACV)(DMSO)(CH₃OH)].0.5CH₃OH*) or water (*[mer-RuCl₃(ACV)(DMSO)(H₂O)].H₂O*) could also have been used as the hydrogen bond acceptor.

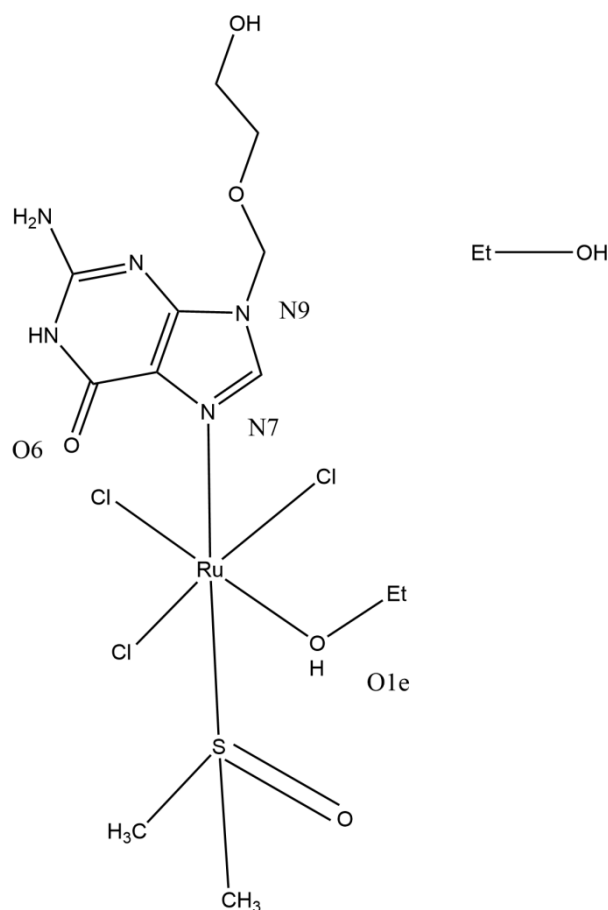


Figure 11 – a molecule structure of *[mer-RuCl₃(ACV)(DMSO)(C₂H₅OH)].C₂H₅OH*.

However, in a 4.5:1 ratio of (NH₄) [*trans-RuCl₄(DMSO)₂*] and ACV, in a mixture of ethanol and hydrochloric acid (1M) (1/1 v/v) that was left for three hours under reflux, red crystals were deposited. Once filtered, washed with diethyl ether and dried, the crystals were analysed by single crystal XRD which showed that it had synthesised to [*trans-RuCl₄(guaH)(DMSO)].2H₂O* in an octahedral structure; ACV had been substituted for guaninium (guaH). This too is similar to NAMI agents that are currently being used to treat cancer. The IR spectra taken from both compounds were similar to each other, but [*trans-RuCl₄(guaH)(DMSO)].2H₂O* showed another peak at 1704 cm⁻¹ for the carbonyl group. The obvious difference between compounds [*mer-*

$\text{RuCl}_3(\text{ACV})(\text{DMSO})(\text{C}_2\text{H}_5\text{OH}) \cdot \text{C}_2\text{H}_5\text{OH}$ and $[\text{trans-RuCl}_4(\text{guaH})(\text{DMSO})] \cdot 2\text{H}_2\text{O}$ is that $[\text{trans-RuCl}_4(\text{guaH})(\text{DMSO})] \cdot 2\text{H}_2\text{O}$ has the carbonyl group facing away from the centre of the molecule whereas the carbonyl group present in $[\text{mer-RuCl}_3(\text{ACV})(\text{DMSO})(\text{C}_2\text{H}_5\text{OH})] \cdot \text{C}_2\text{H}_5\text{OH}$ is facing inwards, forming an intramolecular bond. This has caused the loss of the peak in the IR spectrum for $[\text{mer-RuCl}_3(\text{ACV})(\text{DMSO})(\text{C}_2\text{H}_5\text{OH})] \cdot \text{C}_2\text{H}_5\text{OH}$. The explanation for the carbonyl group facing outwards from the centre is the loss of the acyclic tail due to the acidic conditions, protonating the N7 to form guaninium, but bonding to the ruthenium through N9. This Ru-N bonding leads to intramolecular bonding: N-H---Cl, as no chloride ion has to be substituted.

Although $[\text{mer-RuCl}_3(\text{ACV})(\text{DMSO})(\text{C}_2\text{H}_5\text{OH})] \cdot \text{C}_2\text{H}_5\text{OH}$, $[\text{mer-RuCl}_3(\text{ACV})(\text{DMSO})(\text{CH}_3\text{OH})] \cdot 0.5\text{CH}_3\text{OH}$ and $[\text{mer-RuCl}_3(\text{ACV})(\text{DMSO})(\text{H}_2\text{O})] \cdot \text{H}_2\text{O}$ bond by N7 to the metal centre, which is more favourable in a neutral pH environment, there are no intramolecular bonds with the chloride atoms in the centre. There is an intramolecular hydrogen bond between O6 (carbonyl group) and O1e (oxygen of the bonded ethanol group), as previously mentioned in Figure 11, present in all three of these compounds. In $[\text{trans-RuCl}_4(\text{guaH})(\text{DMSO})] \cdot 2\text{H}_2\text{O}$ there is a distorted octahedral structure with chloride atoms in the equatorial plane. The DMSO and guaninium ligand is bonded in the axial planes. The guaninium N9 bonds to the ruthenium atom obtaining the shortest bond amongst all of the compounds in this study. In addition to the short and strong Ru-N bond, the C=O in $[\text{trans-RuCl}_4(\text{guaH})(\text{DMSO})] \cdot 2\text{H}_2\text{O}$ is shorter than that found in compounds $[\text{mer-RuCl}_3(\text{ACV})(\text{DMSO})(\text{C}_2\text{H}_5\text{OH})] \cdot \text{C}_2\text{H}_5\text{OH}$, $[\text{mer-RuCl}_3(\text{ACV})(\text{DMSO})(\text{CH}_3\text{OH})] \cdot 0.5\text{CH}_3\text{OH}$ and $[\text{mer-RuCl}_3(\text{ACV})(\text{DMSO})(\text{H}_2\text{O})] \cdot \text{H}_2\text{O}$ which is explained by the rare form of bonding. Turel et al. comment on the 'relatively rare' [18] coordination of guaninium to ruthenium through N9. The position that the guaninium takes when bonding to the ruthenium allows intramolecular hydrogen bonding between N3 and the chloride atoms as they have not been substituted, as is the case in the other compounds, leading to an energetically more favourable compound.

UV-Vis spectroscopy was used to analyse both $[trans-RuCl_4(guaH)(DMSO)].2H_2O$ and $[mer-RuCl_3(ACV)(DMSO)(H_2O)].H_2O$. $[trans-RuCl_4(guaH)(DMSO)].2H_2O$ had a 5% decrease in the UV-Vis data, at 395 nm, after four hours owing to hydrolysis of the DMSO. This decreased further as the wavelength dropped from 351 nm to 336 nm as the release of a chloride atom occurred. A similar observation was made in $[mer-RuCl_3(ACV)(DMSO)(H_2O)].H_2O$, however, this occurred a lot faster, happening in 40 minutes, due to this complex having less chloride atoms than $[trans-RuCl_4(guaH)(DMSO)].2H_2O$ which, as previously explained, has a stronger intramolecular bond framework.

Biological tests of compounds $[trans-RuCl_4(guaH)(DMSO)].2H_2O$, $[mer-RuCl_3(ACV)(DMSO)(CH_3OH)].0.5CH_3OH$ and $[mer-RuCl_3(ACV)(DMSO)(H_2O)].H_2O$ against adenocarcinoma cells showed fairly similar results. $[trans-RuCl_4(guaH)(DMSO)].2H_2O$ initially inhibited 12% of the cells in 24 hours, increasing to 35% in 48 hours, but then disappears after 72 hours. $[mer-RuCl_3(ACV)(DMSO)(CH_3OH)].0.5CH_3OH$ begins higher than $[trans-RuCl_4(guaH)(DMSO)].2H_2O$ at 38% in 24 hours, however, this plateaus at 48 hours, and is then partially lost after 72 hours. Finally, $[mer-RuCl_3(ACV)(DMSO)(H_2O)].H_2O$ inhibits 25% of the cells in 24 hours, rising to 30% in 48 hours. However, consistent with the other two compounds, after 72 hours it is completely lost. Nevertheless, $[trans-RuCl_4(guaH)(DMSO)].2H_2O$ allowed cells more uptake of ruthenium than the other two compounds, even though it was not the most effective in inhibiting the cells. Although the ruthenium in $[mer-RuCl_3(ACV)(DMSO)(CH_3OH)].0.5CH_3OH$ and $[mer-RuCl_3(ACV)(DMSO)(H_2O)].H_2O$ was absorbed into the cells, it was less effective than $[trans-RuCl_4(guaH)(DMSO)].2H_2O$; $[trans-RuCl_4(guaH)(DMSO)].2H_2O$ absorbed 89% of the ruthenium, compared to 18.5% by $[mer-RuCl_3(ACV)(DMSO)(CH_3OH)].0.5CH_3OH$ and 11.7% by $[mer-RuCl_3(ACV)(DMSO)(H_2O)].H_2O$ [18] (Figure 12).

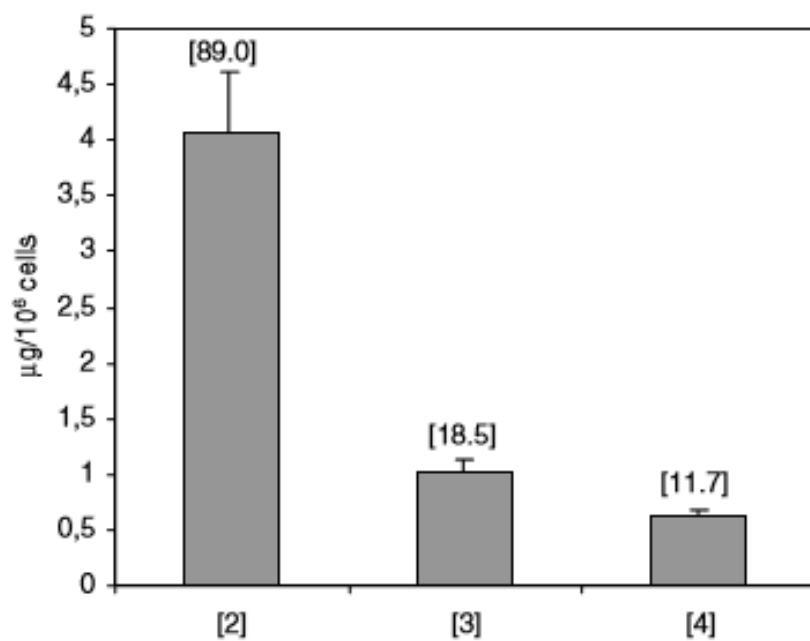


Figure 12 – ruthenium uptake from $[\text{trans-RuCl}_4(\text{guaH})(\text{DMSO})] \cdot 2\text{H}_2\text{O}$ (2), $[\text{mer-RuCl}_3(\text{ACV})(\text{DMSO})(\text{CH}_3\text{OH})] \cdot 0.5\text{CH}_3\text{OH}$ (3) and $[\text{mer-RuCl}_3(\text{ACV})(\text{DMSO})(\text{H}_2\text{O})] \cdot \text{H}_2\text{O}$ (4) into adenocarcinoma cells, [18].

1.3. Aims

The synthesis of new metal-ACV structures, with the potential to form structures that can be used in future studies regarding their use in the biochemical and/or the medical field, is necessary to develop patient treatments for viral conditions, such as complications with the herpes virus. This study aims to synthesise, observe and classify novel metal-ACV molecules, in particular: copper, zinc and silver. Different crystallisation methods will be used and observations made in either solid or solution state prior to classification through x-ray diffraction.

2. Experimental

2.1. Synthesising Single Crystals of 1-9

2.1.1. General Method

Metal (Cu^{2+} , Zn^{2+} , Ag^{+}) tetrafluoroborate salt and acyclovir (ACV) were added in the appropriate ratio (vide infra, Table 1, Table 2 and Table 3) to a glass vial and methanol or ethanol (5-7 mL) was added. The solution was briefly sonicated (<1 minute) with heating to aid dissolution. Vials were left open and allowed to slowly evaporate. Before complete evaporation, crops of single crystals formed that were isolated by taking them out with a spatula and placing them in a new glass vial and analysed initially by single crystal X-ray diffraction (SCXRD) methods, followed by powder X-ray diffraction (PXRD), infrared (IR) spectroscopy, and scanning electron microscopy/energy-dispersive X-ray (SEM/EDX). The vials were later sealed.

2.1.2. Equipment and Chemicals

The ligand (Acyclovir) used in this study was purchased from Sigma Aldrich as a bulk stock. The product's CAS number is 59277-89-3 and has 100% assay; IR (cm^{-1}): 1695, 1647, 1575, 1541, 1489, 1477, 1419, 1386, 1361, 1340, 1307, 1226, 1182, 1103, 1047, 1014. The metal salts used were also bought from Sigma Aldrich: silver tetrafluoroborate (CAS: 14104-20-2, 98%), copper tetrafluoroborate (CAS: 207121-39-9) and zinc tetrafluoroborate (CAS: 27860-83-9). All metal tetrafluoroborates are hazardous, corrosive and are irritants, which may cause severe burning and irritation to the respiratory system.

2.1.3. Copper Compounds 1-5

As per the general method, copper tetrafluoroborate [$\text{Cu}(\text{BF}_4)_2$] (~10 mg, 0.042 mM) and ACV (~10 mg, 0.044 mM) were added to a 7 mL glass vial. The solvent was then added and the solution was fully mixed. After evaporation, between 4-6 days, a majority of crystals were green in colour,

however, some were colourless in appearance. Green crystals were selected for SCXRD analysis as these crystals were certain to have reacted.

Other solutions including copper were also made. By varying the metal to ligand ratio of copper tetrafluoroborate and ACV, increasing the ligand to 20 mg and 30 mg in solutions. The final conditions are stated in Table 1.

Table 1: Summary of conditions for synthesis of copper complexes 1-5

Compound	Formula	Mol. of Cu(BF ₄) ₂ / mM	Mol. of ACV / mM	Solvent	Crystallisation method	Crystal Colour and Types
1	[Cu(ACV) ₂ (H ₂ O) ₃]•2BF ₄	0.44	0.88	Methanol	Evaporation	Green Blocks
2	[Cu(ACV) ₂ (H ₂ O) ₂ (OH) ₂]•ACV + H ₂ O	0.44	0.88	Ethanol	Evaporation	Light Green Plates
3	[Cu(ACV) ₄ (H ₂ O)]•2BF ₄	0.44	0.44	Ethanol	Evaporation	Green Blocks
4	[Cu(ACV) ₂ (H ₂ O) ₂]•BF ₄	0.44	0.44	Acetone	Evaporation	Green Needles
5	[Cu(ACV) ₂ (BF ₄) ₂]•ACV + H ₂ O	0.44	0.44	Ethanol	Evaporation	Dark Green Needles

1: $[\text{Cu}(\text{ACV})_2(\text{H}_2\text{O})_3] \cdot 2\text{BF}_4$

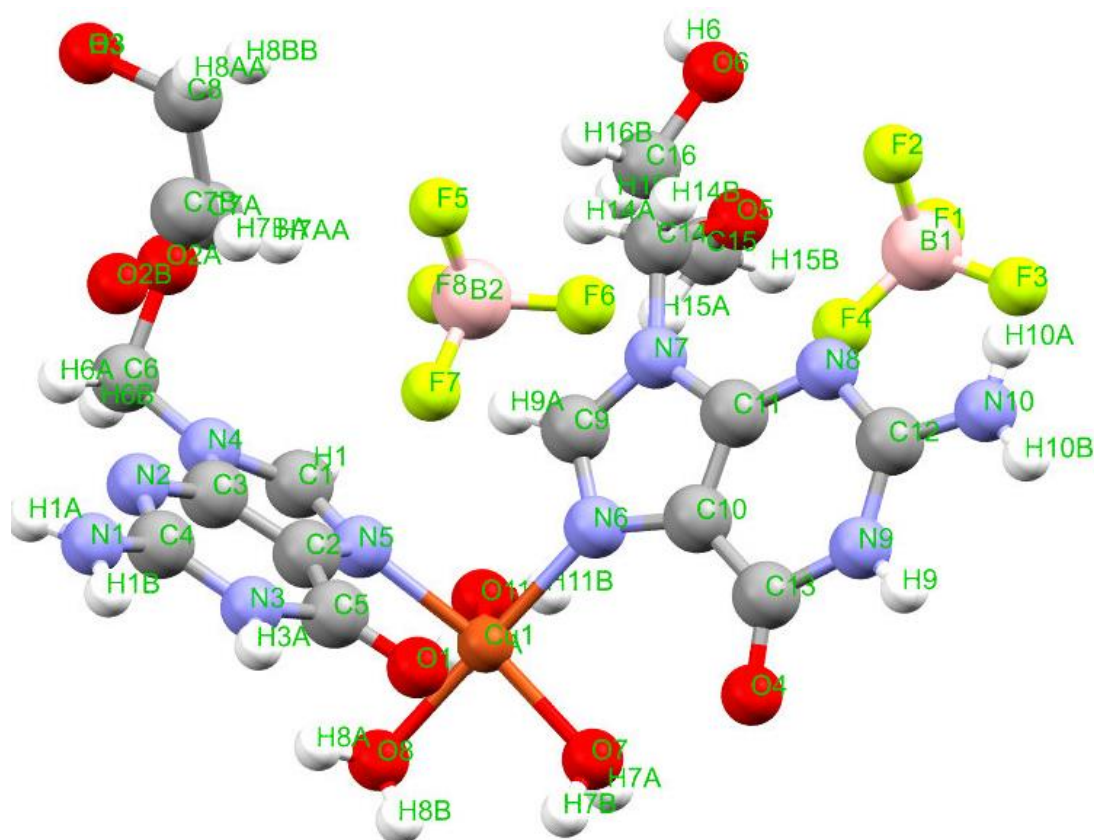


Figure 13 – the molecule structure of complex 1: $[\text{Cu}(\text{ACV})_2(\text{H}_2\text{O})_3] \cdot 2\text{BF}_4$ labelled.

2: $[\text{Cu}(\text{ACV})_2(\text{H}_2\text{O})_2(\text{OH})_2] \cdot \text{ACV} + 2\text{H}_2\text{O}$

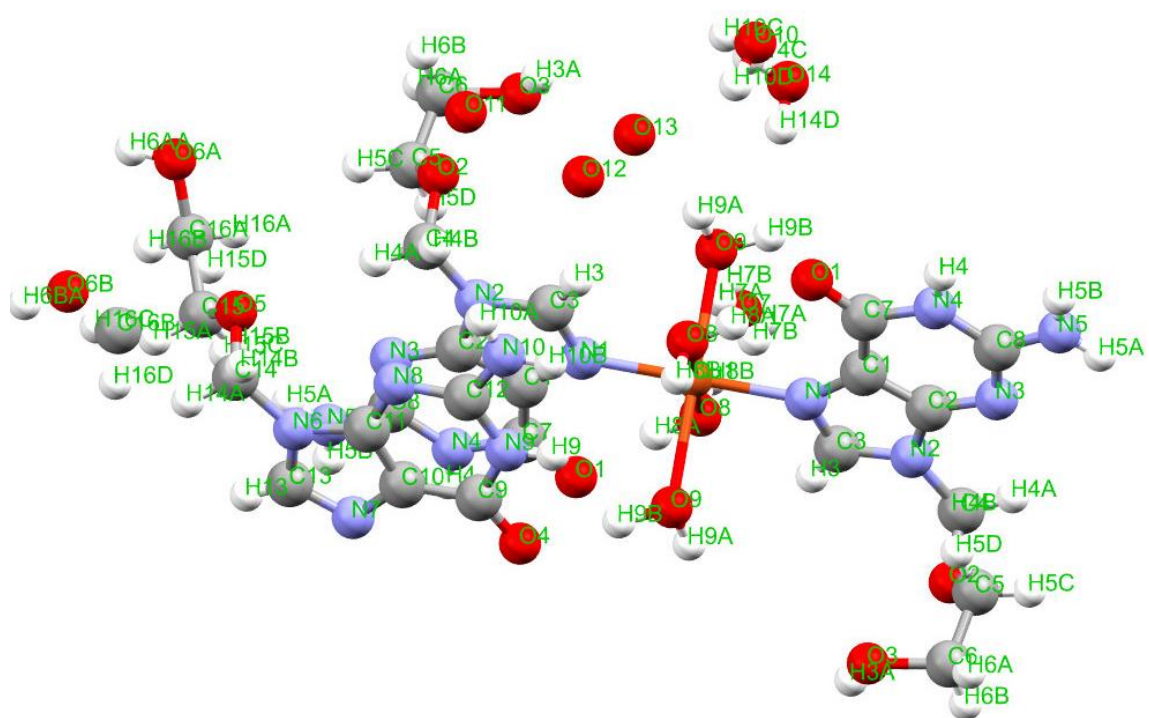


Figure 14 – the molecule structure of complex 2: $[\text{Cu}(\text{ACV})_2(\text{H}_2\text{O})_2(\text{OH})_2] \cdot \text{ACV} + 2\text{H}_2\text{O}$ labelled.

3: $[\text{Cu}(\text{ACV})_4(\text{H}_2\text{O})] \cdot 2\text{BF}_4$

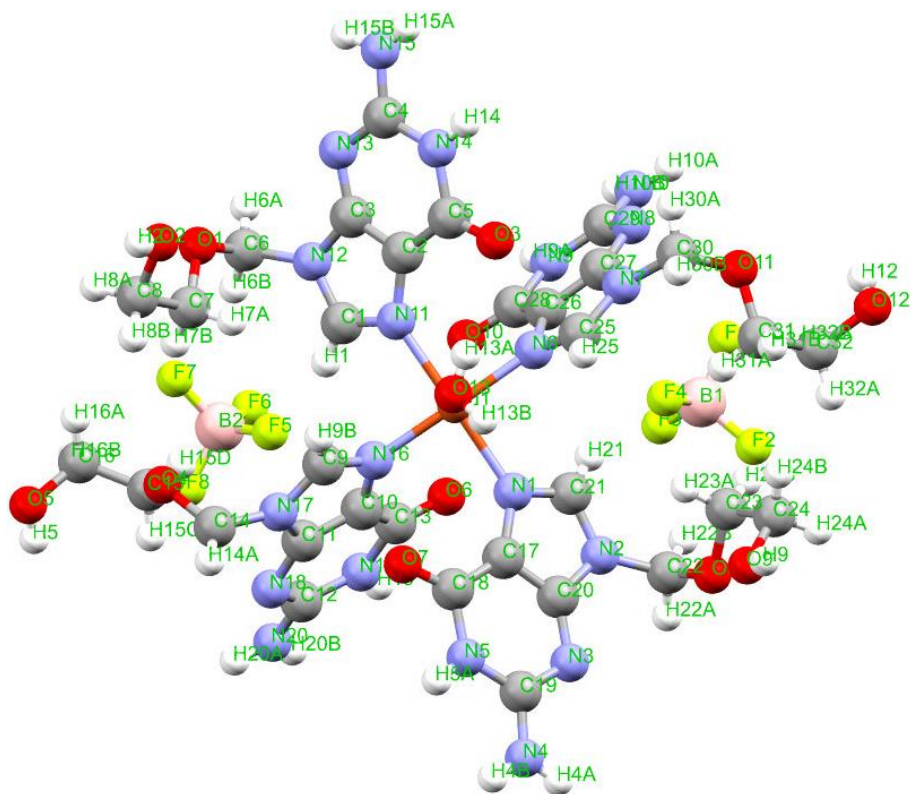


Figure 15 – the molecule structure of complex 3: $[\text{Cu}(\text{ACV})_4(\text{H}_2\text{O})] \cdot 2\text{BF}_4$ labelled.

4: $[\text{Cu}(\text{ACV})_2(\text{H}_2\text{O})_2] \cdot 2\text{BF}_4$

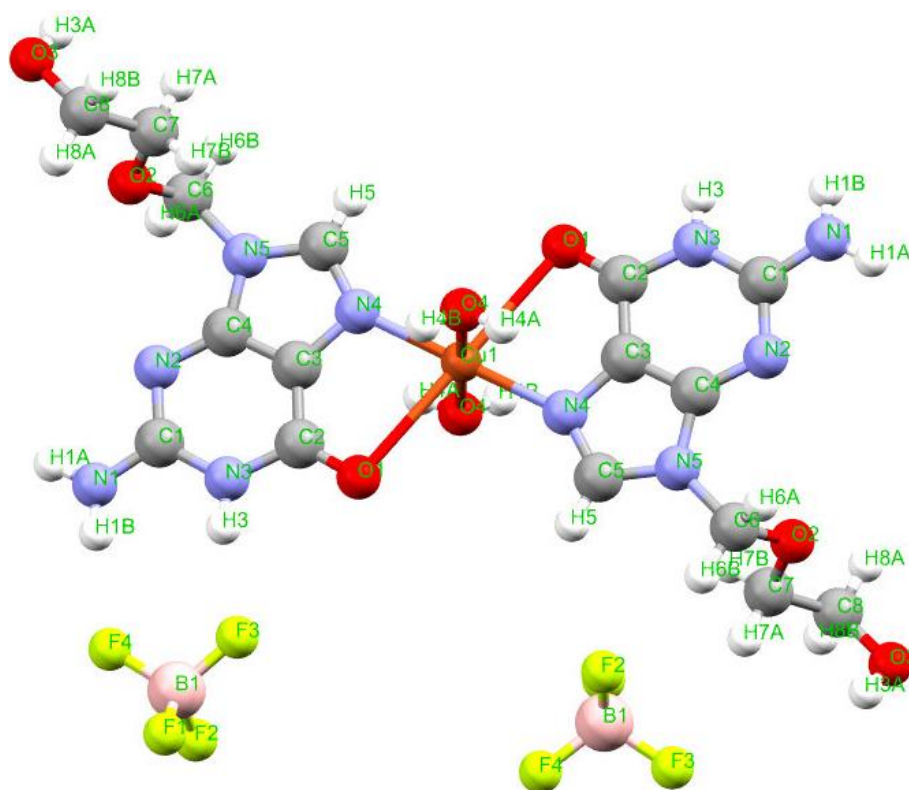


Figure 16 – the molecule structure of complex 4: $[\text{Cu}(\text{ACV})_2(\text{H}_2\text{O})_2] \cdot 2\text{BF}_4$ labelled.

5: $[\text{Cu}(\text{ACV})_2(\text{BF}_4)_2] \cdot \text{ACV} + 2\text{H}_2\text{O}$

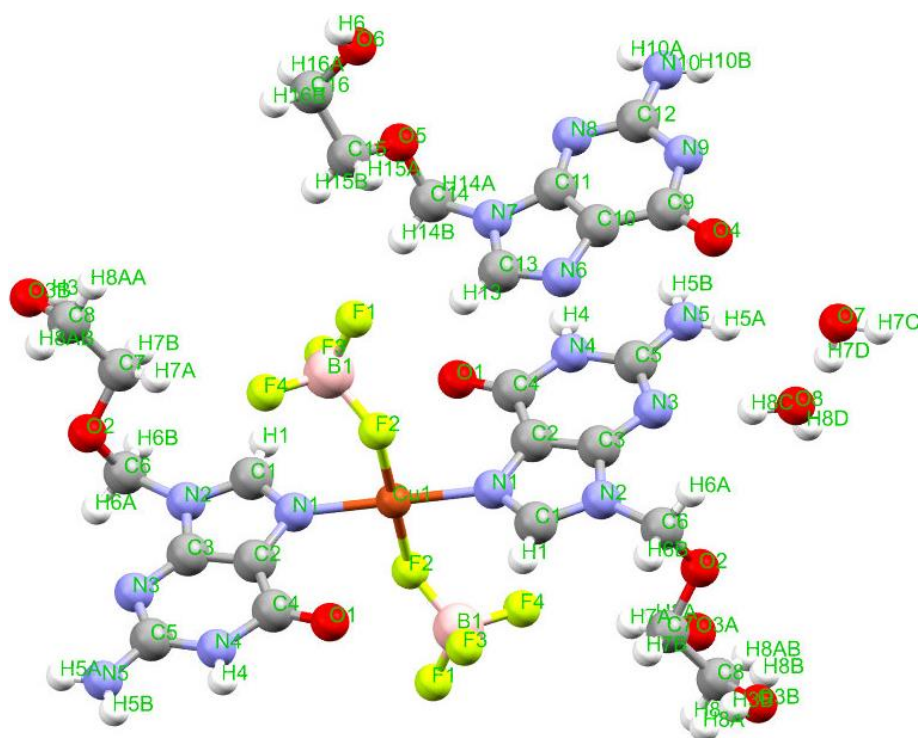


Figure 17 – the molecule structure of complex 5: $[\text{Cu}(\text{ACV})_2(\text{BF}_4)_2] \cdot \text{ACV} + 2\text{H}_2\text{O}$ labelled.

2.1.4. Zinc Compound 6

A zinc compound was synthesised according to the general method. Zinc tetrafluoroborate ($\text{Zn}(\text{BF}_4)_2$) (~10 mg, 0.042 mM) and ACV (~10 mg, 0.044 mM) were added to a glass vial. The solvent was then added and the solution was fully mixed (Table 2). After evaporation, between 5-7 days, selected clear, colourless crystals were picked for SCXRD analysis.

Other solutions were also made, however, when the ratio of metal to ligand was changed by increasing ACV to 20 mg and 30 mg, no change in motif was observed.

Table 2: Summary of conditions for synthesis of zinc complex 6

Compound	Formula	Mol. of $\text{Zn}(\text{BF}_4)_2$ / mM	Mol. of ACV / mM	Solvent	Crystallisation method
6	$[\text{Zn}(\text{ACV})_4] \cdot \text{SiF}_6$ + H_2O	0.44	0.88	Ethanol	Evaporation / layering

6: [Zn(ACV)₄]•SiF₆ + H₂O

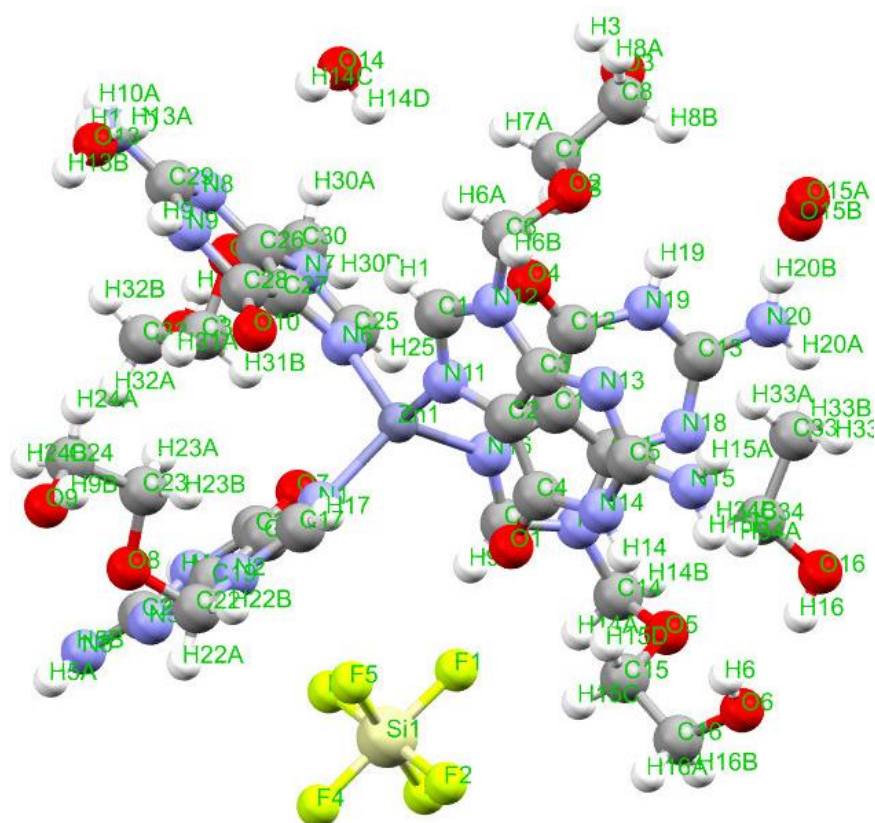


Figure 18 – the molecule structure of complex 6: [Zn(ACV)₄]•SiF₆ + H₂O labelled.

2.1.5. Silver Compounds 7-9

As per the general method, silver tetrafluoroborate (AgBF₄) (~8 mg, 0.044 mM) and ACV (~10 mg, 0.044 mM) were added to a glass vial and wrapped in aluminium foil to prevent the light sensitive silver from reducing. The solvent was then added and the solution was fully mixed (Table 3). After evaporation, selected clear, colourless crystals were picked for SCXRD analysis.

Other solutions were also made, however, the ratio of metal to ligand was changed, with ACV increasing to 20 mg and 30 mg in other solutions.

Table 3: Summary of conditions for synthesis of silver complexes 7-9

Compound	Formula	Mol. of AgBF ₄ / mM	Mol. of ACV / mM	Solvent	Crystallisation method
7	2[Ag ₂ (ACV) ₃]•2SiF ₆ + 3H ₂ O	0.44	0.44	Methanol	Evaporation
8	2[Ag(ACV)]•SiF ₆ + 2H ₂ O	0.44	0.44	Ethanol	Evaporation
9	2[Ag(ACV) ₂]•SiF ₆ + 2H ₂ O	0.44	0.88	Ethanol	Evaporation

7: 2[Ag₂(ACV)₃]•2SiF₆ + 3H₂O

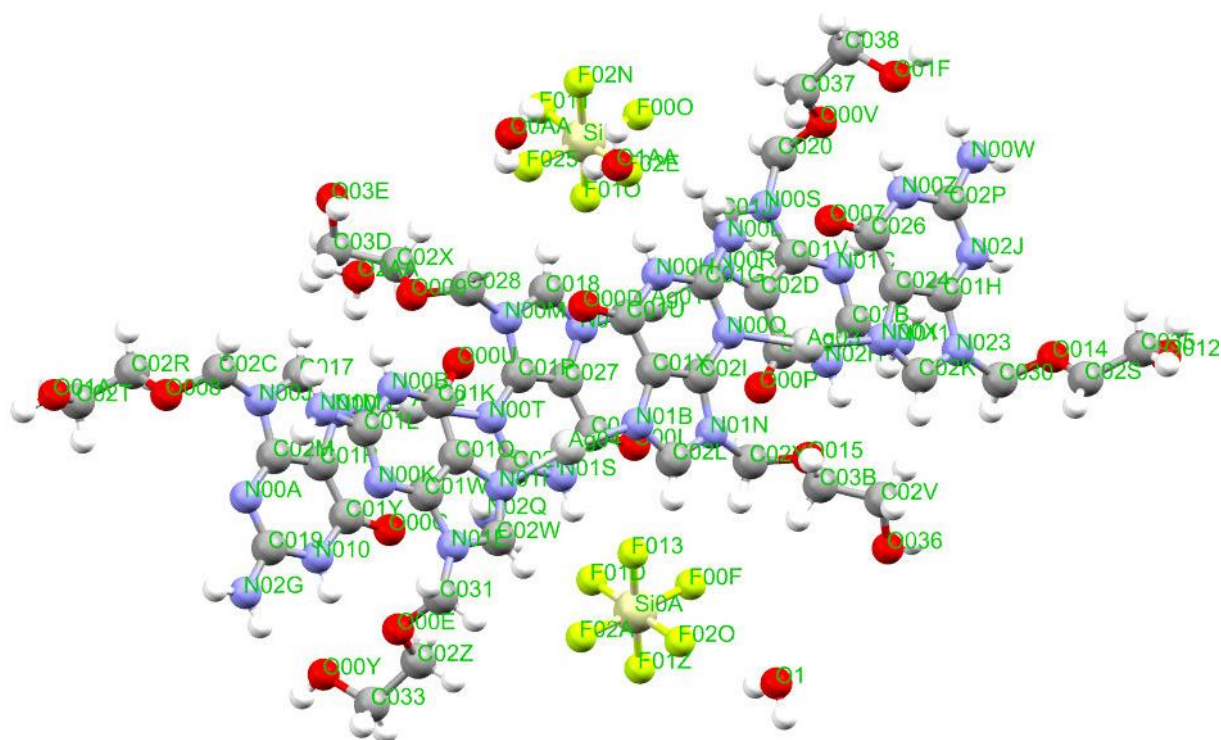


Figure 19 – the molecule structure of complex 7: 2[Ag₂(ACV)₃]•2SiF₆ + 3H₂O labelled.

8: $2[\text{Ag}(\text{ACV})] \cdot \text{SiF}_6 + 2\text{H}_2\text{O}$

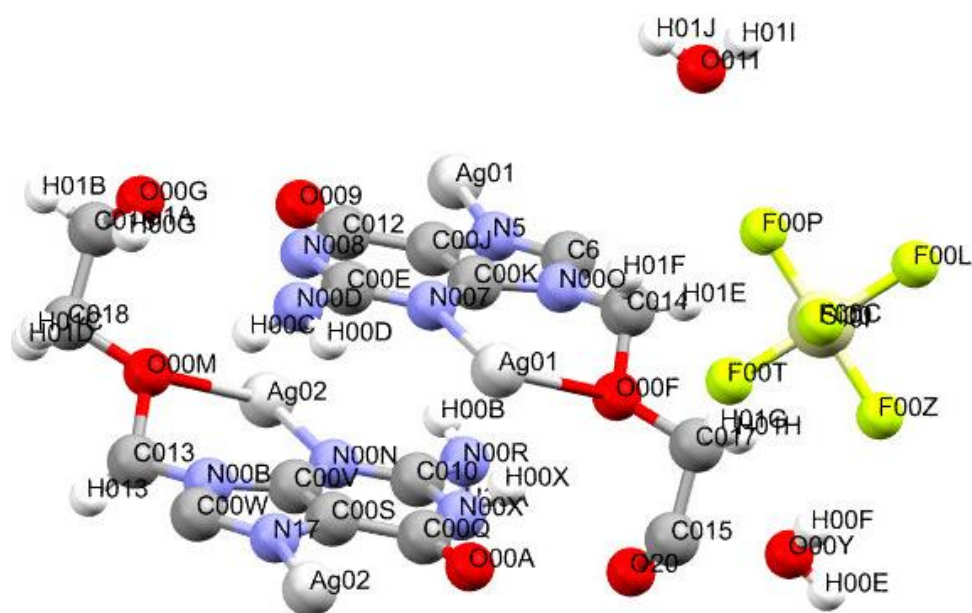


Figure 20 – the molecule structure of complex 8: $2[\text{Ag}(\text{ACV})] \cdot \text{SiF}_6 + 2\text{H}_2\text{O}$ labelled.

9: $2[\text{Ag}(\text{ACV})_2] \cdot \text{SiF}_6 + 2\text{H}_2\text{O}$

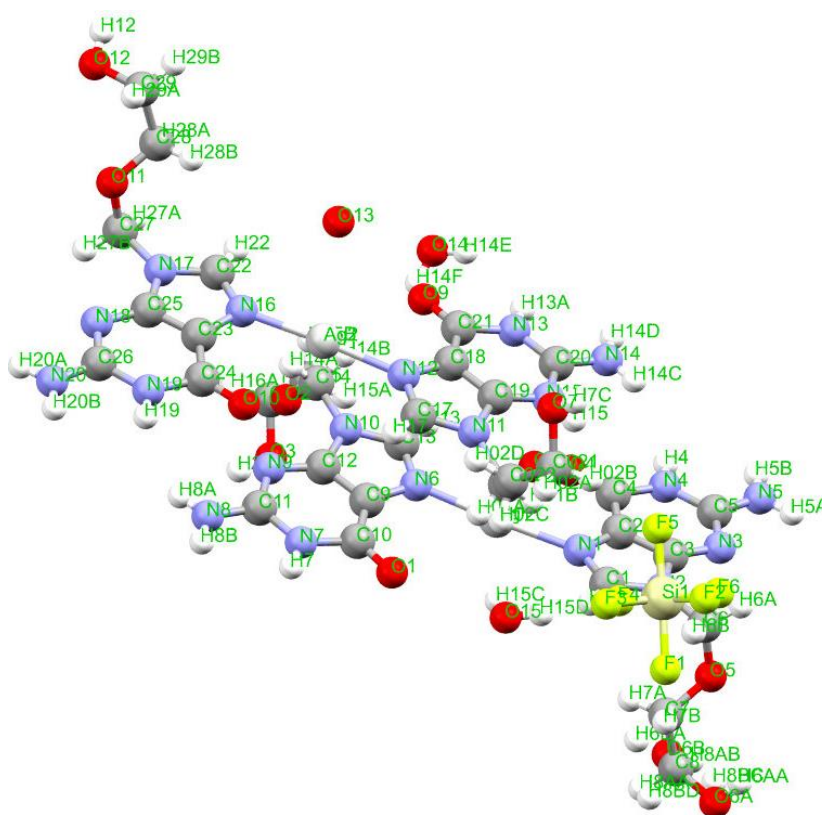


Figure 21 – the molecule structure of complex 9: $2[\text{Ag}(\text{ACV})_2] \cdot \text{SiF}_6 + 2\text{H}_2\text{O}$ labelled.

2.1.6. Scaling Up the synthesis of 1-9

For further analysis, the crystallisations were scaled up by a factor of 10 to isolate more material to enable analysis by Powder X-Ray Diffraction (PXRD). Therefore, the metal salt (100 mg, 4.44 mM) and ACV (100 mg, 4.44 mM) were added to a vial and solvent added (as referenced in Tables 1, 2, and 3). Heating and sonication was applied to assist the reaction.

2.2. Synthesising Powder Samples

2.2.1. General Method 1 – Evaporation

All syntheses relating to this method were carried out as described below, unless stated otherwise. A range of solvents were used in this method: methanol (MeOH), ethanol (EtOH), acetonitrile (MeCN) and acetone (AcO). Metal (Cu^{2+} , Zn^{2+} , Ag^+) tetrafluoroborate (4.44 mM) and Acyclovir (100 mg, 4.44 mM) were added to a 10 mL glass vial. The selected solvent was then added to the glass vial (7 mL). The sample was sonicated for <1 minute and heated to promote dissolution and reaction. The solution was then filtered through a plug of cotton wool and Celite® 545. After filtration was complete, the vial containing the solution was covered with parafilm and a small hole made in the top to allow slow evaporation.

2.2.2. General Method 2 – Layering

A range of solvents were used in this method: methanol (MeOH), ethanol (EtOH), acetonitrile (MeCN), and acetone (AcO). Metal Salt (4.44 mM) and Acyclovir (100 mg, 4.44 mM) were added to a 10 mL glass vial. The solvent was added to the glass vial (7 mL). The sample was sonicated for <1 minute and heated to promote dissolution and reaction. The solution would then be filtered through a glass pipette containing cotton wool and Celite® 545. In a separate clean glass vial a layer of dichloromethane (DCM) (~1 mL, 0.01 M) was placed. A 1:1 buffer solution (~2 mL) of DCM and the chosen solvent was then slowly layered on top of the DCM using a 1mL needle and syringe to deposit it down the side of the vial. Finally, the metal/ligand solution (~1 mL) was layered on top of the buffer by needle and syringe and a cap would be screwed on top to prevent solvent evaporation. Over time, the three layers slowly combined, resulting in crystallisation of the complex.

2.3. Synthesis of 1 ($[\text{Cu}(\text{ACV})_2(\text{H}_2\text{O})_3] \cdot 2\text{BF}_4$)

Both general methods 1 and 2 were used to synthesise this product. Two ratios were used when producing these samples: 1:1 and 2:1 ligand to metal. The synthesis of the 1:1 sample is as described

in the general methods. The 2:1 sample was created by ACV (200 mg, 0.88 mM) and $\text{Cu}(\text{BF}_4)_2$ (100 mg, 0.44 mM) being added to a vial, after which a chosen solvent was added to the vial. Both heating and sonication was used to aid reaction. Both the evaporation method and layering method were then used. The final product synthesised by the evaporation method was green blocks indicating the 2:1 ratio to be the most effective approach. IR (cm^{-1}): 1697, 1635, 1589, 1541, 1490, 1419, 1363, 1178, 1080, 1051, 1010. However, once the measured PXRD data was compared to the predicted (Appendix A Fig.1), the pattern showed the sample to be largely consist of copper complex 1.

2.4. Synthesis of 2 ($[\text{Cu}(\text{ACV})_2(\text{H}_2\text{O})_2(\text{OH})_2] \cdot \text{ACV} + 2\text{H}_2\text{O}$)

Both general methods 1 and 2 were used to synthesise this product. Two ratios were used when producing these samples: 1:1 and 2:1 ligand to metal. The synthesis of the 1:1 sample is as described in the general methods. The 2:1 sample was created by adding ACV (200 mg, 0.88 mM) and $\text{Cu}(\text{BF}_4)_2$ (100 mg, 0.44 mM) to a vial and a chosen solvent would be added to the vial. Both heating and sonication was used to aid reaction. Both the evaporation method and layering method were then used. Evaporation proved to be the better method with a 2:1 ratio of ligand to metal which produced light green plates with a visibly larger yield. IR (cm^{-1}): 1697, 1635, 1589, 1541, 1490, 1419, 1363, 1178, 1080, 1051, 1010. When analysing the PXRD comparison between the predicted Cu 2 and the product (Appendix A Fig.2), the pattern showed the sample to largely consist of copper complex 2.

2.5. Synthesis of 3 ($[\text{Cu}(\text{ACV})_4(\text{H}_2\text{O})] \cdot 2\text{BF}_4$)

Both general methods 1 and 2 were used to synthesise this product. Three ratios were used when producing these samples: 1:1, 2:1 and 3:1 ligand to metal. The 1:1 sample is as described in the general methods. The 2:1 sample was created by adding ACV (200 mg, 0.88 mM) and $\text{Cu}(\text{BF}_4)_2$ (100 mg, 0.44 mM) and a chosen solvent to the vial. The 3:1 sample was created by adding ACV (3:1, 300 mg, 1.33 mM) and $\text{Cu}(\text{BF}_4)_2$ (100 mg, 0.44 mM) and a chosen solvent to the vial. Both heating and

sonication was used to aid reaction. Both the evaporation method and layering method were then used. The evaporation method was more effective in a 1:1 ratio which showed green block crystals which, compared to the other samples, gave a larger yield. IR (cm^{-1}): 1689, 1655, 1598, 1490, 1425, 1359, 1346, 1290, 1274, 1257, 1219, 1193, 1132, 1093, 1047, 1002. The PXRD comparison showed a similar pattern in both the measured and the predicted data, hence this species is the dominant product.

2.6. Synthesis of 4 ($[\text{Cu}(\text{ACV})_2(\text{H}_2\text{O})_2] \cdot 2\text{BF}_4$)

As per general method 1, this sample was replicated to form a sufficient sample to perform the analytical techniques PXRD and infrared spectroscopy. The solvent used in this sample was limited to acetone, as the single crystal was formed from copper and acyclovir in acetone. Both ratios 1:1 and 2:1, ligand to metal, were used in the synthesis. For example, the 2:1 product would be formed from $\text{Cu}(\text{BF}_4)_2$ (100 mg, 0.44 mM) and ACV (200 mg, 0.88 mM) in a vial, then acetone (~5 mL, 0.08 mM) was added. Heating and sonication was used to assist the reaction process. Although method 1 was predominantly chosen for the better yield and better quality crystals, which were dark green needles, a layered approach was also undertaken. The PXRD comparison data can be seen in Appendix A Fig.4 and Fig. 5 which demonstrate that the evaporation approach provides better bulk material of Cu 4. IR (cm^{-1}): 1685, 1653, 1598, 1544, 1489, 1357, 1346, 1193, 1132, 1095, 1045, 1004.

2.7. Synthesis of 5 ($[\text{Cu}(\text{ACV})_2(\text{BF}_4)_2] \cdot \text{ACV} + 2\text{H}_2\text{O}$)

Cu 5 was synthesised by both general methods 1 and 2 to increase the likelihood of achieving single crystals. Using ethanol as the solvent to achieve Cu 5, the crystals synthesised using the evaporation method were of a higher quantity and quality. For Cu 5, a 1:1 ratio was used: ACV (100 mg, 0.44 mM) and $\text{Cu}(\text{BF}_4)_2$ (100 mg, 0.44 mM) were added to a vial along with ethanol (~5 mL, 1 mM). Heating and sonication was needed to promote a full reaction. Overall, evaporation was a better method for producing Cu 5 crystals which were dark green bunched needles. IR (cm^{-1}): 1689, 1655, 1598, 1490, 1425, 1359, 1346, 1290, 1274, 1257, 1219, 1193, 1132, 1093, 1047, 1002. The

comparative PXRD data (Appendix A, Fig. 6) show both the measured and the predicted data to be mainly low intensity peaks with considerable similarities. Some differences were however seen, such as at $\sim 27^\circ$ there is a double peak in the measured data that only appears as a single peak in the predicted data. Additionally, there is a large stacked peak at $\sim 34^\circ$ in the measured data which is not in the predicted; these differences suggest that there may be a mixture of polymorphs within the Cu 5 sample.

2.8. Synthesis of 6 ($[\text{Zn}(\text{ACV})_4] \cdot \text{SiF}_6 + \text{H}_2\text{O}$)

The zinc compound was synthesised by both general methods 1 and 2. All solvent options were explored to achieve this particular crystal. Ligand to metal ratios 1:1 and 2:1 were used. ACV (100 mg/200 mg, 0.44 mM/0.88 mM), $\text{Zn}(\text{BF}_4)_2$ (100 mg, 0.44 mM) and Na_2SiF_6 (~ 7 mg, 0.44 mM) were added to a vial and the solvent (~ 5 mL) added. This solution was sonicated and heated to aid the reaction. In order to achieve a yield of crystals, the only method that was found to effectively synthesise a product was layering in a 2:1 ratio of ligand to metal which resulted in cloudy, white blocks. IR (cm^{-1}): 1691, 1653, 1647, 1637, 1577, 1541, 1489, 1477, 1419, 1386, 1363, 1340, 1311, 1226, 1182, 1045. The PXRD comparison of the measured and the predicted data (Appendix A, Fig.7) demonstrated a largely similar pattern and intensity of peaks. However, low crystallinity/amorphous nature hindered matching of this sample.

2.9. Synthesis of 7 ($2[\text{Ag}(\text{ACV})_3] \cdot \text{SiF}_6 + 3\text{H}_2\text{O}$)

Crystals of Ag 1 were synthesised by general methods 1 and 2. A range of solvents were trialled to form this particular crystal. Ratios 1:1, 2:1 and 3:1 of ligand to metal were used. ACV (80 mg/160 mg/240 mg, 0.44 mM/0.88 mM/1.3 mM), AgBF_4 (100 mg, 0.44 mM) and Na_2SiF_6 (~ 7 mg, 0.44 mM) were added to a vial along with the solvent (~ 5 mL). This solution was sonicated and heated to aid the reaction. Evaporation was the best method for Ag 1 in a 1:1 ratio which gave colourless plated crystals which, when left exposed to air, became very tacky, suggesting hygroscopic behaviour. IR (cm^{-1}): 1693, 1629, 1577, 1539, 1477, 1386, 1361, 1340, 1311, 1226, 1182, 1045, 1016, 985. The

PXRD data comparing the measured data and the predicted data indicated some strong similarities in the powder patterns (Appendix A, Fig. 8). However, a low crystallinity/amorphous nature hindered matching of this sample.

2.10. Synthesis of 8 ($2[\text{Ag}(\text{ACV})]\cdot\text{SiF}_6+ 2\text{H}_2\text{O}$)

The Ag 2 crystal was synthesised by general methods 1 and 2. A range of solvents were trialled separately to form this particular crystal with two ligand to metal ratios, 1:1 and 2:1, tested. ACV (80 mg/160 mg, 0.44 mM/0.88 mM), AgBF_4 (100 mg, 0.44 mM) and Na_2SiF_6 (~7 mg, 0.44 mM) were added to a vial along with the solvent (~5mL). This solution was sonicated and heated to aid the reaction. When synthesising the Ag 2 crystal, the best method for yield and quality was by evaporation in a 1:1 ratio, forming colourless crystal plates which, when left exposed to air, would become tacky. IR (cm^{-1}): 1693, 1629, 1577, 1539, 1386, 1361, 1311, 1226, 1182, 1045, 1016. The PXRD data comparing the measured and predicted data was inconclusive as the measured data was highly amorphous (Appendix A, Fig. 9) and therefore did not show many analytical peaks.

2.11. Synthesis of 9 ($2[\text{Ag}(\text{ACV})_2]\cdot\text{SiF}_6+ 2\text{H}_2\text{O}$)

Ag 3 was synthesised by general methods 1 and 2 with a range of solvents used in separate trials to form this crystal. Two different ratios of ligand to metals were used: 1:1 and 2:1. ACV (80 mg/160 mg, 0.44 mM/0.88 mM), AgBF_4 (100 mg, 0.44 mM) and Na_2SiF_6 (~7 mg, 0.44 mM) were added to a vial along with the solvent (~5 mL). This solution was sonicated and heated to aid the reaction. Evaporation method with a 2:1 ratio of ligand to metal was used and synthesised colourless crystal plates which, when left exposed to air, would become tacky. IR (cm^{-1}): 1693, 1629, 1577, 1539, 1386, 1361, 1311, 1226, 1182, 1045, 1016. Comparative PXRD showed that the measured data line shows broad similarities to the predicted data pattern (Appendix A, Fig. 10). However, as with the other silver complexes, the somewhat amorphous nature of the samples prevents unambiguous matching.

3. Results and Discussion

3.1. Acyclovir (ACV) (Ligand)

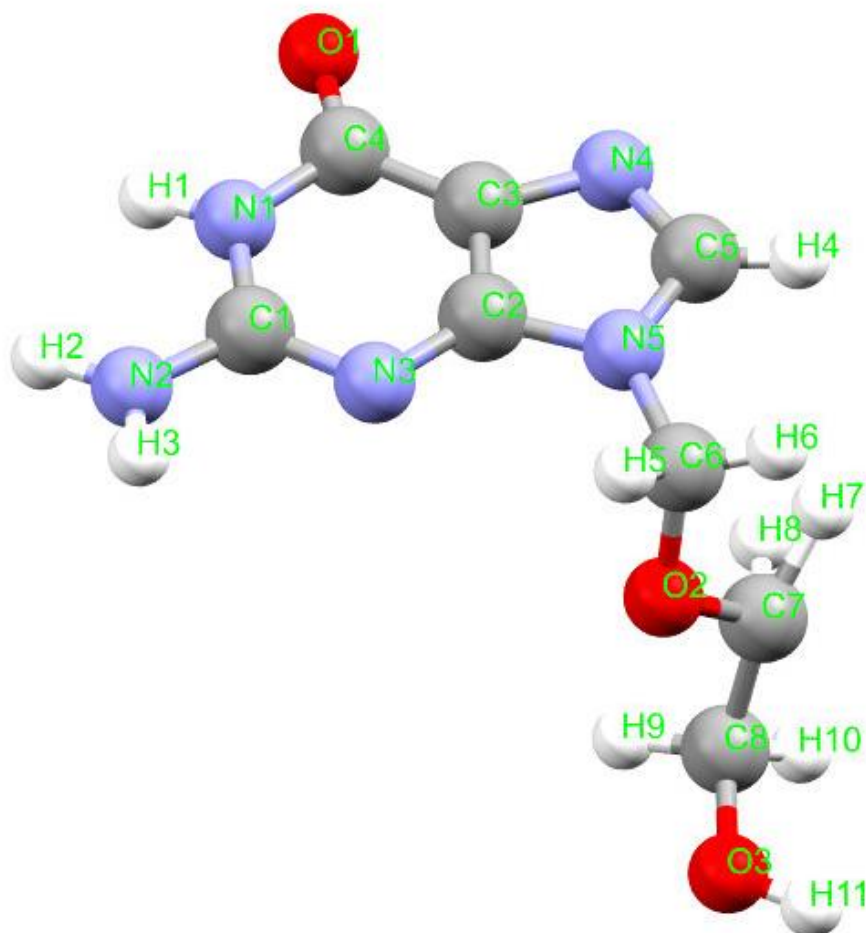


Figure 22 – labelled stick and ball model of acyclovir ligand.

Acyclovir has been used as a ligand in this study. It consists of a neutral, purine ring with an attached ethylene glycol tail, C6-O3 (to be further referred to as the *'tail'*) (Figure 22). The majority of the bonding with the metal occurs at the 5-membered ring at N4, with other examples bonding at O1 and N3 (Figure 23), [16].

3.1.1. Bonding

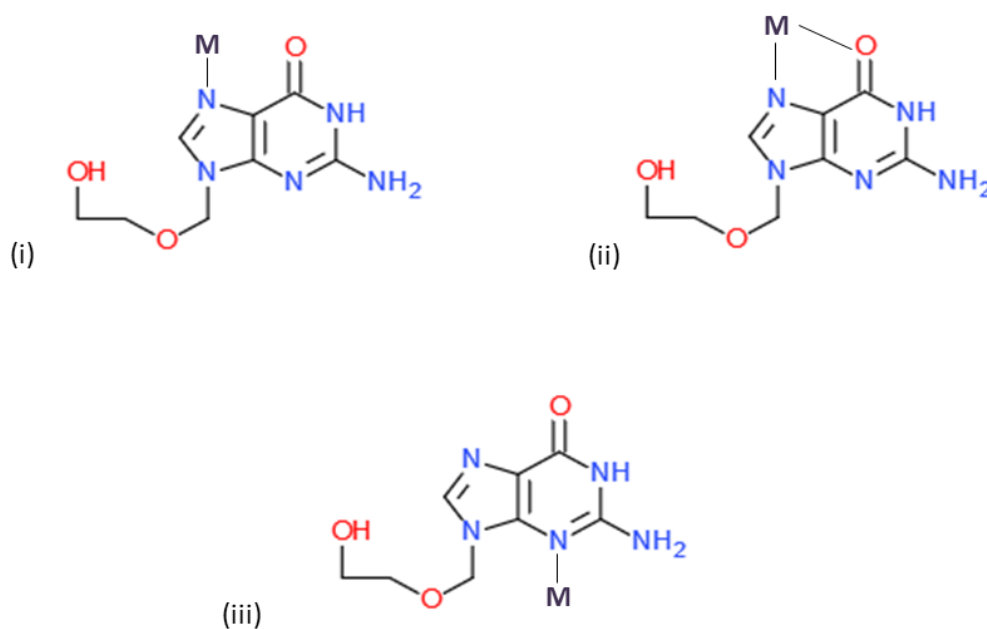


Figure 23 – Metal (M) bonding to N4 (i), N4 and O1 (ii), and N3 (iii) in metal-ACV complexes. Within this study, these are the three outcomes of the metal to ligand bonding.

The binding modes shown in Figure 23 were all observed in this work, in which the metal ion (M) corresponds to Cu^{2+} , Zn^{2+} or Ag^+ . In Figure 23(i), the metal ion is seen to bond with one of the nitrogen atoms of ACV in the 5 membered ring, N4. In Fig.23 (ii) and Fig. 23(iii), the metal bonds at other points of the acyclovir ligand whilst simultaneously bonding with N4. Examples of the N4 bonding have been seen in other research work. A study by Garcia-Raso et al. into the structural synthesis and characteristics of metal-acyclovir including Nickel, Zinc, and Cadmium, all of which bonded to the acyclovir ligand by N4, [16].

3.1.2. Packing

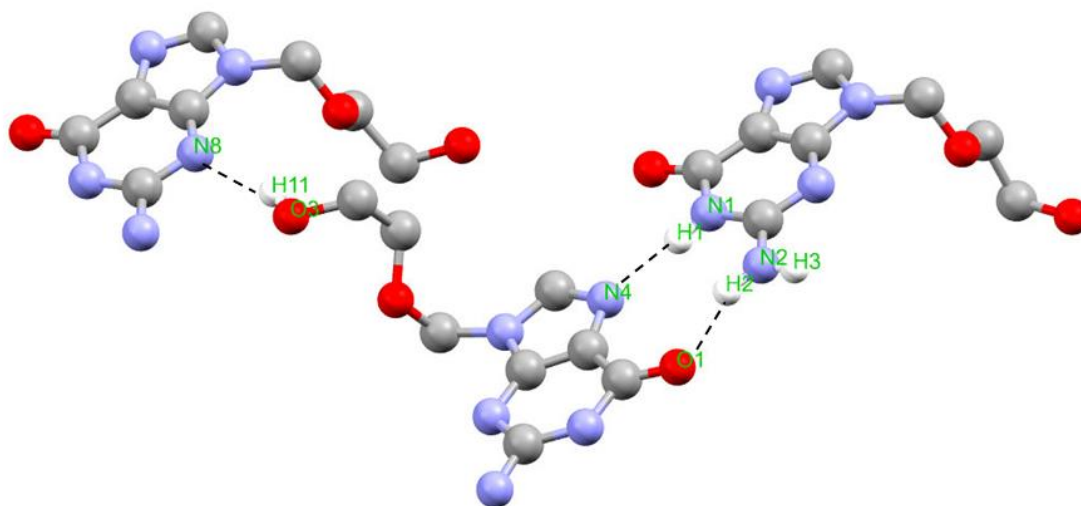


Figure 24 – sheets of acyclovir bonded together through N2-H...O1, N1- H...N4 and O3-H...N8 hydrogen bonds at the purine rings. Not all Hydrogen atoms are shown.

Acyclovir can form in sheets where the molecules assemble with tail up then tail down, alternating between up and down (Figure 24). The sheets are constructed from two hydrogen bonds; N2-H...O1 and N1-H...N4 allow acyclovir molecules to link into sheets. To facilitate stacking, the tails of ACV also form hydrogen bonds with other ACV molecules when forming the crystal through the O3-H...N8 bond.

3.1.3. Predicted Infrared Bands

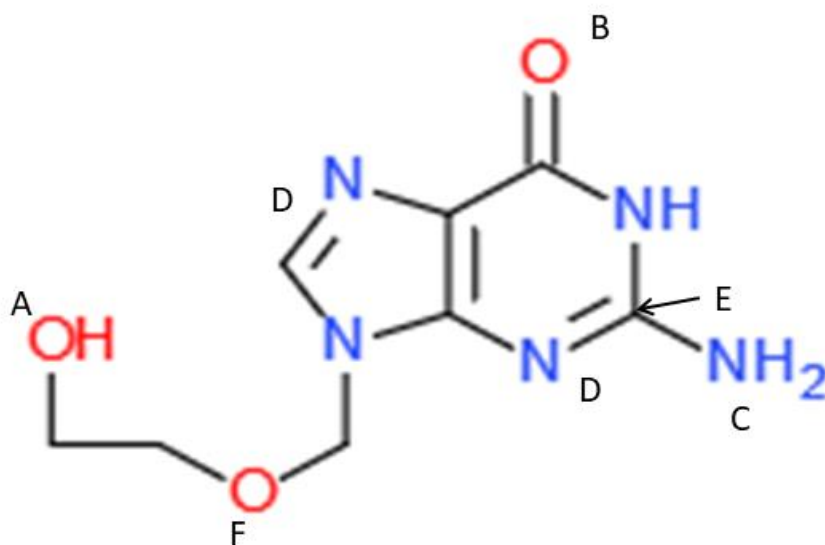


Figure 25 – Functional groups (A-F) that would give infrared absorption data of Acyclovir.

Functional groups A-F (Figure 25) were used when assigning infrared bands for all metal-ACV compounds or ACV. The (-OH)^(A) bond is expected to show a broad band between 3550-3200 cm⁻¹. The (C=O)^(B) in the aromatic ring would display a medium peak 1725-1695 cm⁻¹ which is hoped to be a diagnostic band for complex formation. The amine group, (NH₂)^(C), would show another broad peak, in the region of 3350-3310 cm⁻¹, that would be combined with the (-OH) band previously mentioned. The carbon nitrogen bonds, (C=N)^(D) and (C-N)^(E), would both have medium intensity peaks at 1690-1640 cm⁻¹ and 1350-1000 cm⁻¹ respectively. Finally, there would be another peak that would be attributed to the ether group in the tail of the acyclovir ligand (C-O-C)^(F) at 1150-1085 cm⁻¹.

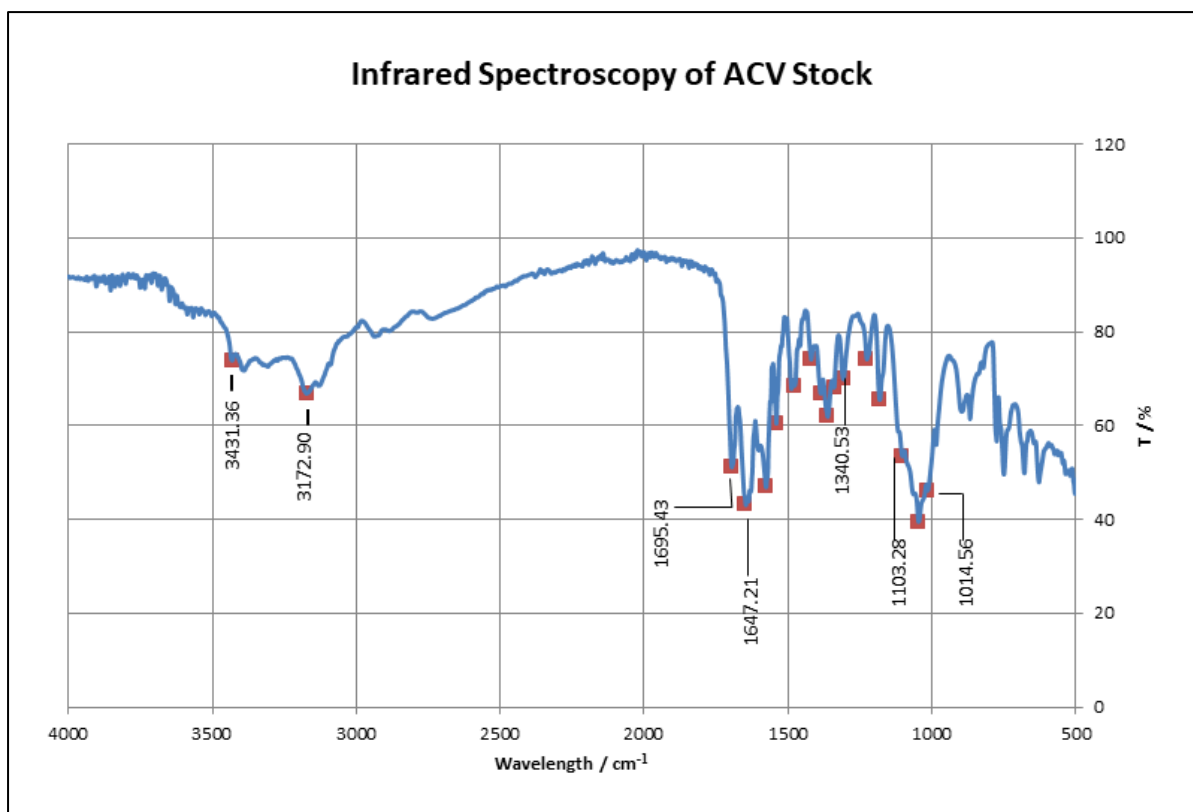


Figure 26 – the experimental IR Spectrum of ACV.

Figure 26 shows the observed infrared spectrum of ACV, taken on the same instrument as the other samples. The red blocks are all significant data points that incorporate data that falls within the ranges previously described. The data points that have specific Figures attached are to show the expected ranges for various functional groups.

3.2. Copper Complexes 1-5

3.2.1. 1 [Cu(ACV)₂(H₂O)₃]•2(BF₄)

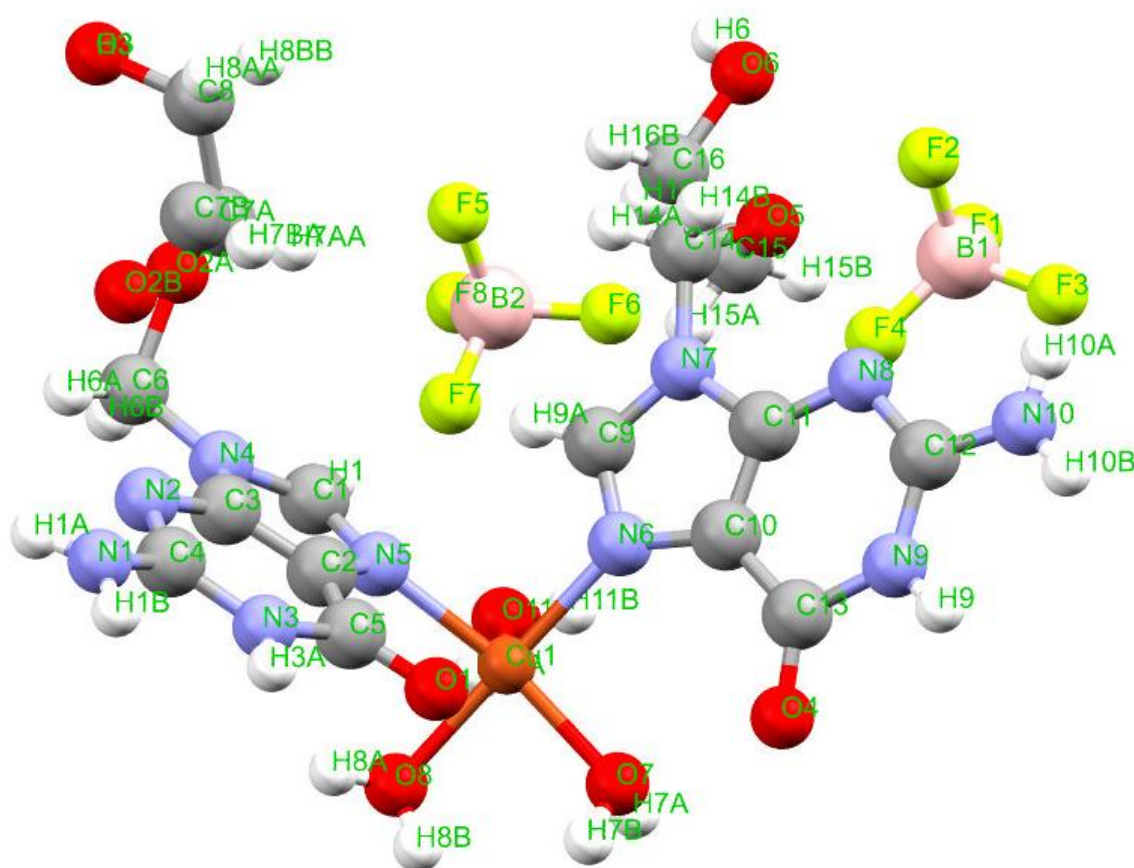


Figure 27 – crystal 1: [Cu(ACV)₂(H₂O)₃]•2(BF₄) labelled

The copper centre adopts the square pyramidal formation comprised of five coordinated ligands, three aqua ligands and two ACV ligands. The single copper centre is coordinated by oxygen atoms (O7, O8 and O11) (Figure 27) from three water molecules. The acyclovir ligands coordinate to the metal via the identical nitrogen location on the five membered ring (N5 and N6), the binding mode seen in Figure 23(i). All ligands attached to the copper ion, both the waters and the acyclovir ligands, are neutral in charge with the metal charge balanced by two tetrafluoroborate anions.

3.2.2. Bond Angles

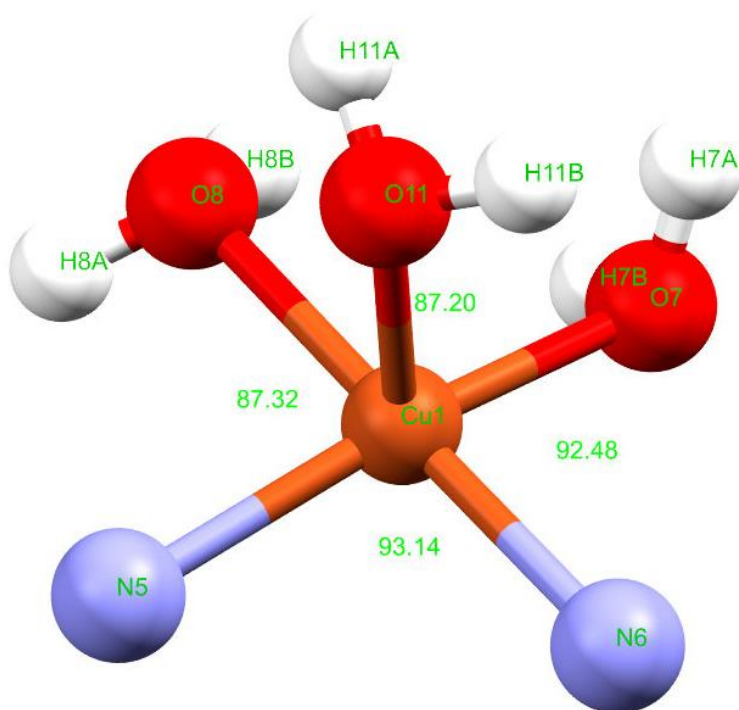


Figure 28 – The angles of the ligand-metal-ligand in the equatorial plane of $[\text{Cu}(\text{ACV})_2(\text{H}_2\text{O})_3] \cdot 2(\text{BF}_4)$.

The angles that the ligands form within the square base of the pyramid formation are shown in Figure 28: (N5-Cu1-N6) 93.14(1)°; (N6-Cu1-O7) 92.48(1)°; (O7-Cu1-O8) 87.20(9)°; (O8-Cu1-N5) 87.32(1)°. While square pyramidal should follow a $\leq 90^\circ$ pattern, these angles are only slightly distorted and are approaching the expected bond angles of a square pyramidal formation.

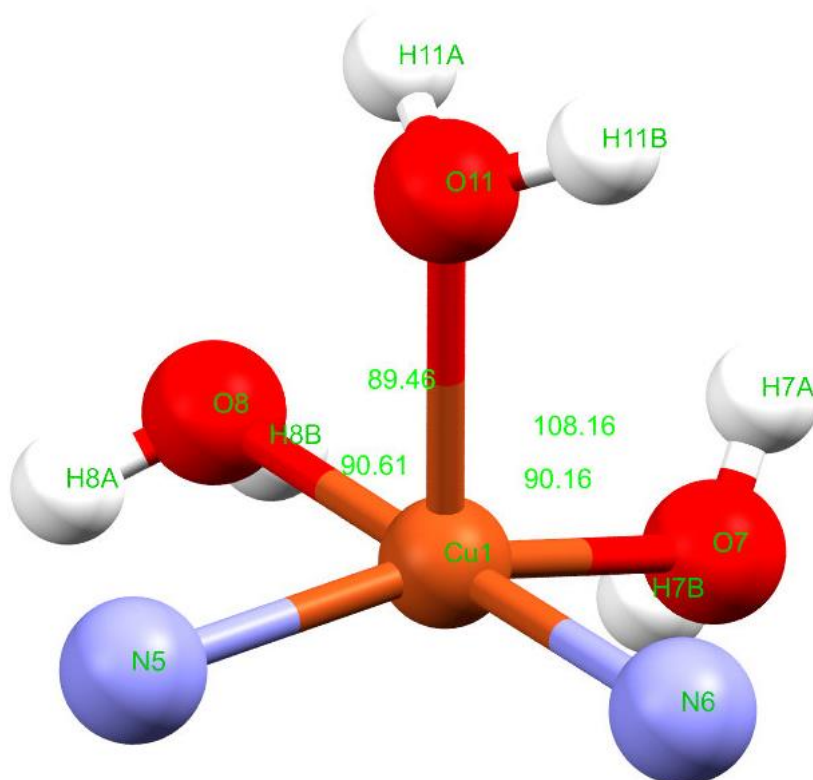


Figure 29 – bond angles from each of the equatorial atoms to O11 of $[\text{Cu}(\text{ACV})_2(\text{H}_2\text{O})_3] \cdot 2(\text{BF}_4)$.

The angles from all the atoms in the equatorial plane to the axial plane (O11) are as follows: (N5-Cu1-O11) $90.61(1)^\circ$, (N6-Cu1-O11) $90.16(1)^\circ$, (O7-Cu1-O11) $108.16(9)^\circ$ and (O8-Cu1-O11) $89.46(9)^\circ$ (Figure 29).

Angle (O8-Cu1-N5) was the smallest angle in the equatorial plane, possibly due to the steric repulsion of the two ACV ligands, or interaction with the water solvents or counter ion, BF_4^- . This interaction would have caused an effect on the spacing of the other coordinating ligands which is why the angles are not all 90° or nearer.

3.2.3. Bond Distances

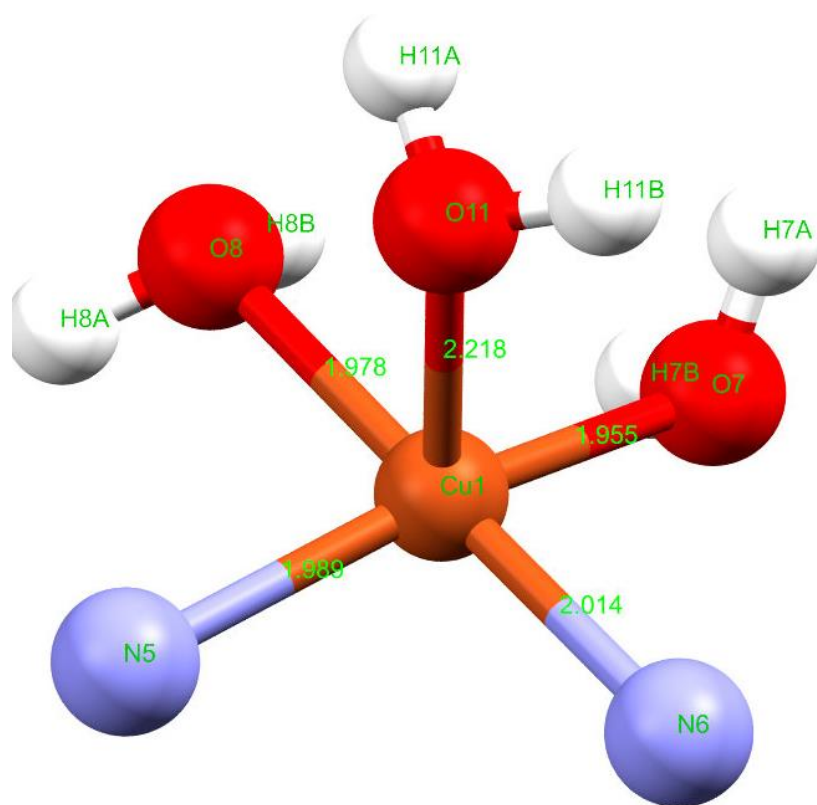


Figure 30 – the bond distances from the bonding ligand atoms and the metal centre of $[\text{Cu}(\text{ACV})_2(\text{H}_2\text{O})_3] \cdot 2(\text{BF}_4)$.

The lengths of the equatorial bonds: (Cu1-O8) 1.978(2) Å; (Cu1-O7) 1.955(2) Å; (Cu1-N6) 2.014(3) Å; and (Cu1-N5) 1.989(3) Å, were all shorter than the axial bond: (Cu1-O11) 2.218(3) Å (Figure 30).

From all of the images of crystal 1, it is possible to describe the complex as a cis model [20]. The square pyramidal formation has what can be described as a square planar around the middle of the complex, with two different ligand types: two acyclovir and two water molecules. Both the water molecules are located on the same side of the complex when viewed down the Z axis and both acyclovir ligands are cis to each other.

In addition to the cis model, the tails of the acyclovir ligands are oriented in different directions. The acyclovir with N30 atom travels through the medial plane whereas, the acyclovir with N13 atom travels through the vertical plane.

3.2.4. Unit Cell, Intermolecular and Intramolecular Bonding

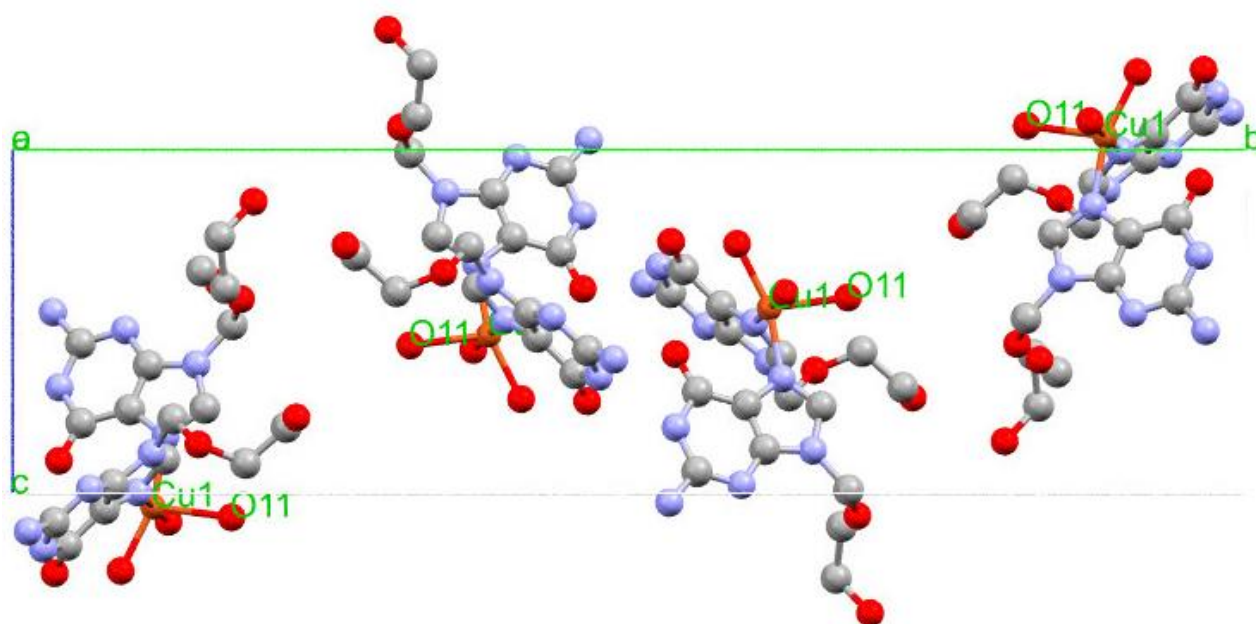


Figure 31- one cell unit of $[\text{Cu}(\text{ACV})_2(\text{H}_2\text{O})_3] \cdot 2(\text{BF}_4)$, viewed from the a plan.

The asymmetric unit fits only a quarter of the unit cell given its space group of $P2_1/n$ (monoclinic). The two single crystals in the centre of the axes have the O11 atom facing in opposite directions to each other, with one of the acyclovir tails facing up in the Y axis whilst the other tail faces down the Y axis (Figure 31). This would likely have happened in order to minimise the energy between each molecule and facilitate intermolecular interactions. However, the remaining two copper complexes to the left and right of the central complexes face into the centre, allowing each of their tails to fill voids that would otherwise be filled by solvent, or counter anions. The remaining voids are also filled by methanol or tetrafluoroborate anions.

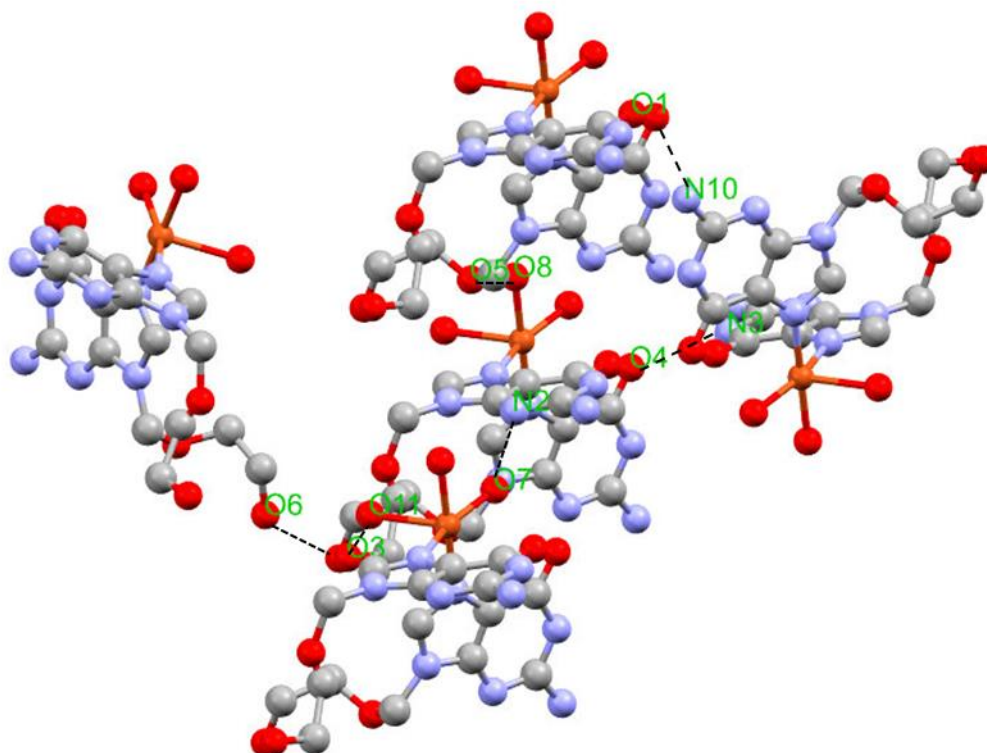


Figure 32 – Selected intermolecular forces in a crystal 1 packed crystal between N3-H...O4, N10-H...O1, O6-H...O3, O11-H...O3, O7-H...N2 and O8-H...O5 (Note: hydrogen atoms not displayed).

Intermolecular forces observed between Cu 1 components are hydrogen bonds, formed from nitrogen-oxygen or oxygen-oxygen donor/acceptor interactions (see Figure 32). There are six unique hydrogen bonding interactions that take place and their corresponding bond distances and angles are as follows: N3-H...O4 (2.845(3) Å), N10-H...O1 (3.059 Å), O6-H...O3 (2.783 Å), O11-H...O3 (2.704 Å), O7-H...N2 (2.798 Å) and O8-H...O5 (2.815 Å) (see Table 1). All of the hydrogen bond lengths fall within the moderate strength region of 2.5-3.2 Å [21], demonstrating that the hydrogen bonding within the crystal is a dominant solid-state stabilising force.

Intermolecular (Donor-Hydrogen...Acceptor)			Object 1	Object 2	Object 3	Angle / °
Object 1	Object 2	Length / Å	Object 1	Object 2	Object 3	Angle / °
N3	O4	2.845(3)	N3	H3A	O4	168.4(18)
H3A	O4	1.997(19)	N10	H10A	O1	160(2)
N10	O1	2.891(3)	O6	H6	O3	162.1(19)
H10A	O1	2.067(17)	O11	H11B	O3	152.6(17)
O6	O3	2.783(3)	O7	H7A	N2	124.6(19)
H6	O3	1.991(2)	O8	H8A	O5	143.3(17)
O11	O3	2.704(4)				
H11B	O3	1.889(3)				
O7	N2	2.798(3)				
H7A	N2	2.216(3)				
O8	O5	2.815(3)				
H8A	O5	2.078(2)				

Table 1 – all of the intermolecular hydrogen bond lengths from Donor to Acceptor, hydrogen to Acceptor and the Donor-Hydrogen...Acceptor angles from $[\text{Cu}(\text{ACV})_2(\text{H}_2\text{O})_3] \cdot 2(\text{BF}_4)$.

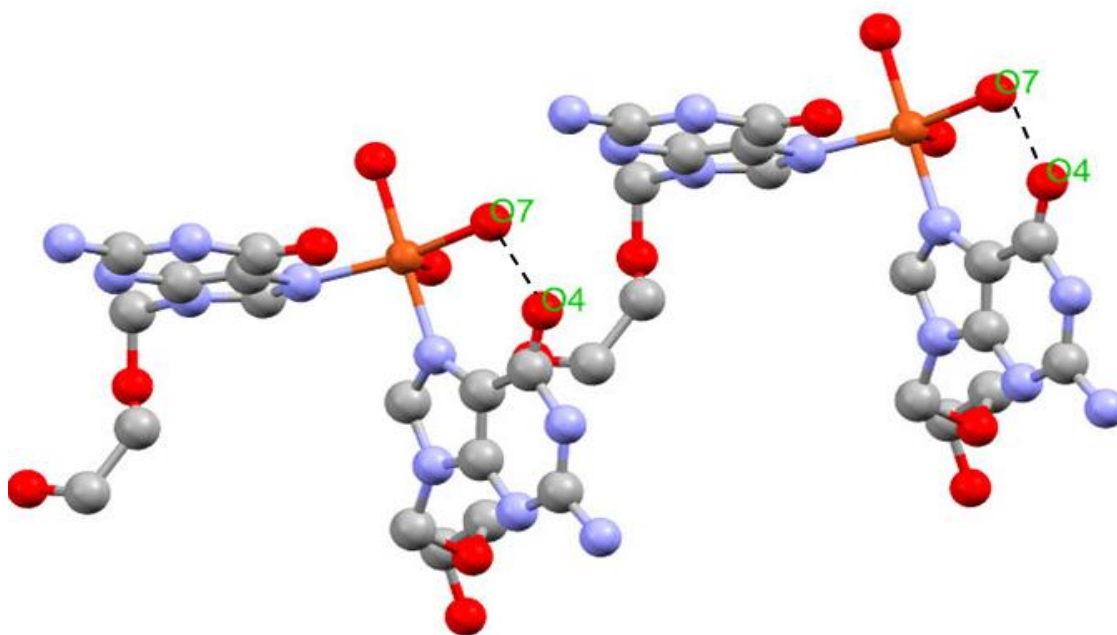


Figure 33 – intramolecular bonding in a single crystal molecular between O7-H...O4 (Note: hydrogen atoms not displayed.)

Within a molecule of Cu 1, there were intramolecular hydrogen bonds between O4-H...O7 (see Figure 33) with a bond length of 2.597 Å (see Table 1). This bond length represents a strong hydrogen bond. Given that hydrogen bonds require a proton acceptor and donor to be present, oxygen 4 in this scenario acts as the acceptor to oxygen 7's proton donor.

Intramolecular (Donor-Hydrogen...Acceptor)			Object 1	Object 2	Object 3	Angle / °
Object 1	Object 2	Length / Å	Object 1	Object 2	Object 3	Angle / °
O7	O4	2.597(3)	O7	H7A	O4	48.7(15)
H7A	O4	3.084(19)				

Table 2 – all of the intramolecular hydrogen bond lengths from Donor to Acceptor, hydrogen to Acceptor and the Donor-Hydrogen...Acceptor angle from $[\text{Cu}(\text{ACV})_2(\text{H}_2\text{O})_3] \cdot 2(\text{BF}_4)$.

3.2.5. Scanning Electron Microscope Data

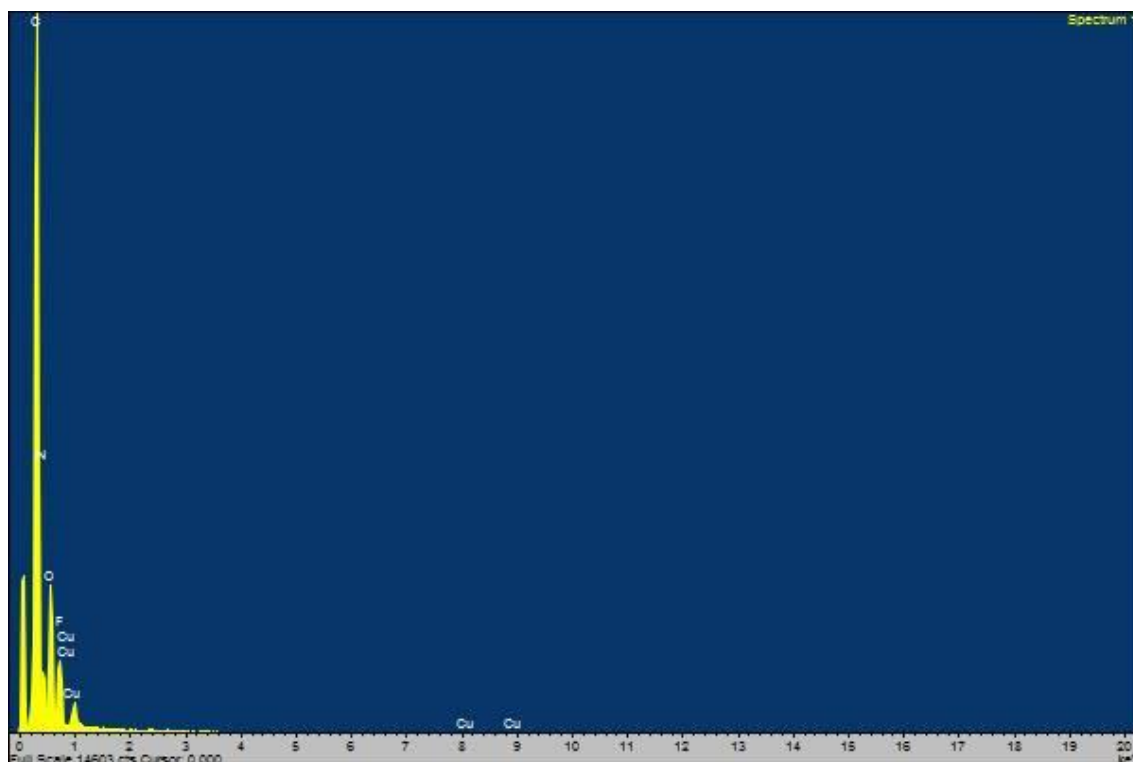


Figure 34 – SEM data from $[\text{Cu}(\text{ACV})_2(\text{H}_2\text{O})_3] \cdot 2(\text{BF}_4)$.

This SEM data (Figure 34) shows what elements the crystal 1 compound was composed of. It was observed that organic elements, such as carbon, nitrogen, oxygen and fluorine which make up the acyclovir ligands and the BF_4^- counter ion, were all present, in addition to copper which was the

metal centre of the compound. SEM instruments have a sensitivity limit which precludes the detection of boron or hydrogen in samples, thus explaining why they are not seen in the spectrum

3.2.6. 2 [Cu(ACV)₂(H₂O)₂(OH)₂] \cdot ACV + 2H₂O

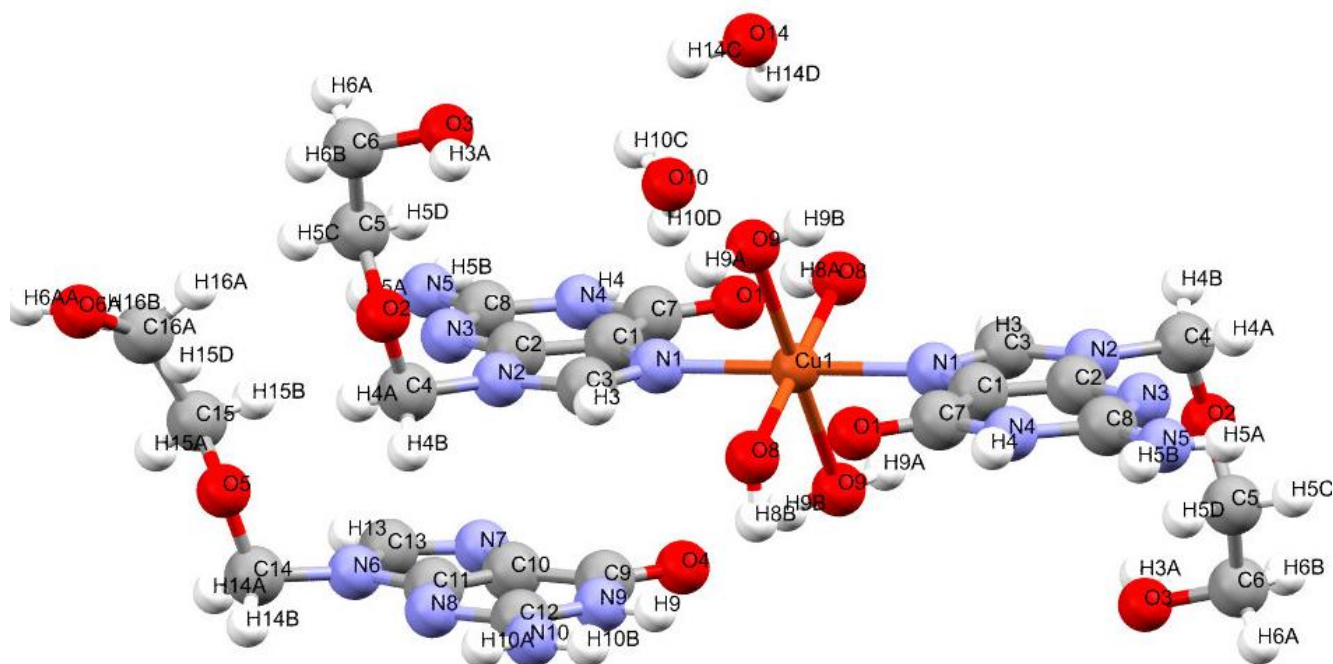


Figure 35 – Crystal 2: [Cu(ACV)₂(H₂O)₂(OH)₂] \cdot ACV + 2H₂O labelled.

This copper centred molecule adopts an octahedral structure with a space group of $P\bar{1}$ (triclinic). It has six total binding ligands, two aqua ligands, two hydroxyl ligands and two ACV ligands to the copper central atom. As demonstrated in Figure 23 (i), the metal is bonded to the ACV via N4 or N1 as it is seen in this crystal (Figure 35). There is also one non-bound ACV molecule in the crystal lattice that also appears in the asymmetric unit, as well as several water solvent molecules. There are no counter ions seen as the main molecule charge balanced by hydroxyl ligands and is thus overall neutral.

3.2.7. Bond Angles

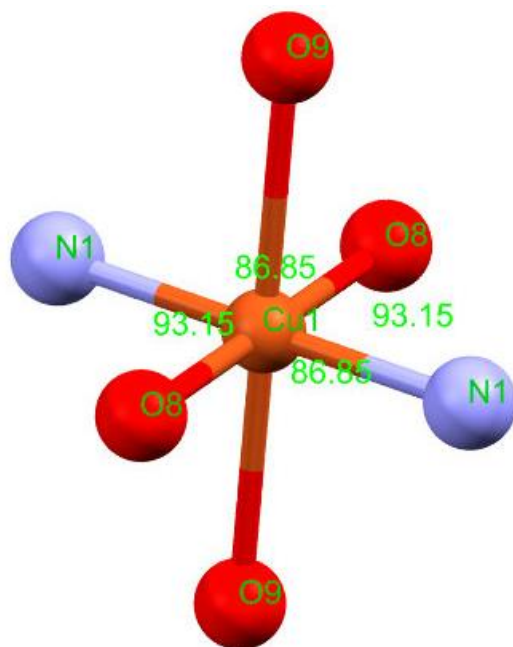


Figure 36 – angles of ligand-metal-ligand in the equatorial plane of $[\text{Cu}(\text{ACV})_2(\text{H}_2\text{O})_2(\text{OH})_2] \cdot \text{ACV} + 2\text{H}_2\text{O}$

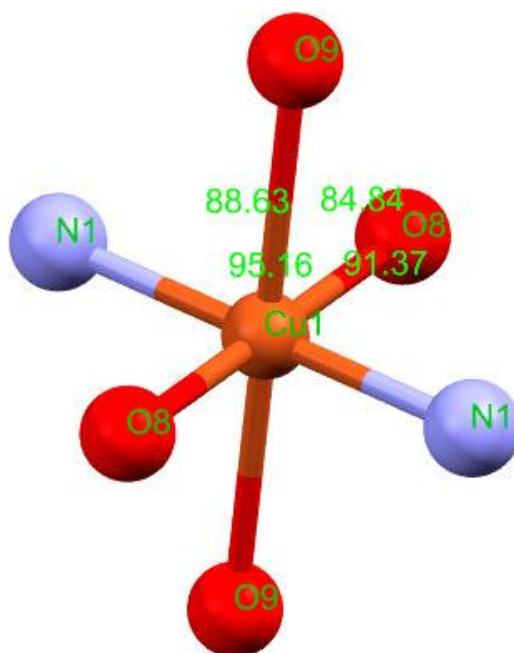


Figure 37 – angles from the equatorial atoms to the axial atoms of $[\text{Cu}(\text{ACV})_2(\text{H}_2\text{O})_2(\text{OH})_2] \cdot \text{ACV} + 2\text{H}_2\text{O}$.

As seen in Figure 36 and 37, the binding ligands of this octahedral complex are two hydroxyl ligands (O8) and two ACV ligands (N1) in the equatorial plane and two aqua ligands (O9) in the axial plane. In the equatorial plane this forms a square planar geometry and has the following angles: (O8-Cu1-N1) 86.85° and (N1-Cu1-O8) 93.15° ; each of these angles are seen twice as there are two hydroxyl and ACV ligands (Figure 36). As for the angles in the axial plane, each angle is different (Figure 37): (a) (O9-Cu1-N1) 88.63° , (b) (O9-Cu1-N1) 91.37° , (a) (O9-Cu1-O8) 84.84° , (b) (O9-Cu1-O8) 95.16° .

A 'perfect' octahedral complex should form 90° angles from each ligand to another. However, in the case of $[\text{Cu}(\text{ACV})_2(\text{H}_2\text{O})_2(\text{OH})_2]$ none of the angles are at an exact 90° which could be explained by any weak force inflicted by solvent molecules in the structure. Another explanation is steric competition between ligands. The water molecules are rather small, while the ACV are much larger in comparison, which may lead to the ligand angles differing from 90° .

3.2.8. Bond Distance

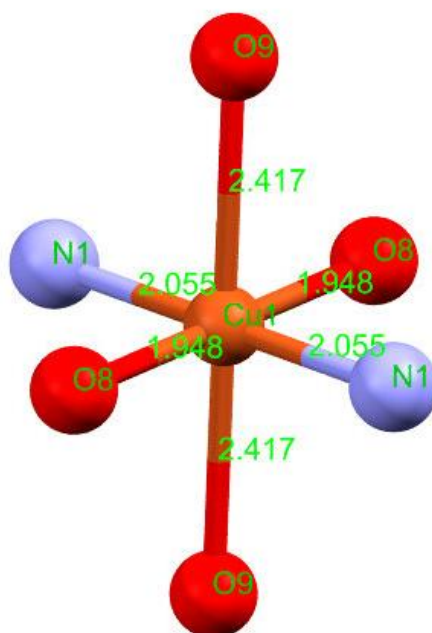


Figure 38 – bond distances from the central copper atom to each of the binding ligand atoms of $[\text{Cu}(\text{ACV})_2(\text{H}_2\text{O})_2(\text{OH})_2] \cdot \text{ACV} + 2\text{H}_2\text{O}$

The bond distances vary, especially the distances from the copper atom to those in the axial plane: (Cu1-O9) 2.417 Å, compared to those in the equatorial plane: (Cu1-O8) 1.948 Å, (Cu1-N1) 2.055 Å. This difference is explained by the Jahn-Teller distortion effect. Here, the molecular geometry changes to become less symmetrical to remove orbital degeneracy, thereby lowering the overall energy of the complex. The Jahn-Teller distortion causes the axial ligands to elongate and the equatorial ligands to contract to achieve this, lowering the energy and improving stability.

In addition, the smaller bond lengths (Cu1-O8) are the hydroxyl ligands as they are more electronegative than the aqua ligands, and are therefore more attracted to the copper centres than the aqua ligands.

Another factor to mention is that the ligands in the equatorial plane can be described as *trans*- as the same ligands are on opposite sides, facing each other [20]. In addition, the two ACV ligands have their tails in different directions which may also help to minimise energy.

3.2.9. Unit Cell, Intermolecular and Intramolecular Bonding

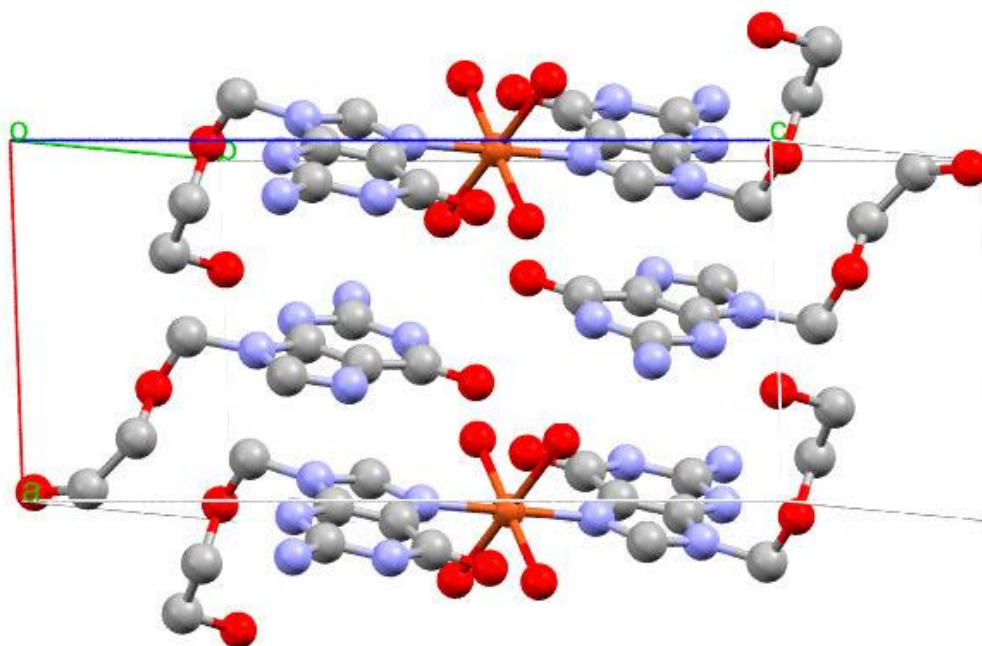


Figure 39 – a cell unit within a unit cell (axes shown) in the b^* plane view of $[\text{Cu}(\text{ACV})_2(\text{H}_2\text{O})_2(\text{OH})_2] \cdot \text{ACV} + 2\text{H}_2\text{O}$.

The asymmetric unit only fits half of the unit cell which is $P\bar{1}$ (triclinic). However, some of the molecules fall on the outside of the axes. Whilst the two non-bonded ACV molecules fit within, half of all the bonded ACV ligands are on the outside along with one equatorial bonded water molecule and one axial bonded water molecule. While the non-bonded ACV molecules fill some of the void within the unit cell, there are still voids that are filled by three ethanol molecules and two water molecules.

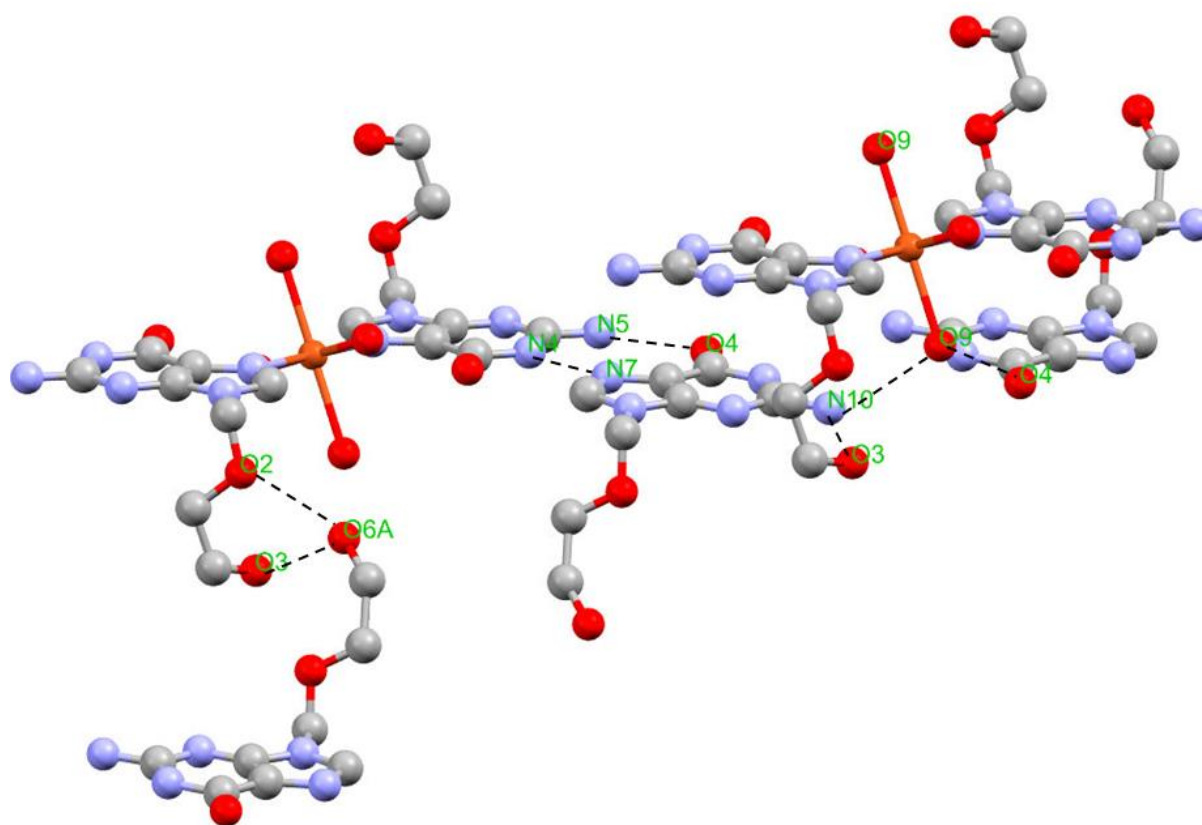


Figure 40 – the intermolecular hydrogen bonding shown: O9-H···O4, N10-H···O9, N10-H···O3, N5-H···O4, N4-H···N7, O6A-H···O2, and O3-H···O6A (Note: hydrogen atoms not displayed).

In a packed cell of crystal 2, there are seven unique intermolecular bonds with three types of hydrogen bonding: O-H···O, O-H···N, and N-H···N. The distances between each of these hydrogen bonds differed slightly: (O9-H···O4) 2.844 Å, (N10-H···O9) 3.009 Å, (N10-H···O3) 2.934 Å, (N5-H···O4) 2.997 Å, (N4-H···N7) 2.757 Å, (O6A-H···O2) 2.848 Å, (O3-H···O6A) 2.701 Å (see Table 3). All of these intermolecular bonds were in the range of 2.5-3.2 Å [21] which suggests that they are all moderate strength hydrogen bonds, and therefore, will have considerable influence on formation of these crystals.

Intermolecular(Donor-Hydrogen...Acceptor)			Object 1	Object 2	Object 3	Angle / °	
	Object 1	Object 2	Length / Å				
	O9	O4	2.844(7)	O9	H9B	O4	168.4(2)
	H9B	O4	1.869(5)	N10	H10B	O9	134.9(3)
	N10	O9	3.009(7)	N10	H10A	O3	173.9(4)
	H10B	O9	2.34(4)	N5	H5B	O4	159.9(5)
	N10	O3	2.934(9)	N4	H4	N7	167.9(6)
	H10A	O3	2.078(7)	O6A	H6AA	O2	48.5(11)
	N5	O4	2.997(5)	O3	H3A	O6A	155.8(9)
	H5B	O4	2.175(3)				
	N4	N7	2.757(6)				
	H4	N7	1.91(5)				
	O6A	O2	2.85(2)				
	H6AA	O2	3.325(5)				
	O3	O6A	2.70(2)				
	H3A	O6A	1.93(2)				

Table 3 - all of the intermolecular hydrogen bond lengths from Donor to Acceptor, hydrogen to Acceptor and the Donor-Hydrogen...Acceptor angles from $[\text{Cu}(\text{ACV})_2(\text{H}_2\text{O})_2(\text{OH})_2] \cdot \text{ACV} + 2\text{H}_2\text{O}$.

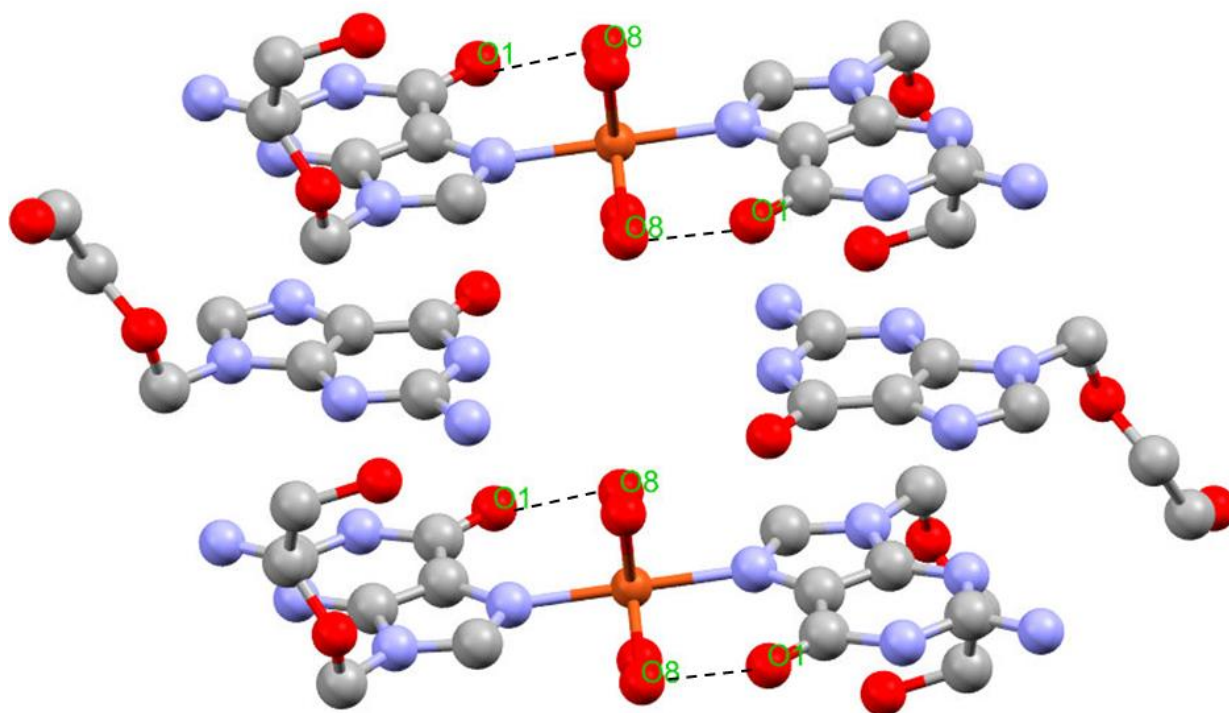


Figure 41 – the intramolecular bonds shown, O8-H...O1 (Note: hydrogen atoms not displayed).

Only one case of intramolecular hydrogen bonds occurred within the Cu 2 crystal, an O-H...O: (O8-H...O1) with a distance of 2.573 Å (see Table 4). At this distance the hydrogen bond is on the boundary of moderate strength, verging on strong, and is an intramolecular interaction meaning a

considerable amount of energy would be needed to break this bond. The intramolecular bond occurs in the equatorial plane between one ACV ligand and one hydroxyl ligand.

Intramolecular(Donor-Hydrogen...Acceptor)			Object 1	Object 2	Object 3	Angle / °
Object 1	Object 2	Length / Å	Object 1	Object 2	Object 3	Angle / °
O8	O1	2.573(6)	O8	H8A	O1	166.4(2)
H8A	O1	1.66(4)				

Table 4 – all of the intramolecular hydrogen bond lengths from Donor to Acceptor, hydrogen to Acceptor and the Donor-Hydrogen...Acceptor angle from $[\text{Cu}(\text{ACV})_2(\text{H}_2\text{O})_2(\text{OH})_2] \cdot \text{ACV} + 2\text{H}_2\text{O}$.

3.2.10. Scanning Electron Microscope Data

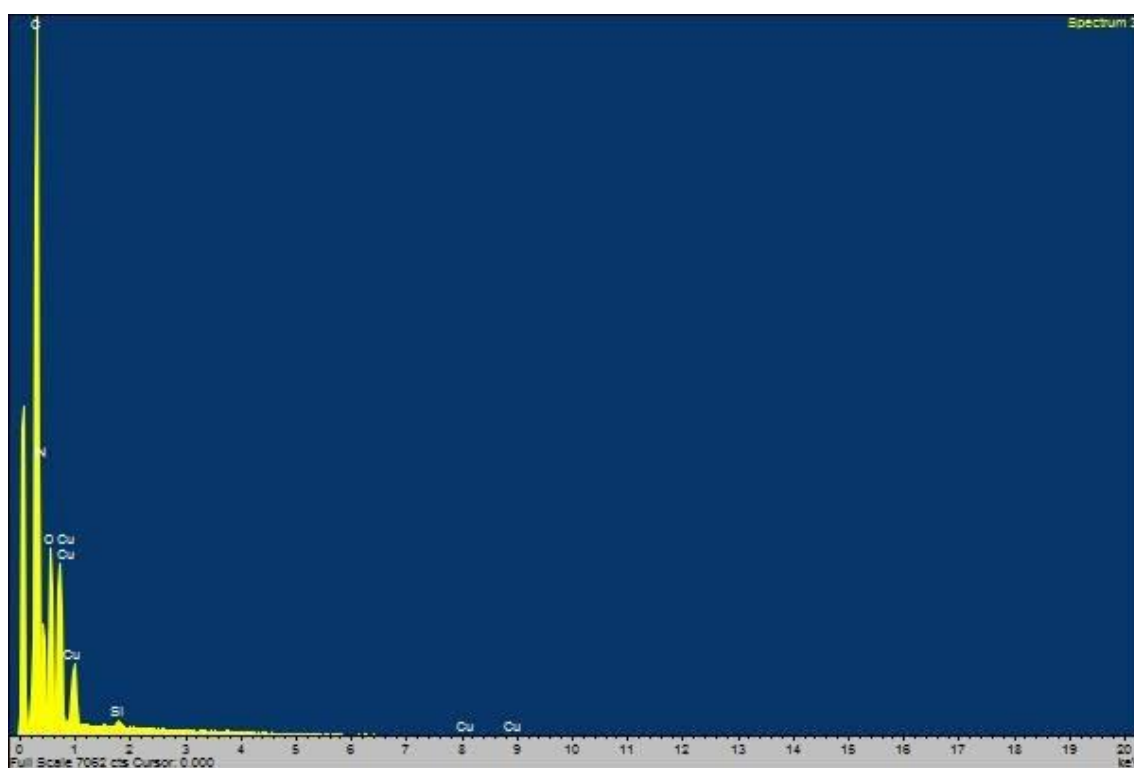


Figure 42 – SEM data of $[\text{Cu}(\text{ACV})_2(\text{H}_2\text{O})_2(\text{OH})_2] \cdot \text{ACV} + 2\text{H}_2\text{O}$

This SEM data (Figure 42) illustrates what elements make up the crystal 2 compound. Organic elements such as carbon, nitrogen and oxygen, which make up the acyclovir ligands, are present. However, there is no fluorine shown, which confirms the absence of BF_4^- counter ions. Copper was found, confirming the metal centre of the compound and silicon was also observed, which is likely derived from the platform the compound was analysed on.

3.2.11. 3 [Cu(ACV)₄H₂O]•2(BF₄)

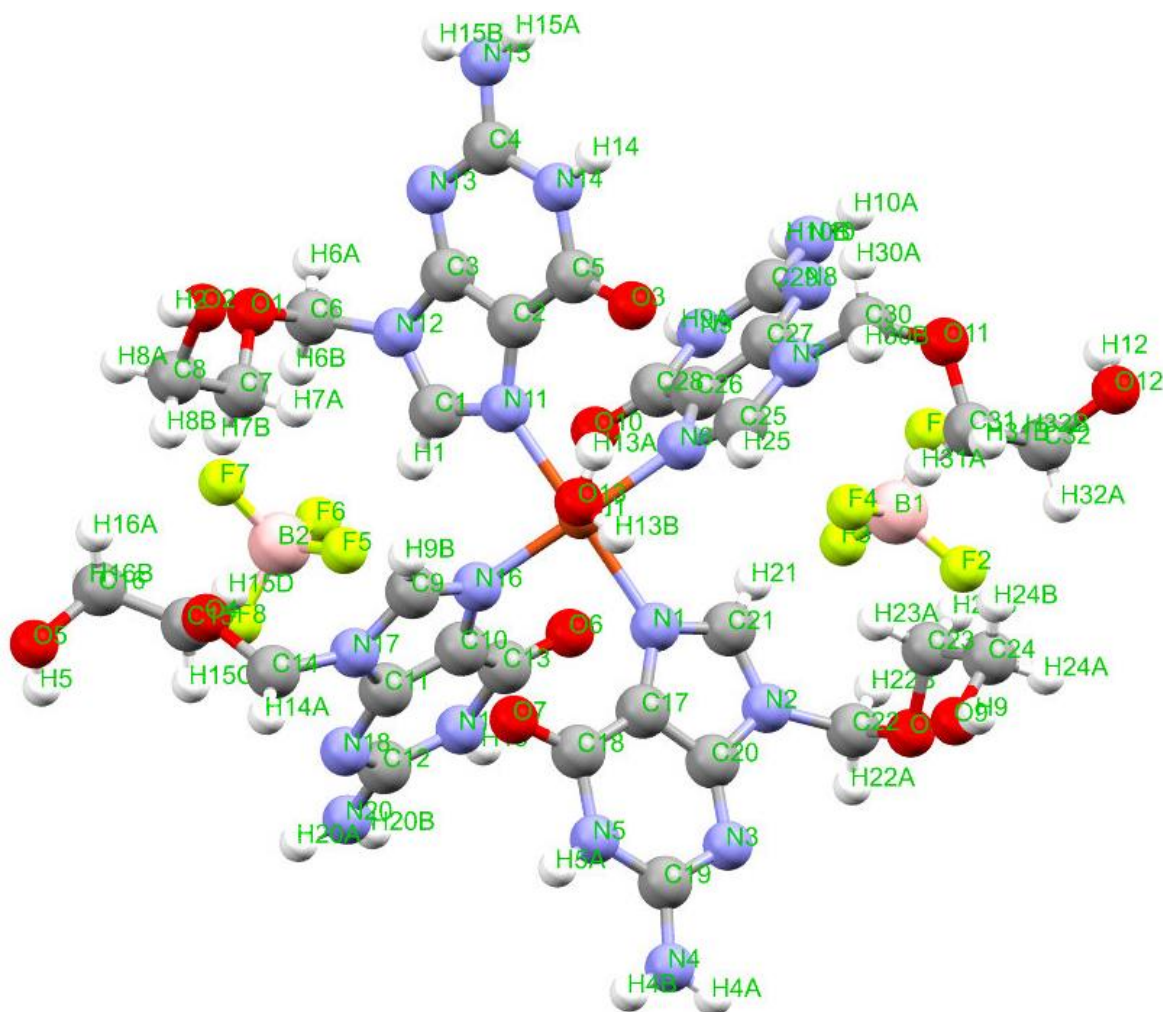


Figure 43 – Crystal 3: [Cu(ACV)₄H₂O]•2(BF₄) labelled

Crystal 3 shows a square pyramidal geometry with five total bonding ligands to the central metal which is copper (Cu²⁺). Four of the ligands are ACV molecules, each of which bond in the format seen in Figure 23(i) at N1, N6, N10, and N16, all in the equatorial plane. The remaining ligand is an aqua ligand which sits in the axial plane. Also observed in the single crystal is the tetrafluoroborate ions which, being anions, act as counter ions that balance the overall charge of the single crystal to a neutral charge. No solvent can be seen within the voids of the molecule and crystal structure, even though ethanol was found to be critical to the synthesis of this crystal.

3.2.12. Bond Angles

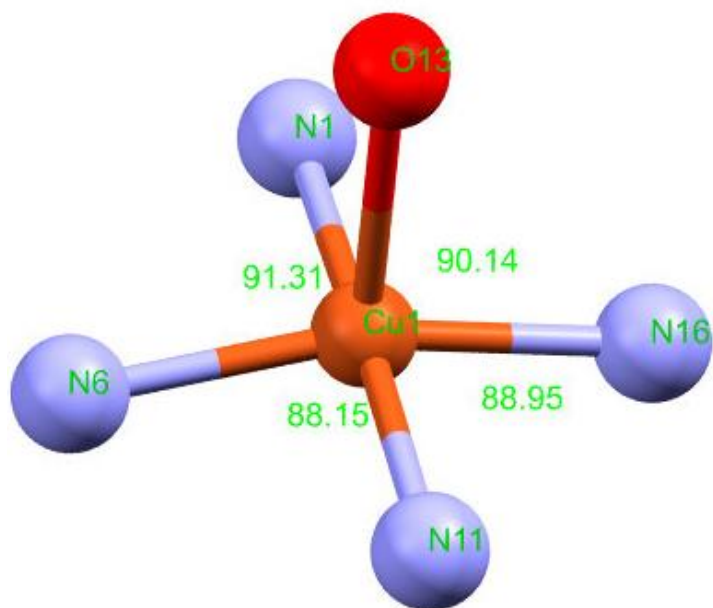


Figure 44 – [Cu(ACV)₄H₂O]•2(BF₄) bond angles in the equatorial plane, ligand-metal-ligand.

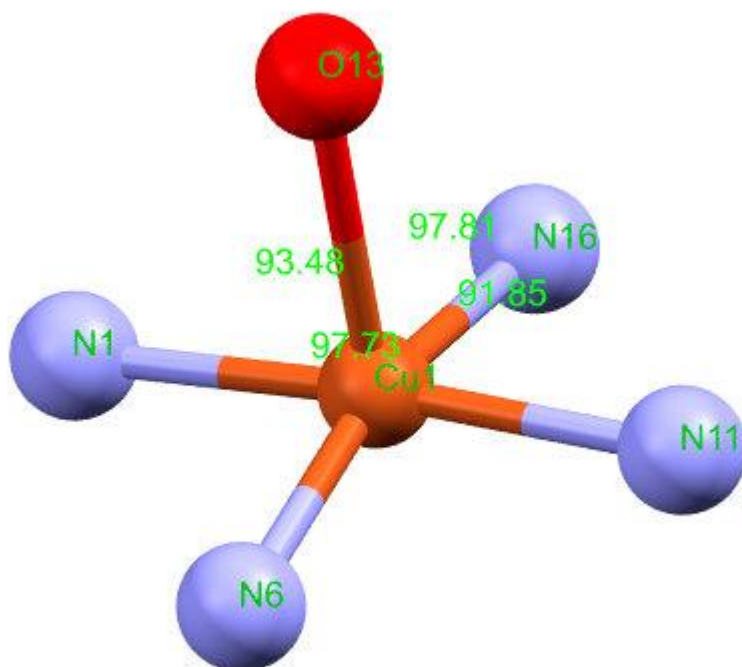


Figure 45 – bond angles of [Cu(ACV)₄H₂O]•2(BF₄) in the equatorial plane, ACV-metal-aqua.

For a square pyramidal-shaped compound, the angles between ligands should be $\leq 90^\circ$. However, the angles in crystal 3 do not equate to this (Figure 44): (N1-Cu1-N6) $91.3(1)^\circ$, (N6-Cu1-N11) $88.15(2)^\circ$, (N11-Cu1-N16) $88.95(1)^\circ$, and (N16-Cu1-N1) $90.14(1)^\circ$ in the equatorial plane. The axial plane also differs from the 'perfect' angle of $\leq 90^\circ$ (Figure 45): (N1-Cu1-O13) $93.48(9)^\circ$, (N6-Cu1-O13) $97.73(1)^\circ$, (N11-Cu1-O13) $91.85(9)^\circ$, and (N16-Cu1-O13) $97.81(9)^\circ$. The ACV ligands (not fully shown in Figures 44 and 45) have their tails orientated in different directions: N1 and N11 have their tails pointing up in the Z axis, while N6 and N16 have their tails pointing down in the Z axis.

The distortion in bond angles is explained by how the counter ions, two tetrafluoroborate (not shown in Figures 44 and 45), fill the voids. This influences the position of the ACV ligand, and therefore, the bond angle which isn't 'perfect'. In addition to this, the tail positions could also influence the final bond angles, as they find the best position to minimise repulsion of the counter anions and the other ligand tail.

3.2.13. Bond Distances

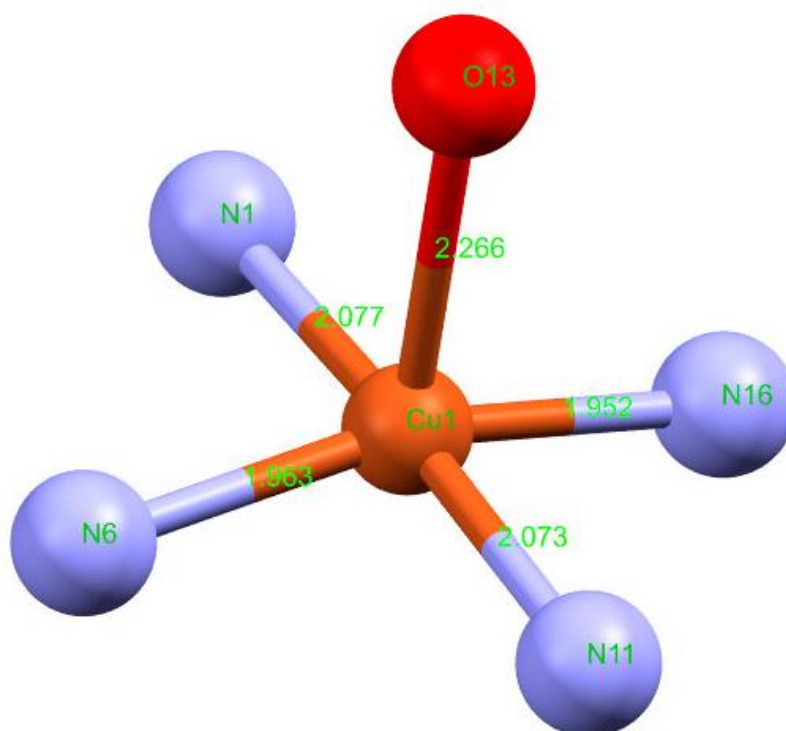


Figure 46 – the bond distances of the bonding ligands to the central metal atom of $[\text{Cu}(\text{ACV})_4\text{H}_2\text{O}] \cdot 2(\text{BF}_4)$.

All of the distances between the bonding ligand atoms and the metal centre differ, with some only by a small amount (Figure 46): (Cu1-N1) 2.077(2) Å, (Cu1-N6) 1.963(3) Å, (Cu1-N11) 2.073(2) Å, (Cu1-N16) 1.952(3) Å, and (Cu1-O13) 2.266(2) Å. The equatorial atoms are all roughly similar, with the exception of the Cu1-O13 distance, measuring the largest; more than ~ 0.200 Å longer than any of the others.

3.2.14. Unit Cell, Intermolecular and Intramolecular Bonding.

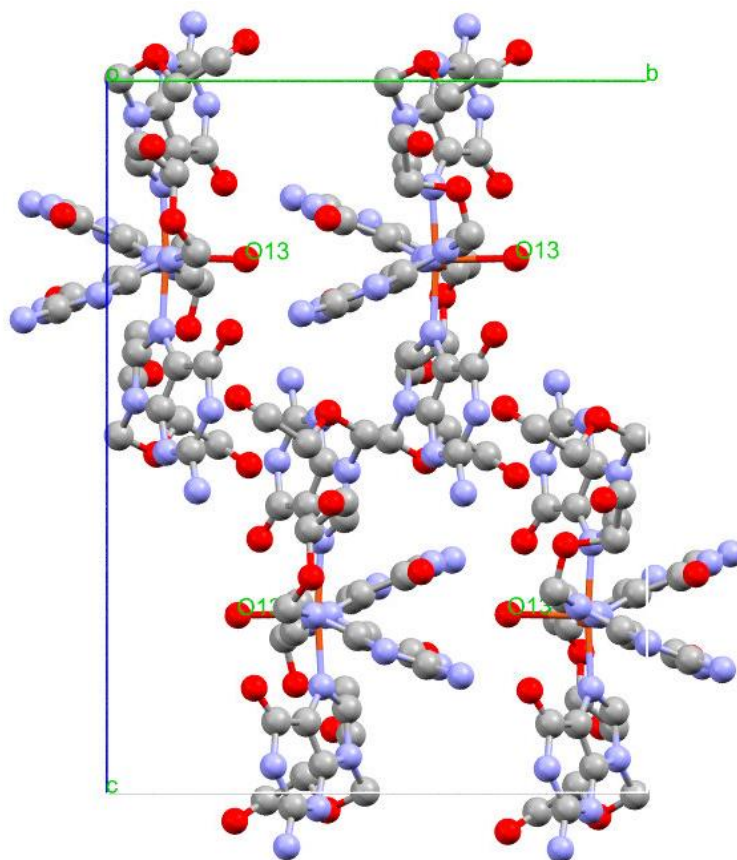


Figure 47 – a cell unit of a $[\text{Cu}(\text{ACV})_4\text{H}_2\text{O}] \cdot 2(\text{BF}_4)$ crystals viewed through the a axis (cell axes are shown).

The asymmetric unit of crystal 3 lies within a quarter of the unit cell which has a space group of $P2_1/n$ (monoclinic). The formation of this crystal is in a specific order, with each Cu 3 molecule stacking asymmetrically. In the example of Figure 47, the O13 on one molecule points left, then the O13 on the next molecule to its side points to the right. This pattern continues to form the wider crystal pattern.

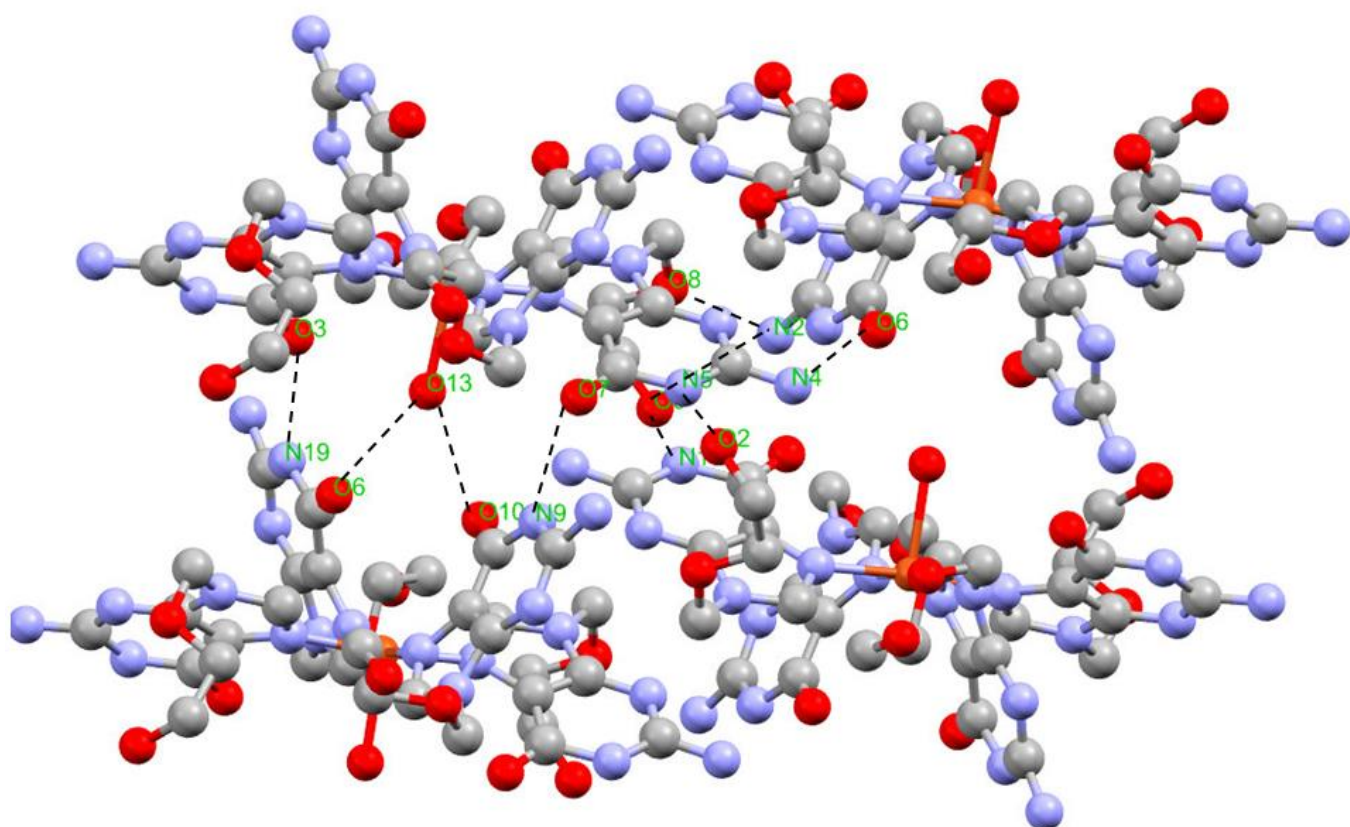


Figure 48 – intermolecular hydrogen bonding between N5-H \cdots O2, O13-H \cdots O10, O6-H \cdots N4, N19-H \cdots O3, N20-H \cdots O8, N20-H \cdots O9, N14-H \cdots O9, N9-H \cdots O7 and O13-H \cdots O6 (Note: hydrogen atoms not displayed).

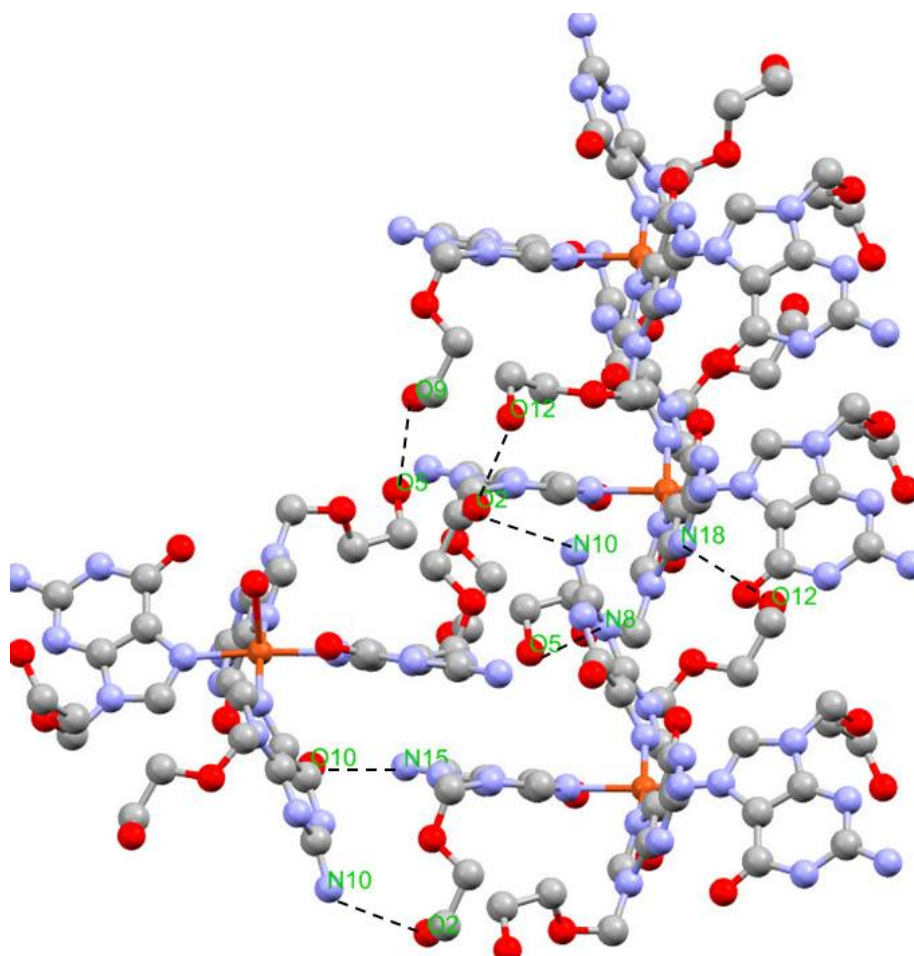


Figure 49 – intermolecular hydrogen bonds between N10-H...O2, O2-H...O12, O5-H...N8, O9-H...O5, N15-H...O10 and O12-H...N18 (Note: hydrogen atoms not displayed).

Within Cu 3 crystals there are fifteen unique intermolecular hydrogen bonds, displayed in both Figures 48 and 49. Each bond is either an O-H...O bond or an O-H...N bond, all with various bond distances: (N5-H...O2) 2.824 Å, (O13-H...O10) 2.852 Å, (N4-H...O6) 2.950 Å, (N19-H...O3) 2.796 Å, (N20-H...O8) 3.026 Å, (N20-H...O9) 3.008 Å, (N14-H...O9) 2.847 Å, (N9-H...O7) 2.730 Å, (O13-H...O6) 2.918 Å, (N10-H...O2) 3.014 Å, (O2-H...O12) 2.692 Å, (O5-H...N8) 2.877 Å, (O9-H...O5) 2.679 Å, (O10-H...N15) 3.033 Å, and (O12-H...N18) 2.942 Å (see Table 5). All these bonds are within the moderate bond strength for intermolecular hydrogen bonds (2.5-3.2 Å) [21] meaning they will have a considerable influence on formation of these crystals.

Intermolecular (Donor-Hydrogen...Acceptor)				Object 1	Object 2	Object 3	Angle / °
Object 1	Object 2	Length / Å		Object 1	Object 2	Object 3	Angle / °
N5	O2	2.824(4)		N5	H5A	O2	158.4(17)
H5A	O2	2.006(2)		O13	H13B	O10	107.4(17)
O13	O10	2.852(3)		N4	H4A	O6	163.9(2)
H13B	O10	2.48(2)		N19	H19	O3	161.3(19)
N4	O6	2.950(3)		N20	H20B	O8	84.1(17)
H4A	O6	2.114(2)		N20	H20B	O9	135.2(18)
N19	O3	2.796(3)		N14	H14	O9	154.7(17)
H19	O3	1.968(2)		N9	H9A	O7	171.2(18)
N20	O8	3.026(3)		O13	H13A	O6	123.7(16)
H20B	O8	2.991(17)		N10	H10B	O2	125.3(2)
N20	O9	3.008(3)		O2	H2	O12	161.6(19)
H20B	O9	2.336(2)		O5	H5	N8	177(4)
N14	O9	2.847(4)		O9	H9	O5	169.8(19)
H14	O9	2.046(2)		N15	H15B	O10	176(4)
N9	O7	2.730(3)		O12	H12	N18	167(5)
H9A	O7	1.877(2)					
O13	O6	2.918(3)					
H13A	O6	2.359(2)					
N10	O2	3.014(3)					
H10B	O2	2.433(2)					
O2	O12	2.692(3)					
H2	O12	1.901(2)					
O5	N8	2.877(4)					
H5	N8	2.10(5)					
O9	O5	2.679(3)					
H9	O5	1.868(2)					
N15	O10	3.033(3)					
H15B	O10	2.19(4)					
O12	N18	2.942(4)					
H12	N18	2.27(5)					

Table 5 – all of the intermolecular hydrogen bond lengths from Donor to Acceptor, hydrogen to Acceptor and the Donor-Hydrogen...Acceptor angles from $[\text{Cu}(\text{ACV})_4\text{H}_2\text{O}] \cdot 2(\text{BF}_4)$.

3.2.15. Scanning Electron Microscope Data

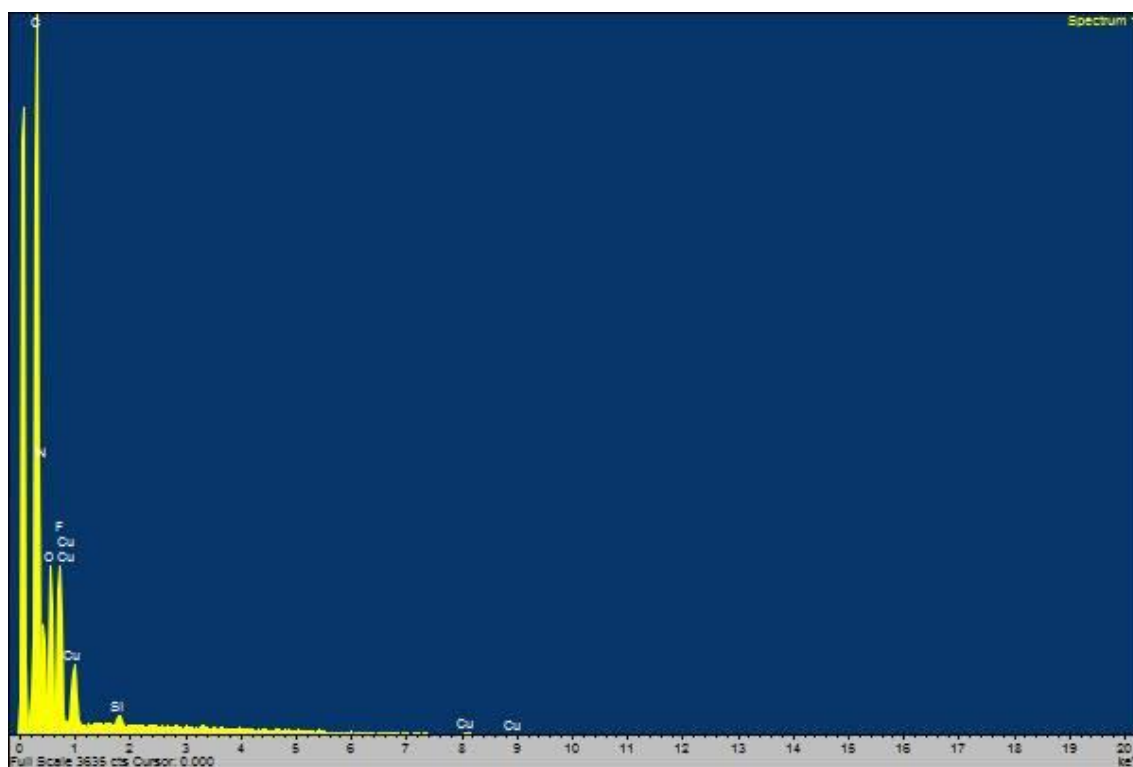


Figure 50 – SEM data of $[\text{Cu}(\text{ACV})_4\text{H}_2\text{O}] \cdot 2(\text{BF}_4)$

This SEM data (Figure 50) shows the elemental composition of the crystal 3 complex. It is observed that there are organic elements such as carbon, nitrogen, oxygen and fluorine, which made up the acyclovir ligands and the BF_4^- counter ion, as well as copper which was the metal centre of the compound. As stated earlier, lighter atoms hydrogen and boron are beyond the detection capabilities of the instrument. There is also silicon identified in this spectrum, which is found within the platform on which the compound was placed.

3.2.16. 4 [Cu(ACV)₂(H₂O)₂]•2BF₄

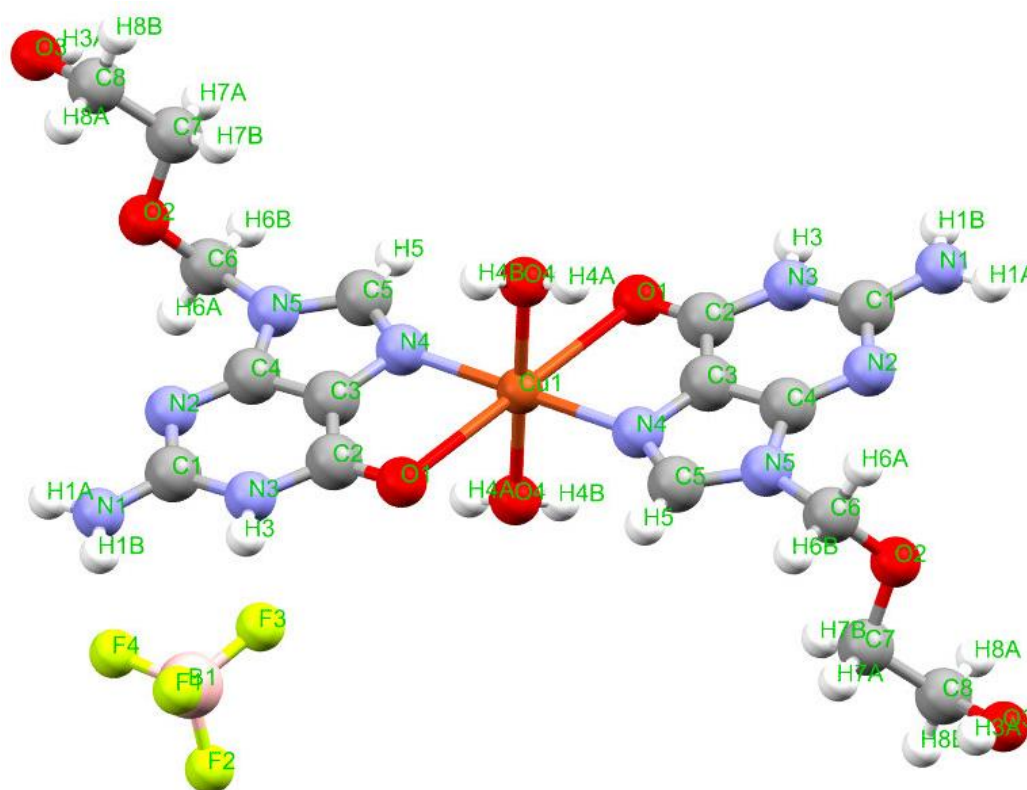


Figure 51 – Crystal 4: [Cu(ACV)₂(H₂O)₂]•2BF₄ labelled. Note: the symmetry-generated tetrafluoroborate anion is omitted.

This copper-centred crystal compound is a monoclinic molecule ($P2_1/n$) which has an octahedral structure. There are two types of ligands coordinated to the copper atom centre: two ACV ligands, with two unique bonding sites, and two aqua ligands. The ACV ligands are coordinated to the metal centre as seen in Figure 23(ii), taking the locations around the equatorial position at O1 and N4. The aqua ligands take both the axial positions above and below the copper centre via symmetry. Two tetrafluoroborate anions were identified which act as counter ions (one grown by symmetry), leading to an overall balanced compound.

3.2.17. Bond Angles

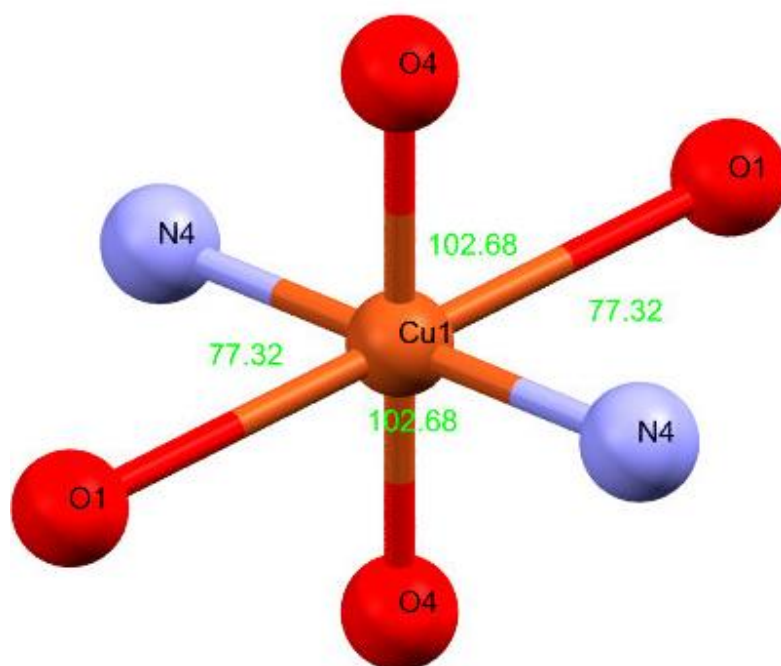


Figure 52 – bond angles between each of the atoms in the equatorial plane of $[\text{Cu}(\text{ACV})_2(\text{H}_2\text{O})_2] \cdot 2\text{BF}_4$

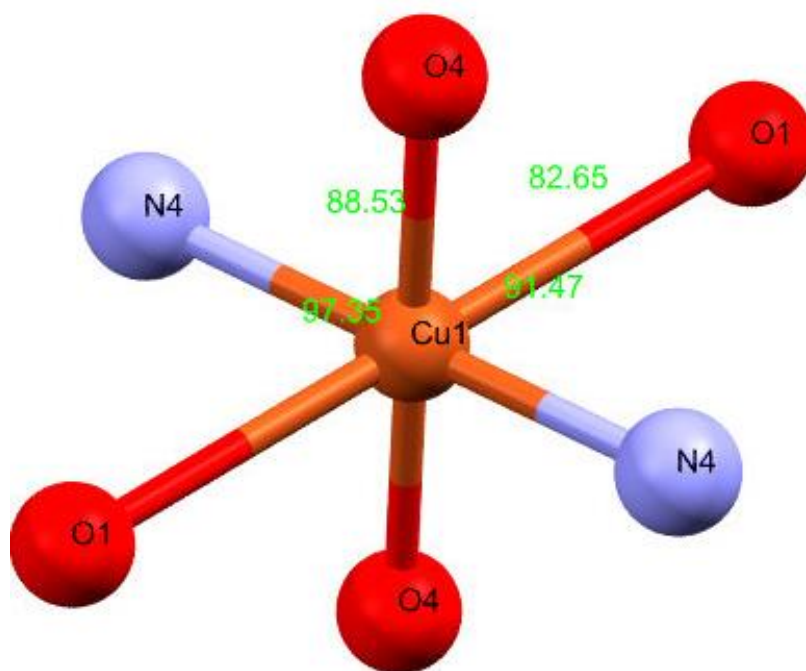


Figure 53– bond angles between the equatorial plane and the atom within the axial plane of $[\text{Cu}(\text{ACV})_2(\text{H}_2\text{O})_2] \cdot 2\text{BF}_4$.

There are four bonding atoms in the equatorial plane, however, two are symmetry-equivalent (Figure 52): two (N4-Cu1-O1) 102.68° and (O1-Cu1-N4) 77.32° . Each of the equatorial atoms have different angles with the atoms in the axial plane (Figure 53) (O1-Cu1-O4)a 82.65° , (O1-Cu1-O4)b 97.35° , (N4-Cu1-O4)a 91.47° , and (N4-Cu1-O4)b 88.53° . These angles in the axial plane are mirrored on the opposite side with the O4 atom seen below the equatorial atoms.

The angles do not correspond to the 'perfect' angles sizes of an octahedral structure which is 90° between each atom and the neighbouring atom. Some of these angles are close to the 90° angle, while others are far from it. This particular crystal is bound to two bidentate ligands in the equatorial plane, each ligand having two bonding sites. The rigid structure of the ligands would mean that some of the bonding atoms would have to compromise the 'perfect' angle of 90° in order to bond.

3.2.18. Bond Distance

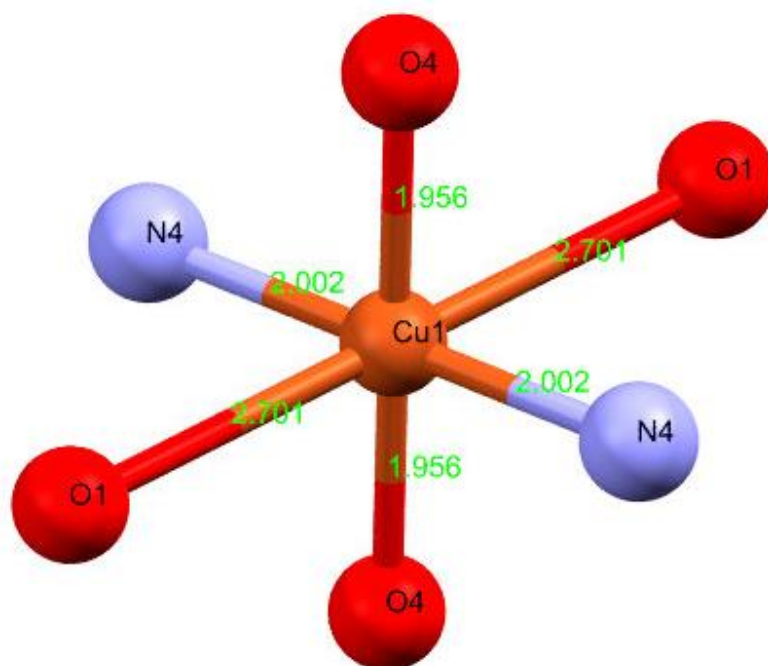


Figure 54 – bond lengths between the copper centre and the bonding atoms of $[\text{Cu}(\text{ACV})_2(\text{H}_2\text{O})_2] \cdot 2\text{BF}_4$

Though there are six bonding atoms from ligands to the metal centre, three are symmetry-equivalent pairs (Figure 54): (O1-Cu1) 2.701 Å, (N4-Cu1) 2.002 Å, and (O4-Cu1) 1.956 Å. The distances of (O4-Cu1) and (N4-Cu1) only differ by ~ 0.050 Å, however (O1-Cu1) was an outlier despite being part of the same ligand as N4.

Compounds with copper that have an octahedral geometry usually show a level of distortion caused by the Jahn-Teller effect. This crystal structure demonstrates this effect, wherein the bonding O1 from the chelating ACV ligand is elongated to 2.701 Å.

3.2.19. Unit Cell, Intermolecular and Intramolecular Bonding

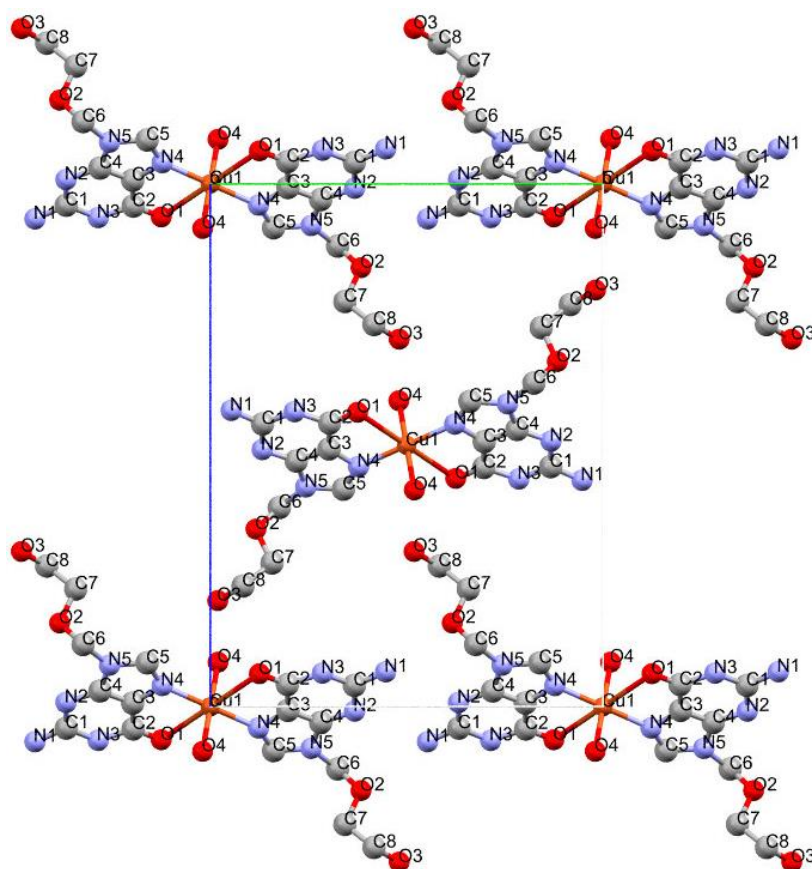


Figure 55 – packing of $[\text{Cu}(\text{ACV})_2(\text{H}_2\text{O})_2] \cdot 2\text{BF}_4$, as seen from view a. Note: hydrogen atoms not displayed.

Crystal 4's asymmetric unit fills only a quarter of the unit cell which has a space group of $P2_1/n$ (monoclinic). Two molecules of Cu 4 next to each other on either end of the axes with a central Cu 4 molecule stack to form a crystal structure (Figure 55). This is replicated in another identical layer underneath the initial layer.

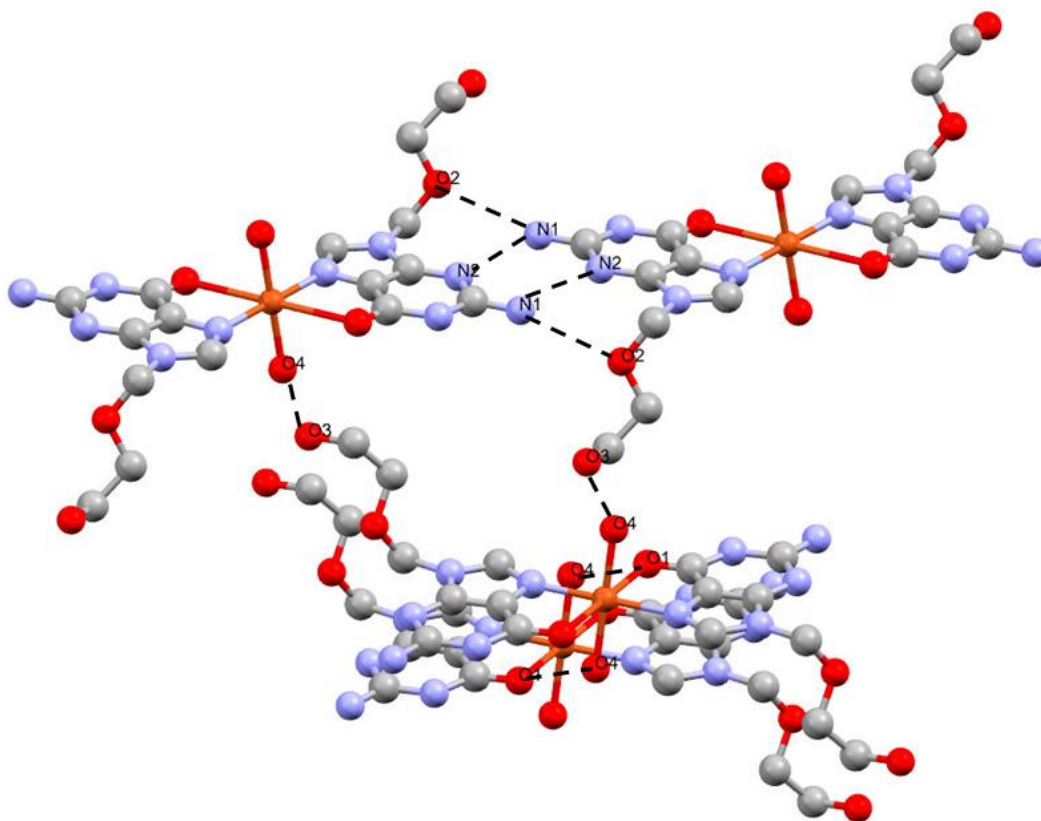


Figure 56 – the intermolecular hydrogen bonding between $[\text{Cu}(\text{ACV})_2(\text{H}_2\text{O})_2] \cdot 2\text{BF}_4$ molecules (Note: hydrogen atoms not displayed)

There are three different intermolecular hydrogen bond types: O-H \cdots O, O-H \cdots N, and N-H \cdots N. These are seen in four unique intermolecular bonds: (O4-H \cdots O1) 2.714 Å, (O3-H \cdots O4) 2.665 Å, (N1-H \cdots O2) 3.010 Å, and (N1-H \cdots N2) 3.048 Å (see Table 6).. All of these bonds fall into the moderate intermolecular hydrogen bond strength region of 2.5-3.2 Å, meaning that these bonds would have a significant impact in the development of the crystal and a moderate amount of energy would be required to break them.

Intermolecular (Donor-Hydrogen...Acceptor)			
Object 1	Object 2	Length / Å	Object 1 Object 2 Object 3 Angle / °
O4	O1	2.714(3)	O3 H3A O4 108.7(2)
H4A	O1	1.943(2)	O4 H4A O1 148.8(18)
O3	O4	2.665(4)	N1 H1A N2 175.2(2)
H3A	O4	2.287(2)	N1 H1B O2 102.8(2)
N1	O2	3.010(4)	
H1B	O2	2.701(2)	
N1	N2	3.048(4)	
H1A	N2	2.19(3)	

Table 6 – all of the intermolecular hydrogen bond lengths from Donor to Acceptor, hydrogen to Acceptor and the Donor-Hydrogen...Acceptor angles from $[\text{Cu}(\text{ACV})_2(\text{H}_2\text{O})_2] \cdot 2\text{BF}_4$.

There were no intramolecular bonds that were observed in crystal 4.

3.2.20. Scanning Electron Microscope Data

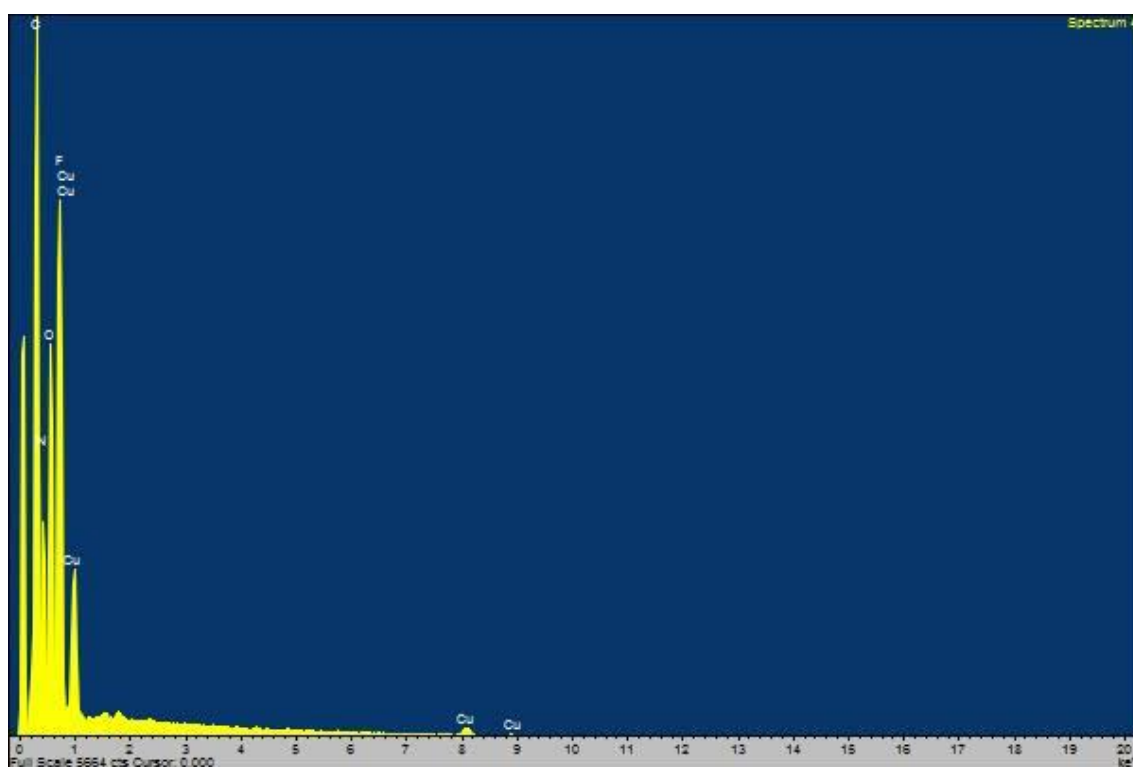


Figure 57 – a SEM spectrum of $[\text{Cu}(\text{ACV})_2(\text{H}_2\text{O})_2] \cdot 2\text{BF}_4$

This SEM data (Figure 57) indicates elements present in the crystal 4 compound. It is observed that there are organic elements such as carbon, nitrogen, oxygen and fluorine, which made up the

acyclovir ligands and the BF_4^- counter ion. Copper was also identified which was the metal centre of the compound.

3.2.21. 5 $[\text{Cu}(\text{ACV})_2(\text{BF}_4)_2] \cdot \text{ACV} + 2\text{H}_2\text{O}$

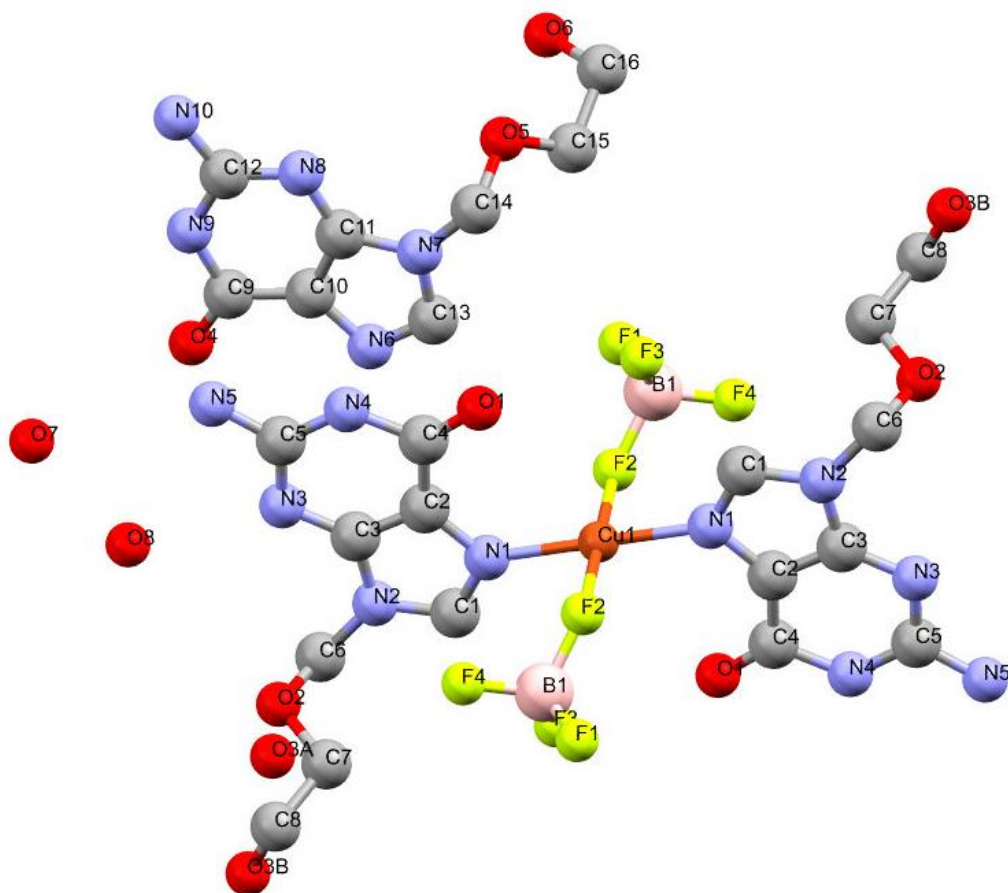


Figure 58 – Crystal 5: $[\text{Cu}(\text{ACV})_2(\text{BF}_4)_2] \cdot \text{ACV} + 2\text{H}_2\text{O}$ labelled. Note: hydrogen atoms not displayed.

Crystal 5 is a square planar structured molecule which is a triclinic space group ($P\bar{1}$) (Figure 58). It has a copper metal centre bound to four ligands, however, there are only two unique ligands: ACV and BF_4^- which are positioned in a *trans* formation with either side of the copper equator having one ACV ligand and one BF_4^- ligand. The ACV ligands bond to the copper centre in the same position as seen in Figure 23(i) bonding to N1. There is one spectating ACV molecule that is not attached in any way to the metal centre or the other ligands. The overall charge of the crystal 5 molecule is neutral as the two BF_4^- ions, which both bond to the Cu^{2+} , balance the charge.

3.2.22. Bond Angles

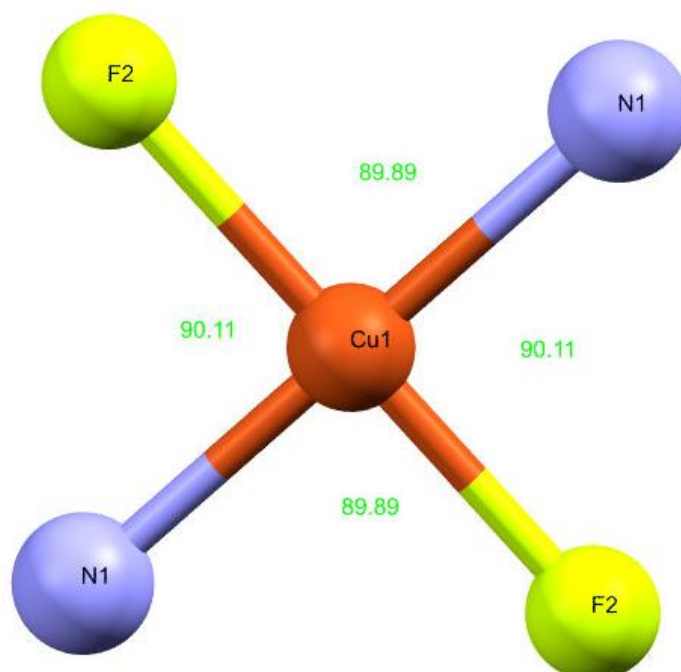


Figure 59 – bond angles between each of the bonding atoms in $[\text{Cu}(\text{ACV})_2(\text{BF}_4)_2] \cdot \text{ACV} + 2\text{H}_2\text{O}$.

Being square planar, there are only four angles in total, and via symmetry, there are only two unique angles (Figure 59): (N1-Cu1-F2) 90.11° and (F2-Cu1-N1) 89.89° . Square planar molecules should have a 90° angle between bonding atoms for the 'perfect' molecule structure. Whilst the angles are not exactly 90° they are only out by $\pm 0.11^\circ$ and are within error. The size of the ligands which bond to the metal centre would cause the slight difference, but there is no distortion occurring.

3.2.23. Bond Distances

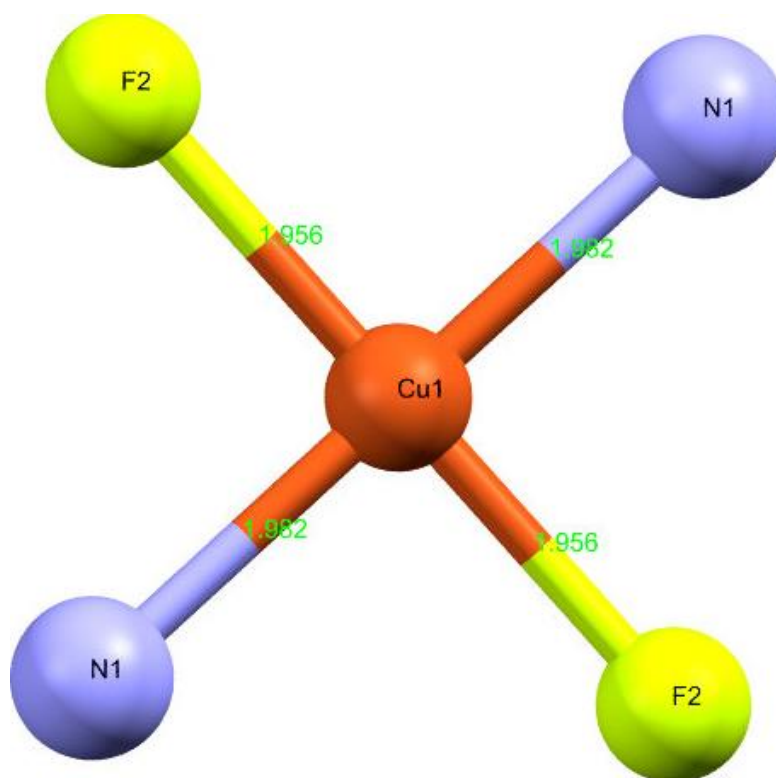


Figure 60 – bond distances from the copper centre to the bonding ligand atoms of the $[\text{Cu}(\text{ACV})_2(\text{BF}_4)_2] \cdot \text{ACV} + 2\text{H}_2\text{O}$

Although there are four bonding atoms to the metal centre, there are only two unique measurements (Figure 60): (Cu1-N1) 1.982 Å and (Cu1-F2) 1.956 Å. The similarities in these distances are very close thus demonstrating the highly-symmetrical nature of this structure. Even though the ligands alter the distances very slightly, crystal 5 can be likened to a ‘perfect’ square planar structure.

3.2.24. Unit Cell, Intermolecular and Intramolecular Bonding

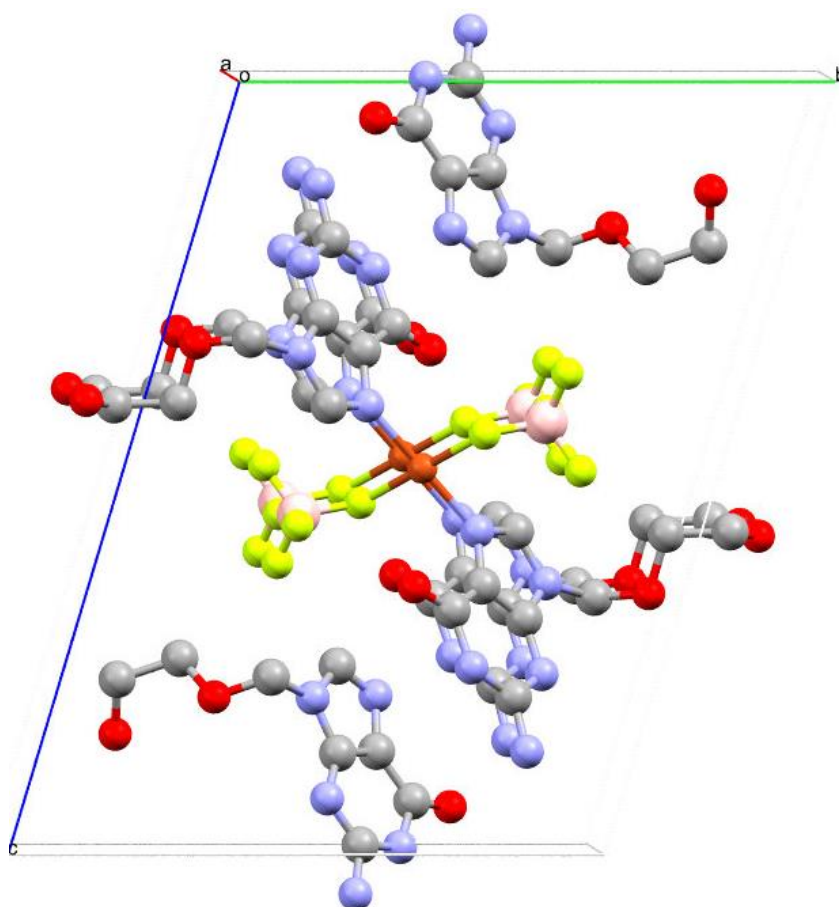


Figure 61 – a cell unit of $[\text{Cu}(\text{ACV})_2(\text{BF}_4)_2] \cdot \text{ACV} + 2\text{H}_2\text{O}$, viewed from the *a* plane. Note: hydrogen atoms not displayed.

The asymmetric unit is $P\bar{1}$ (triclinic). Some atoms from the bonding ACV and observing ACV grow outside of the cell unit axes (Figure 61), but largely fall within them. The crystal packing of crystal 5 is of one molecule layering another, with the secondary complex staggered off to one side. The spectating ACV sandwiches these stacked molecules.

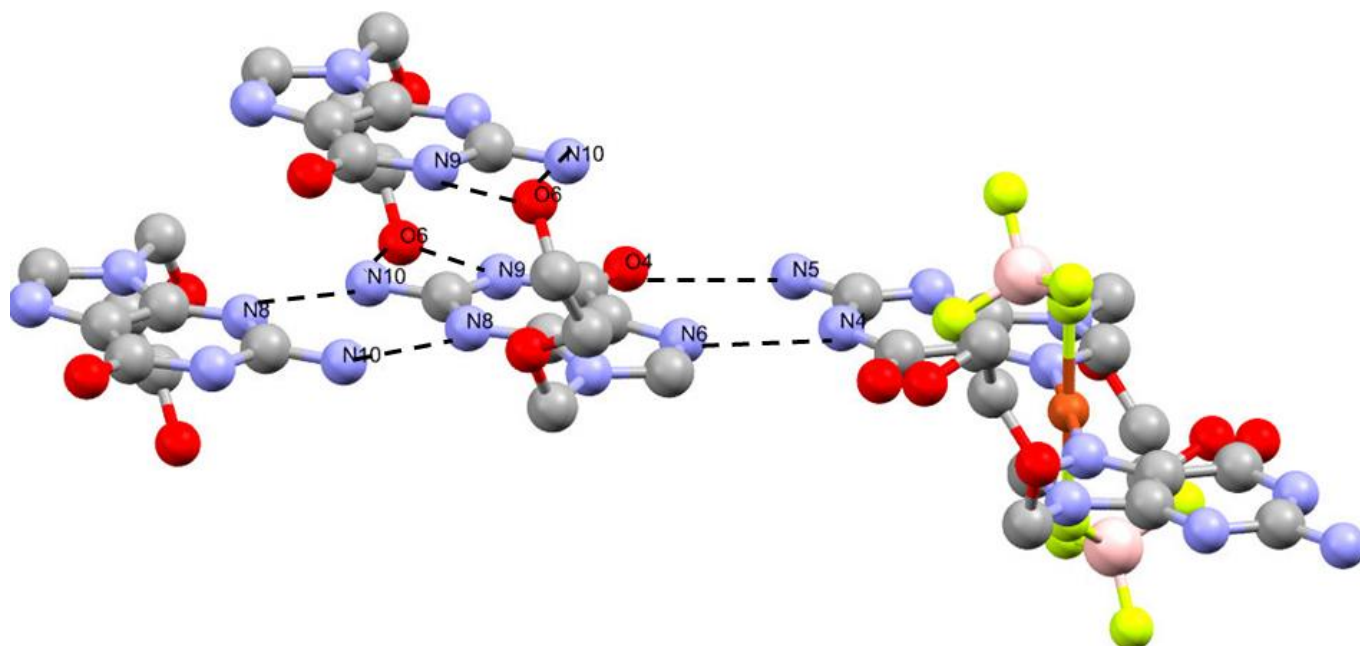


Figure 62 – intermolecular hydrogen bonds in $[\text{Cu}(\text{ACV})_2(\text{BF}_4)_2] \cdot \text{ACV} + 2\text{H}_2\text{O}$ are $\text{N4-H}\cdots\text{N6}$, $\text{N5-H}\cdots\text{O4}$, $\text{N10-H}\cdots\text{N8}$, $\text{N10-H}\cdots\text{O6}$, and $\text{O6-H}\cdots\text{N9}$. (Note: hydrogen atoms not displayed).

There are five unique intermolecular hydrogen bonds consisting of $\text{N-H}\cdots\text{N}$ and $\text{O-H}\cdots\text{N}$ (Figure 62): ($\text{N4-H}\cdots\text{N6}$) 2.850 Å, ($\text{N5-H}\cdots\text{O4}$) 2.825 Å, ($\text{N10-H}\cdots\text{N8}$) 2.983 Å, ($\text{N10-H}\cdots\text{O6}$) 3.018 Å, and ($\text{O6-H}\cdots\text{N9}$) 2.787 Å (see Table 7). All of these hydrogen bonds fall into the moderate region of hydrogen bond strength, between 2.5-3.2 Å, which means that these bonds are significant in the forming of this crystal; a moderate amount of energy would be needed to break them.

Intermolecular (Donor-Hydrogen...Acceptor)			Object 1	Object 2	Object 3	Angle / °
Object 1	Object 2	Length / Å	Object 1	Object 2	Object 3	Angle / °
N4	N6	2.850(4)	N4	H4	N6	172.6(16)
H4	N6	1.995(3)	N5	H5B	O4	156.4(17)
N5	O4	2.825(4)	N10	H10A	N8	160.4(3)
H5B	O4	2.015(3)	N10	H10B	O6	143(4)
N10	N8	2.983(4)	O6	H6	N9	47.9(2)
H10A	N8	2.155(3)				
N10	O6	3.018(5)				
H10B	O6	2.39(5)				
O6	N9	2.787(4)				
H6	N9	3.269(2)				

Table 7 – all of the intermolecular hydrogen bond lengths from Donor to Acceptor, hydrogen to Acceptor and the Donor-Hydrogen...Acceptor angles from $[\text{Cu}(\text{ACV})_2(\text{BF}_4)_2] \cdot \text{ACV} + 2\text{H}_2\text{O}$

3.2.25. Scanning Electron Microscope Data

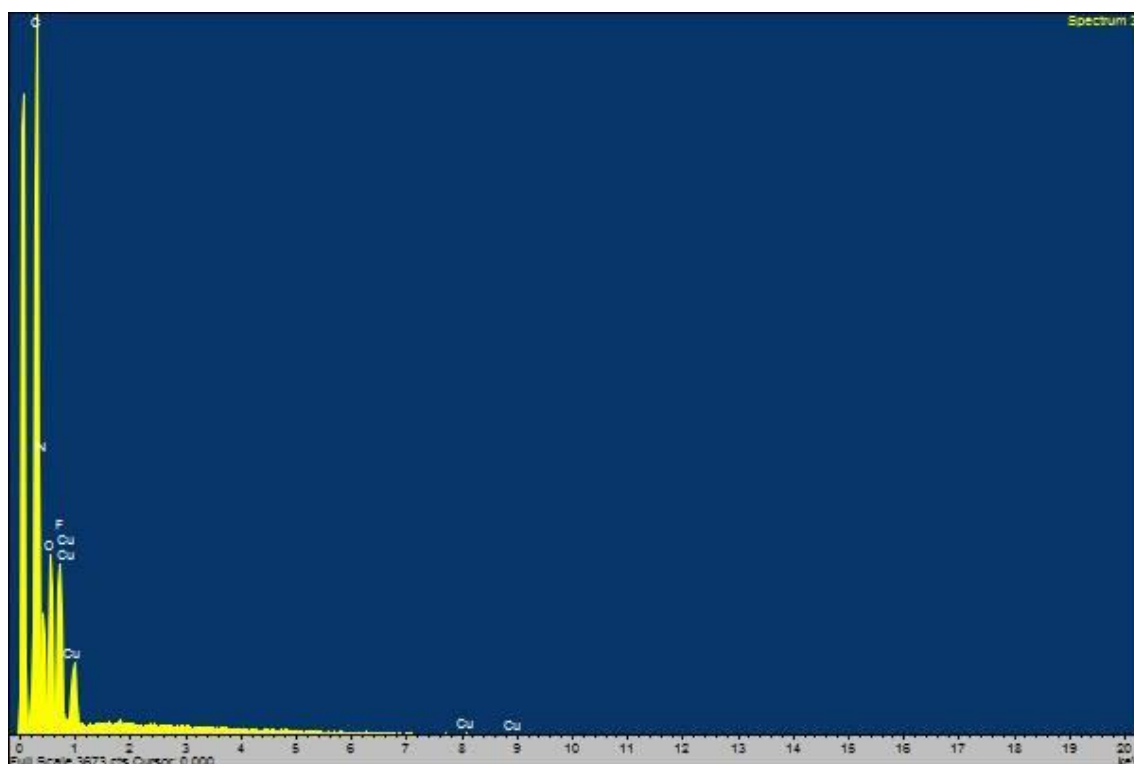


Figure 63 – SEM data of $[\text{Cu}(\text{ACV})_2(\text{BF}_4)_2] \cdot \text{ACV} + 2\text{H}_2\text{O}$

This SEM data (Figure 63) shows what elements made up the crystal 5 compound. There are the organic elements such as carbon, nitrogen, oxygen and fluorine, which made up the acyclovir ligands and the BF_4^- counter ion, as well as copper which was the metal centre of the compound.

3.3. Zinc Complexes 6

3.3.1. 6 $[\text{Zn}(\text{ACV})_4] \cdot \text{SiF}_6 + \text{H}_2\text{O}$

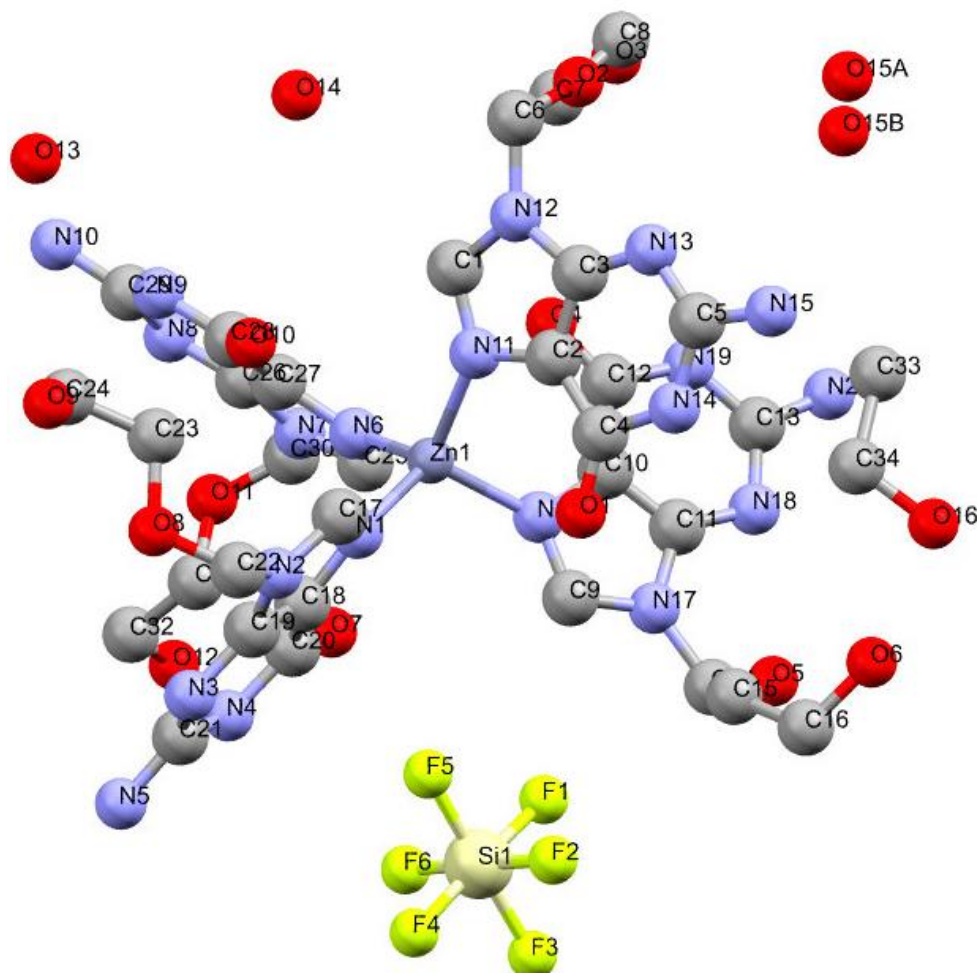


Figure 64 – Crystal 6: $[\text{Zn}(\text{ACV})_4] \cdot \text{SiF}_6 + \text{H}_2\text{O}$ labelled. Note: hydrogen atoms not displayed.

The only zinc containing crystal in this study's selection is crystal 6. It has a triclinic, $P\bar{1}$ space group and is tetrahedral molecule in nature. Bonding to the zinc metal centre are four ACV ligands, each bonding by N1, N6, N11, and N16. Each of the coordinating ACV nitrogen atoms bonds in the mode reported in Figure 23(i) with each of the tails alternating in orientation, never facing each other for geometric optimisation. The overall charge of the molecule is neutral because of a single counter anion, SiF_6^{2-} , which balances the positively charged zinc atom. The counter ion is postulated to form from the breakdown of BF_4^- , which then interacts with silica sourced from the glassware.

3.3.2. Bond Angles

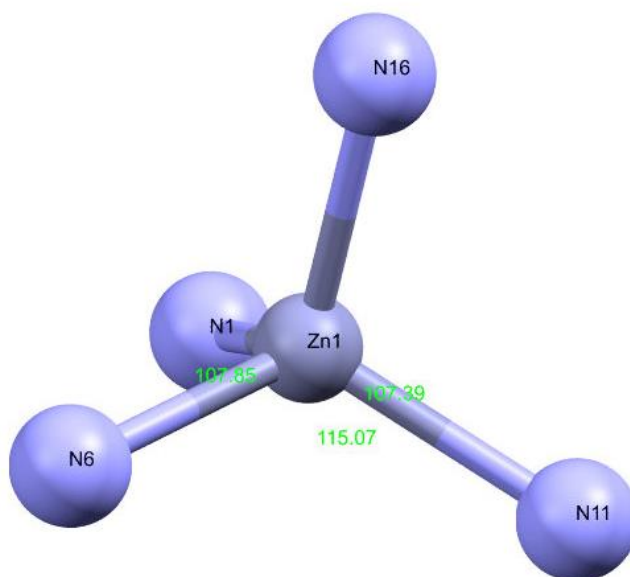


Figure 65 – the angles of each of the three surrounding atoms (N1, N6, N11) with each other in $[\text{Zn}(\text{ACV})_4] \cdot \text{SiF}_6 + \text{H}_2\text{O}$.

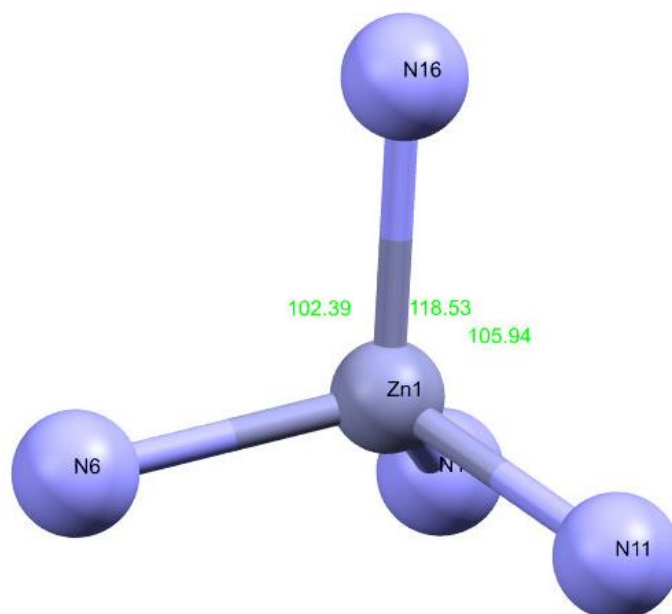


Figure 66 – the angles from each of the surrounding atoms (N1, N6, N11) to the remaining atom (N16) in $[\text{Zn}(\text{ACV})_4] \cdot \text{SiF}_6 + \text{H}_2\text{O}$.

Tetrahedral structures have atoms surrounding the central metal atom. The three angles surrounding the zinc centre are (N1-Zn1-N6) 107.85(1)°, (N6-Zn1-N11) 115.07(1)°, and (N16-Zn1-N1) 107.39(1)° (Figure 65). For a tetrahedral shaped structure, the ideal bond angle would be 109.5°, which none of these angles are. However, two angles in this compound are close to this ‘perfect’ measurement whilst one of the angles was vastly different with a measurement of 115.07°. The explanation could be that while the ligands would find a place of geometric stability, they may have to be further than ideal from each other, leading to this larger bond angle.

As for the bond angles to the remaining atom, they differed to the ideal too (Figure 66): (N1-Zn1-N16) 118.53(1)°, (N6-Zn1-N16) 102.39(1)°, and (N11-Zn1-N16) 105.94(1)°. As previously mentioned, the geometric optimisation of the ligands would try to minimise any energy caused by steric repulsion of the ligands which leads to these bond angles differing from the ideal measurements.

3.3.3. Bond Distances

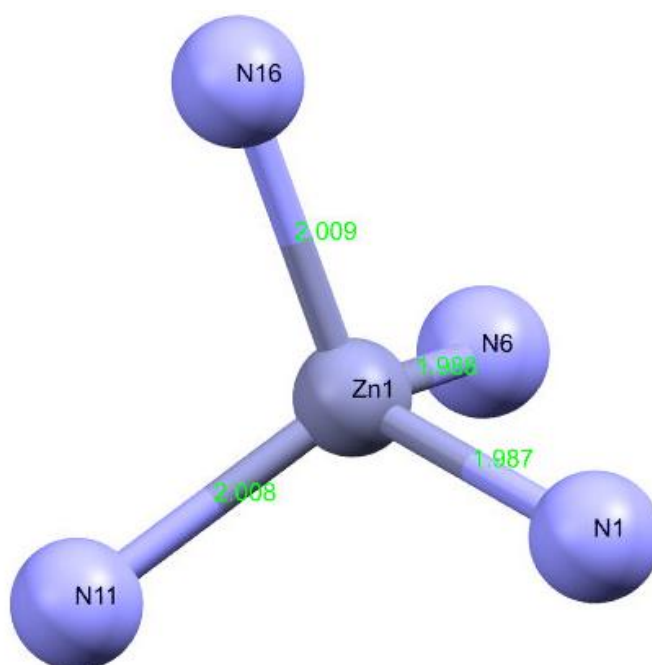


Figure 67 – the bond lengths between the Zinc centre and the bonding ACV ligands in [Zn(ACV)₄] \cdot SiF₆ \cdot H₂O.

In crystal 6, there are four unique bond lengths (Figure 67): (Zn1-N1) 1.987(3) Å, (Zn1-N6) 1.988(3) Å, (Zn1-N11) 2.008(2) Å, and (Zn1-N16) 2.009(2) Å. Whilst all of these bond lengths differ, they are very similar, all being within a ~ 0.020 Å range. The slight difference is very close to the error margin, and may be caused by the ligand steric repulsion as previously explained.

3.3.4. Unit Cell, Intermolecular and Intramolecular Bonding

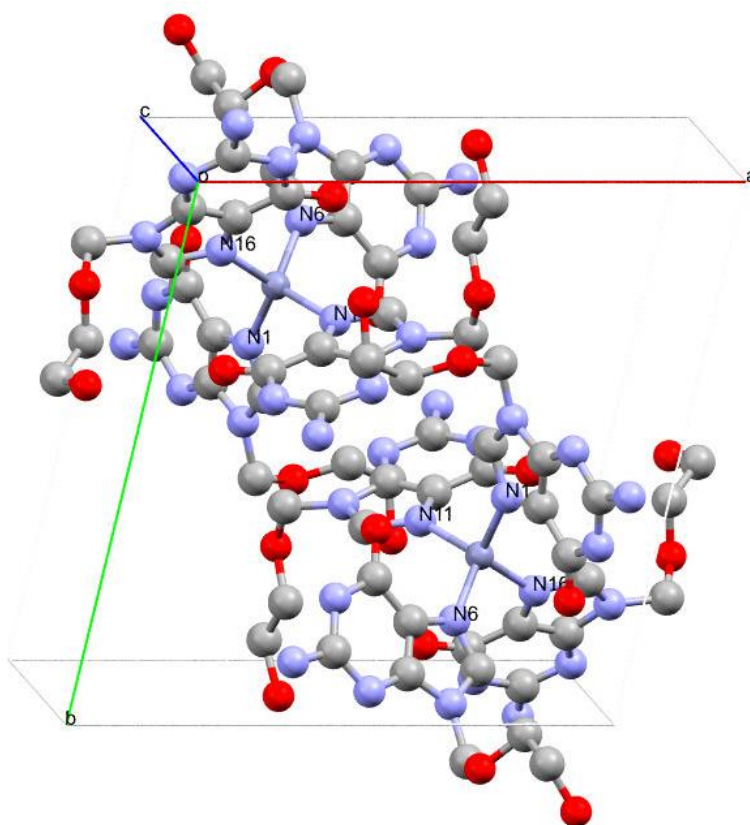


Figure 68 – cell unit of $[\text{Zn}(\text{ACV})_4] \cdot \text{SiF}_6 \cdot \text{H}_2\text{O}$, viewed through C^* . Note: hydrogen atoms not displayed.

The packing of this crystal involves considerable stacking with rows of complexes facing each other, in seemingly reverse mirror image.

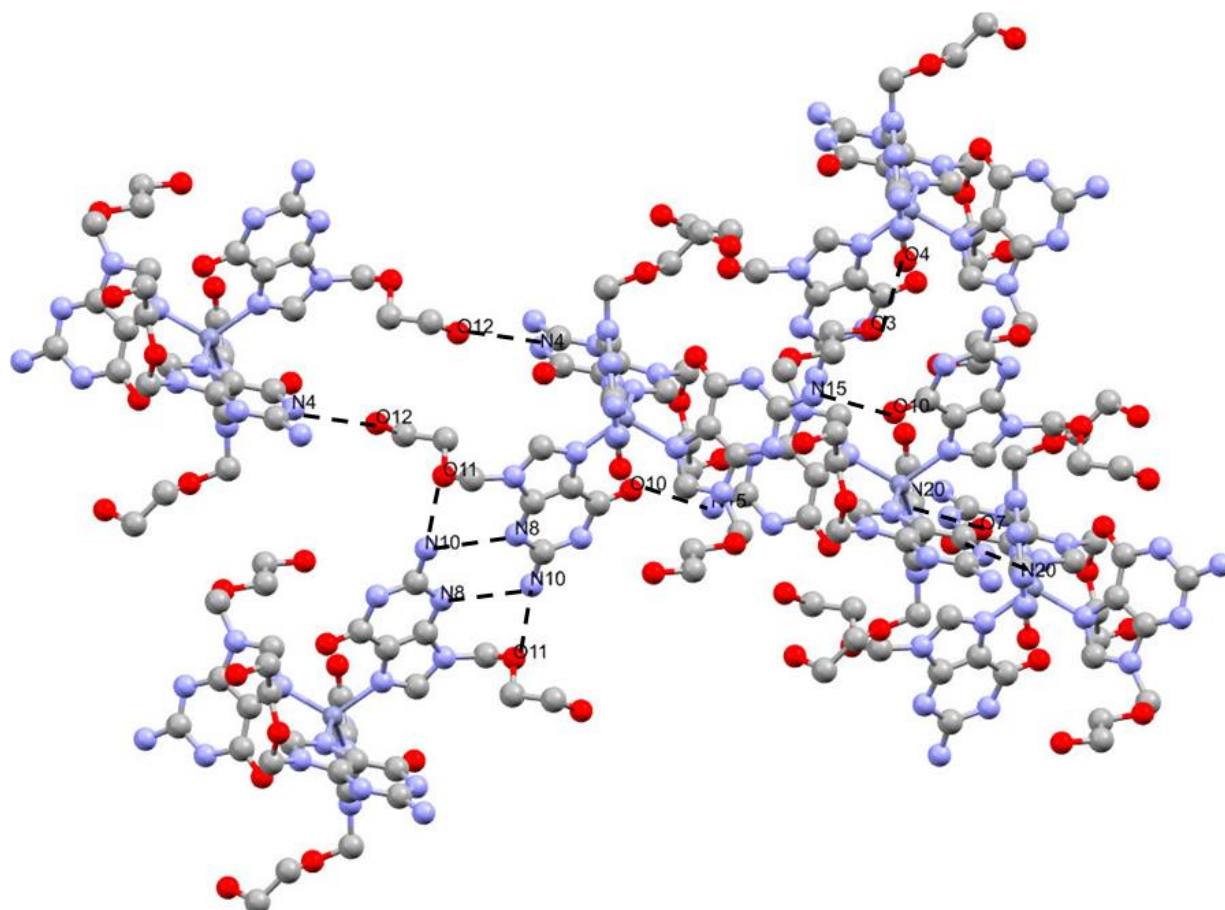


Figure 69– the intermolecular hydrogen bonds between $[Zn(ACV)_4] \cdot SiF_6 \cdot H_2O$ molecules: N15-H \cdots O10, N4-H \cdots O12, N10-H \cdots N8, N10-H \cdots O11, N20-H \cdots O7, and O3-H \cdots O4 (Note: hydrogen atoms not displayed).

Between crystal 6 molecules there are six unique intermolecular hydrogen bonds consisting of O-H \cdots O, O-H \cdots N, N-H \cdots N, and N-H \cdots O bonds (Figure 69): (N15-H \cdots O10) 2.795 Å, (N4-H \cdots O12) 2.804 Å, (N10-H \cdots N8) 3.027 Å, (N10-H \cdots O11) 2.834 Å, (N20-H \cdots O7) 2.779 Å, and (O3-H \cdots O4) 2.714 Å (see Table 8). Each of these bonds fall within the moderate strength region for hydrogen bonds, meaning that they have a significant influence on the formation of this crystal structure, and that it would take a moderate amount of energy to break these bonds.

Intermolecular (Donor-Hydrogen...Acceptor)						
Object 1	Object 2	Length / Å	Object 1	Object 2	Object 3	Angle / °
N15	O10	2.795(3)	N15	H15A	O10	120.4(19)
H15A	O10	2.26(2)	N4	H4	O12	175.3(2)
N4	O12	2.804(5)	N10	H10A	N8	151(2)
H4	O12	1.945(4)	N10	H10B	O11	105.9(2)
N10	N8	3.027(4)	N20	H20A	O7	140.3(19)
H10A	N8	2.246(3)	O3	H3	O4	176.7(19)
N10	O11	2.834(4)				
H10B	O11	2.475(2)				
N20	O7	2.779(3)				
H20A	O7	2.063(19)				
O3	O4	2.714(4)				
H3	O4	1.896(2)				

Table 8 – all of the intermolecular hydrogen bond lengths from Donor to Acceptor, hydrogen to Acceptor and the Donor-Hydrogen...Acceptor angles from $[\text{Zn}(\text{ACV})_4] \cdot \text{SiF}_6 + \text{H}_2\text{O}$

3.3.5. Scanning Electron Microscope Data

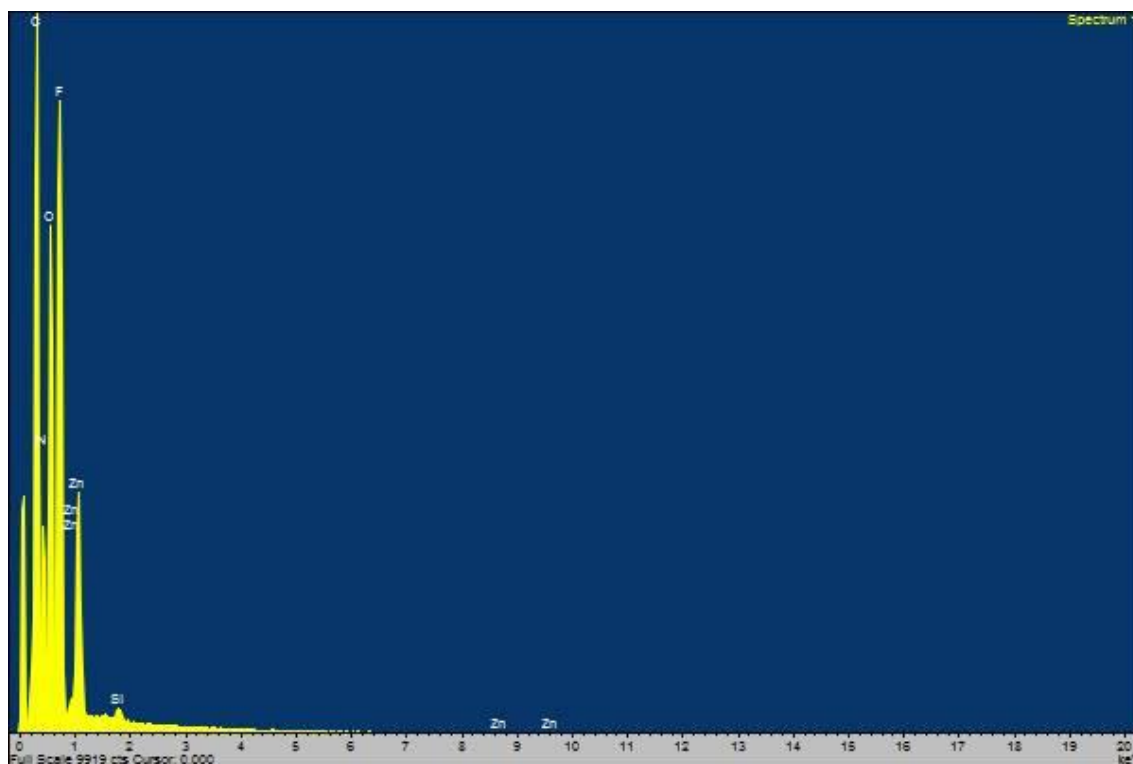


Figure 70 – the SEM data for $[\text{Zn}(\text{ACV})_4] \cdot \text{SiF}_6 + \text{H}_2\text{O}$.

This SEM data for crystal 6 (Figure 70) indicated the elements that make up the crystal. There are organic elements such as carbon, nitrogen, oxygen and fluorine, which make up the acyclovir ligands

and the SiF_6^{2-} counter ion. Additionally, zinc was identified which was the metal centre of the compound and silicon which is found in the counter ion as well as the SEM instrument platform.

3.4.2. Bond Angles

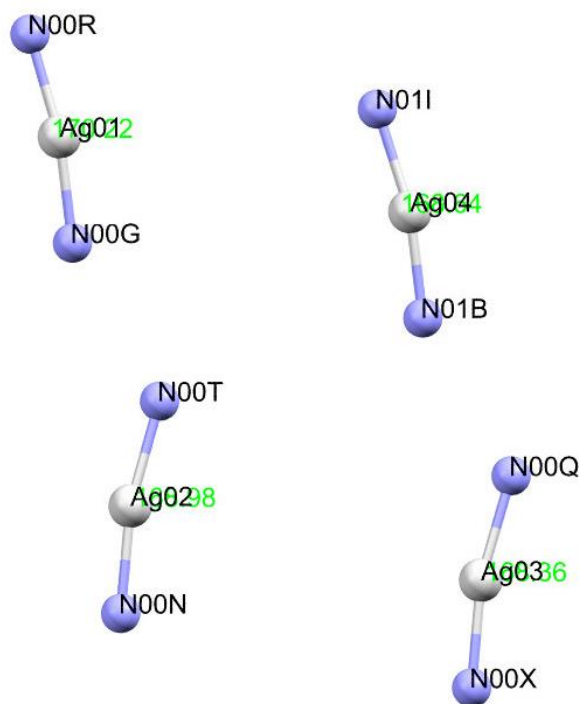


Figure 72 – cropped image showing the bond angles from ligand-metal-ligand from the $2[\text{Ag}_2(\text{ACV})_3] \cdot 2\text{SiF}_6 + 3\text{H}_2\text{O}$ complex.

In total there are four unique bond angles involving the bonding of the ligand atom to the silver metal centre and the other bonding ligand atom (Figure 72). These bond angles are (N00R-Ag01-N00G) $170.22(3)^\circ$, (N00T-Ag02-N00N) $168.98(3)^\circ$, (N00X-Ag03-N00Q) $168.36(4)^\circ$, and (N01B-Ag04-N01I) $168.64(4)^\circ$; all of these bond angles are very similar with the largest deviation being 1.86° . The similarities of these angles show that they all follow a similar pattern of linear coordination.

3.4.3. Bond Distances

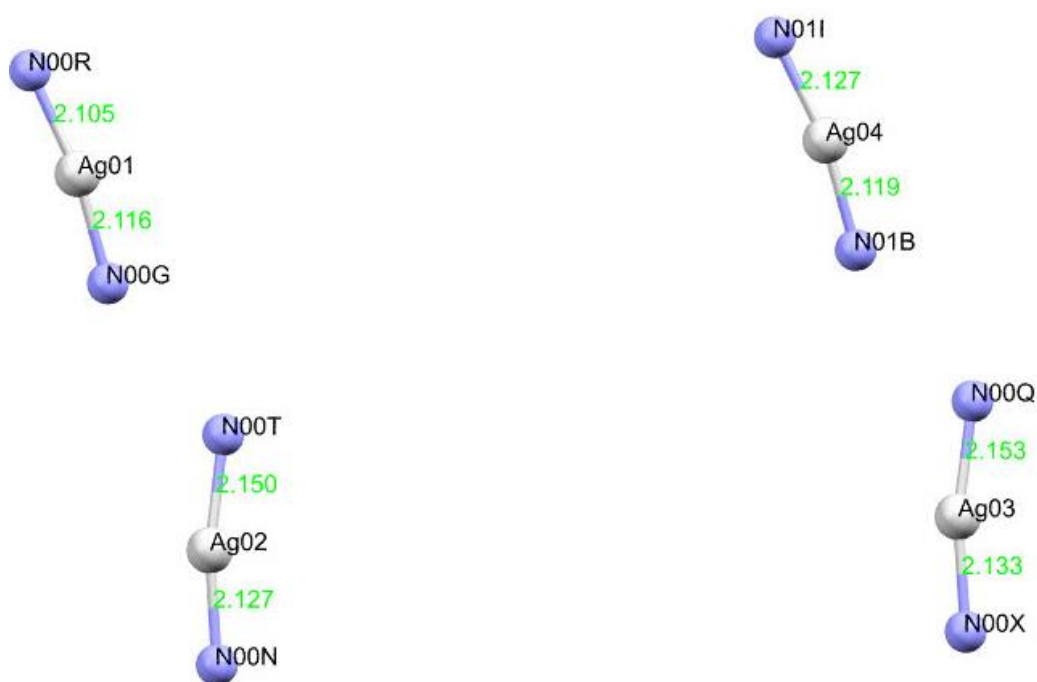


Figure 73 – cropped image showing the bond distances from the bonding ligand atom to the central metal atom in $2[\text{Ag}_2(\text{ACV})_3] \cdot 2\text{SiF}_6 + 3\text{H}_2\text{O}$.

In an asymmetric cell of crystal 7 there are eight unique bond lengths (Figure 73): (Ag1-N00R) 2.105(1) Å, (Ag1-N00G) 2.116(9) Å, (Ag2-N00T) 2.150(1) Å, (Ag2-N00N) 2.127(9) Å, (Ag3-N00Q) 2.153(9) Å, (Ag3-N00X) 2.133(1) Å, (Ag4-N011) 2.127(1) Å, and (Ag4-N01B) 2.119(1) Å. The sum of these bond lengths differs by up to 0.048 Å, which is within experimental error.

3.4.4. Unit Cell, Intermolecular and Intramolecular Bonding

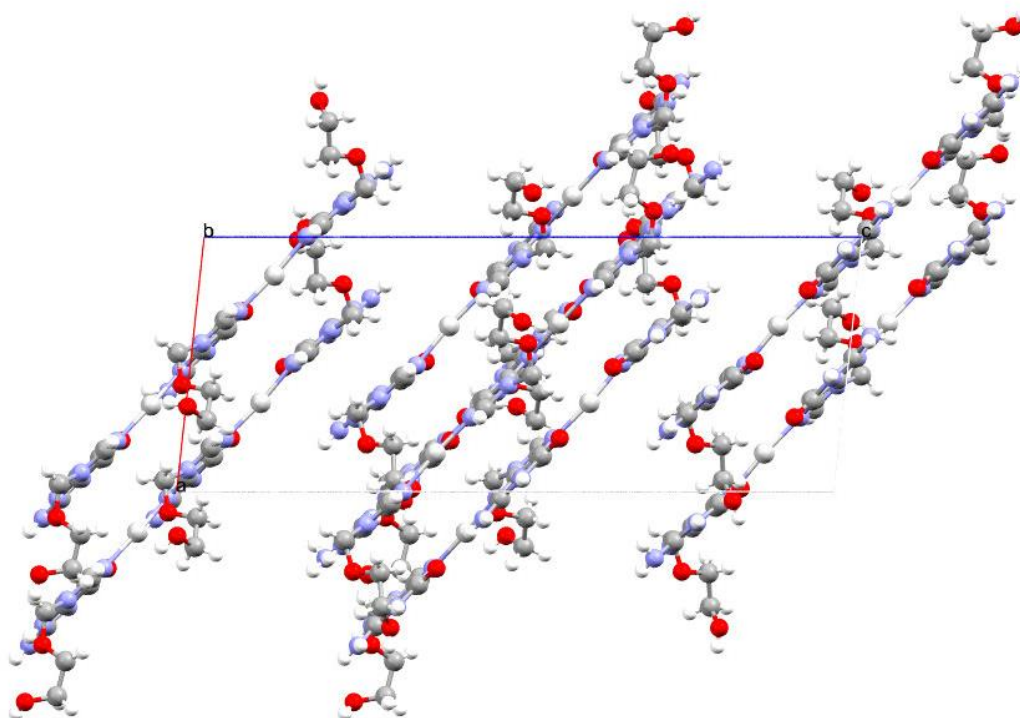


Figure 74 – a cell unit of $2[\text{Ag}_2(\text{ACV})_3] \cdot 2\text{SiF}_6 + 3\text{H}_2\text{O}$, viewed through B.

The asymmetric unit of crystal 7 fits a quarter of the cell contents and has a space group of $P2/c$ (monoclinic). The asymmetric unit consists of two complexes staggered relative to one another; these grow to form layers that overlap.

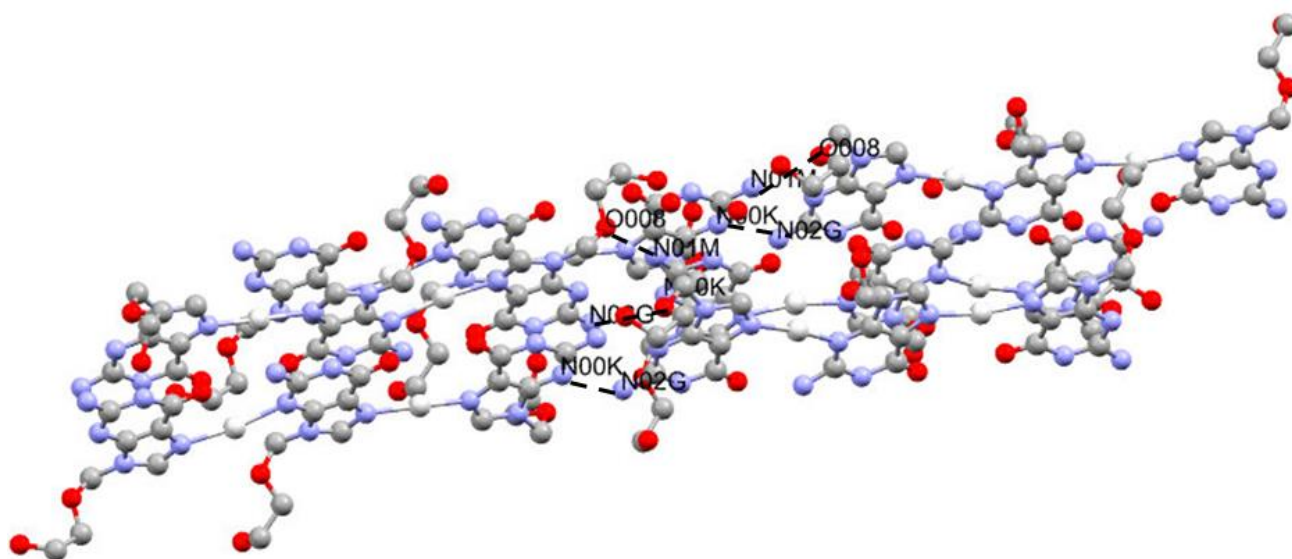


Figure 75 – intermolecular hydrogen bonds between molecules in $2[\text{Ag}_2(\text{ACV})_3] \cdot 2\text{SiF}_6 + 3\text{H}_2\text{O}$ (Note: hydrogen atoms not displayed).

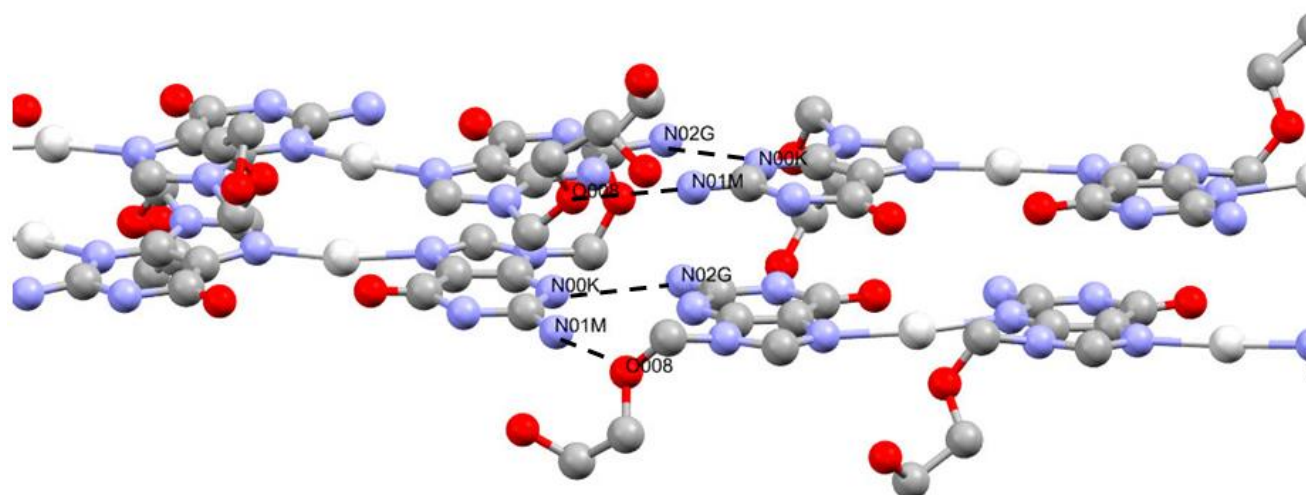


Figure 76 – expanded view of the intermolecular hydrogen bonds between molecule: N00K-N02G and N01M-O008 (Note: hydrogen atoms not displayed).

There are two unique intermolecular hydrogen bonds made up of N-H...N and N-H...O (Figure 75 and Figure 76): (N02G-H...N00K) 2.953 Å and (N01M-H...O008) 2.847 Å (see Table 9). These hydrogen bond lengths are within the moderate bond length range and therefore are significant bonds in the formation of this crystal. It also means that a moderate amount of energy would be needed to break these bonds.

Intermolecular (Donor-Hydrogen...Acceptor)						
Object 1	Object 2	Length / Å	Object 1	Object 2	Object 3	Angle / °
N02G	N00K	2.95(1)	N01M	H01A	O008	105.6(6)
H02H	N00K	2.094(9)	N02G	H02H	N00K	176.4(7)
N01M	O008	2.85(1)				
H01A	O008	2.493(8)				

Table 9 - all of the intermolecular hydrogen bond lengths from Donor to Acceptor, hydrogen to Acceptor and the Donor-Hydrogen...Acceptor angles from $2[\text{Ag}_2(\text{ACV})_3] \cdot 2\text{SiF}_6 + 3\text{H}_2\text{O}$

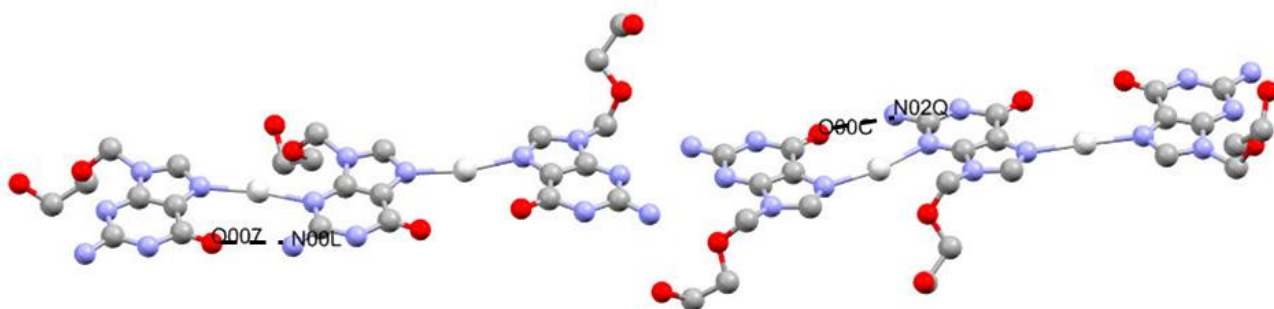


Figure 77 – intramolecular hydrogen bonds seen within $2[\text{Ag}_2(\text{ACV})_3] \cdot 2\text{SiF}_6 + 3\text{H}_2\text{O}$: N00L -H...O007 and N02Q -H...O00C (Note: hydrogen atoms not displayed).

The two intramolecular hydrogen bonds are the same bond type, N-H...O (Figure 77). (N00L-H...O007) 2.911 Å and (N02Q-H...O00C) 2.862 Å (see Table 10), both falling in the moderate region of hydrogen bond strength, meaning that they would both need moderate energy to break them.

Intramolecular (Donor-Hydrogen...Acceptor)						
Object 1	Object 2	Length / Å	Object 1	Object 2	Object 3	Angle / °
N02Q	O00C	2.86(2)	N02Q	H02O	O00C	116.5(9)
H02O	O00C	2.371(9)	N00L	H00A	O007	164(7)
N00L	O007	2.91(1)				
H00A	O007	2.074(8)				

Table 10 – all of the intramolecular hydrogen bond lengths from Donor to Acceptor, hydrogen to Acceptor and the Donor-Hydrogen...Acceptor angles from $2[\text{Ag}_2(\text{ACV})_3] \cdot 2\text{SiF}_6 + 3\text{H}_2\text{O}$

3.4.5. Scanning Electron Microscope Data

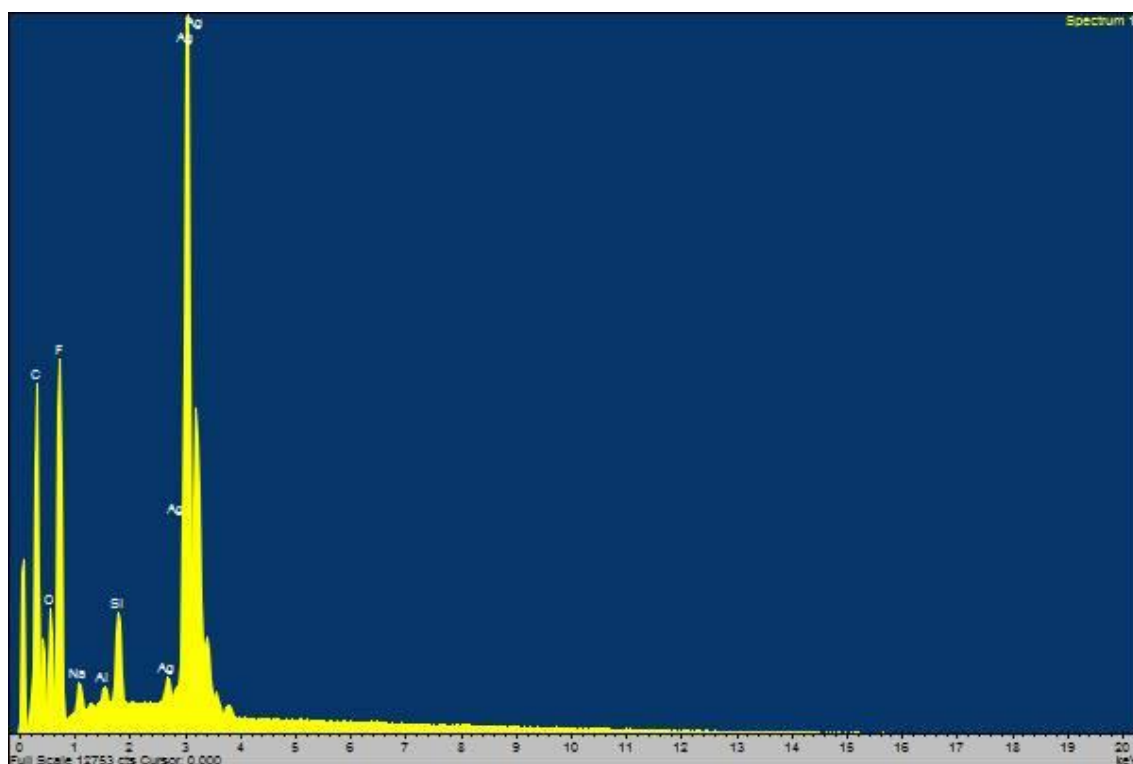


Figure 78 – the SEM data for $2[\text{Ag}_2(\text{ACV})_3] \cdot 2\text{SiF}_6 + 3\text{H}_2\text{O}$

This SEM data for crystal 7 (Figure 78) shows the elemental composition of the compound. There are organic elements such as carbon, nitrogen, oxygen and fluorine, which make up the acyclovir ligands and the SiF_6^{2-} counter ion, as well as silver which was the metal of the compound's framework. Silicon could be found in the counter ion as well as the SEM instrument platform.

3.4.6. 8 $2[\text{Ag}(\text{ACV})]\cdot\text{SiF}_6 + 2\text{H}_2\text{O}$

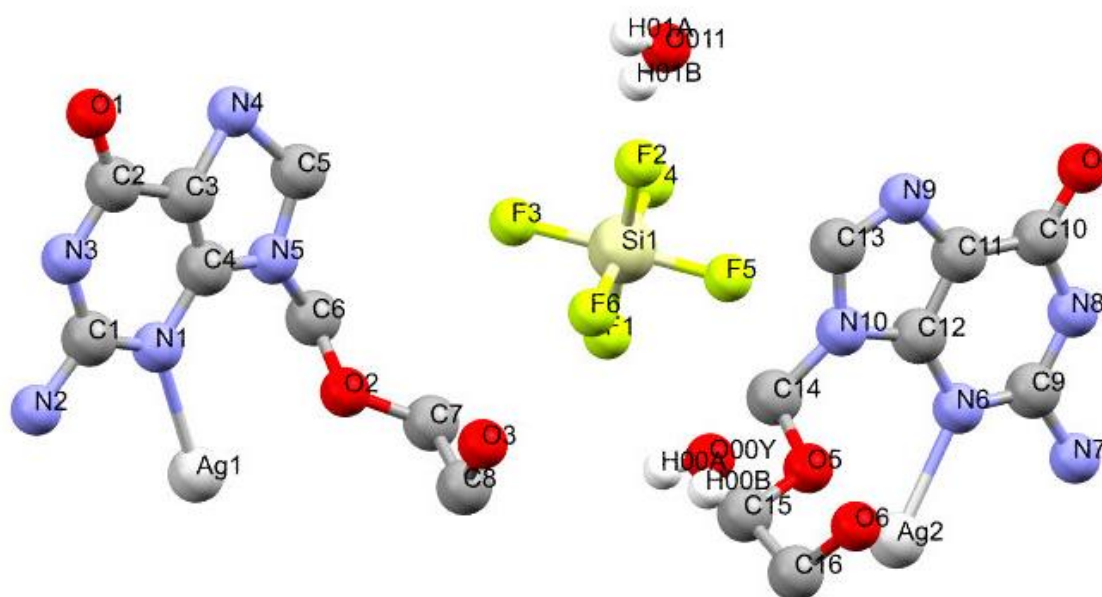


Figure 79 – Crystal 8: $2[\text{Ag}(\text{ACV})]\cdot\text{SiF}_6 + 2\text{H}_2\text{O}$ labelled asymmetric unit. Note: some hydrogen atoms omitted.

This monoclinic structure with a space group of $P2_1$ does not appear to have a typical structure, given that the ACV molecule bonds to a silver atom (Figure 79). The silver atoms bond to their individual ACV molecules in the fashion seen in Figure 23 (iii). Within one asymmetric unit of crystal 8, there are two molecules of ACV with the bonding silver atoms. Also observed is a SiF_6^{2-} molecule which acts as a counter ion leading to an overall charge of crystal 8 to be neutral.

3.4.7. Bond Angles

In each molecule observed in crystal 8, both silver atoms had the angles of interest measured: (N1-Ag1-N4) $162.06(2)^\circ$ and (N6-Ag2-N9) $155.78(1)^\circ$ differing by only 6.28° . The complex's structure is a polymer as there is a continuous chain of each respective monomer unit (the monomers seen in Figure 80). Crystal 8 is a linear polymer and does not have an ideal bonding angle. However, the angles explored are similar which could indicate that they follow a similar pattern.

3.4.8. Bond Distances

Both silver atoms and the bonding atom were measured for length: (Ag1-N1) 2.192(3) Å and (Ag2-N6) 2.207(3) Å. As previously stated, the crystal complex is a linear polymer consisting of repeating units with identical bond lengths. Both lengths are similar, differing by 0.015 Å. The similarities show that this is a well distributed molecule with little distortion.

3.4.9. Unit Cell, Intermolecular and Intramolecular Bonding

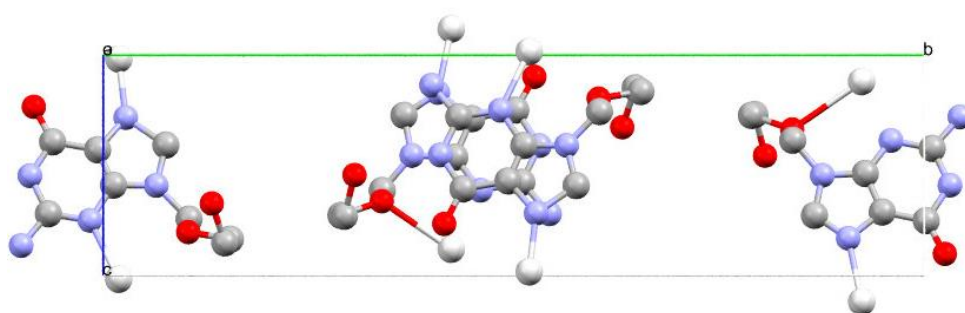


Figure 80 – a cell unit of $2[\text{Ag}(\text{ACV})]\cdot\text{SiF}_6 + 2\text{H}_2\text{O}$, viewed from a. Note: hydrogen atoms not displayed.

The asymmetric unit fits a quarter of the cell of this monoclinic crystal ($P2_1$), packing these monomers units together. Two of these units are in the centre of the cell axes, stacked on top of each other and slightly staggered (Figure 80). One monomer unit of crystal 8 polymer is on either side of the central asymmetric unit, each facing a different way to the other. Some atoms of the cell unit do fall on the outside of the axes, however, a majority are within.

As previously discussed, crystal 8 is a polymer formed from many of the individual monomer units. Due to the nature of this polymer, there is no intermolecular bonding that occurs.

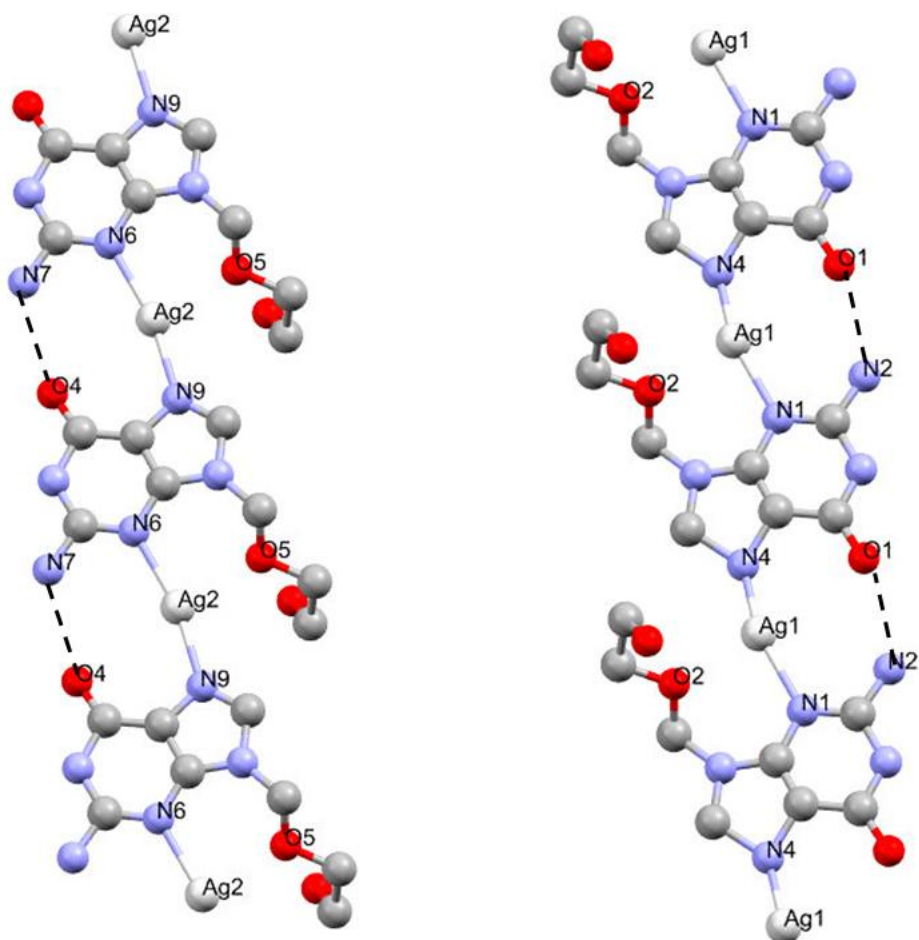


Figure 81 – Both intramolecular Hydrogen Bonds coordination bonds between $2[\text{Ag}(\text{ACV})]\cdot\text{SiF}_6 + 2\text{H}_2\text{O}$ molecules (Note: hydrogen atoms not displayed).

There are two unique intramolecular hydrogen bonds between the crystal 8 polymer consisting of N-H...O bonds (Figure 81): (N2-H...O1) 2.825 Å, and (N7-H...O4) 2.901 Å (see Table 11). As one monomer of crystal 8 has the silver atom in the position described in Figure 23 (iii), when it forms into a polymer the silver atom of an adjoining monomer will bond in the format seen in Figure 23 (i). These bonds are within the moderate region of hydrogen bond strength which means they are significant to the formation of the crystals, and would need a moderate amount of energy to break them.

Intramolecular (Donor-Hydrogen...Acceptor)				Object 1	Object 2	Object 3	Angle / °
Object 1	Object 2	Length / Å		Object 1	Object 2	Object 3	Angle / °
N7	O4	2.90(5)		N2	H2A	O1	160(19)
H7A	O4	2.06(3)		N7	H7A	O4	154(2)
N2	O1	2.82(4)					
H2A	O1	2.00(2)					

Table 11 – all of the intramolecular hydrogen bond lengths from Donor to Acceptor, hydrogen to Acceptor and the Donor-Hydrogen...Acceptor angles from $2[\text{Ag}(\text{ACV})] \cdot \text{SiF}_6 + 2\text{H}_2\text{O}$

The crystal data from this complex suggested an intramolecular bond between the silver atoms and the oxygen atom in the ACV tail ($\text{Ag1} \cdots \text{O2}$ and $\text{Ag2} \cdots \text{O5}$). However, the data around this bond isn't strongly reassuring to conclusively accept this bond, as well as the chemical impossibility of these bonds as the oxygen atoms are not protonated.

3.4.10. Scanning Electron Microscope Data

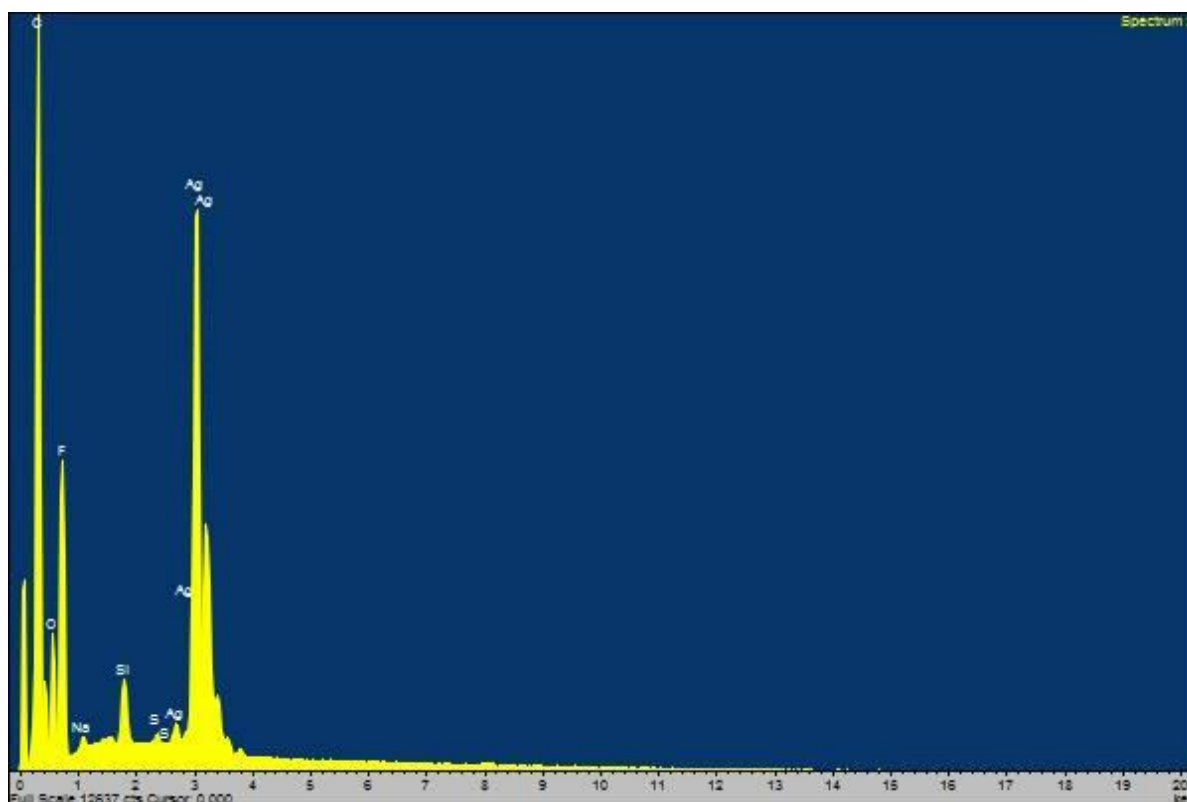


Figure 82 – the SEM data for $2[\text{Ag}(\text{ACV})] \cdot \text{SiF}_6 + 2\text{H}_2\text{O}$.

This SEM data for crystal 8 (Figure 82) shows what elements are present within the crystal. There are organic elements such as carbon, nitrogen, oxygen and fluorine, which make up the acyclovir ligands and the SiF_6^{2-} counter ion, as well as silver which is the metal within this complex. Silicon is also identified which could be found in the counter ion as well as the SEM instrument platform.

3.4.11. 9 $2[\text{Ag}(\text{ACV})_2] \cdot \text{SiF}_6 + 2\text{H}_2\text{O}$

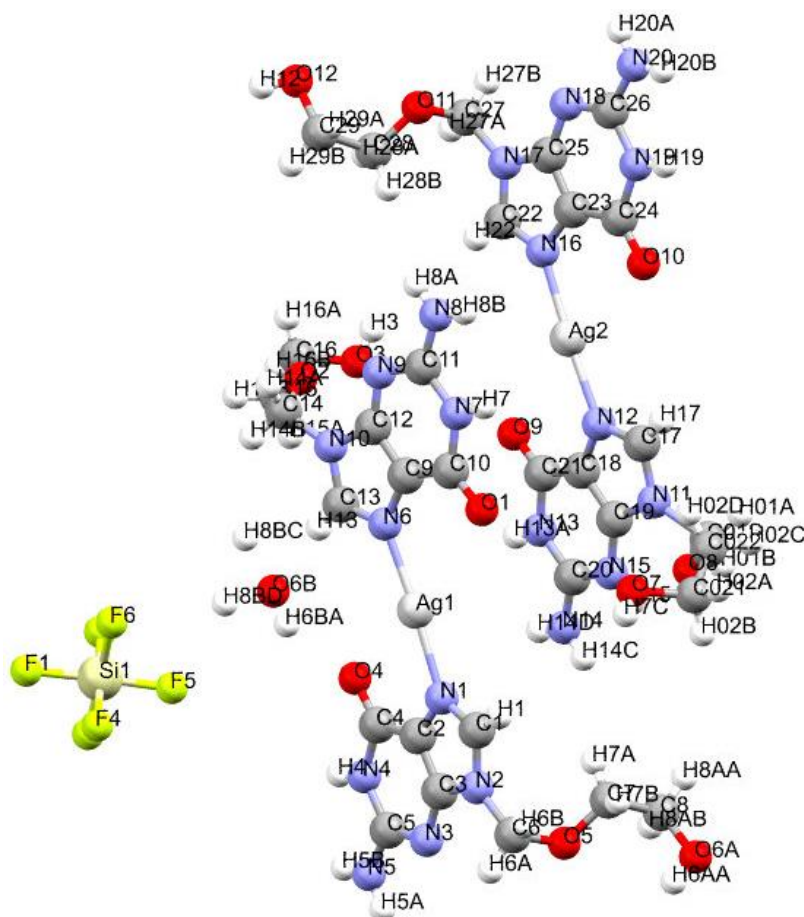


Figure 83 –Crystal 9: $2[\text{Ag}(\text{ACV})_2] \cdot \text{SiF}_6 + 2\text{H}_2\text{O}$ labelled

Crystal 9 is a triclinic compound with a space group of $P\bar{1}$ that forms in sheets of the single molecules that make up the asymmetric unit (Figure 83). One asymmetric unit is made up of two molecules of a silver centred molecule with two ACV ligands to either side of it. These ACV ligands bond to the silver in the same way as seen in Figure 23 (i). In this example, the bonding atoms are N1, N6, N12, and N16. The two complexes are aligned in a staggered way. The observed counter ion was a SiF_6^{2-} anion which charge-balances the complex to achieve overall neutrality.

3.4.12. Bond Angles

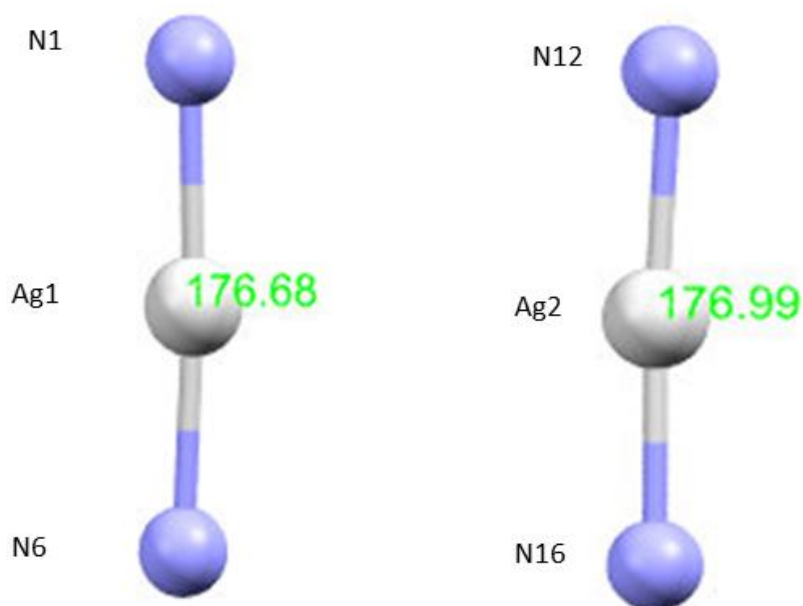


Figure 84 – cropped image comparing the bond angles measured from the bonded atom to the silver to the other bonded atom in $2[\text{Ag}(\text{ACV})_2] \cdot \text{SiF}_6 + 2\text{H}_2\text{O}$.

The bond angles are taken from the two ACV nitrogen atoms of either ligand, through the silver atom (Figure 84): (N1-Ag1-N6) $176.68(2)^\circ$ and (N12-Ag2-N16) $176.99(2)^\circ$. The two angles are very similar, only differing by 0.31° , which is within experimental error.

3.4.13. Bond Distances

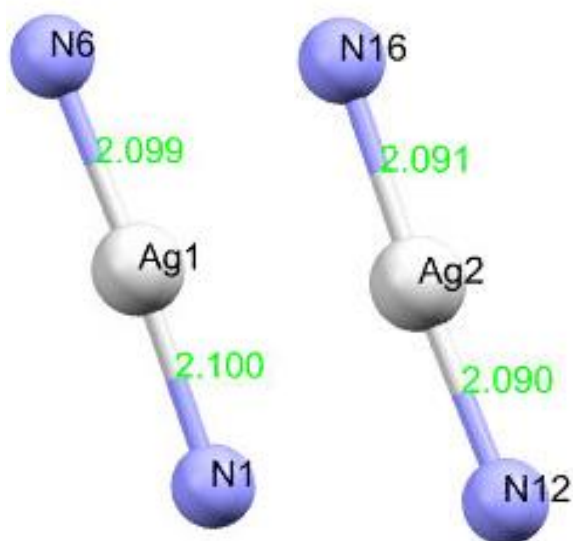


Figure 85 – cropped image comparing bond distances measured from the silver atom to the bonding atoms in $2[\text{Ag}(\text{ACV})_2] \cdot \text{SiF}_6 + 2\text{H}_2\text{O}$.

There are four unique lengths between the silver atom and the bonding atom from the ACV ligand (Figure 85): (Ag1-N1) 2.100(5) Å, (Ag1-N6) 2.099(5) Å, (Ag2-N12) 2.090(5) Å, and (Ag2-N16) 2.091(5) Å. All the bond lengths are consistent with each other differing by 0.10 Å, which is within experimental error.

3.4.14. Unit Cell, Intermolecular and Intramolecular Bonding

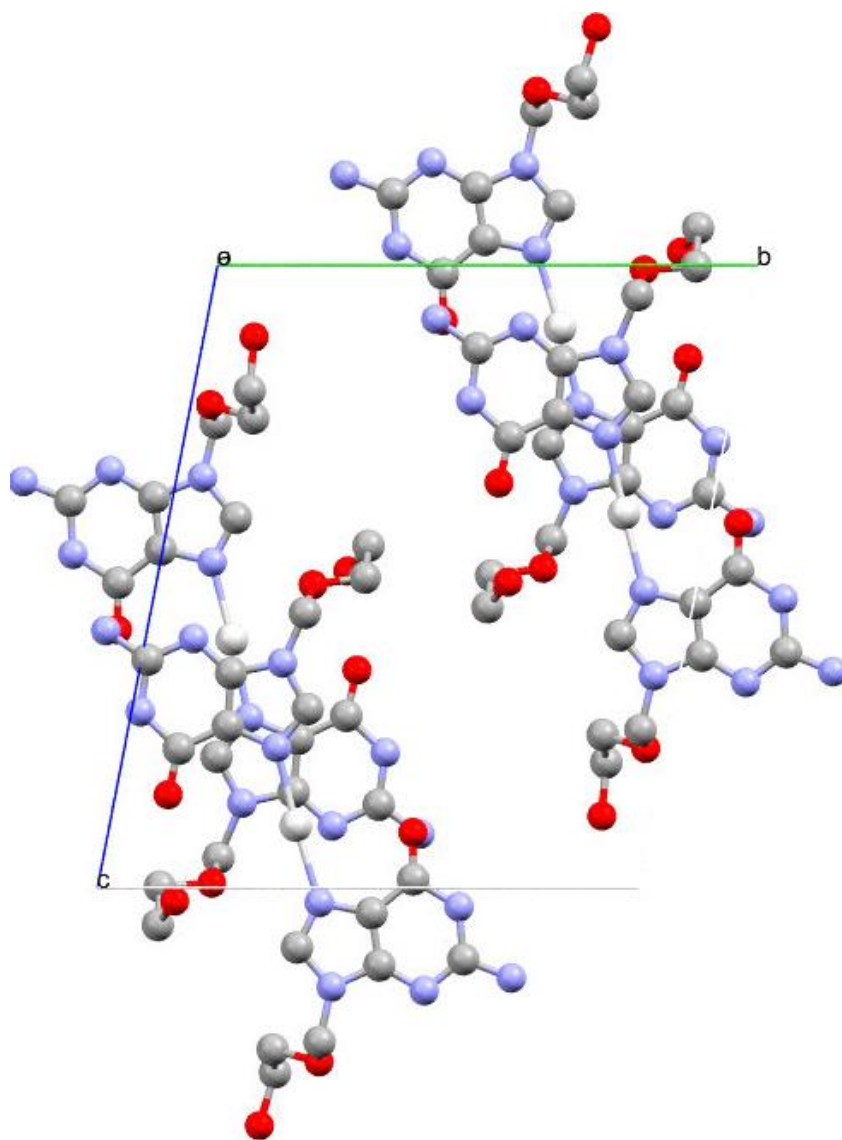


Figure 86 – unit cell of $2[\text{Ag}(\text{ACV})_2] \cdot \text{SiF}_6 + 2\text{H}_2\text{O}$, viewed through a. Note: hydrogen atoms not displayed.

This $P\bar{1}$, triclinic asymmetric unit takes up half of the cell unit (Figure 86) with the packing of crystal 9 consisting of two silver-ACV complexes staggered relative to one another, with each complex having the same composition.

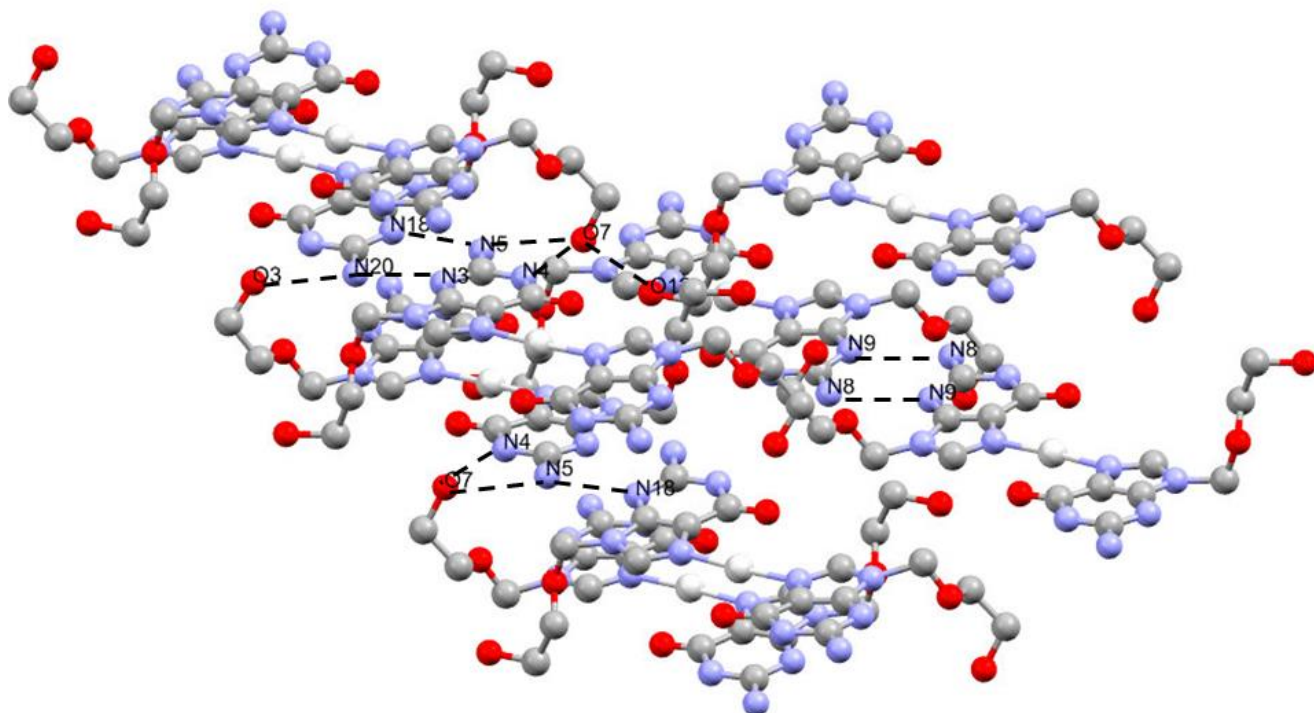


Figure 87 – the intermolecular hydrogen bonds between $2[\text{Ag}(\text{ACV})_2] \cdot \text{SiF}_6 + 2\text{H}_2\text{O}$ molecules: $\text{N}8\text{-H}\cdots\text{N}9$, $\text{O}7\text{-H}\cdots\text{O}12$, $\text{N}4\text{-H}\cdots\text{O}7$, $\text{N}5\text{-H}\cdots\text{O}7$, $\text{N}20\text{-H}\cdots\text{O}3$, $\text{N}20\text{-H}\cdots\text{N}3$, and $\text{N}5\text{-H}\cdots\text{N}18$. (Note: hydrogen atoms not displayed).

Intermolecular hydrogen bonding between crystal 9 molecules consists of seven unique bonds made up of $\text{N-H}\cdots\text{N}$, $\text{O-H}\cdots\text{O}$, $\text{N-H}\cdots\text{O}$, and $\text{O-H}\cdots\text{N}$ (Figure 87): ($\text{N}8\text{-H}\cdots\text{N}9$) 3.054 Å, ($\text{O}7\text{-H}\cdots\text{O}12$) 2.802 Å, ($\text{N}5\text{-H}\cdots\text{O}7$) 2.993 Å, ($\text{N}4\text{-H}\cdots\text{O}7$) 2.793 Å, ($\text{N}20\text{-H}\cdots\text{O}3$) 3.006 Å, ($\text{N}20\text{-H}\cdots\text{N}3$) 3.018 Å, and ($\text{N}5\text{-H}\cdots\text{N}18$) 3.056 Å (see Table 12). These bond lengths all fall within the moderate region of hydrogen bond strength, meaning they are all significant in the formation of the crystal 9 complex and would need a moderate amount of energy to break them.

Intermolecular (Donor-Hydrogen...Acceptor)				Object 1	Object 2	Object 3	Angle / °
Object 1	Object 2	Length / Å		Object 1	Object 2	Object 3	Angle / °
N8	N9	3.054(7)		N8	H8A	N9	172.4(4)
H8A	N9	2.2(5)		N4	H4	O7	159.1(5)
O7	O12	2.80(1)		N5	H5B	O7	145(4)
H7C	O12	2.03(10)		O7	H7C	O12	157.2(5)
N5	O7	2.99(1)		N20	H20A	N3	171.8(4)
H5B	O7	2.247(7)		N5	H5A	N18	178.6(7)
N4	O7	2.793(9)		N20	H20B	O3	146.1(4)
H4	O7	1.973(6)					
N20	N3	3.018(7)					
H20A	N3	2.164(5)					
N5	N18	3.056(8)					
H5A	N18	2.196(5)					
N20	O3	3.006(9)					
H20B	O3	2.254(7)					

Table 12 – all of the intermolecular hydrogen bond lengths from Donor to Acceptor, hydrogen to Acceptor and the Donor-Hydrogen...Acceptor angles from $2[\text{Ag}(\text{ACV})_2] \cdot \text{SiF}_6 + 2\text{H}_2\text{O}$

In crystal 9, there are no observed intramolecular hydrogen bonds between molecules.

3.4.15. Scanning Electron Microscope Data

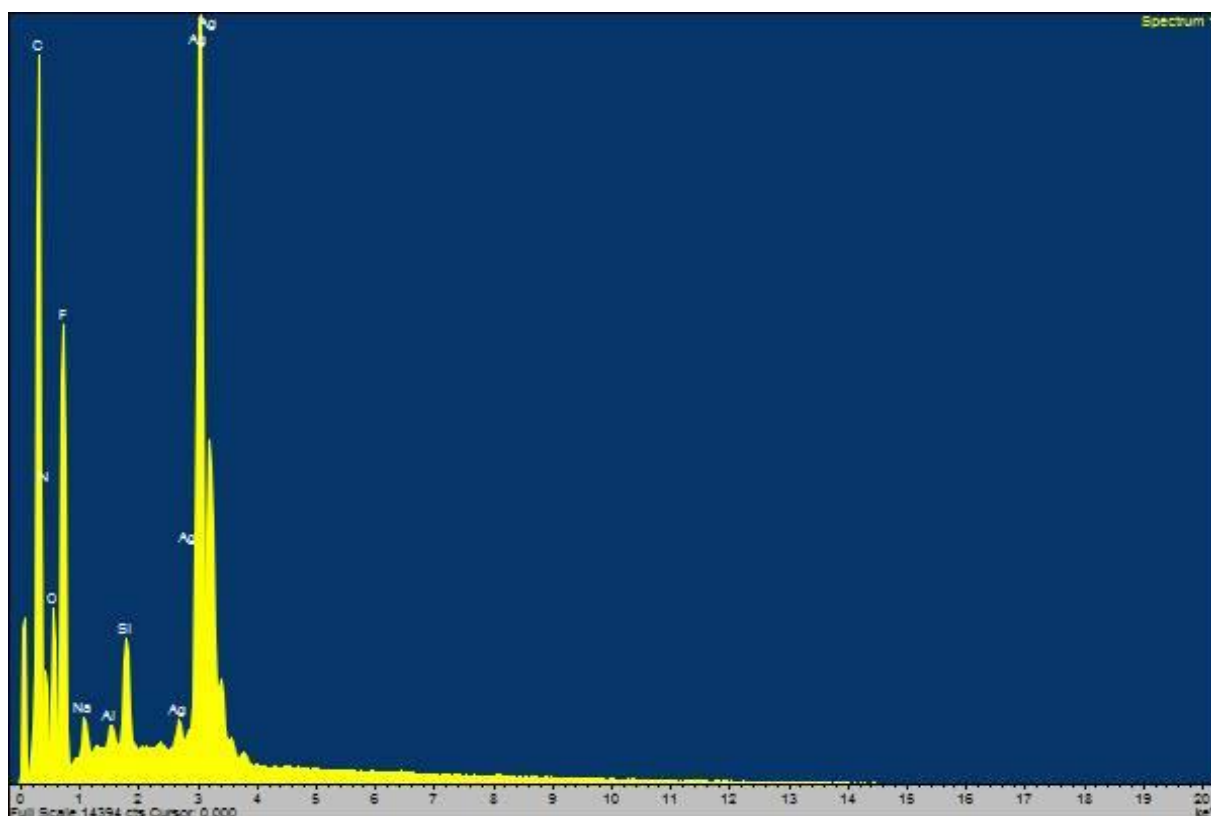


Figure 88 – the SEM data for $2[\text{Ag}(\text{ACV})_2] \cdot \text{SiF}_6 \cdot 2\text{H}_2\text{O}$.

This SEM data for crystal 9 (Figure 88) indicates what elements are within the crystal. There are organic elements such as carbon, nitrogen, oxygen and fluorine, which made up the acyclovir ligands and the SiF_6^{2-} counter ion, as well as silver which was the metal used in the synthesis of this compound. Silicon was also identified which could be found in the counter ion as well as the SEM instrument platform.

4.1. Conclusion

In this study, the focus was synthesising new crystalline forms of metal-ACV complexes, in order to characterise as many polymorphs as possible, and to analyse the metal-ligand bonding. In addition, the use of ACV as the ligand allowed for the scope of the study to incorporate the synthesis of potential antiviral medication and chemotherapeutic drugs which are highly sought after in medicine. Although the use of metal-ACV complexes have been the focus of other studies, only a few selected metals and a limited range of microbials and viruses had been examined. Furthermore, this study, as well as other studies, notes the insolubility of ACV in aqueous mediums and only partial solubility in certain organic solvents, such as methanol and ethanol.

During this study, several crystallisations successfully led to the synthesis of new complexes with metal tetrafluoroborate salts and ACV ligands using different solvent mixtures and a variation of crystallisation methods. The process of characterising these different crystal structures involved powder X-ray diffraction (PXRD), infrared (IR) spectroscopy, and scanning electron microscope energy dispersive X-ray (SEM/EDX) analysis. Each of the three transition metal salts studied formed at least one unique crystal structure.

The largest family of new crystal structures discovered were copper based complexes, with five distinctive crystals observed. These different crystal types were found using different ratios of metal to ligand as well as two different types of alcohol solvent: methanol and ethanol. The solubility of ACV in these solvents was similar to that described in existing literature. Nevertheless, when dissolved with the metal salt, the solubility of ACV increased; this was observed in all the crystallisations. Each copper complex took the geometric form of one of three coordination geometries: octahedral, square pyramidal, or square planar. Each allowed for unique bonding arrangements to occur between metal and ligand.

The first three copper crystals were either square pyramidal (crystals 1 and 3) or octahedral (crystal 2) and all bonded via N4 of the purine ring (see 'Results and Discussion' Figure 22 and 23 (i)), a

common bonding point for ACV to a metal in both this study and others in existing literature. However, in crystal 4 the ACV ligands bonded through two sites as bidentate ligands at N4 and via the carbonyl group on the purine ring, O1 (see 'Results and Discussion' Figure 23 (ii)). This is rarely observed in ACV ligands, prompting discussion in the 'Literature Analysis' of ACV's pseudo bidentate nature. The moderate strength of observed hydrogen bonding from O1 to the copper centre ensures that crystal 4 adopts an octahedral geometry.

Crystal 5, the final copper centred crystal, is the only square planar crystal observed in this study to be bonded with its counter ion, BF_4^- . This unique bond is through one of the fluoride atoms directly to the copper centre. No evidence of a crystal of this kind, where both ACV and tetrafluoroborate ligands attached to the copper centre, could be found within the existing literature.

The remaining four crystals are comprised of one zinc-based crystal, and three silver-based crystals. The only zinc crystal observed in this study is also the only structure with tetrahedral geometry, bonded to four ACV ligands, all by the N4 atom of the ACV molecule (see 'Results and Discussion' Figure 23 (i)). Crystals 7 and 9 were formed in a linear geometric shape, with both crystals containing one silver atom bound to two ACV ligands. Crystal 7 has one ACV ligand bonded by the N4 position, which is commonly seen; the other ACV ligand coordinates via the N3 position. In crystal 9, ACV only bonds through N4. Both of these crystals are unique because they form a polymeric chain of repeating units within their solid-state structures. Although polymeric chains have been discussed in literature, [16], it is seldom mentioned that they replicate units outwards from the metal centre.

The final silver crystal, crystal 8, contains two symmetrical monomers formed of one ACV bonding to one silver atom via the N3 position. Crystal 8 is a polymer that forms a continuous chain from each separate monomer, bonding via the silver atom in the N3 position of the ACV ligands to another monomer's ACV ligand in the N4 position (see 'Results and Discussion' Figure 23 (i) and (iii)). Also observed was $\text{Ag}\cdots\text{O}$ interactions, however, it was a chemical impossibility which did not have strong data to support it.

PXRD data of samples containing their individual polymorphs was collected; however, there were several samples that were either of low crystallinity, or a combination of other crystal polymorphs. Crystals 3 and 4 all matched when the measured PXRD data was compared to that of the predicted PXRD data. All the other crystals' data was similar to their predicted data pattern, which was to be expected as they contained a quantity of the corresponding crystal polymorph. Discrepancies between predicted and observed data were as a consequence of polymorphs that had either not been isolated or accounted for.

4.2. Future Work

Furthering this study into the polymorphs of biologically relevant metals with ACV, a wider range of solvents will need to be evaluated, as previously discussed, due to some polymorphic structures being dependent on the medium they are dissolved and react in. A range of organic and inorganic solvents, such as water, hexane and toluene, would be a few to suggest for future study. Moreover, mixtures of solvents, such as a water/methanol or water/ethanol solution may also be worthy of further investigation. Finding strategies to increase the yield of each product using different solvents is also required, as this is necessary for undertaking the analytical techniques for characterisation.

Evaluating a broader range of metal tetrafluoroborates is necessary for further studies to ensure that ACV can retain its function as an antiviral and that the metal does not cause any adverse effects to the patient through in vitro and animal testing. For example, metals already found in existing medications and biologically relevant metals. Metals such as iron ($\text{Fe}(\text{BF}_4)_2$), and magnesium ($\text{Mg}(\text{BF}_4)_2$) could be used as they each have specific in vivo roles.

Different crystallisation methods could also be assessed as these are another way to synthesise new potential polymorphs. Two techniques which could be considered are vapour diffusion and sublimation. These techniques are a suitable expansion of this study, as the solvents already in use, such as methanol and ethanol, have low boiling points and are therefore well suited to vapour-based crystallisation methods.

Mixtures observed in the PXRD data, particularly for the zinc compound for which this study only isolated one polymorph, requires further study. These mixtures will need to be separated in order for the single crystals to be isolated and analysed by single crystal XRD.

Other analytical techniques may also be applied, such as thermal analysis. Using methods such as thermogravimetric analysis (TGA) and differential scanning calorimetry (DSC) would give insight into the solvents within each crystal's structure and the identity of bound solvent to the metal centre. As

well as knowledge of the solvents, polymorphs can switch under different temperatures, and would be identifiable on a TGA spectrum.

Further work into bioactivity and antiviral studies of the crystals featured in this thesis will have to be completed prior to practical application. As previous studies have shown (see in Literature Analysis), metal-ACV complexes are active against fungi microbials, have an impact on viruses for up to 3 consecutive days, and have been used effectively against adenocarcinoma cell (metal dependent). By testing the crystals in this study, new medical beneficial activity could be found.

Bibliography

- [1] W. H. Organization, "Essential medicines and health products," World Health Organization, August 2017. [Online]. Available: <https://www.who.int/medicines/publications/essentialmedicines/en/>. [Accessed 2 April 2019].
- [2] W. Bergmann and R. Feeney, "Contributions to the Study of Marine Products. The Nucleosides of Sponges," *Journal of Organic Chemistry*, vol. 16, no. 6, pp. 981-987, 1951.
- [3] E. De Clercq and H. Field, "Antiviral prodrugs - the development of successful prodrug strategies for antiviral chemotherapy," *British Journal of Pharmacology*, vol. 147, no. 1, pp. 1-11, 2006.
- [4] K. Sepcic, "Bioactive Alkylpyridinium Compounds from Marine Sponges," *Toxin Review*, vol. 19, no. 2, pp. 139-160, 2000.
- [5] E.-C. Mar and e. al., "Inhibition of Cellular DNA Polymerase α and Human Cytomegalovirus-Induced DNA Polymerase by the Triphosphates of 9-(2-Hydroxyethoxymethyl)Guanine and 9-(1,3-Dihydroxy-2-Propoxymethyl)Guanine," *Journal of Virology*, vol. 53, no. 3, pp. 776-780, 1985.
- [6] J. F. Committe, "British National Formulary," in *British National Formulary*, London, BMJ Group and Pharmaceutical Press, 2017, pp. 599-600.
- [7] B. Alberts, *Molecular Biology of the Cell*, New York: Garland Science, 2002.
- [8] K. Guille and W. Clegg, "Anhydrous guanine: a synchrotron study," *Acta Crystallographica Section C*, vol. 62, no. 8, pp. 515-517, 2006.

- [9] D. e. a. Gur, "Guanine Crystallization in Aqueous Solution Enables Control over Crystal Size and Polymorphism," *Crystal Growth & Design*, vol. 16, no. 9, pp. 4975-4980, 2016.
- [10] G. I. Birnbaum and M. Cygler, "Conformational features of acyclonucleosides: structure of acyclovir, an antiherpes agent," *Canadian Journal of Chemistry*, vol. 62, no. 12, pp. 2646-2652, 1984.
- [11] C. Bergstrom and e. al., "Experimental and Computational Screening Models for Prediction of Aqueous Drug Solubility," *Pharmaceutical Research*, vol. 19, no. 2, pp. 182-188, 2002.
- [12] K. Lutker and e. al., "Polymorphs and Hydrates of Acyclovir," *Journal of Pharmaceutical Sciences*, vol. 100, no. 3, pp. 949-963, 2011.
- [13] J. Shamshina and e. al., "Acyclovir as an Ionic Liquid Cation or Anion Can Improve Aqueous Solubility," *ACS Omega*, vol. 2, no. 7, pp. 3483-3493, 2017.
- [14] N. England, "Improving Outcomes Through Personalised Medicine," 7th September 2016. [Online]. Available: <https://www.england.nhs.uk/wp-content/uploads/2016/09/improving-outcomes-personalised-medicine.pdf>. [Accessed 16 August 2020].
- [15] P. Matak and e. al., "Copper Deficiency Leads to Anemia, Duodenal Hypoxia Upregulation of HIF-2 α and Altered Expression of Iron Absorption Genes in Mice," *PLoS One*, vol. 8, no. 3, p. e59538, 2013.
- [16] A. Garcia-Raso and e. al., "Synthesis and structural characteristics of metal acyclovir (ACV) complexes: [Ni(or Co)(ACV)₂(H₂O)₄]Cl₂.2ACV, [Zn(ACV)-Cl₂(H₂O)], Cd(ACV)Cl₂.H₂O and [Hg(ACV)Cl₂]_x. Recognition of acyclovir by Ni-ACV," *Journal of the Chemical Society, Dalton Transactions*, no. 2, pp. 167-173, 1999.
- [17] M. V. Avcioglu and A. Golcu, "Synthesis of Acyclovir Metal Complexes: Spectral, Electrochemical,

- Thermal and DNA Binding Studies," *Synthesis and Reactivity in Inorganic, Metal-Organic, and Nano-Metal Chemistry*, vol. 45, no. 4, pp. 581-590, 2013.
- [18] I. Turel and e. al., "Solution, solid state and biological characterization of ruthenium(III)-DMSO complexes with purine base derivatives," *Journal of Inorganic Biochemistry*, vol. 98, no. 2, pp. 393-401, 2004.
- [19] J. Coverdale and e. al., "Designing Ruthenium Anticancer Drugs: What Have We Learnt from the Key Drug Candidates," *Inorganics*, vol. 7, no. 3, p. 31, 2019.
- [20] P. Matthews, *Advanced Chemistry: Physical and Industrial*, Cambridge: Cambridge University, 2003.
- [21] G. A. Jeffrey, *An Introduction to Hydrogen Bonding*, Oxford: Oxford University Press, 1997.
- [22] I. Turel and e. al., "New studies in the copper (II) acyclovir (acv) system. NMR relaxation studies and the X-ray crystal structure of $[Cu(acv)_2(H_2O)_2](NO_3)_2$," *Polyhedron*, vol. 17, no. 23-24, pp. 4195-4201, 1998.

Appendix A

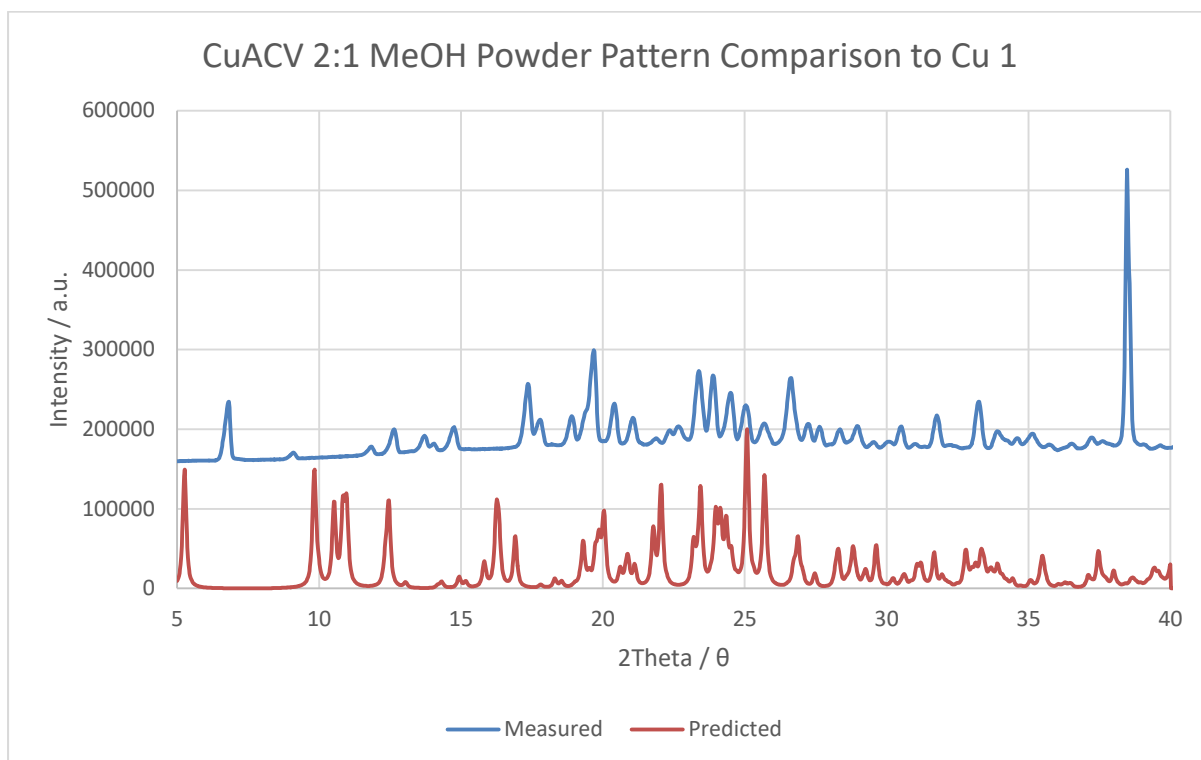


Figure 89

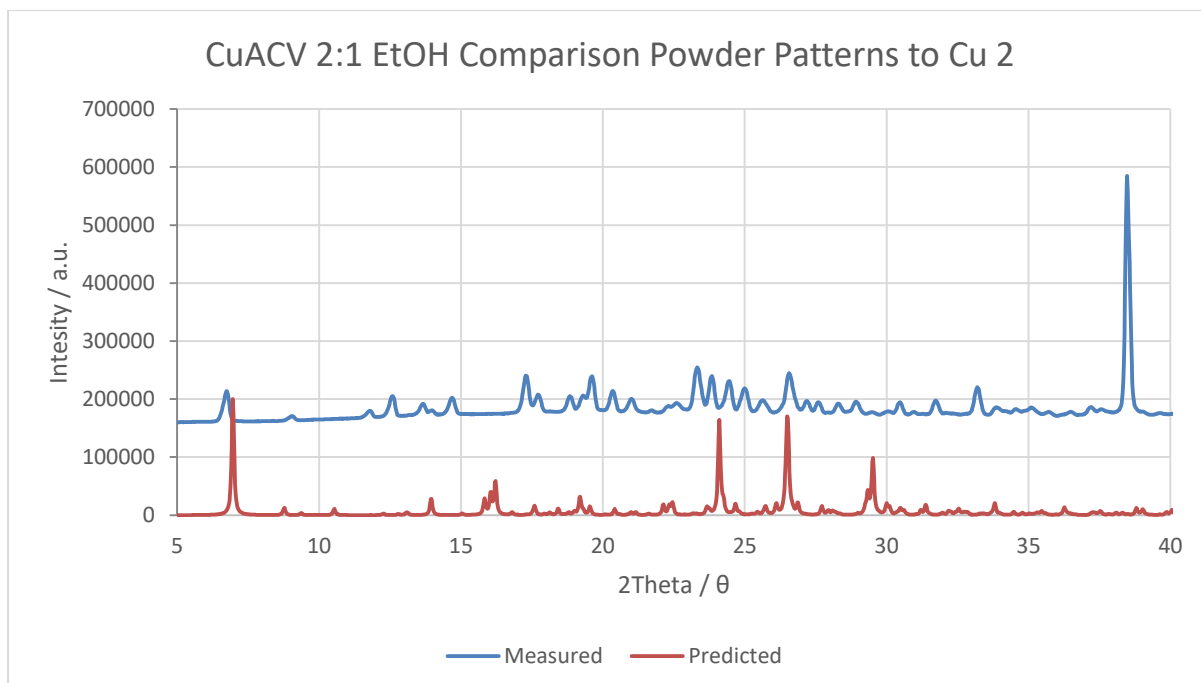


Figure 90

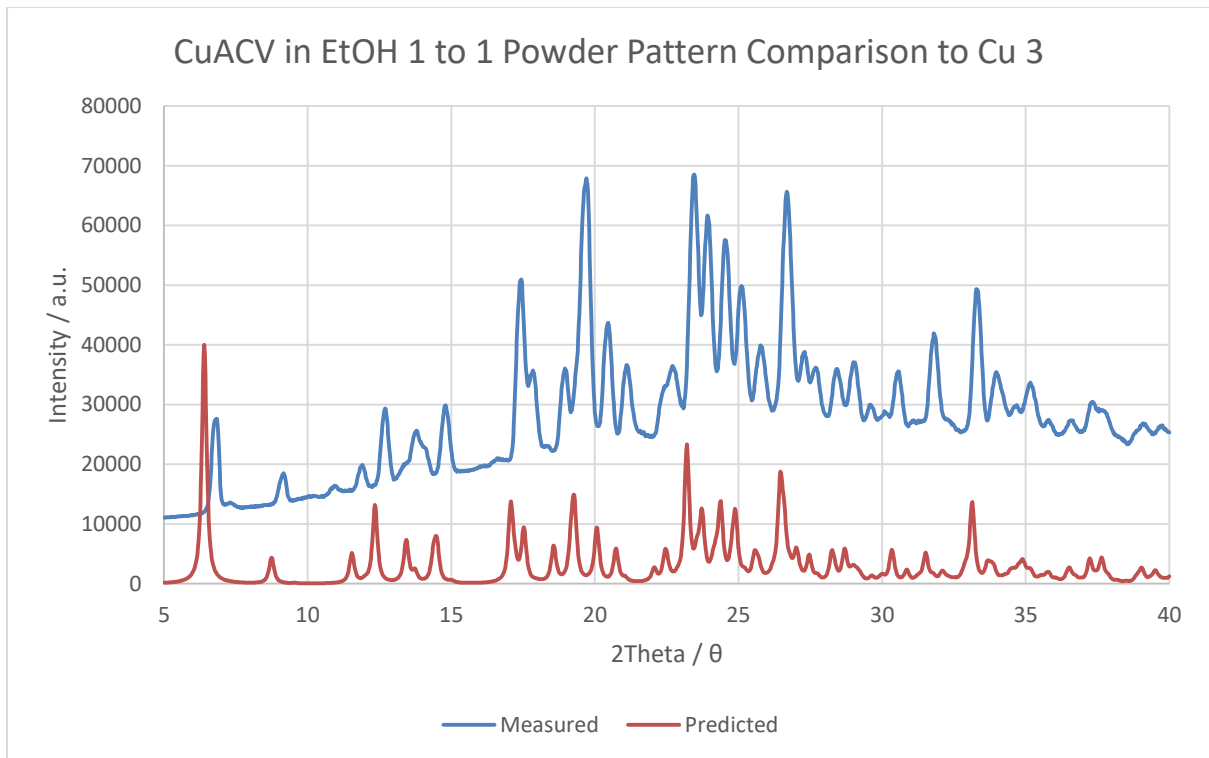


Figure 91

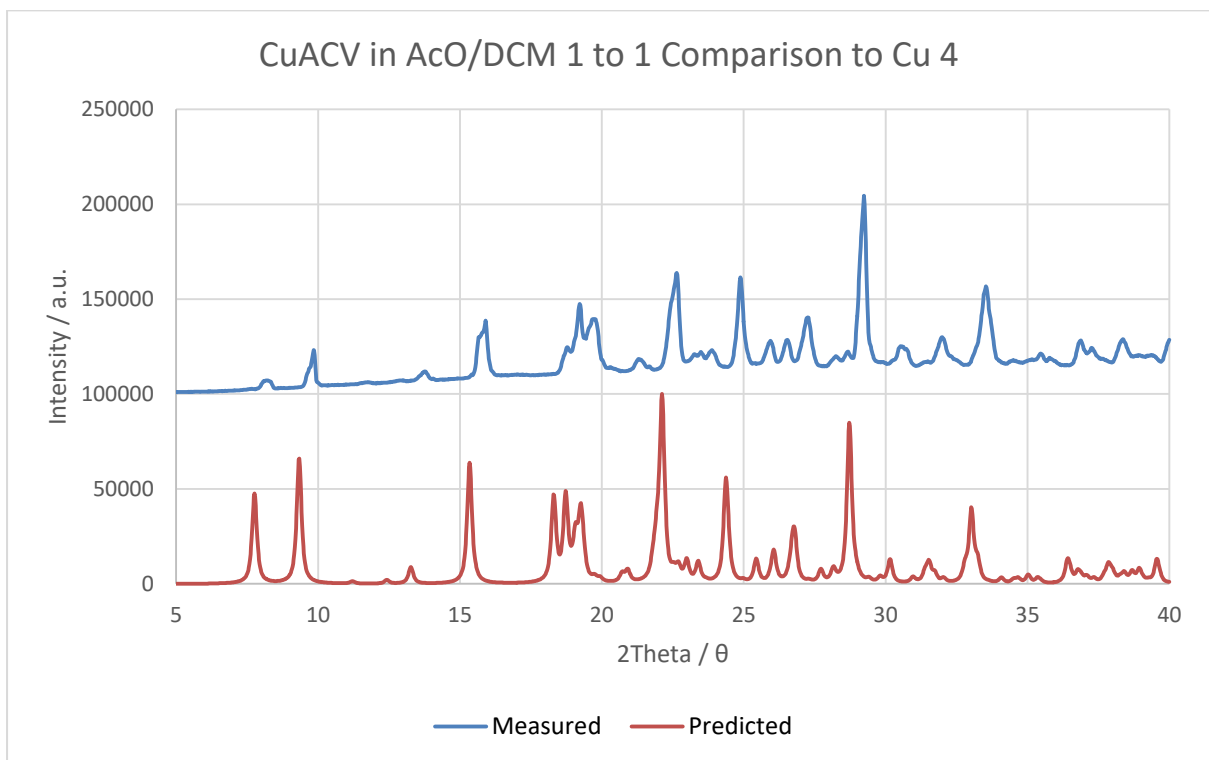


Figure 92

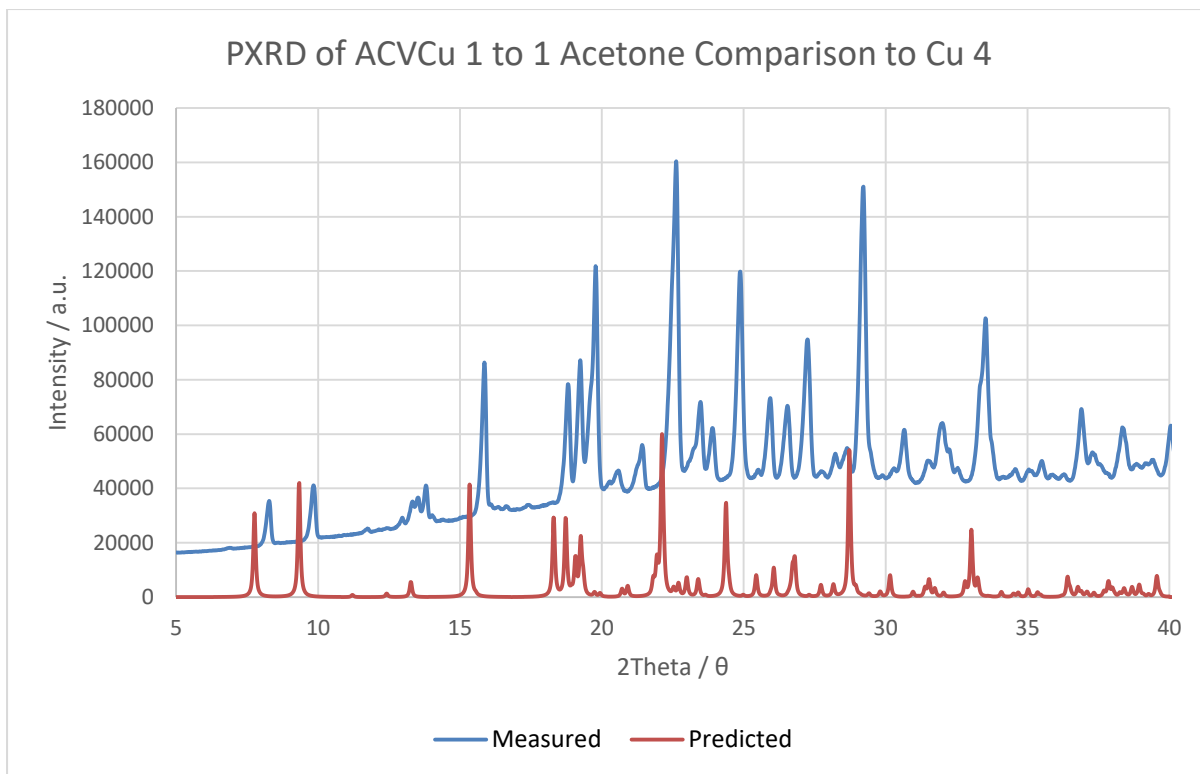


Figure 93

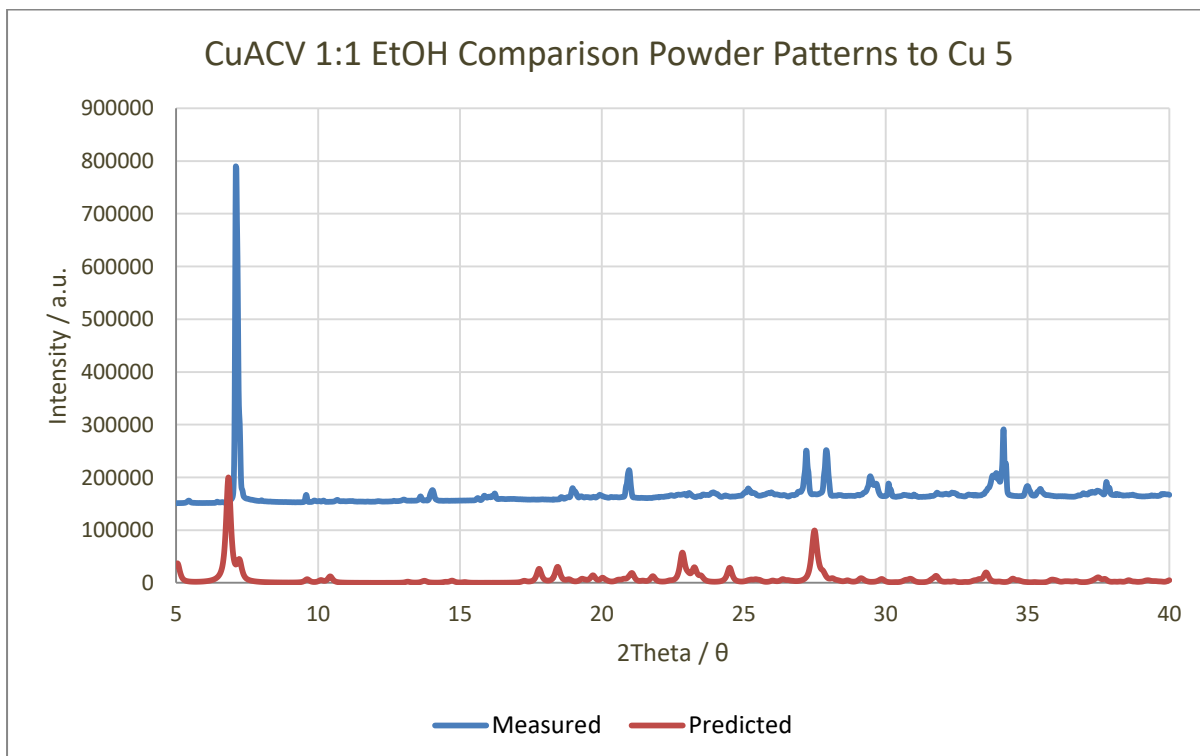


Figure 94

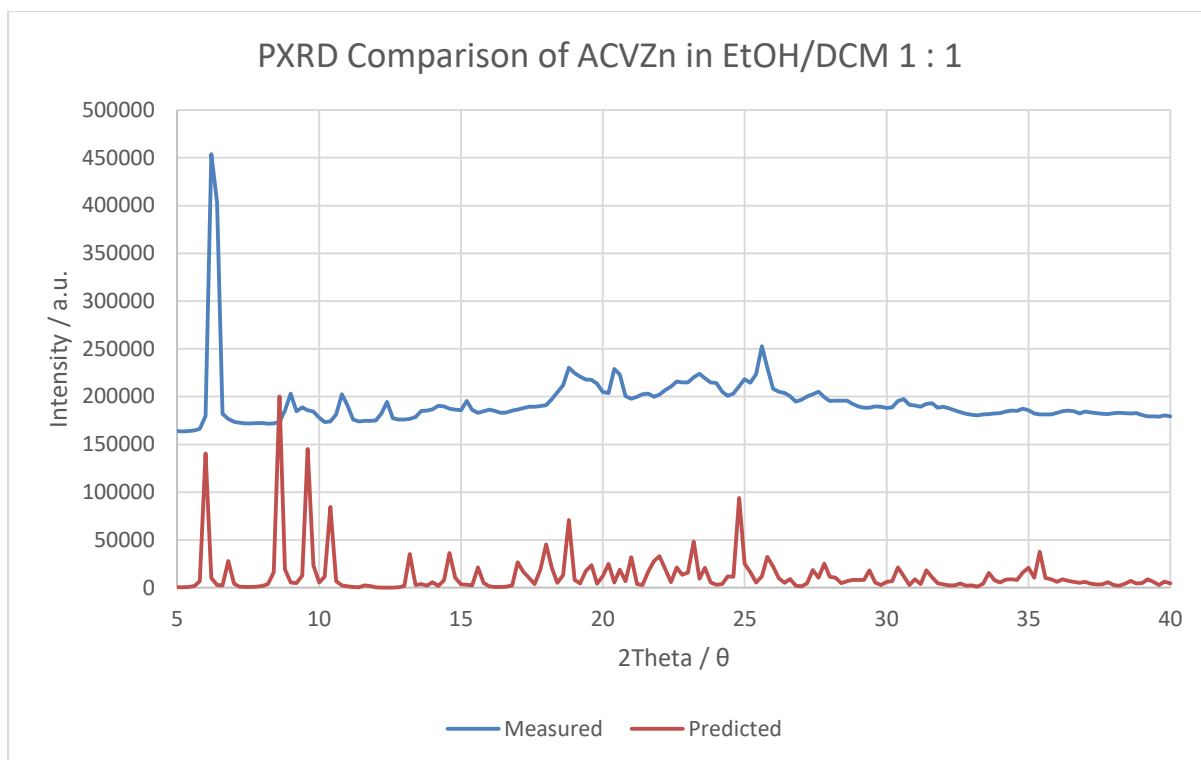


Figure 95

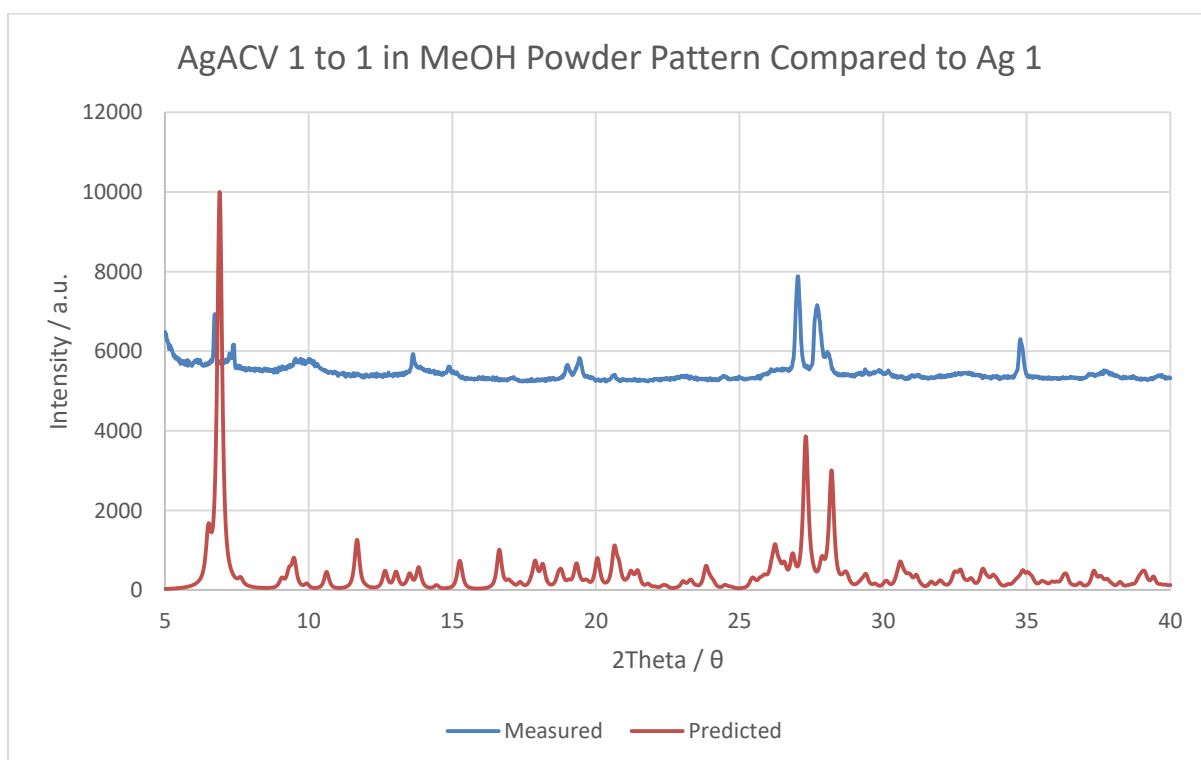


Figure 96

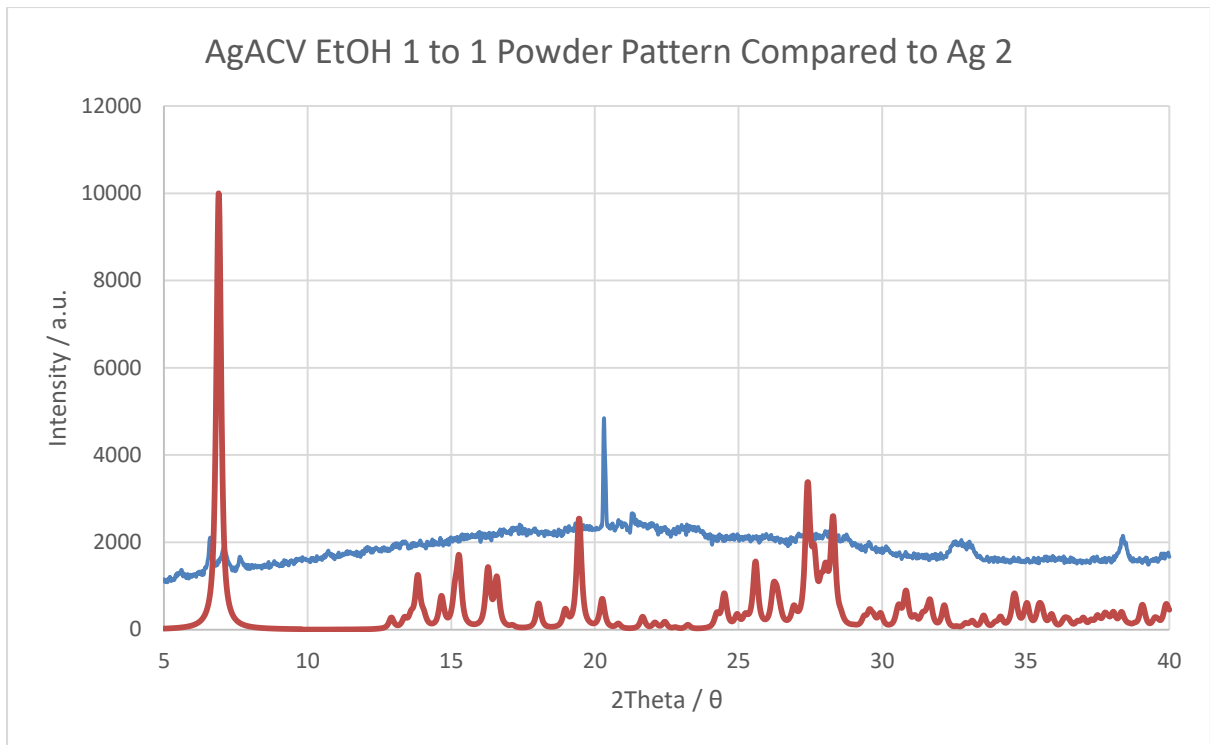


Figure 97

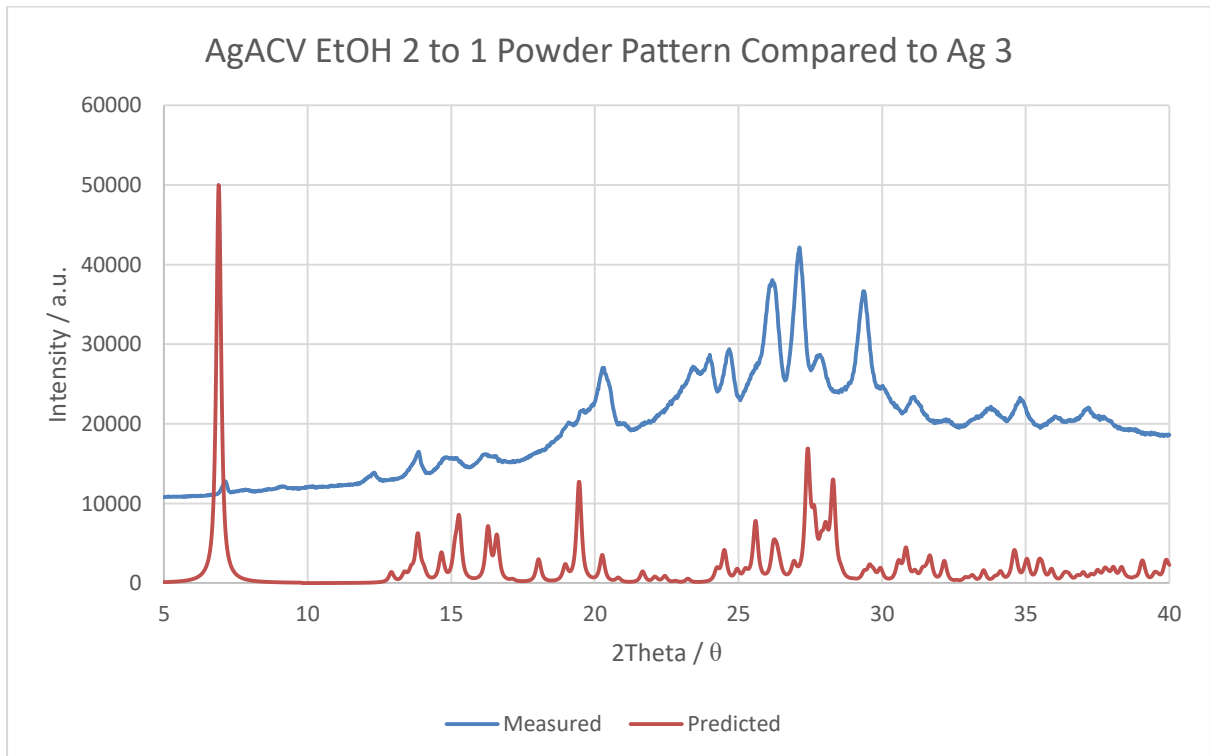


Figure 98

Appendix B

Cu 1 Crystal Data

Identification code	acvcu_002
Empirical formula	C8 H14.69 B Cu0.50 F4 N5 O5.50
Formula weight	387.51
Temperature	99.99(10) K
Wavelength	1.54184 Å
Crystal system	Monoclinic
Space group	P 1 21/n 1
Unit cell dimensions	a = 9.4165(3) Å α = 90° b = 33.5821(9) Å β = 102.693(3)° c = 9.5634(3) Å γ = 90°
Volume	2950.29(16) Å ³
Z	8
Density (calculated)	1.745 Mg/m ³
Absorption coefficient	2.179 mm ⁻¹
F(000)	1577
Theta range for data collection	4.920 to 61.703°
Index ranges	-10 ≤ h ≤ 7, -38 ≤ k ≤ 38, -10 ≤ l ≤ 10
Reflections collected	15245
Independent reflections	4512 [R(int) = 0.0353]
Completeness to theta = 61.703°	98.30%
Absorption correction	Semi-empirical from equivalents
Max. and min. transmission	1.00000 and 0.94070
Refinement method	Full-matrix least-squares on F ²
Data / restraints / parameters	4512 / 5 / 475
Goodness-of-fit on F ²	1.041
Final R indices [I > 2σ(I)]	R1 = 0.0401, wR2 = 0.0993
R indices (all data)	R1 = 0.0517, wR2 = 0.1059
Extinction coefficient	n/a
Largest diff. peak and hole	0.547 and -0.443 e.Å ⁻³

Table 13 – crystal data obtained from CIF data for Cu 1.

Cu 2 Crystal Data

Identification code	acv_cu_1to1
Empirical formula	C10.67 H21.41 Cu0.33 N6.67 O8.71
Formula weight	403.58
Temperature	100.00(10) K
Wavelength	1.54184 Å
Crystal system	Triclinic

Space group	P -1
Unit cell dimensions	a = 7.3965(4) Å α= 69.836(9)°. b = 12.4980(12) Å β= 87.977(6)°. c = 15.5796(14) Å γ = 87.476(6)°.
Volume	1350.3(2) Å ³
Z	3
Density (calculated)	1.489 Mg/m ³
Absorption coefficient	1.466 mm ⁻¹
F(000)	634
Theta range for data collection	3.770 to 72.539°.
Index ranges	-9<=h<=6, -15<=k<=15, -19<=l<=17
Reflections collected	9162
Independent reflections	5152 [R(int) = 0.0446]
Completeness to theta = 67.684°	99.60%
Absorption correction	Semi-empirical from equivalents
Max. and min. transmission	1.00000 and 0.87367
Refinement method	Full-matrix least-squares on F ²
Data / restraints / parameters	5152 / 5 / 354
Goodness-of-fit on F ²	1.252
Final R indices [I>2sigma(I)]	R1 = 0.1077, wR2 = 0.3005
R indices (all data)	R1 = 0.1302, wR2 = 0.3289
Extinction coefficient	n/a
Largest diff. peak and hole	1.835 and -0.858 e.Å ⁻³

Table 14 – crystal data obtained from CIF data for Cu 2.

Cu 3 Crystal Data

Identification code	acvcu_004
Empirical formula	C32 H45 B2 Cu F8 N20 O13
Formula weight	1155.04
Temperature	291.45(10) K
Wavelength	1.54184 Å
Crystal system	Monoclinic
Space group	P 1 21/c 1
Unit cell dimensions	a = 14.1928(8) Å α= 90°. b = 15.3243(7) Å β= 103.552(5)° c = 20.7830(9) Å γ = 90°.
Volume	4394.3(4) Å ³
Z	4
Density (calculated)	1.746 Mg/m ³
Absorption coefficient	1.807 mm ⁻¹
F(000)	2368
Theta range for data collection	3.620 to 70.298°.
Index ranges	-17<=h<=16, -16<=k<=18, -18<=l<=25

Reflections collected	17786
Independent reflections	8113 [R(int) = 0.0459]
Completeness to theta = 67.684°	99.00%
Absorption correction	Semi-empirical from equivalents
Max. and min. transmission	1.00000 and 0.84000
Refinement method	Full-matrix least-squares on F2
Data / restraints / parameters	8113 / 0 / 712
Goodness-of-fit on F2	1.013
Final R indices [I>2sigma(I)]	R1 = 0.0466, wR2 = 0.1049
R indices (all data)	R1 = 0.0791, wR2 = 0.1207
Extinction coefficient	n/a
Largest diff. peak and hole	0.816 and -0.528 e.Å ⁻³

Table 15 – crystal data obtained from CIF data for Cu 3.

Cu 4 Crystal Data

Identification code	cu_acetone
Empirical formula	C8 H13 B Cu0.50 F4 N5 O4
Formula weight	361.81
Temperature	300.00(15) K
Wavelength	1.54184 Å
Crystal system	Monoclinic
Space group	P 1 21/n 1
Unit cell dimensions	a = 4.9311(3) Å α= 90°. b = 14.2453(6) Å β= 93.914(4)°. c = 18.9826(8) Å γ = 90°
Volume	1330.32(11) Å ³
Z	4
Density (calculated)	1.806 Mg/m ³
Absorption coefficient	2.278 mm ⁻¹
F(000)	734
Theta range for data collection	3.883 to 61.552°.
Index ranges	-5<=h<=3, -15<=k<=7, -16<=l<=21
Reflections collected	3799
Independent reflections	2035 [R(int) = 0.0270]
Completeness to theta = 61.552°	98.10%
Absorption correction	Semi-empirical from equivalents
Max. and min. transmission	1.00000 and 0.91685
Refinement method	Full-matrix least-squares on F2
Data / restraints / parameters	2035 / 0 / 215
Goodness-of-fit on F2	1.074
Final R indices [I>2sigma(I)]	R1 = 0.0408, wR2 = 0.1052
R indices (all data)	R1 = 0.0571, wR2 = 0.1142
Extinction coefficient	n/a

Largest diff. peak and hole	0.489 and -0.424 e.Å ⁻³
-----------------------------	------------------------------------

Table 16 – crystal data obtained from CIF data for Cu 4.

Cu 5 Crystal Data

Identification code	cuacv4
Empirical formula	C16 H24 B Cu0.50 F4 N10 O8.00
Formula weight	603.39
Temperature	263(50) K
Wavelength	1.54184 Å
Crystal system	Triclinic
Space group	P -1
Unit cell dimensions	a = 5.0065(3) Å α= 106.683(4)°. b = 13.5389(6) Å β= 91.482(4)°. c = 18.2983(8) Å γ = 94.832(4)°
Volume	1182.25(11) Å ³
Z	2
Density (calculated)	1.695 Mg/m ³
Absorption coefficient	1.758 mm ⁻¹
F(000)	619
Theta range for data collection	3.616 to 70.126°.
Index ranges	-5<=h<=6, -16<=k<=15, -22<=l<=21
Reflections collected	7599
Independent reflections	4335 [R(int) = 0.0343]
Completeness to theta = 67.684°	99.20%
Absorption correction	Semi-empirical from equivalent
Max. and min. transmission	1.00000 and 0.73562
Refinement method	Full-matrix least-squares on F ²
Data / restraints / parameters	4335 / 0 / 389
Goodness-of-fit on F ²	1.039
Final R indices [I>2σ(I)]	R1 = 0.0573, wR2 = 0.1590
R indices (all data)	R1 = 0.0638, wR2 = 0.1692
Extinction coefficient	n/a
Largest diff. peak and hole	0.801 and -0.761 e.Å ⁻³

Table 17 – crystal data obtained from CIF data for Cu 5.

Zn 1 Crystal Data

Identification code	acvzn_001
Empirical formula	C34 H54 F6 N20 O16 Si Zn
Formula weight	1206.43
Temperature	149.99(10) K
Wavelength	1.54184 Å
Crystal system	Triclinic
Space group	P -1
Unit cell dimensions	a = 13.1171(2) Å α= 94.6280(10)°

	b = 13.3905(2) Å β= 95.3660(10)°. c = 14.8131(2) Å γ = 103.6360(10)°
Volume	2503.19(6) Å ³
Z	2
Density (calculated)	1.601 Mg/m ³
Absorption coefficient	1.891 mm ⁻¹
F(000)	1248
Theta range for data collection	3.491 to 72.378°.
Index ranges	-16<=h<=15, -16<=k<=16, -18<=l<=18
Reflections collected	37222
Independent reflections	9745 [R(int) = 0.0349]
Completeness to theta = 67.684°	99.90%
Absorption correction	Semi-empirical from equivalents
Max. and min. transmission	1.00000 and 0.83757
Refinement method	Full-matrix least-squares on F ²
Data / restraints / parameters	9745 / 0 / 725
Goodness-of-fit on F ²	1.045
Final R indices [I>2sigma(I)]	R1 = 0.0531, wR2 = 0.1393
R indices (all data)	R1 = 0.0605, wR2 = 0.1449
Extinction coefficient	n/a
Largest diff. peak and hole	1.412 and -0.714 e.Å ⁻³

Table 18 – crystal data obtained from CIF data for Zn 1.

Ag 1 Crystal Data

Identification code	acvag_001
Empirical formula	C40 H60 Ag4 B0.25 F13 N49 O14 P2 Si0.25
Formula weight	2201.51
Temperature	150.00(10) K
Wavelength	1.54184 Å
Crystal system	Monoclinic
Space group	P 1 2/c 1
Unit cell dimensions	a = 10.6064(4) Å α= 90°. b = 25.5910(11) Å β= 96.192(4)° c = 27.2880(12) Å γ = 90°.
Volume	7363.5(5) Å ³
Z	4
Density (calculated)	1.986 Mg/m ³
Absorption coefficient	10.004 mm ⁻¹
F(000)	4379
Theta range for data collection	3.454 to 61.720°.
Index ranges	-12<=h<=11, -28<=k<=13, -29<=l<=31
Reflections collected	21889
Independent reflections	11243 [R(int) = 0.0320]

Completeness to theta = 61.720°	97.80%
Absorption correction	Semi-empirical from equivalents
Max. and min. transmission	1.00000 and 0.79986
Refinement method	Full-matrix least-squares on F2
Data / restraints / parameters	11243 / 0 / 493
Goodness-of-fit on F2	1.037
Final R indices [$I > 2\sigma(I)$]	R1 = 0.1079, wR2 = 0.2940
R indices (all data)	R1 = 0.1564, wR2 = 0.3401
Extinction coefficient	n/a
Largest diff. peak and hole	4.017 and -1.463 e.Å ⁻³

Table 19 – crystal data obtained from CIF data for Ag 1.

Ag 2 Crystal Data

Identification code	acvag_002
Empirical formula	C15 H0.50 Ag F4 N6 O3 Si0.50
Formula weight	521.44
Temperature	100.00(10) K
Wavelength	1.54184 Å
Crystal system	Monoclinic
Space group	P 1 21 1
Unit cell dimensions	a = 7.0464(2) Å α = 90° b = 25.5833(8) Å β = 112.646(4)° c = 7.4217(2) Å γ = 90°
Volume	1234.76(7) Å ³
Z	2
Density (calculated)	1.402 Mg/m ³
Absorption coefficient	7.292 mm ⁻¹
F(000)	503
Theta range for data collection	6.462 to 66.319°.
Index ranges	-8 ≤ h ≤ 8, -30 ≤ k ≤ 30, -8 ≤ l ≤ 8
Reflections collected	20405
Independent reflections	4274 [R(int) = 0.0665]
Completeness to theta = 66.319°	99.20%
Absorption correction	Semi-empirical from equivalents
Max. and min. transmission	1.00000 and 0.76044
Refinement method	Full-matrix least-squares on F2
Data / restraints / parameters	4274 / 1 / 377
Goodness-of-fit on F2	1.727
Final R indices [$I > 2\sigma(I)$]	R1 = 0.1546, wR2 = 0.3459
R indices (all data)	R1 = 0.1550, wR2 = 0.3466
Absolute structure parameter	0.178(9)
Extinction coefficient	n/a
Largest diff. peak and hole	19.922 and -2.885 e.Å ⁻³

Table 20 – crystal data obtained from CIF data for Ag 2.

Ag 3 Crystal Data

Identification code	acvag2to1
Empirical formula	C32 H49 Ag2 F6 N20 O15 Si
Formula weight	1311.74
Temperature	291.45(10) K
Wavelength	1.54184 Å
Crystal system	Triclinic
Space group	P -1
Unit cell dimensions	a = 10.1680(3) Å α = 97.841(2)°. b = 14.9186(5) Å β = 97.279(2)°. c = 16.6814(5) Å γ = 108.993(3)°
Volume	2330.43(13) Å ³
Z	2
Density (calculated)	1.869 Mg/m ³
Absorption coefficient	8.006 mm ⁻¹
F(000)	1326
Theta range for data collection	3.781 to 70.205°.
Index ranges	-9<=h<=12, -17<=k<=18, -19<=l<=20
Reflections collected	16243
Independent reflections	8625 [R(int) = 0.0346]
Completeness to theta = 67.684°	99.50%
Absorption correction	Semi-empirical from equivalents
Max. and min. transmission	1.00000 and 0.51167
Refinement method	Full-matrix least-squares on F ²
Data / restraints / parameters	8625 / 3 / 706
Goodness-of-fit on F ²	1.049
Final R indices [I>2sigma(I)]	R1 = 0.0685, wR2 = 0.1830
R indices (all data)	R1 = 0.0746, wR2 = 0.1908
Extinction coefficient	n/a
Largest diff. peak and hole	1.628 and -1.505 e.Å ⁻³

Table 21 – crystal data obtained from CIF data for Ag 3.

Appendix C

Crystal 1

Bond Lengths (Å)		Bond Angles (°)	
Cu(1)-O(8)	1.9772	O(8)-Cu(1)-O(11)	89.469
Cu(1)-O(11)	2.2182	O(8)-Cu(1)-N(6)	179.3911
Cu(1)-O(7)	1.9552	O(8)-Cu(1)-N(5)	87.331
Cu(1)-N(6)	2.0143	O(7)-Cu(1)-O(8)	87.219
Cu(1)-N(5)	1.9893	O(7)-Cu(1)-O(11)	108.171
F(8)-B(2)	1.3804	O(7)-Cu(1)-N(6)	92.471
F(6)-B(2)	1.4064	O(7)-Cu(1)-N(5)	160.4011
F(5)-B(2)	1.3824	N(6)-Cu(1)-O(11)	90.151
F(7)-B(2)	1.3965	N(5)-Cu(1)-O(11)	90.591
O(4)-C(13)	1.2474	N(5)-Cu(1)-N(6)	93.141
O(5)-C(14)	1.4134	C(14)-O(5)-C(15)	113.52
O(5)-C(15)	1.4454	Cu(1)-O(8)-H(8A)	110.4
O(1)-C(5)	1.2304	Cu(1)-O(8)-H(8B)	110
F(4)-B(1)	1.3855	H(8A)-O(8)-H(8B)	104
F(1)-B(1)	1.3685	C(8)-O(3)-H(3)	109.5
O(8)-H(8A)	0.8606	C(16)-O(6)-H(6)	109.5
O(8)-H(8B)	0.8587	Cu(1)-O(11)-H(11A)	111.3
F(3)-B(1)	1.3895	Cu(1)-O(11)-H(11B)	111
O(3)-H(3)	0.82	H(11A)-O(11)-H(11B)	102.8
O(3)-C(8)	1.4294	Cu(1)-O(7)-H(7A)	110.2
O(6)-H(6)	0.82	Cu(1)-O(7)-H(7B)	110.7
O(6)-C(16)	1.4384	H(7A)-O(7)-H(7B)	103.5
O(11)-H(11A)	0.8842	C(13)-N(9)-H(9)	116.9
O(11)-H(11B)	0.8838	C(12)-N(9)-H(9)	116.9
O(7)-H(7A)	0.8638	C(12)-N(9)-C(13)	126.23
O(7)-H(7B)	0.8663	C(10)-N(6)-Cu(1)	137.22
F(2)-B(1)	1.4065	C(9)-N(6)-Cu(1)	118.42
N(9)-H(9)	0.86	C(9)-N(6)-C(10)	104.43
N(9)-C(13)	1.3844	C(1)-N(5)-Cu(1)	134.22
N(9)-C(12)	1.3754	C(1)-N(5)-C(2)	105.32
N(6)-C(10)	1.4064	C(2)-N(5)-Cu(1)	119.32
N(6)-C(9)	1.3134	C(11)-N(7)-C(14)	125.73
N(5)-C(1)	1.3144	C(9)-N(7)-C(11)	106.93
N(5)-C(2)	1.3844	C(9)-N(7)-C(14)	127.43
N(7)-C(11)	1.3754	H(10C)-O(10)-H(10D)	104.6
N(7)-C(14)	1.4574	C(4)-N(2)-C(3)	112.33
N(7)-C(9)	1.3564	C(3)-N(4)-C(6)	127.23
O(10)-H(10C)	0.8508	C(1)-N(4)-C(3)	106.72
O(10)-H(10D)	0.8496	C(1)-N(4)-C(6)	126.03
N(2)-C(3)	1.3614	C(12)-N(8)-C(11)	112.13

N(2)-C(4)	1.3204	C(5)-N(3)-H(3A)	117.2
N(4)-C(3)	1.3754	C(4)-N(3)-H(3A)	117.2
N(4)-C(1)	1.3654	C(4)-N(3)-C(5)	125.53
N(4)-C(6)	1.4684	H(10A)-N(10)-H(10B)	120
N(8)-C(11)	1.3444	C(12)-N(10)-H(10A)	120
N(8)-C(12)	1.3314	C(12)-N(10)-H(10B)	120
N(3)-H(3A)	0.86	H(9B)-O(9)-H(9C)	104.3
N(3)-C(5)	1.3984	H(1A)-N(1)-H(1B)	131
N(3)-C(4)	1.3724	C(4)-N(1)-H(1A)	110.1
N(10)-H(10A)	0.86	C(4)-N(1)-H(1B)	1122
N(10)-H(10B)	0.86	N(6)-C(10)-C(13)	132.93
N(10)-C(12)	1.3334	C(11)-C(10)-N(6)	109.53
O(9)-H(9B)	0.8518	C(11)-C(10)-C(13)	117.53
O(9)-H(9C)	0.8513	N(7)-C(11)-C(10)	105.93
N(1)-H(1A)	0.8626	N(8)-C(11)-N(7)	124.23
N(1)-C(4)	1.3454	N(8)-C(11)-C(10)	129.83
N(1)-H(1B)	0.85119	N(2)-C(3)-N(4)	126.53
C(10)-C(11)	1.3814	N(2)-C(3)-C(2)	127.43
C(10)-C(13)	1.4214	C(2)-C(3)-N(4)	106.03
C(3)-C(2)	1.3644	N(5)-C(1)-N(4)	111.93
C(1)-H(1)	0.93	N(5)-C(1)-H(1)	124.1
C(2)-C(5)	1.4164	N(4)-C(1)-H(1)	124.1
C(14)-H(14A)	0.97	O(4)-C(13)-N(9)	119.73
C(14)-H(14B)	0.97	O(4)-C(13)-C(10)	128.53
C(9)-H(9A)	0.93	N(9)-C(13)-C(10)	111.83
C(6)-H(6A)	0.97	N(5)-C(2)-C(5)	129.33
C(6)-H(6B)	0.97	C(3)-C(2)-N(5)	110.13
C(6)-O(2B)	1.3425	C(3)-C(2)-C(5)	120.63
C(6)-O(2A)	1.5018	O(1)-C(5)-N(3)	122.33
C(15)-H(15A)	0.97	O(1)-C(5)-C(2)	127.53
C(15)-H(15B)	0.97	N(3)-C(5)-C(2)	110.23
C(15)-C(16)	1.4915	N(8)-C(12)-N(9)	122.53
C(8)-H(8BB)	1.019	N(8)-C(12)-N(10)	119.83
C(8)-C(7A)	1.5599	N(10)-C(12)-N(9)	117.73
C(8)-C(7B)	1.4179	N(2)-C(4)-N(3)	123.63
C(8)-H(8AA)	0.796	N(2)-C(4)-N(1)	119.33
C(16)-H(16A)	0.97	N(1)-C(4)-N(3)	117.03
C(16)-H(16B)	0.97	O(5)-C(14)-N(7)	111.12
O(2B)-C(7B)	1.2969	O(5)-C(14)-H(14A)	109.4
C(7A)-H(7AA)	0.93	O(5)-C(14)-H(14B)	109.4
C(7A)-O(2A)	0.9088	N(7)-C(14)-H(14A)	109.4
C(7B)-H(7BA)	0.93	N(7)-C(14)-H(14B)	109.4
		H(14A)-C(14)-H(14B)	108
		N(6)-C(9)-N(7)	113.23
		N(6)-C(9)-H(9A)	123.4
		N(7)-C(9)-H(9A)	123.4

N(4)-C(6)-H(6A)	109.8
N(4)-C(6)-H(6B)	109.8
N(4)-C(6)-O(2A)	109.53
H(6A)-C(6)-H(6B)	108.2
O(2B)-C(6)-N(4)	112.43
O(2A)-C(6)-H(6A)	109.8
O(2A)-C(6)-H(6B)	109.8
O(5)-C(15)-H(15A)	108.9
O(5)-C(15)-H(15B)	108.9
O(5)-C(15)-C(16)	113.23
H(15A)-C(15)-H(15B)	107.8
C(16)-C(15)-H(15A)	108.9
C(16)-C(15)-H(15B)	108.9
O(3)-C(8)-H(8BB)	1055
O(3)-C(8)-C(7A)	112.14
O(3)-C(8)-H(8AA)	1074
H(8BB)-C(8)-H(8AA)	1026
C(7A)-C(8)-H(8AA)	1284
C(7B)-C(8)-O(3)	114.74
C(7B)-C(8)-H(8BB)	1255
C(7B)-C(8)-H(8AA)	1004
O(6)-C(16)-C(15)	112.43
O(6)-C(16)-H(16A)	109.1
O(6)-C(16)-H(16B)	109.1
C(15)-C(16)-H(16A)	109.1
C(15)-C(16)-H(16B)	109.1
H(16A)-C(16)-H(16B)	107.9
F(8)-B(2)-F(6)	109.03
F(8)-B(2)-F(5)	110.13
F(8)-B(2)-F(7)	110.73
F(5)-B(2)-F(6)	109.13
F(5)-B(2)-F(7)	109.93
F(7)-B(2)-F(6)	108.13
F(4)-B(1)-F(3)	109.54
F(4)-B(1)-F(2)	110.03
F(1)-B(1)-F(4)	110.93
F(1)-B(1)-F(3)	110.83
F(1)-B(1)-F(2)	108.64
F(3)-B(1)-F(2)	107.03
C(7B)-O(2B)-C(6)	136.77
C(8)-C(7A)-H(7AA)	113.1
O(2A)-C(7A)-C(8)	133.88
O(2A)-C(7A)-H(7AA)	113.1
C(7A)-O(2A)-C(6)	141.89
C(8)-C(7B)-H(7BA)	115.3
O(2B)-C(7B)-C(8)	129.47

Table 22

Crystal 2

Bond Lengths (Å)		Bond Angles (°)	
Cu(1)-O(8)	1.9483	O(8)-Cu(1)-O(8)#1	180.02
Cu(1)-O(8)#1	1.9483	O(8)-Cu(1)-O(9)#1	84.8315
Cu(1)-O(9)#1	2.4174	O(8)#1-Cu(1)-O(9)#1	95.1715
Cu(1)-O(9)	2.4174	O(8)-Cu(1)-O(9)	95.1715
Cu(1)-N(1)	2.0564	O(8)#1-Cu(1)-O(9)	84.8315
Cu(1)-N(1)#1	2.0564	O(8)-Cu(1)-N(1)	86.8615
O(1)-C(7)	1.2507	O(8)-Cu(1)-N(1)#1	93.1415
O(8)-H(8A)	0.9297	O(8)#1-Cu(1)-N(1)	93.1415
O(8)-H(8B)	0.9262	O(8)#1-Cu(1)-N(1)#1	86.8615
O(4)-C(9)	1.2447	O(9)-Cu(1)-O(9)#1	180
O(9)-H(9A)	0.9883	N(1)-Cu(1)-O(9)#1	88.6315
O(9)-H(9B)	0.9874	N(1)#1-Cu(1)-O(9)#1	91.3715
N(4)-H(4)	0.86	N(1)-Cu(1)-O(9)	91.3715
N(4)-C(7)	1.3806	N(1)#1-Cu(1)-O(9)	88.6315
N(4)-C(8)	1.3777	N(1)-Cu(1)-N(1)#1	180.02
N(9)-H(9)	0.86	Cu(1)-O(8)-H(8A)	114.3
N(9)-C(9)	1.3907	Cu(1)-O(8)-H(8B)	114
N(9)-C(12)	1.3638	H(8A)-O(8)-H(8B)	99.7
N(3)-C(2)	1.3476	Cu(1)-O(9)-H(9A)	115.3
N(3)-C(8)	1.3198	Cu(1)-O(9)-H(9B)	115
N(8)-C(11)	1.3387	H(9A)-O(9)-H(9B)	98.6
N(8)-C(12)	1.3377	C(7)-N(4)-H(4)	117.4
N(7)-C(10)	1.3926	C(8)-N(4)-H(4)	117.4
N(7)-C(13)	1.3048	C(8)-N(4)-C(7)	125.35
N(1)-C(3)	1.3107	C(9)-N(9)-H(9)	117
N(1)-C(1)	1.3966	C(12)-N(9)-H(9)	117
O(2)-C(4)	1.3878	C(12)-N(9)-C(9)	126.04
O(2)-C(5)	1.4488	C(8)-N(3)-C(2)	112.55
N(2)-C(2)	1.3717	C(12)-N(8)-C(11)	111.45
N(2)-C(3)	1.3706	C(13)-N(7)-C(10)	105.25
N(2)-C(4)	1.4677	C(3)-N(1)-Cu(1)	120.33
C(7)-C(1)	1.4287	C(3)-N(1)-C(1)	104.84
N(6)-C(11)	1.3797	C(1)-N(1)-Cu(1)	134.94
N(6)-C(13)	1.3828	C(4)-O(2)-C(5)	112.75
N(6)-C(14)	1.4749	C(2)-N(2)-C(4)	127.44
N(5)-H(5A)	0.86	C(3)-N(2)-C(2)	107.14
N(5)-H(5B)	0.86	C(3)-N(2)-C(4)	125.45
N(5)-C(8)	1.3387	O(1)-C(7)-N(4)	119.45
N(10)-H(10A)	0.86	O(1)-C(7)-C(1)	128.74
N(10)-H(10B)	0.86	N(4)-C(7)-C(1)	112.05
N(10)-C(12)	1.3427	C(11)-N(6)-C(13)	106.65

C(10)-C(9)	1.4117	C(11)-N(6)-C(14)	125.95
C(10)-C(11)	1.3908	C(13)-N(6)-C(14)	127.55
C(2)-C(1)	1.3777	H(5A)-N(5)-H(5B)	120
O(5)-C(15)	1.40816	C(8)-N(5)-H(5A)	120
O(5)-C(14)	1.37711	C(8)-N(5)-H(5B)	120
C(3)-H(3)	0.93	H(10A)-N(10)-H(10B)	120
O(3)-H(3A)	0.82	C(12)-N(10)-H(10A)	120
O(3)-C(6)	1.45913	C(12)-N(10)-H(10B)	120
C(13)-H(13)	0.93	N(7)-C(10)-C(9)	130.75
C(4)-H(4A)	0.97	C(11)-C(10)-N(7)	110.14
C(4)-H(4B)	0.97	C(11)-C(10)-C(9)	119.15
C(5)-H(5C)	0.97	O(4)-C(9)-N(9)	120.95
C(5)-H(5D)	0.97	O(4)-C(9)-C(10)	128.25
C(5)-C(6)	1.47213	N(9)-C(9)-C(10)	110.95
C(6)-H(6A)	0.97	N(3)-C(2)-N(2)	125.75
C(6)-H(6B)	0.97	N(3)-C(2)-C(1)	128.75
C(15)-H(15A)	0.97	N(2)-C(2)-C(1)	105.64
C(15)-H(15B)	0.97	N(8)-C(11)-N(6)	125.75
C(15)-H(15C)	0.97	N(8)-C(11)-C(10)	128.95
C(15)-H(15D)	0.97	N(6)-C(11)-C(10)	105.45
C(15)-C(16A)	1.552	N(3)-C(8)-N(4)	123.45
C(15)-C(16B)	1.563	N(3)-C(8)-N(5)	120.65
C(16A)-H(16A)	0.97	N(5)-C(8)-N(4)	116.05
C(16A)-H(16B)	0.97	C(14)-O(5)-C(15)	115.49
C(16A)-O(6A)	1.47315	N(1)-C(3)-N(2)	112.35
O(6A)-H(6AA)	0.82	N(1)-C(3)-H(3)	123.8
C(16B)-H(16C)	0.97	N(2)-C(3)-H(3)	123.8
C(16B)-H(16D)	0.97	N(1)-C(1)-C(7)	131.75
C(16B)-O(6B)	1.46716	C(2)-C(1)-N(1)	110.14
O(6B)-H(6BA)	0.82	C(2)-C(1)-C(7)	118.24
C(14)-H(14A)	0.97	C(6)-O(3)-H(3A)	109.5
C(14)-H(14B)	0.97	N(8)-C(12)-N(9)	123.85
O(7)-H(7A)	1.0579	N(8)-C(12)-N(10)	118.85
O(7)-H(7B)	0.561	N(10)-C(12)-N(9)	117.35
O(7)-H(7B)#2	0.561	N(7)-C(13)-N(6)	112.65
O(14)-H(14C)	0.9183	N(7)-C(13)-H(13)	123.7
O(14)-H(14D)	0.8508	N(6)-C(13)-H(13)	123.7
O(10)-H(10C)	0.8356	O(2)-C(4)-N(2)	112.04
O(10)-H(10D)	0.8504	O(2)-C(4)-H(4A)	109.2
		O(2)-C(4)-H(4B)	109.2
		N(2)-C(4)-H(4A)	109.2
		N(2)-C(4)-H(4B)	109.2
		H(4A)-C(4)-H(4B)	107.9
		O(2)-C(5)-H(5C)	109.8
		O(2)-C(5)-H(5D)	109.8
		O(2)-C(5)-C(6)	109.27

H(5C)-C(5)-H(5D)	108.3
C(6)-C(5)-H(5C)	109.8
C(6)-C(5)-H(5D)	109.8
O(3)-C(6)-C(5)	109.67
O(3)-C(6)-H(6A)	109.7
O(3)-C(6)-H(6B)	109.7
C(5)-C(6)-H(6A)	109.7
C(5)-C(6)-H(6B)	109.7
H(6A)-C(6)-H(6B)	108.2
O(5)-C(15)-H(15A)	108.7
O(5)-C(15)-H(15B)	108.7
O(5)-C(15)-H(15C)	110
O(5)-C(15)-H(15D)	110
O(5)-C(15)-C(16A)	114.115
O(5)-C(15)-C(16B)	108.518
H(15A)-C(15)-H(15B)	107.6
H(15C)-C(15)-H(15D)	108.4
C(16A)-C(15)-H(15A)	108.7
C(16A)-C(15)-H(15B)	108.7
C(16B)-C(15)-H(15C)	110
C(16B)-C(15)-H(15D)	110
C(15)-C(16A)-H(16A)	102.2
C(15)-C(16A)-H(16B)	102.2
H(16A)-C(16A)-H(16B)	104.8
O(6A)-C(16A)-C(15)	1392
O(6A)-C(16A)-H(16A)	102.2
O(6A)-C(16A)-H(16B)	102.2
C(16A)-O(6A)-H(6AA)	109.5
C(15)-C(16B)-H(16C)	105.8
C(15)-C(16B)-H(16D)	105.8
H(16C)-C(16B)-H(16D)	106.2
O(6B)-C(16B)-C(15)	1263
O(6B)-C(16B)-H(16C)	105.8
O(6B)-C(16B)-H(16D)	105.8
C(16B)-O(6B)-H(6BA)	109.5
N(6)-C(14)-H(14A)	109.1
N(6)-C(14)-H(14B)	109.1
O(5)-C(14)-N(6)	112.65
O(5)-C(14)-H(14A)	109.1
O(5)-C(14)-H(14B)	109.1
H(14A)-C(14)-H(14B)	107.8
H(7A)-O(7)-H(7B)#2	72.5
H(7A)-O(7)-H(7B)	107.5
H(7B)-O(7)-H(7B)#2	180
H(14C)-O(14)-H(14D)	105.5
H(10C)-O(10)-H(10D)	90.8

Table 23

Crystal 3

Bond Length (Å)		Bond Angles(°)	
Cu(1)-O(13)	2.266(2)	N(16)-Cu(1)-O(13)	97.82(10)
Cu(1)-N(16)	1.952(3)	N(16)-Cu(1)-N(11)	88.96(10)
Cu(1)-N(11)	2.074(2)	N(16)-Cu(1)-N(1)	90.14(10)
Cu(1)-N(1)	2.077(2)	N(16)-Cu(1)-N(6)	164.27(10)
Cu(1)-N(6)	1.963(3)	N(11)-Cu(1)-O(13)	91.85(9)
F(1)-B(1)	1.394(4)	N(11)-Cu(1)-N(1)	174.68(10)
F(6)-B(2)	1.406(4)	N(1)-Cu(1)-O(13)	93.47(9)
F(3)-B(1)	1.395(4)	N(6)-Cu(1)-O(13)	97.73(10)
F(4)-B(1)	1.391(4)	N(6)-Cu(1)-N(11)	88.15(10)
F(8)-B(2)	1.390(4)	N(6)-Cu(1)-N(1)	91.31(10)
F(2)-B(1)	1.384(4)	C(22)-O(8)-C(23)	112.3(2)
F(5)-B(2)	1.388(4)	C(6)-O(1)-C(7)	113.6(2)
O(8)-C(22)	1.392(4)	C(24)-O(9)-H(9)	109.5
O(8)-C(23)	1.436(4)	C(30)-O(11)-C(31)	113.6(2)
F(7)-B(2)	1.375(4)	C(16)-O(5)-H(5)	103(3)
O(1)-C(6)	1.401(4)	C(14)-O(4)-C(15)	112.8(2)
O(1)-C(7)	1.432(4)	C(8)-O(2)-H(2)	109.5
O(3)-C(5)	1.235(4)	C(32)-O(12)-H(12)	100(4)
O(9)-H(9)	0.82	Cu(1)-O(13)-H(13A)	109.3
O(9)-C(24)	1.432(4)	Cu(1)-O(13)-H(13B)	109.3
O(6)-C(13)	1.234(4)	H(13A)-O(13)-H(13B)	104.5
O(11)-C(30)	1.399(4)	C(4)-N(13)-C(3)	112.3(2)
O(11)-C(31)	1.429(4)	C(19)-N(3)-C(20)	112.4(2)
O(10)-C(28)	1.231(4)	C(13)-N(19)-H(19)	117.1
O(5)-C(16)	1.429(4)	C(12)-N(19)-H(19)	117.1
O(5)-H(5)	0.77(5)	C(12)-N(19)-C(13)	125.7(3)
O(7)-C(18)	1.235(4)	C(9)-N(17)-C(11)	106.4(2)
O(4)-C(14)	1.403(4)	C(9)-N(17)-C(14)	126.6(2)
O(4)-C(15)	1.435(4)	C(11)-N(17)-C(14)	126.9(3)
O(2)-H(2)	0.82	C(12)-N(18)-C(11)	112.3(3)
O(2)-C(8)	1.432(4)	C(10)-N(16)-Cu(1)	126.5(2)
O(12)-C(32)	1.429(4)	C(9)-N(16)-Cu(1)	127.3(2)
O(12)-H(12)	0.69(5)	C(9)-N(16)-C(10)	105.8(3)
O(13)-H(13A)	0.8514	C(1)-N(11)-Cu(1)	120.0(2)
O(13)-H(13B)	0.8502	C(1)-N(11)-C(2)	105.0(2)
N(13)-C(4)	1.315(4)	C(2)-N(11)-Cu(1)	134.7(2)
N(13)-C(3)	1.354(4)	C(19)-N(5)-H(5A)	117.1
N(3)-C(19)	1.317(4)	C(19)-N(5)-C(18)	125.8(3)
N(3)-C(20)	1.352(4)	C(18)-N(5)-H(5A)	117.1
N(19)-H(19)	0.86	C(20)-N(2)-C(22)	125.2(2)
N(19)-C(13)	1.394(4)	C(21)-N(2)-C(20)	106.7(2)
N(19)-C(12)	1.372(4)	C(21)-N(2)-C(22)	127.5(3)
N(17)-C(9)	1.359(4)	C(1)-N(12)-C(6)	125.4(3)

N(17)-C(11)	1.383(4)	C(3)-N(12)-C(1)	106.6(2)
N(17)-C(14)	1.465(4)	C(3)-N(12)-C(6)	126.7(2)
N(18)-C(12)	1.322(4)	C(27)-N(7)-C(30)	126.4(3)
N(18)-C(11)	1.357(4)	C(25)-N(7)-C(27)	107.1(2)
N(16)-C(10)	1.386(4)	C(25)-N(7)-C(30)	126.6(3)
N(16)-C(9)	1.316(4)	C(17)-N(1)-Cu(1)	135.0(2)
N(11)-C(1)	1.314(4)	C(21)-N(1)-Cu(1)	119.7(2)
N(11)-C(2)	1.403(4)	C(21)-N(1)-C(17)	104.8(2)
N(5)-H(5A)	0.86	C(25)-N(6)-Cu(1)	125.4(2)
N(5)-C(19)	1.373(4)	C(25)-N(6)-C(26)	105.7(3)
N(5)-C(18)	1.398(4)	C(26)-N(6)-Cu(1)	127.7(2)
N(2)-C(20)	1.368(4)	C(4)-N(15)-H(15A)	125(3)
N(2)-C(21)	1.364(4)	C(4)-N(15)-H(15B)	112(3)
N(2)-C(22)	1.464(4)	H(15A)-N(15)-H(15B)	122(4)
N(12)-C(1)	1.371(4)	C(29)-N(9)-H(9A)	117.1
N(12)-C(3)	1.367(4)	C(29)-N(9)-C(28)	125.8(3)
N(12)-C(6)	1.463(4)	C(28)-N(9)-H(9A)	117.1
N(7)-C(27)	1.379(4)	C(4)-N(14)-H(14)	117.4
N(7)-C(25)	1.360(4)	C(4)-N(14)-C(5)	125.2(3)
N(7)-C(30)	1.469(4)	C(5)-N(14)-H(14)	117.4
N(1)-C(17)	1.403(4)	C(29)-N(8)-C(27)	111.8(3)
N(1)-C(21)	1.315(4)	H(4A)-N(4)-H(4B)	120
N(6)-C(25)	1.312(4)	C(19)-N(4)-H(4A)	120
N(6)-C(26)	1.396(4)	C(19)-N(4)-H(4B)	120
N(15)-C(4)	1.347(4)	H(20A)-N(20)-H(20B)	120
N(15)-H(15A)	0.74(4)	C(12)-N(20)-H(20A)	120
N(15)-H(15B)	0.85(4)	C(12)-N(20)-H(20B)	120
N(9)-H(9A)	0.86	H(10A)-N(10)-H(10B)	120
N(9)-C(29)	1.368(4)	C(29)-N(10)-H(10A)	120
N(9)-C(28)	1.404(4)	C(29)-N(10)-H(10B)	120
N(14)-H(14)	0.86	N(11)-C(1)-N(12)	112.5(3)
N(14)-C(4)	1.377(4)	N(11)-C(1)-H(1)	123.7
N(14)-C(5)	1.402(4)	N(12)-C(1)-H(1)	123.7
N(8)-C(27)	1.349(4)	N(3)-C(19)-N(5)	123.1(3)
N(8)-C(29)	1.322(4)	N(3)-C(19)-N(4)	119.3(3)
N(4)-H(4A)	0.86	N(4)-C(19)-N(5)	117.6(3)
N(4)-H(4B)	0.86	N(3)-C(20)-N(2)	124.2(3)
N(4)-C(19)	1.346(4)	N(3)-C(20)-C(17)	129.3(3)
N(20)-H(20A)	0.86	N(2)-C(20)-C(17)	106.5(2)
N(20)-H(20B)	0.86	N(7)-C(27)-C(26)	106.0(3)
N(20)-C(12)	1.344(4)	N(8)-C(27)-N(7)	125.3(3)
N(10)-H(10A)	0.86	N(8)-C(27)-C(26)	128.8(3)
N(10)-H(10B)	0.86	O(6)-C(13)-N(19)	121.0(3)
N(10)-C(29)	1.349(4)	O(6)-C(13)-C(10)	128.0(3)
C(1)-H(1)	0.93	N(19)-C(13)-C(10)	110.9(3)
C(20)-C(17)	1.392(4)	N(18)-C(12)-N(19)	123.4(3)

C(27)-C(26)	1.380(4)	N(18)-C(12)-N(20)	119.7(3)
C(13)-C(10)	1.424(4)	N(20)-C(12)-N(19)	116.9(3)
C(10)-C(11)	1.374(4)	N(16)-C(10)-C(13)	131.1(3)
C(25)-H(25)	0.93	C(11)-C(10)-N(16)	109.1(3)
C(9)-H(9B)	0.93	C(11)-C(10)-C(13)	119.3(3)
C(5)-C(2)	1.422(4)	N(13)-C(4)-N(15)	119.2(3)
C(17)-C(18)	1.421(4)	N(13)-C(4)-N(14)	123.4(3)
C(3)-C(2)	1.378(4)	N(15)-C(4)-N(14)	117.4(3)
C(26)-C(28)	1.422(4)	N(7)-C(25)-H(25)	123.9
C(6)-H(6A)	0.97(4)	N(6)-C(25)-N(7)	112.1(3)
C(6)-H(6B)	1.06(4)	N(6)-C(25)-H(25)	123.9
C(21)-H(21)	0.93	N(17)-C(9)-H(9B)	123.9
C(30)-H(30A)	0.97	N(16)-C(9)-N(17)	112.1(3)
C(30)-H(30B)	0.97	N(16)-C(9)-H(9B)	123.9
C(22)-H(22A)	0.97	O(3)-C(5)-N(14)	119.5(3)
C(22)-H(22B)	0.97	O(3)-C(5)-C(2)	128.9(3)
C(24)-H(24A)	0.97	N(14)-C(5)-C(2)	111.6(2)
C(24)-H(24B)	0.97	N(1)-C(17)-C(18)	133.7(3)
C(24)-C(23)	1.506(4)	C(20)-C(17)-N(1)	108.9(3)
C(23)-H(23A)	0.97	C(20)-C(17)-C(18)	117.3(3)
C(23)-H(23B)	0.97	N(18)-C(11)-N(17)	125.3(3)
C(14)-H(14A)	0.93	N(18)-C(11)-C(10)	128.2(3)
C(16)-H(16A)	0.97	C(10)-C(11)-N(17)	106.5(3)
C(16)-H(16B)	0.97	N(13)-C(3)-N(12)	124.0(3)
C(16)-C(15)	1.505(4)	N(13)-C(3)-C(2)	129.2(3)
C(32)-H(32A)	0.97	N(12)-C(3)-C(2)	106.8(3)
C(32)-H(32B)	0.97	O(7)-C(18)-N(5)	119.1(3)
C(32)-C(31)	1.507(5)	O(7)-C(18)-C(17)	129.0(3)
C(8)-H(8A)	0.97	N(5)-C(18)-C(17)	111.9(2)
C(8)-H(8B)	0.97	N(11)-C(2)-C(5)	132.9(3)
C(8)-C(7)	1.500(4)	C(3)-C(2)-N(11)	109.1(3)
C(15)-H(15C)	0.97	C(3)-C(2)-C(5)	117.9(3)
C(15)-H(15D)	0.97	N(6)-C(26)-C(28)	131.4(3)
C(7)-H(7A)	0.97	C(27)-C(26)-N(6)	109.2(3)
C(7)-H(7B)	0.97	C(27)-C(26)-C(28)	119.2(3)
C(31)-H(31A)	0.97	O(1)-C(6)-N(12)	110.8(2)
C(31)-H(31B)	0.97	O(1)-C(6)-H(6A)	108(2)
		O(1)-C(6)-H(6B)	114(2)
		N(12)-C(6)-H(6A)	107(2)
		N(12)-C(6)-H(6B)	108.0(19)
		H(6A)-C(6)-H(6B)	110(3)
		N(2)-C(21)-H(21)	123.5
		N(1)-C(21)-N(2)	113.1(3)
		N(1)-C(21)-H(21)	123.5
		O(11)-C(30)-N(7)	111.2(2)
		O(11)-C(30)-H(30A)	109.4

O(11)-C(30)-H(30B)	109.4
N(7)-C(30)-H(30A)	109.4
N(7)-C(30)-H(30B)	109.4
H(30A)-C(30)-H(30B)	108
N(8)-C(29)-N(9)	123.7(3)
N(8)-C(29)-N(10)	119.7(3)
N(10)-C(29)-N(9)	116.5(3)
O(8)-C(22)-N(2)	111.6(2)
O(8)-C(22)-H(22A)	109.3
O(8)-C(22)-H(22B)	109.3
N(2)-C(22)-H(22A)	109.3
N(2)-C(22)-H(22B)	109.3
H(22A)-C(22)-H(22B)	108
O(9)-C(24)-H(24A)	110.1
O(9)-C(24)-H(24B)	110.1
O(9)-C(24)-C(23)	107.9(2)
H(24A)-C(24)-H(24B)	108.4
C(23)-C(24)-H(24A)	110.1
C(23)-C(24)-H(24B)	110.1
O(8)-C(23)-C(24)	108.7(2)
O(8)-C(23)-H(23A)	110
O(8)-C(23)-H(23B)	110
C(24)-C(23)-H(23A)	110
C(24)-C(23)-H(23B)	110
H(23A)-C(23)-H(23B)	108.3
O(4)-C(14)-N(17)	113.0(2)
O(4)-C(14)-H(14A)	123.5
N(17)-C(14)-H(14A)	123.5
O(5)-C(16)-H(16A)	109.2
O(5)-C(16)-H(16B)	109.2
O(5)-C(16)-C(15)	111.9(3)
H(16A)-C(16)-H(16B)	107.9
C(15)-C(16)-H(16A)	109.2
C(15)-C(16)-H(16B)	109.2
O(10)-C(28)-N(9)	120.7(3)
O(10)-C(28)-C(26)	128.8(3)
N(9)-C(28)-C(26)	110.5(3)
O(12)-C(32)-H(32A)	109.4
O(12)-C(32)-H(32B)	109.4
O(12)-C(32)-C(31)	111.1(3)
H(32A)-C(32)-H(32B)	108
C(31)-C(32)-H(32A)	109.4
C(31)-C(32)-H(32B)	109.4
O(2)-C(8)-H(8A)	110.2
O(2)-C(8)-H(8B)	110.2
O(2)-C(8)-C(7)	107.5(3)

H(8A)-C(8)-H(8B)	108.5
C(7)-C(8)-H(8A)	110.2
C(7)-C(8)-H(8B)	110.2
O(4)-C(15)-C(16)	108.4(2)
O(4)-C(15)-H(15C)	110
O(4)-C(15)-H(15D)	110
C(16)-C(15)-H(15C)	110
C(16)-C(15)-H(15D)	110
H(15C)-C(15)-H(15D)	108.4
O(1)-C(7)-C(8)	108.6(2)
O(1)-C(7)-H(7A)	110
O(1)-C(7)-H(7B)	110
C(8)-C(7)-H(7A)	110
C(8)-C(7)-H(7B)	110
H(7A)-C(7)-H(7B)	108.3
O(11)-C(31)-C(32)	107.2(3)
O(11)-C(31)-H(31A)	110.3
O(11)-C(31)-H(31B)	110.3
C(32)-C(31)-H(31A)	110.3
C(32)-C(31)-H(31B)	110.3
H(31A)-C(31)-H(31B)	108.5
F(1)-B(1)-F(3)	110.4(3)
F(4)-B(1)-F(1)	109.6(3)
F(4)-B(1)-F(3)	109.9(3)
F(2)-B(1)-F(1)	109.5(3)
F(2)-B(1)-F(3)	109.4(3)
F(2)-B(1)-F(4)	108.1(3)
F(8)-B(2)-F(6)	109.8(3)
F(5)-B(2)-F(6)	108.5(3)
F(5)-B(2)-F(8)	110.1(3)
F(7)-B(2)-F(6)	109.2(3)
F(7)-B(2)-F(8)	109.9(3)
F(7)-B(2)-F(5)	109.3(3)

Table 24

Crystal 4

Bond Lengths (Å)		Bond Angles (°)	
Cu(1)-O(4)	1.9562	O(4)-Cu(1)-O(4)#1	180
Cu(1)-O(4)#1	1.9562	O(4)-Cu(1)-N(4)	88.531
Cu(1)-N(4)#1	2.0023	O(4)-Cu(1)-N(4)#1	91.471
Cu(1)-N(4)	2.0023	O(4)#1-Cu(1)-N(4)	91.471
O(2)-C(6)	1.3855	O(4)#1-Cu(1)-N(4)#1	88.531
O(2)-C(7)	1.4374	N(4)#1-Cu(1)-N(4)	180.008
O(4)-H(4A)	0.8576	C(6)-O(2)-C(7)	114.33
O(4)-H(4B)	0.8571	Cu(1)-O(4)-H(4A)	109.5
O(1)-C(2)	1.2384	Cu(1)-O(4)-H(4B)	109.9

F(1)-B(1)	1.3826	H(4A)-O(4)-H(4B)	103.9
F(4)-B(1)	1.3796	C(1)-N(2)-C(4)	112.93
F(3)-B(1)	1.3936	C(4)-N(5)-C(6)	124.83
N(2)-C(4)	1.3444	C(5)-N(5)-C(4)	107.23
N(2)-C(1)	1.3365	C(5)-N(5)-C(6)	128.03
N(5)-C(4)	1.3734	C(1)-N(3)-H(3)	117.4
N(5)-C(6)	1.4794	C(2)-N(3)-H(3)	117.4
N(5)-C(5)	1.3675	C(2)-N(3)-C(1)	125.23
N(3)-H(3)	0.86	C(3)-N(4)-Cu(1)	111.22
N(3)-C(1)	1.3794	C(5)-N(4)-Cu(1)	143.63
N(3)-C(2)	1.3754	C(5)-N(4)-C(3)	104.83
F(2)-B(1)	1.3726	C(8)-O(3)-H(3A)	109.5
N(4)-C(3)	1.3904	H(1A)-N(1)-H(1B)	120
N(4)-C(5)	1.3104	C(1)-N(1)-H(1A)	120
O(3)-H(3A)	0.82	C(1)-N(1)-H(1B)	120
O(3)-C(8)	1.4245	N(2)-C(4)-N(5)	127.93
N(1)-H(1A)	0.86	N(2)-C(4)-C(3)	126.83
N(1)-H(1B)	0.86	C(3)-C(4)-N(5)	105.33
N(1)-C(1)	1.3165	N(4)-C(3)-C(2)	128.73
C(4)-C(3)	1.3725	C(4)-C(3)-N(4)	110.53
C(3)-C(2)	1.4085	C(4)-C(3)-C(2)	120.83
C(6)-H(6A)	1.004	N(2)-C(1)-N(3)	123.03
C(6)-H(6B)	1.045	N(1)-C(1)-N(2)	119.83
C(5)-H(5)	0.93	N(1)-C(1)-N(3)	117.13
C(7)-H(7A)	0.97	O(1)-C(2)-N(3)	123.63
C(7)-H(7B)	0.97	O(1)-C(2)-C(3)	125.13
C(7)-C(8)	1.4756	N(3)-C(2)-C(3)	111.33
C(8)-H(8A)	0.97	O(2)-C(6)-N(5)	111.63
C(8)-H(8B)	0.97	O(2)-C(6)-H(6A)	1072
		O(2)-C(6)-H(6B)	1142
		N(5)-C(6)-H(6A)	1072
		N(5)-C(6)-H(6B)	1062
		H(6A)-C(6)-H(6B)	1113
		N(5)-C(5)-H(5)	123.9
		N(4)-C(5)-N(5)	112.13
		N(4)-C(5)-H(5)	123.9
		O(2)-C(7)-H(7A)	109.9
		O(2)-C(7)-H(7B)	109.9
		O(2)-C(7)-C(8)	108.93
		H(7A)-C(7)-H(7B)	108.3
		C(8)-C(7)-H(7A)	109.9
		C(8)-C(7)-H(7B)	109.9
		O(3)-C(8)-C(7)	113.24
		O(3)-C(8)-H(8A)	108.9
		O(3)-C(8)-H(8B)	108.9
		C(7)-C(8)-H(8A)	108.9

C(7)-C(8)-H(8B)	108.9
H(8A)-C(8)-H(8B)	107.7
F(1)-B(1)-F(3)	108.94
F(4)-B(1)-F(1)	110.94
F(4)-B(1)-F(3)	108.53
F(2)-B(1)-F(1)	109.33
F(2)-B(1)-F(4)	109.34
F(2)-B(1)-F(3)	110.04

Table 25

Crystal 5

Bond Lengths (Å)		Bond Angle (°)	
Cu1-F2	1.9562	F2-Cu1-F2#1	180
Cu1-F2#1	1.9562	F2-Cu1-N1	90.119
Cu1-N1#1	1.9822	F2#1-Cu1-N1	89.899
Cu1-N1	1.9822	F2-Cu1-N1#1	89.899
F4-B1	1.3934	F2#1-Cu1-N1#1	90.119
F1-B1	1.3964	N1#1-Cu1-N1	180
F3-B1	1.3784	B1-F2-Cu1	125.72
F2-B1	1.4834	C6-O2-C7	113.33
O2-C6	1.3904	C4-N4-H4	117.4
O2-C7	1.4364	C5-N4-H4	117.4
O1-C4	1.2284	C5-N4-C4	125.13
O4-C9	1.2344	C2-N1-Cu1	124.12
N4-H4	0.86	C1-N1-Cu1	130.12
N4-C4	1.3984	C1-N1-C2	105.82
N4-C5	1.3714	C14-O5-C15	113.33
N1-C2	1.3924	C1-N2-C3	106.42
N1-C1	1.3084	C1-N2-C6	126.83
O5-C14	1.3845	C3-N2-C6	126.73
O5-C15	1.3955	C11-N7-C14	126.13
N2-C1	1.3664	C13-N7-C11	106.13
N2-C3	1.3764	C13-N7-C14	127.73
N2-C6	1.4674	C5-N3-C3	112.23
N7-C11	1.3784	C12-N8-C11	112.23
N7-C13	1.3764	C13-N6-C10	104.33
N7-C14	1.4584	C12-N9-C9	125.33
N3-C5	1.3314	H5A-N5-H5B	120
N3-C3	1.3484	C5-N5-H5A	120
N8-C12	1.3244	C5-N5-H5B	120
N8-C11	1.3514	H10A-N10-H10B	123.7
N6-C13	1.3014	C12-N10-H10A	109.8
N6-C10	1.3924	C12-N10-H10B	121.3
N9-C12	1.3704	N1-C2-C4	130.93
N9-C9	1.3914	C3-C2-N1	108.93
N5-H5A	0.86	C3-C2-C4	120.23

N5-H5B	0.86	O1-C4-N4	120.93
N5-C5	1.3404	O1-C4-C2	128.33
N10-H10A	0.863	N4-C4-C2	110.82
N10-C12	1.3444	C16-O6-H6	109.5
N10-H10B	0.745	N1-C1-N2	112.33
C2-C4	1.4164	N1-C1-H1	123.9
C2-C3	1.3754	N2-C1-H1	123.9
O6-H6	0.82	N3-C5-N4	123.93
O6-C16	1.4155	N3-C5-N5	119.53
C1-H1	0.93	N5-C5-N4	116.63
C9-C10	1.4165	N3-C3-N2	125.53
C11-C10	1.3795	N3-C3-C2	127.83
C13-H13	0.93	C2-C3-N2	106.62
C14-H14A	1.014	N8-C12-N9	123.83
C14-H14B	0.944	N8-C12-N10	119.93
C6-H6A	0.97	N10-C12-N9	116.33
C6-H6B	0.97	O4-C9-N9	120.23
O3B-H3B	0.82	O4-C9-C10	128.33
O3B-C8	1.4496	N9-C9-C10	111.43
C7-H7A	0.97	N7-C11-C10	105.53
C7-H7B	0.97	N8-C11-N7	126.33
C7-C8	1.4765	N8-C11-C10	128.13
C16-H16A	0.97	N7-C13-H13	123.3
C16-H16B	0.97	N6-C13-N7	113.53
C16-C15	1.4996	N6-C13-H13	123.3
C8-H8AA	0.97	N6-C10-C9	130.23
C8-H8AB	0.97	C11-C10-N6	110.63
C8-H8A	0.97	C11-C10-C9	119.23
C8-H8B	0.97	O5-C14-N7	113.83
C8-O3A	1.812	O5-C14-H14A	1052
C15-H15A	0.97	O5-C14-H14B	1132
C15-H15B	0.97	N7-C14-H14A	1102
O8-H8C	0.8502	N7-C14-H14B	1072
O8-H8D	0.8497	H14A-C14-H14B	1073
O7-H7C	0.8504	O2-C6-N2	111.93
O7-H7D	0.8492	O2-C6-H6A	109.2
O3A-H3A	0.82	O2-C6-H6B	109.2
		N2-C6-H6A	109.2
		N2-C6-H6B	109.2
		H6A-C6-H6B	107.9
		C8-O3B-H3B	109.5
		O2-C7-H7A	109.6
		O2-C7-H7B	109.6
		O2-C7-C8	110.13
		H7A-C7-H7B	108.2
		C8-C7-H7A	109.6

C8-C7-H7B	109.6
F4-B1-F1	109.33
F4-B1-F2	109.13
F1-B1-F2	108.33
F3-B1-F4	109.73
F3-B1-F1	110.53
F3-B1-F2	109.93
O6-C16-H16A	109.8
O6-C16-H16B	109.8
O6-C16-C15	109.64
H16A-C16-H16B	108.2
C15-C16-H16A	109.8
C15-C16-H16B	109.8
O3B-C8-C7	106.04
O3B-C8-H8AA	110.5
O3B-C8-H8AB	110.5
C7-C8-H8AA	110.5
C7-C8-H8AB	110.5
C7-C8-H8A	115.1
C7-C8-H8B	115.1
C7-C8-O3A	80.98
H8AA-C8-H8AB	108.7
H8A-C8-H8B	112.2
O3A-C8-H8A	115.1
O3A-C8-H8B	115.1
O5-C15-C16	110.94
O5-C15-H15A	109.5
O5-C15-H15B	109.5
C16-C15-H15A	109.5
C16-C15-H15B	109.5
H15A-C15-H15B	108
H8C-O8-H8D	104.5
H7C-O7-H7D	104.5
C8-O3A-H3A	109.5

Table 26

Crystal 6

Bond Length (Å)		Bond Angles (°)	
Zn(1)-N(16)	2.0102	N(11)-Zn(1)-N(16)	105.959
Zn(1)-N(11)	2.0082	N(1)-Zn(1)-N(16)	118.531
Zn(1)-N(1)	1.9872	N(1)-Zn(1)-N(11)	107.391
Zn(1)-N(6)	1.9882	N(1)-Zn(1)-N(6)	107.851
Si(1)-F(6)	1.6802	N(6)-Zn(1)-N(16)	102.399
Si(1)-F(4)	1.6772	N(6)-Zn(1)-N(11)	115.079
Si(1)-F(3)	1.6893	F(6)-Si(1)-F(3)	90.1414
Si(1)-F(1)	1.6693	F(4)-Si(1)-F(6)	90.2112

Si(1)-F(2)	1.6763	F(4)-Si(1)-F(3)	88.3413
Si(1)-F(5)	1.6613	F(1)-Si(1)-F(6)	88.7713
O(5)-C(14)	1.3954	F(1)-Si(1)-F(4)	177.3618
O(5)-C(15)	1.4444	F(1)-Si(1)-F(3)	89.2315
O(7)-C(20)	1.2264	F(1)-Si(1)-F(2)	91.2615
O(11)-C(30)	1.3804	F(2)-Si(1)-F(6)	178.9716
O(11)-C(31)	1.4385	F(2)-Si(1)-F(4)	89.7215
O(10)-C(28)	1.2314	F(2)-Si(1)-F(3)	88.8315
O(1)-C(4)	1.2304	F(5)-Si(1)-F(6)	91.2014
O(4)-C(12)	1.2334	F(5)-Si(1)-F(4)	91.7618
O(2)-C(6)	1.3864	F(5)-Si(1)-F(3)	178.6516
O(2)-C(7)	1.4394	F(5)-Si(1)-F(1)	90.6919
N(16)-C(9)	1.3104	F(5)-Si(1)-F(2)	89.8215
N(16)-C(10)	1.3924	C(14)-O(5)-C(15)	114.22
O(13)-H(13A)	0.8504	C(30)-O(11)-C(31)	116.23
O(13)-H(13B)	0.85	C(6)-O(2)-C(7)	112.83
O(8)-C(22)	1.3904	C(9)-N(16)-Zn(1)	128.32
O(8)-C(23)	1.4374	C(9)-N(16)-C(10)	105.52
N(11)-C(2)	1.3894	C(10)-N(16)-Zn(1)	125.2018
N(11)-C(1)	1.3094	H(13A)-O(13)-H(13B)	104.5
N(17)-C(9)	1.3704	C(22)-O(8)-C(23)	112.93
N(17)-C(11)	1.3814	C(2)-N(11)-Zn(1)	120.7518
N(17)-C(14)	1.4673	C(1)-N(11)-Zn(1)	132.62
N(12)-C(3)	1.3844	C(1)-N(11)-C(2)	105.42
N(12)-C(1)	1.3634	C(9)-N(17)-C(11)	107.02
N(12)-C(6)	1.4664	C(9)-N(17)-C(14)	126.82
N(3)-C(19)	1.3534	C(11)-N(17)-C(14)	126.02
N(3)-C(21)	1.3294	C(3)-N(12)-C(6)	126.92
N(14)-H(14)	0.86	C(1)-N(12)-C(3)	107.42
N(14)-C(5)	1.3794	C(1)-N(12)-C(6)	125.63
N(14)-C(4)	1.3954	C(21)-N(3)-C(19)	112.33
N(1)-C(18)	1.3863	C(5)-N(14)-H(14)	117.3
N(1)-C(17)	1.3174	C(5)-N(14)-C(4)	125.42
N(13)-C(3)	1.3534	C(4)-N(14)-H(14)	117.3
N(13)-C(5)	1.3294	C(18)-N(1)-Zn(1)	125.4819
N(6)-C(27)	1.3784	C(17)-N(1)-Zn(1)	128.3019
N(6)-C(25)	1.3094	C(17)-N(1)-C(18)	105.42
N(7)-C(26)	1.3774	C(5)-N(13)-C(3)	112.12
N(7)-C(25)	1.3644	C(27)-N(6)-Zn(1)	127.1818
N(7)-C(30)	1.4674	C(25)-N(6)-Zn(1)	127.02
N(2)-C(19)	1.3824	C(25)-N(6)-C(27)	105.72
N(2)-C(17)	1.3644	C(26)-N(7)-C(30)	127.92
N(2)-C(22)	1.4624	C(25)-N(7)-C(26)	107.02
N(18)-C(11)	1.3514	C(25)-N(7)-C(30)	125.12
N(18)-C(13)	1.3324	C(19)-N(2)-C(22)	127.02
N(20)-H(20A)	0.86	C(17)-N(2)-C(19)	106.92

N(20)-H(20B)	0.86	C(17)-N(2)-C(22)	126.02
N(20)-C(13)	1.3364	C(13)-N(18)-C(11)	112.02
N(15)-H(15A)	0.86	H(20A)-N(20)-H(20B)	120
N(15)-H(15B)	0.86	C(13)-N(20)-H(20A)	120
N(15)-C(5)	1.3394	C(13)-N(20)-H(20B)	120
N(4)-H(4)	0.86	H(15A)-N(15)-H(15B)	120
N(4)-C(20)	1.3874	C(5)-N(15)-H(15A)	120
N(4)-C(21)	1.3714	C(5)-N(15)-H(15B)	120
O(3)-H(3)	0.82	C(20)-N(4)-H(4)	117.2
O(3)-C(8)	1.4105	C(21)-N(4)-H(4)	117.2
N(19)-H(19)	0.86	C(21)-N(4)-C(20)	125.53
N(19)-C(12)	1.3954	C(8)-O(3)-H(3)	109.5
N(19)-C(13)	1.3734	C(12)-N(19)-H(19)	117.1
N(8)-C(26)	1.3554	C(13)-N(19)-H(19)	117.1
N(8)-C(29)	1.3314	C(13)-N(19)-C(12)	125.83
N(9)-H(9)	0.86	C(29)-N(8)-C(26)	111.92
N(9)-C(28)	1.3864	C(28)-N(9)-H(9)	117.3
N(9)-C(29)	1.3694	C(29)-N(9)-H(9)	117.3
O(6)-H(6)	0.82	C(29)-N(9)-C(28)	125.32
O(6)-C(16)	1.4145	C(16)-O(6)-H(6)	109.5
C(9)-H(9A)	0.93	N(16)-C(9)-N(17)	112.12
C(2)-C(3)	1.3764	N(16)-C(9)-H(9A)	124
C(2)-C(4)	1.4194	N(17)-C(9)-H(9A)	124
C(27)-C(26)	1.3724	N(11)-C(2)-C(4)	129.52
C(27)-C(28)	1.4164	C(3)-C(2)-N(11)	110.32
C(12)-C(10)	1.4184	C(3)-C(2)-C(4)	119.93
C(11)-C(10)	1.3804	N(6)-C(27)-C(28)	129.63
N(5)-H(5A)	0.86	C(26)-C(27)-N(6)	110.12
N(5)-H(5B)	0.86	C(26)-C(27)-C(28)	120.23
N(5)-C(21)	1.3404	N(13)-C(3)-N(12)	126.92
N(10)-H(10A)	0.86	N(13)-C(3)-C(2)	128.13
N(10)-H(10B)	0.86	C(2)-C(3)-N(12)	104.92
N(10)-C(29)	1.3294	O(4)-C(12)-N(19)	120.93
C(19)-C(18)	1.3744	O(4)-C(12)-C(10)	128.03
C(18)-C(20)	1.4174	N(19)-C(12)-C(10)	111.02
C(1)-H(1)	0.93	N(18)-C(11)-N(17)	125.92
C(25)-H(25)	0.93	N(18)-C(11)-C(10)	128.63
C(17)-H(17)	0.93	C(10)-C(11)-N(17)	105.52
C(14)-H(14A)	0.97	H(5A)-N(5)-H(5B)	120
C(14)-H(14B)	0.97	C(21)-N(5)-H(5A)	120
O(16)-H(16)	0.82	C(21)-N(5)-H(5B)	120
O(16)-C(34)	1.4337	N(16)-C(10)-C(12)	130.82
C(22)-H(22A)	0.97	C(11)-C(10)-N(16)	109.92
C(22)-H(22B)	0.97	C(11)-C(10)-C(12)	119.23
C(30)-H(30A)	0.97	H(10A)-N(10)-H(10B)	120
C(30)-H(30B)	0.97	C(29)-N(10)-H(10A)	120

O(9)-H(9B)	0.82	C(29)-N(10)-H(10B)	120
O(9)-C(24)	1.4267	N(3)-C(19)-N(2)	126.63
O(14)-H(14C)	0.8495	N(3)-C(19)-C(18)	127.73
O(14)-H(14D)	0.8498	C(18)-C(19)-N(2)	105.72
C(6)-H(6A)	0.97	N(13)-C(5)-N(14)	123.63
C(6)-H(6B)	0.97	N(13)-C(5)-N(15)	120.83
C(15)-H(15C)	0.97	N(15)-C(5)-N(14)	115.53
C(15)-H(15D)	0.97	N(1)-C(18)-C(20)	130.13
C(15)-C(16)	1.4915	C(19)-C(18)-N(1)	110.02
C(7)-H(7A)	0.97	C(19)-C(18)-C(20)	119.93
C(7)-H(7B)	0.97	N(8)-C(26)-N(7)	127.03
C(7)-C(8)	1.5055	N(8)-C(26)-C(27)	127.63
C(8)-H(8A)	0.97	C(27)-C(26)-N(7)	105.52
C(8)-H(8B)	0.97	O(10)-C(28)-N(9)	122.43
C(16)-H(16A)	0.97	O(10)-C(28)-C(27)	126.83
C(16)-H(16B)	0.97	N(9)-C(28)-C(27)	110.82
O(12)-H(12)	0.82	N(11)-C(1)-N(12)	112.03
O(12)-C(32)	1.4026	N(11)-C(1)-H(1)	124
C(23)-H(23A)	0.97	N(12)-C(1)-H(1)	124
C(23)-H(23B)	0.97	N(18)-C(13)-N(20)	120.73
C(23)-C(24)	1.5066	N(18)-C(13)-N(19)	123.33
C(32)-H(32A)	0.97	N(20)-C(13)-N(19)	116.03
C(32)-H(32B)	0.97	N(6)-C(25)-N(7)	111.72
C(32)-C(31)	1.4975	N(6)-C(25)-H(25)	124.2
C(31)-H(31A)	0.97	N(7)-C(25)-H(25)	124.2
C(31)-H(31B)	0.97	N(1)-C(17)-N(2)	112.02
C(24)-H(24A)	0.97	N(1)-C(17)-H(17)	124
C(24)-H(24B)	0.97	N(2)-C(17)-H(17)	124
C(34)-H(34A)	0.97	O(1)-C(4)-N(14)	121.23
C(34)-H(34B)	0.97	O(1)-C(4)-C(2)	127.93
C(34)-C(33)	1.5529	N(14)-C(4)-C(2)	110.82
C(33)-H(33A)	0.96	O(7)-C(20)-N(4)	121.73
C(33)-H(33B)	0.96	O(7)-C(20)-C(18)	127.23
C(33)-H(33C)	0.96	N(4)-C(20)-C(18)	111.12
		N(3)-C(21)-N(4)	123.53
		N(3)-C(21)-N(5)	119.93
		N(5)-C(21)-N(4)	116.63
		O(5)-C(14)-N(17)	112.72
		O(5)-C(14)-H(14A)	109.1
		O(5)-C(14)-H(14B)	109.1
		N(17)-C(14)-H(14A)	109.1
		N(17)-C(14)-H(14B)	109.1
		H(14A)-C(14)-H(14B)	107.8
		C(34)-O(16)-H(16)	109.5
		O(8)-C(22)-N(2)	112.53
		O(8)-C(22)-H(22A)	109.1

O(8)-C(22)-H(22B)	109.1
N(2)-C(22)-H(22A)	109.1
N(2)-C(22)-H(22B)	109.1
H(22A)-C(22)-H(22B)	107.8
N(8)-C(29)-N(9)	123.93
N(10)-C(29)-N(8)	119.83
N(10)-C(29)-N(9)	116.23
O(11)-C(30)-N(7)	112.33
O(11)-C(30)-H(30A)	109.1
O(11)-C(30)-H(30B)	109.1
N(7)-C(30)-H(30A)	109.1
N(7)-C(30)-H(30B)	109.1
H(30A)-C(30)-H(30B)	107.9
C(24)-O(9)-H(9B)	109.5
H(14C)-O(14)-H(14D)	104.6
O(2)-C(6)-N(12)	111.53
O(2)-C(6)-H(6A)	109.3
O(2)-C(6)-H(6B)	109.3
N(12)-C(6)-H(6A)	109.3
N(12)-C(6)-H(6B)	109.3
H(6A)-C(6)-H(6B)	108
O(5)-C(15)-H(15C)	109.9
O(5)-C(15)-H(15D)	109.9
O(5)-C(15)-C(16)	108.93
H(15C)-C(15)-H(15D)	108.3
C(16)-C(15)-H(15C)	109.9
C(16)-C(15)-H(15D)	109.9
O(2)-C(7)-H(7A)	110.6
O(2)-C(7)-H(7B)	110.6
O(2)-C(7)-C(8)	105.93
H(7A)-C(7)-H(7B)	108.7
C(8)-C(7)-H(7A)	110.6
C(8)-C(7)-H(7B)	110.6
O(3)-C(8)-C(7)	111.63
O(3)-C(8)-H(8A)	109.3
O(3)-C(8)-H(8B)	109.3
C(7)-C(8)-H(8A)	109.3
C(7)-C(8)-H(8B)	109.3
H(8A)-C(8)-H(8B)	108
O(6)-C(16)-C(15)	114.13
O(6)-C(16)-H(16A)	108.7
O(6)-C(16)-H(16B)	108.7
C(15)-C(16)-H(16A)	108.7
C(15)-C(16)-H(16B)	108.7
H(16A)-C(16)-H(16B)	107.6
C(32)-O(12)-H(12)	109.5

O(8)-C(23)-H(23A)	110
O(8)-C(23)-H(23B)	110
O(8)-C(23)-C(24)	108.43
H(23A)-C(23)-H(23B)	108.4
C(24)-C(23)-H(23A)	110
C(24)-C(23)-H(23B)	110
O(12)-C(32)-H(32A)	109.9
O(12)-C(32)-H(32B)	109.9
O(12)-C(32)-C(31)	108.94
H(32A)-C(32)-H(32B)	108.3
C(31)-C(32)-H(32A)	109.9
C(31)-C(32)-H(32B)	109.9
O(11)-C(31)-C(32)	106.73
O(11)-C(31)-H(31A)	110.4
O(11)-C(31)-H(31B)	110.4
C(32)-C(31)-H(31A)	110.4
C(32)-C(31)-H(31B)	110.4
H(31A)-C(31)-H(31B)	108.6
O(9)-C(24)-C(23)	113.55
O(9)-C(24)-H(24A)	108.9
O(9)-C(24)-H(24B)	108.9
C(23)-C(24)-H(24A)	108.9
C(23)-C(24)-H(24B)	108.9
H(24A)-C(24)-H(24B)	107.7
O(16)-C(34)-H(34A)	109.5
O(16)-C(34)-H(34B)	109.5
O(16)-C(34)-C(33)	110.95
H(34A)-C(34)-H(34B)	108
C(33)-C(34)-H(34A)	109.5
C(33)-C(34)-H(34B)	109.5
C(34)-C(33)-H(33A)	109.5
C(34)-C(33)-H(33B)	109.5
C(34)-C(33)-H(33C)	109.5
H(33A)-C(33)-H(33B)	109.5
H(33A)-C(33)-H(33C)	109.5
H(33B)-C(33)-H(33C)	109.5

Table 27

Crystal 7

Bond Lengths (Å)		Bond Angle (°)	
Ag(01)-N(00G)	2.11311	N(00R)-Ag(01)-N(00G)	170.44
Ag(01)-N(00R)	2.10912	N(00N)-Ag(02)-N(00T)	168.94
Ag(02)-N(00N)	2.1261	N(00Q)-Ag(03)-N(00X)	168.65
Ag(02)-N(00T)	2.15111	N(01I)-Ag(04)-N(01B)	169.05
Ag(03)-N(00Q)	2.14411	F(00O)-Si(00)-F(01O)	90.16
Ag(03)-N(00X)	2.13013	F(00O)-Si(00)-F(025)	177.86

Ag(04)-N(01B)	2.12813	F(00O)-Si(00)-F(02E)	90.47
Ag(04)-N(01I)	2.11612	F(00O)-Si(00)-F(02N)	90.26
Si(00)-F(00O)	1.65111	F(01O)-Si(00)-F(025)	88.67
Si(00)-F(01O)	1.66813	F(01O)-Si(00)-F(02N)	177.97
Si(00)-F(01T)	1.66014	F(01T)-Si(00)-F(00O)	90.06
Si(00)-F(025)	1.67214	F(01T)-Si(00)-F(01O)	92.17
Si(00)-F(02E)	1.65415	F(01T)-Si(00)-F(025)	88.27
Si(00)-F(02N)	1.67115	F(01T)-Si(00)-F(02E)	179.68
Si(0A)-F(00F)	1.66811	F(01T)-Si(00)-F(02N)	85.87
Si(0A)-F(013)	1.65214	F(02E)-Si(00)-F(01O)	87.87
Si(0A)-F(01D)	1.64916	F(02E)-Si(00)-F(025)	91.47
Si(0A)-F(01Z)	1.552	F(02E)-Si(00)-F(02N)	94.37
Si(0A)-F(02A)	1.74118	F(02N)-Si(00)-F(025)	90.97
Si(0A)-F(02O)	1.692	F(00F)-Si(0A)-F(013)	88.86
O(007)-C(026)	1.20718	F(00F)-Si(0A)-F(01D)	90.27
O(008)-C(02C)	1.39115	F(00F)-Si(0A)-F(02A)	170.38
O(008)-C(02R)	1.46716	F(00F)-Si(0A)-F(02O)	87.69
O(009)-C(028)	1.37718	F(013)-Si(0A)-F(02A)	84.28
O(009)-C(02X)	1.452	F(013)-Si(0A)-F(02O)	90.81
N(00A)-C(019)	1.32317	F(01D)-Si(0A)-F(013)	86.68
N(00A)-C(02M)	1.35817	F(01D)-Si(0A)-F(02A)	96.09
N(00B)-C(01K)	1.38817	F(01D)-Si(0A)-F(02O)	176.711
N(00B)-C(01L)	1.41217	F(01Z)-Si(0A)-F(00F)	93.89
O(00C)-C(01Y)	1.24616	F(01Z)-Si(0A)-F(013)	171.91
O(00D)-C(01U)	1.25015	F(01Z)-Si(0A)-F(01D)	101.01
O(00E)-C(02Z)	1.432	F(01Z)-Si(0A)-F(02A)	92.31
O(00E)-C(031)	1.41118	F(01Z)-Si(0A)-F(02O)	81.612
N(00G)-C(018)	1.31717	F(02O)-Si(0A)-F(02A)	85.91
N(00G)-C(027)	1.39518	C(02C)-O(008)-C(02R)	114.21
N(00H)-C(01G)	1.38917	C(028)-O(009)-C(02X)	114.213
N(00H)-C(01U)	1.39617	C(019)-N(00A)-C(02M)	113.411
O(00I)-C(029)	1.22219	C(01K)-N(00B)-C(01L)	124.611
N(00J)-C(017)	1.40216	C(031)-O(00E)-C(02Z)	113.912
N(00J)-C(02C)	1.45417	C(018)-N(00G)-Ag(01)	123.99
N(00J)-C(02M)	1.35517	C(018)-N(00G)-C(027)	106.211
N(00K)-C(01L)	1.32316	C(027)-N(00G)-Ag(01)	129.99
N(00K)-C(01W)	1.33117	C(01G)-N(00H)-C(01U)	125.111
N(00L)-C(01G)	1.32418	C(017)-N(00J)-C(02C)	124.511
N(00M)-C(018)	1.37317	C(02M)-N(00J)-C(017)	106.711
N(00M)-C(01P)	1.41117	C(02M)-N(00J)-C(02C)	127.411
N(00M)-C(028)	1.47719	C(01L)-N(00K)-C(01W)	113.211
N(00N)-C(017)	1.31816	C(018)-N(00M)-C(01P)	105.311
N(00N)-C(01R)	1.38117	C(018)-N(00M)-C(028)	126.612
O(00P)-C(039)	1.24619	C(01P)-N(00M)-C(028)	127.312
N(00Q)-C(01G)	1.33118	C(017)-N(00N)-Ag(02)	134.99
N(00Q)-C(02I)	1.38617	C(017)-N(00N)-C(01R)	105.81

N(00R)-C(01J)	1.34918	C(01R)-N(00N)-Ag(02)	119.18
N(00R)-C(02D)	1.35518	C(01G)-N(00Q)-Ag(03)	122.89
N(00S)-C(01J)	1.36317	C(01G)-N(00Q)-C(02I)	114.111
N(00S)-C(01V)	1.34417	C(02I)-N(00Q)-Ag(03)	122.99
N(00S)-C(020)	1.48718	C(01J)-N(00R)-Ag(01)	125.99
N(00T)-C(01P)	1.34517	C(01J)-N(00R)-C(02D)	105.412
N(00T)-C(02F)	1.32918	C(02D)-N(00R)-Ag(01)	127.89
O(00U)-C(01K)	1.24016	C(01J)-N(00S)-C(020)	124.011
O(00V)-C(020)	1.40618	C(01V)-N(00S)-C(01J)	108.511
O(00V)-C(037)	1.43419	C(01V)-N(00S)-C(020)	127.011
N(00W)-C(02P)	1.33919	C(01P)-N(00T)-Ag(02)	124.09
N(00X)-C(024)	1.392	C(02F)-N(00T)-Ag(02)	122.49
N(00X)-C(02K)	1.312	C(02F)-N(00T)-C(01P)	113.012
O(00Y)-C(033)	1.442	C(020)-O(00V)-C(037)	111.811
N(00Z)-C(026)	1.40719	C(024)-N(00X)-Ag(03)	117.41
N(00Z)-C(02P)	1.36619	C(02K)-N(00X)-Ag(03)	135.812
N(010)-C(019)	1.39117	C(02K)-N(00X)-C(024)	106.114
N(010)-C(01Y)	1.38516	C(02P)-N(00Z)-C(026)	126.412
N(011)-C(02B)	1.362	C(019)-N(010)-C(01Y)	125.411
O(012)-C(035)	1.442	C(030)-O(014)-C(02S)	115.615
O(014)-C(02S)	1.362	C(02Y)-O(015)-C(03B)	112.513
O(014)-C(030)	1.382	N(00N)-C(017)-N(00J)	110.911
O(015)-C(02Y)	1.41717	N(00G)-C(018)-N(00M)	112.912
O(015)-C(03B)	1.412	N(00A)-C(019)-N(010)	123.212
C(019)-N(02G)	1.33019	N(00A)-C(019)-N(02G)	120.312
O(01A)-C(02T)	1.44718	N(02G)-C(019)-N(010)	116.412
N(01B)-C(01X)	1.39518	C(01X)-N(01B)-Ag(04)	128.71
N(01B)-C(02L)	1.352	C(02L)-N(01B)-Ag(04)	124.61
N(01C)-C(01V)	1.37518	C(02L)-N(01B)-C(01X)	106.612
N(01C)-C(02B)	1.32619	C(02B)-N(01C)-C(01V)	111.912
N(01E)-C(01W)	1.42119	C(01W)-N(01E)-C(031)	126.512
N(01E)-C(02W)	1.38619	C(02W)-N(01E)-C(01W)	106.612
N(01E)-C(031)	1.462	C(02W)-N(01E)-C(031)	126.513
O(01F)-C(038)	1.422	N(00L)-C(01G)-N(00H)	116.512
C(01H)-N(023)	1.37319	N(00Q)-C(01G)-N(00H)	122.412
C(01H)-C(024)	1.382	N(00Q)-C(01G)-N(00L)	121.113
C(01H)-N(02J)	1.37419	N(023)-C(01H)-C(024)	107.413
N(01D)-C(01Q)	1.38518	N(023)-C(01H)-N(02J)	125.013
N(01D)-C(02W)	1.322	N(02J)-C(01H)-C(024)	127.613
C(01K)-C(01Q)	1.40719	C(01Q)-N(01I)-Ag(04)	125.39
C(01L)-N(01M)	1.33317	C(02W)-N(01I)-Ag(04)	127.31
N(01N)-C(02I)	1.34618	C(02W)-N(01D)-C(01Q)	106.412
N(01N)-C(02L)	1.35319	N(00R)-C(01J)-N(00S)	109.812
N(01N)-C(02Y)	1.49119	N(00B)-C(01K)-C(01Q)	112.612
C(01P)-C(027)	1.382	O(00U)-C(01K)-N(00B)	119.712
C(01Q)-C(01W)	1.38419	O(00U)-C(01K)-C(01Q)	127.713

C(01R)-C(01Y)	1.42518	N(00K)-C(01L)-N(00B)	121.811
C(01R)-C(02M)	1.38319	N(00K)-C(01L)-N(01M)	121.312
N(01S)-C(029)	1.402	N(01M)-C(01L)-N(00B)	116.811
N(01S)-C(02F)	1.35919	C(02I)-N(01N)-C(02L)	109.912
C(01U)-C(01X)	1.42018	C(02I)-N(01N)-C(02Y)	128.212
C(01V)-C(02D)	1.38019	C(02L)-N(01N)-C(02Y)	119.912
C(01X)-C(02I)	1.37319	N(00T)-C(01P)-N(00M)	126.612
N(023)-C(02K)	1.372	N(00T)-C(01P)-C(027)	126.813
N(023)-C(030)	1.482	C(027)-C(01P)-N(00M)	106.612
C(024)-C(026)	1.422	N(01I)-C(01Q)-C(01K)	131.313
C(027)-C(029)	1.392	C(01W)-C(01Q)-N(01I)	110.812
C(02B)-N(02H)	1.402	C(01W)-C(01Q)-C(01K)	117.912
C(02D)-C(039)	1.432	N(00N)-C(01R)-C(01Y)	129.412
C(02F)-N(02Q)	1.362	N(00N)-C(01R)-C(02M)	110.011
N(02H)-C(039)	1.392	C(02M)-C(01R)-C(01Y)	120.612
N(02J)-C(02P)	1.33019	C(02F)-N(01S)-C(029)	126.313
C(02R)-C(02T)	1.492	O(00D)-C(01U)-N(00H)	120.411
C(02S)-C(035)	1.543	O(00D)-C(01U)-C(01X)	127.512
C(02V)-O(036)	1.413	N(00H)-C(01U)-C(01X)	112.111
C(02V)-C(03B)	1.513	N(00S)-C(01V)-N(01C)	126.712
C(02X)-C(03D)	1.563	N(00S)-C(01V)-C(02D)	105.712
C(02Z)-C(033)	1.533	N(01C)-C(01V)-C(02D)	127.613
C(037)-C(038)	1.512	N(00K)-C(01W)-N(01E)	125.712
C(03D)-O(03E)	1.483	N(00K)-C(01W)-C(01Q)	129.613
		C(01Q)-C(01W)-N(01E)	104.712
		N(01B)-C(01X)-C(01U)	131.212
		N(01B)-C(01X)-C(02I)	108.212
		C(02I)-C(01X)-C(01U)	120.312
		O(00C)-C(01Y)-N(010)	119.111
		O(00C)-C(01Y)-C(01R)	130.012
		N(010)-C(01Y)-C(01R)	110.911
		O(00V)-C(020)-N(00S)	111.911
		C(01H)-N(023)-C(02K)	105.513
		C(01H)-N(023)-C(030)	126.614
		C(02K)-N(023)-C(030)	126.915
		N(00X)-C(024)-C(026)	131.714
		C(01H)-C(024)-N(00X)	108.313
		C(01H)-C(024)-C(026)	120.013
		O(007)-C(026)-N(00Z)	121.914
		O(007)-C(026)-C(024)	127.615
		N(00Z)-C(026)-C(024)	110.413
		C(01P)-C(027)-N(00G)	109.012
		C(01P)-C(027)-C(029)	121.014
		C(029)-C(027)-N(00G)	129.713
		O(009)-C(028)-N(00M)	112.412
		O(00I)-C(029)-N(01S)	120.314

O(00I)-C(029)-C(027)	129.615
C(027)-C(029)-N(01S)	110.013
N(011)-C(02B)-N(02H)	115.214
N(01C)-C(02B)-N(011)	119.714
N(01C)-C(02B)-N(02H)	124.814
O(008)-C(02C)-N(00J)	110.31
N(00R)-C(02D)-C(01V)	110.612
N(00R)-C(02D)-C(039)	130.313
C(01V)-C(02D)-C(039)	119.213
N(00T)-C(02F)-N(01S)	122.713
N(02Q)-C(02F)-N(00T)	118.913
N(02Q)-C(02F)-N(01S)	118.414
C(039)-N(02H)-C(02B)	123.613
N(00Q)-C(02I)-C(01X)	125.712
N(01N)-C(02I)-N(00Q)	127.612
N(01N)-C(02I)-C(01X)	106.712
C(02P)-N(02J)-C(01H)	112.013
N(00X)-C(02K)-N(023)	112.716
N(01N)-C(02L)-N(01B)	108.513
N(00A)-C(02M)-N(00J)	127.012
N(00A)-C(02M)-C(01R)	126.412
N(00J)-C(02M)-C(01R)	106.511
N(00W)-C(02P)-N(00Z)	115.513
N(02J)-C(02P)-N(00W)	121.014
N(02J)-C(02P)-N(00Z)	123.514
O(008)-C(02R)-C(02T)	104.911
O(014)-C(02S)-C(035)	105.715
O(01A)-C(02T)-C(02R)	110.912
O(036)-C(02V)-C(03B)	105.117
N(01I)-C(02W)-N(01E)	111.413
O(009)-C(02X)-C(03D)	109.817
O(015)-C(02Y)-N(01N)	112.211
O(00E)-C(02Z)-C(033)	106.914
O(014)-C(030)-N(023)	111.115
O(00E)-C(031)-N(01E)	110.912
O(00Y)-C(033)-C(02Z)	108.415
O(012)-C(035)-C(02S)	108.815
O(00V)-C(037)-C(038)	107.813
O(01F)-C(038)-C(037)	108.914
O(00P)-C(039)-C(02D)	126.414
O(00P)-C(039)-N(02H)	120.814
N(02H)-C(039)-C(02D)	112.713
O(015)-C(03B)-C(02V)	109.817
O(03E)-C(03D)-C(02X)	1012

Table 28

Crystal 8

Bond Lengths (Å)		Bond Angles (°)	
Ag(01)-N(007)#1	2.203	N(5)-Ag(01)-N(007)#1	166.81
Ag(01)-N(5)	2.153	N(17)#1-Ag(02)-N(00N)	164.61
Ag(02)-N(00N)	2.183	F(00C)-Si(00)-F(00L)	88.211
Ag(02)-N(17)#1	2.113	F(00C)-Si(00)-F(00P)	91.811
Si(00)-F(00C)	1.662	F(00C)-Si(00)-F(00T)	89.412
Si(00)-F(00I)	1.652	F(00C)-Si(00)-F(00Z)	87.711
Si(00)-F(00L)	1.722	F(00I)-Si(00)-F(00C)	178.712
Si(00)-F(00P)	1.692	F(00I)-Si(00)-F(00L)	93.011
Si(00)-F(00T)	1.682	F(00I)-Si(00)-F(00P)	88.511
Si(00)-F(00Z)	1.682	F(00I)-Si(00)-F(00T)	89.412
N(007)-C(00E)	1.324	F(00I)-Si(00)-F(00Z)	92.111
N(007)-C(00K)	1.405	F(00P)-Si(00)-F(00L)	89.611
N(008)-C(00E)	1.344	F(00T)-Si(00)-F(00L)	177.513
N(008)-C(012)	1.424	F(00T)-Si(00)-F(00P)	89.711
O(009)-C(012)	1.234	F(00T)-Si(00)-F(00Z)	90.812
O(00A)-C(00Q)	1.284	F(00Z)-Si(00)-F(00L)	89.811
N(00B)-C(00V)	1.365	F(00Z)-Si(00)-F(00P)	179.212
N(00B)-C(00W)	1.384	C(00E)-N(007)-Ag(01)#2	1242
N(00B)-C(013)	1.484	C(00E)-N(007)-C(00K)	1143
N(00D)-C(00E)	1.384	C(00K)-N(007)-Ag(01)#2	1212
O(00F)-C(014)	1.394	C(00E)-N(008)-C(012)	1243
O(00F)-C(017)	1.464	C(00V)-N(00B)-C(00W)	1063
O(00G)-C(016)	1.414	C(00V)-N(00B)-C(013)	1323
C(00J)-C(00K)	1.375	C(00W)-N(00B)-C(013)	1223
C(00J)-C(012)	1.405	N(007)-C(00E)-N(008)	1253
C(00J)-N(5)	1.394	N(007)-C(00E)-N(00D)	1203
C(00K)-N(00O)	1.365	N(008)-C(00E)-N(00D)	1163
O(00M)-C(013)	1.444	C(014)-O(00F)-C(017)	1162
O(00M)-C(018)	1.443	C(00K)-C(00J)-C(012)	1233
N(00N)-C(00V)	1.395	C(00K)-C(00J)-N(5)	1073
N(00N)-C(010)	1.325	C(012)-C(00J)-N(5)	1293
N(00O)-C(014)	1.435	C(00J)-C(00K)-N(007)	1223
N(00O)-C(6)	1.374	N(00O)-C(00K)-N(007)	1283
C(00Q)-C(00S)	1.445	N(00O)-C(00K)-C(00J)	1093
C(00Q)-N(00X)	1.365	C(018)-O(00M)-C(013)	1122
N(00R)-C(010)	1.355	C(00V)-N(00N)-Ag(02)	1252
C(00S)-C(00V)	1.295	C(010)-N(00N)-Ag(02)	1232
C(00S)-N(17)	1.384	C(010)-N(00N)-C(00V)	1133
C(00W)-N(17)	1.364	C(00K)-N(00O)-C(014)	1273
N(00X)-C(010)	1.385	C(00K)-N(00O)-C(6)	1043
C(015)-C(017)	1.505	C(6)-N(00O)-C(014)	1283
C(015)-O(20)	1.455	O(00A)-C(00Q)-C(00S)	1283
C(016)-C(018)	1.515	O(00A)-C(00Q)-N(00X)	1213

N(5)-C(6)	1.304	N(00X)-C(00Q)-C(00S)	1113
		C(00V)-C(00S)-C(00Q)	1213
		C(00V)-C(00S)-N(17)	1134
		N(17)-C(00S)-C(00Q)	1273
		N(00B)-C(00V)-N(00N)	1243
		C(00S)-C(00V)-N(00B)	1084
		C(00S)-C(00V)-N(00N)	1273
		N(17)-C(00W)-N(00B)	1113
		C(00Q)-N(00X)-C(010)	1253
		N(00N)-C(010)-N(00R)	1203
		N(00N)-C(010)-N(00X)	1233
		N(00R)-C(010)-N(00X)	1173
		O(009)-C(012)-N(008)	1213
		O(009)-C(012)-C(00J)	1283
		C(00J)-C(012)-N(008)	1113
		O(00M)-C(013)-N(00B)	1063
		O(00F)-C(014)-N(00O)	1083
		O(20)-C(015)-C(017)	1153
		O(00G)-C(016)-C(018)	1103
		O(00F)-C(017)-C(015)	1073
		O(00M)-C(018)-C(016)	1063
		C(00J)-N(5)-Ag(01)	1192
		C(6)-N(5)-Ag(01)	1352
		C(6)-N(5)-C(00J)	1063
		N(5)-C(6)-N(00O)	1133
		C(00S)-N(17)-Ag(02)#2	1252
		C(00W)-N(17)-Ag(02)#2	1332
		C(00W)-N(17)-C(00S)	1033

Table 29

Crystal 9

Bond Lengths (Å)		Bond Angles (°)	
Ag(1)-N(6)	2.0995	N(6)-Ag(1)-N(1)	176.72
Ag(1)-N(1)	2.1005	N(16)-Ag(2)-N(12)	177.03
Ag(2)-N(16)	2.0905	F(3)-Si(1)-F(4)	88.92
Ag(2)-N(12)	2.0905	F(3)-Si(1)-F(1)	87.42
Si(1)-F(3)	1.6844	F(6)-Si(1)-F(3)	179.42
Si(1)-F(6)	1.6784	F(6)-Si(1)-F(4)	90.72
Si(1)-F(4)	1.6974	F(6)-Si(1)-F(1)	92.22
Si(1)-F(2)	1.6534	F(4)-Si(1)-F(1)	88.72
Si(1)-F(1)	1.6984	F(2)-Si(1)-F(3)	90.52
Si(1)-F(5)	1.6584	F(2)-Si(1)-F(6)	89.92
O(11)-C(27)	1.3957	F(2)-Si(1)-F(4)	177.72
O(11)-C(28)	1.4247	F(2)-Si(1)-F(1)	89.13
O(10)-C(24)	1.2247	F(2)-Si(1)-F(5)	93.23
O(5)-C(6)	1.3928	F(5)-Si(1)-F(3)	91.72

O(5)-C(7)	1.4398	F(5)-Si(1)-F(6)	88.72
O(2)-C(14)	1.3847	F(5)-Si(1)-F(4)	89.12
O(2)-C(15)	1.4117	F(5)-Si(1)-F(1)	177.62
N(9)-C(12)	1.3357	C(27)-O(11)-C(28)	111.25
N(9)-C(11)	1.3297	C(6)-O(5)-C(7)	112.65
N(18)-C(25)	1.3547	C(14)-O(2)-C(15)	115.45
N(18)-C(26)	1.3188	C(11)-N(9)-C(12)	112.55
N(8)-H(8A)	0.86	C(26)-N(18)-C(25)	112.25
N(8)-H(8B)	0.86	H(8A)-N(8)-H(8B)	120
N(8)-C(11)	1.3337	C(11)-N(8)-H(8A)	120
N(10)-C(12)	1.3847	C(11)-N(8)-H(8B)	120
N(10)-C(14)	1.4557	C(12)-N(10)-C(14)	126.25
N(10)-C(13)	1.3737	C(13)-N(10)-C(12)	106.84
O(4)-C(4)	1.2278	C(13)-N(10)-C(14)	127.05
N(16)-C(23)	1.3898	C(23)-N(16)-Ag(2)	117.84
N(16)-C(22)	1.3138	C(22)-N(16)-Ag(2)	137.04
N(17)-C(27)	1.4667	C(22)-N(16)-C(23)	105.25
N(17)-C(25)	1.3727	C(25)-N(17)-C(27)	126.35
N(17)-C(22)	1.3727	C(25)-N(17)-C(22)	107.25
O(9)-C(21)	1.2288	C(22)-N(17)-C(27)	126.35
N(15)-H(15)	0.86	C(20)-N(15)-H(15)	123
N(15)-C(20)	1.3298	C(20)-N(15)-C(19)	113.95
N(15)-C(19)	1.3468	C(19)-N(15)-H(15)	123
O(1)-C(10)	1.2368	C(13)-N(6)-Ag(1)	127.14
N(6)-C(13)	1.3038	C(13)-N(6)-C(9)	105.35
N(6)-C(9)	1.3957	C(9)-N(6)-Ag(1)	127.64
N(3)-C(3)	1.3438	C(5)-N(3)-C(3)	112.05
N(3)-C(5)	1.3069	H(14C)-N(14)-H(14D)	120
N(14)-H(14C)	0.86	C(20)-N(14)-H(14C)	120
N(14)-H(14D)	0.86	C(20)-N(14)-H(14D)	120
N(14)-C(20)	1.3178	C(26)-N(19)-H(19)	117.3
N(19)-H(19)	0.86	C(26)-N(19)-C(24)	125.45
N(19)-C(26)	1.3928	C(24)-N(19)-H(19)	117.3
N(19)-C(24)	1.4038	C(20)-N(13)-H(13A)	116.9
N(13)-H(13A)	0.86	C(20)-N(13)-C(21)	126.26
N(13)-C(20)	1.3737	C(21)-N(13)-H(13A)	116.9
N(13)-C(21)	1.3989	C(3)-N(2)-C(6)	126.45
N(2)-C(3)	1.3768	C(1)-N(2)-C(3)	106.75
N(2)-C(6)	1.4687	C(1)-N(2)-C(6)	126.86
N(2)-C(1)	1.3678	C(2)-N(1)-Ag(1)	118.44
N(1)-C(2)	1.3899	C(1)-N(1)-Ag(1)	136.65
N(1)-C(1)	1.3108	C(1)-N(1)-C(2)	105.05
N(7)-H(7)	0.86	C(11)-N(7)-H(7)	117.2
N(7)-C(11)	1.3747	C(11)-N(7)-C(10)	125.65
N(7)-C(10)	1.3918	C(10)-N(7)-H(7)	117.2
O(14)-H(14E)	0.8494	H(14E)-O(14)-H(14F)	109.6

O(14)-H(14F)	0.8497	C(16)-O(3)-H(3)	109.5
O(3)-H(3)	0.82	H(20A)-N(20)-H(20B)	120
O(3)-C(16)	1.3809	C(26)-N(20)-H(20A)	120
N(20)-H(20A)	0.86	C(26)-N(20)-H(20B)	120
N(20)-H(20B)	0.86	C(18)-N(12)-Ag(2)	125.55
N(20)-C(26)	1.3348	C(17)-N(12)-Ag(2)	127.85
N(12)-C(18)	1.3929	C(17)-N(12)-C(18)	106.36
N(12)-C(17)	1.32612	N(9)-C(12)-N(10)	125.85
C(12)-C(9)	1.3798	N(9)-C(12)-C(9)	128.95
C(27)-H(27A)	0.97	C(9)-C(12)-N(10)	105.35
C(27)-H(27B)	0.97	O(11)-C(27)-N(17)	112.84
O(8)-C(01S)	1.3209	O(11)-C(27)-H(27A)	109
O(8)-C(022)	1.4199	O(11)-C(27)-H(27B)	109
C(14)-H(14A)	0.97	N(17)-C(27)-H(27A)	109
C(14)-H(14B)	0.97	N(17)-C(27)-H(27B)	109
O(15)-H(15C)	0.8498	H(27A)-C(27)-H(27B)	107.8
O(15)-H(15D)	0.8496	C(01S)-O(8)-C(022)	114.67
C(25)-C(23)	1.3768	O(2)-C(14)-N(10)	112.95
C(23)-C(24)	1.4159	O(2)-C(14)-H(14A)	109
C(13)-H(13)	0.93	O(2)-C(14)-H(14B)	109
N(4)-H(4)	0.86	N(10)-C(14)-H(14A)	109
N(4)-C(4)	1.3929	N(10)-C(14)-H(14B)	109
N(4)-C(5)	1.3758	H(14A)-C(14)-H(14B)	107.8
C(9)-C(10)	1.4198	N(9)-C(11)-N(8)	120.55
C(3)-C(2)	1.3768	N(9)-C(11)-N(7)	123.05
C(21)-C(18)	1.3961	N(8)-C(11)-N(7)	116.55
C(6)-H(6A)	0.97	N(15)-C(20)-N(13)	121.75
C(6)-H(6B)	0.97	N(14)-C(20)-N(15)	120.25
C(18)-C(19)	1.3918	N(14)-C(20)-N(13)	118.15
O(7)-H(7C)	0.82	H(15C)-O(15)-H(15D)	104.7
O(7)-C(021)	1.45002	N(18)-C(25)-N(17)	126.55
C(19)-N(11)	1.3849	N(18)-C(25)-C(23)	127.95
C(2)-C(4)	1.4009	N(17)-C(25)-C(23)	105.55
N(5)-H(5A)	0.86	N(16)-C(23)-C(24)	129.05
N(5)-H(5B)	0.86	C(25)-C(23)-N(16)	110.25
N(5)-C(5)	1.3431	C(25)-C(23)-C(24)	120.85
C(16)-H(16A)	0.97	N(18)-C(26)-N(19)	123.75
C(16)-H(16B)	0.97	N(18)-C(26)-N(20)	120.85
C(16)-C(15)	1.4611	N(20)-C(26)-N(19)	115.45
C(22)-H(22)	0.93	N(10)-C(13)-H(13)	123.8
N(11)-C(01S)	1.6021	N(6)-C(13)-N(10)	112.55
N(11)-C(17)	1.3809	N(6)-C(13)-H(13)	123.8
C(7)-H(7A)	0.97	C(4)-N(4)-H(4)	117.2
C(7)-H(7B)	0.97	C(5)-N(4)-H(4)	117.2
C(7)-C(8)	1.4761	C(5)-N(4)-C(4)	125.66
C(15)-H(15A)	0.97	N(6)-C(9)-C(10)	131.15

C(15)-H(15B)	0.97	C(12)-C(9)-N(6)	110.15
C(01S)-H(01A)	0.97	C(12)-C(9)-C(10)	118.75
C(01S)-H(01B)	0.97	N(3)-C(3)-N(2)	126.25
C(28)-H(28A)	0.97	N(3)-C(3)-C(2)	128.06
C(28)-H(28B)	0.97	N(2)-C(3)-C(2)	105.86
C(28)-C(29)	1.50311	O(10)-C(24)-N(19)	121.76
C(1)-H(1)	0.93	O(10)-C(24)-C(23)	128.36
C(8)-H(8AA)	0.97	N(19)-C(24)-C(23)	110.05
C(8)-H(8AB)	0.97	O(9)-C(21)-N(13)	120.07
C(8)-H(8BC)	0.97	O(9)-C(21)-C(18)	128.77
C(8)-H(8BD)	0.97	C(18)-C(21)-N(13)	111.25
C(8)-O(6A)	1.45002	O(5)-C(6)-N(2)	112.15
C(8)-O(6B)	1.45002	O(5)-C(6)-H(6A)	109.2
O(12)-H(12)	0.82	O(5)-C(6)-H(6B)	109.2
O(12)-C(29)	1.42013	N(2)-C(6)-H(6A)	109.2
C(021)-H(02A)	0.97	N(2)-C(6)-H(6B)	109.2
C(021)-H(02B)	0.97	H(6A)-C(6)-H(6B)	107.9
C(021)-C(022)	1.50112	N(12)-C(18)-C(21)	131.36
C(022)-H(02C)	0.97	C(19)-C(18)-N(12)	108.66
C(022)-H(02D)	0.97	C(19)-C(18)-C(21)	119.96
C(17)-H(17)	0.93	C(021)-O(7)-H(7C)	109.5
C(29)-H(29A)	0.97	N(15)-C(19)-C(18)	126.86
C(29)-H(29B)	0.97	N(15)-C(19)-N(11)	126.16
O(6A)-H(6AA)	0.82	N(11)-C(19)-C(18)	107.06
O(6B)-H(6BA)	0.82	N(1)-C(2)-C(4)	129.66
		C(3)-C(2)-N(1)	110.06
		C(3)-C(2)-C(4)	120.46
		O(1)-C(10)-N(7)	120.76
		O(1)-C(10)-C(9)	128.06
		N(7)-C(10)-C(9)	111.25
		H(5A)-N(5)-H(5B)	120
		C(5)-N(5)-H(5A)	120
		C(5)-N(5)-H(5B)	120
		O(3)-C(16)-H(16A)	109.5
		O(3)-C(16)-H(16B)	109.5
		O(3)-C(16)-C(15)	110.56
		H(16A)-C(16)-H(16B)	108.1
		C(15)-C(16)-H(16A)	109.5
		C(15)-C(16)-H(16B)	109.5
		N(16)-C(22)-N(17)	111.85
		N(16)-C(22)-H(22)	124.1
		N(17)-C(22)-H(22)	124.1
		C(19)-N(11)-C(01S)	125.15
		C(17)-N(11)-C(19)	106.16
		C(17)-N(11)-C(01S)	128.27
		O(5)-C(7)-H(7A)	109.8

O(5)-C(7)-H(7B)	109.8
O(5)-C(7)-C(8)	109.25
H(7A)-C(7)-H(7B)	108.3
C(8)-C(7)-H(7A)	109.8
C(8)-C(7)-H(7B)	109.8
O(2)-C(15)-C(16)	110.46
O(2)-C(15)-H(15A)	109.6
O(2)-C(15)-H(15B)	109.6
C(16)-C(15)-H(15A)	109.6
C(16)-C(15)-H(15B)	109.6
H(15A)-C(15)-H(15B)	108.1
O(8)-C(01S)-N(11)	107.27
O(8)-C(01S)-H(01A)	110.3
O(8)-C(01S)-H(01B)	110.3
N(11)-C(01S)-H(01A)	110.3
N(11)-C(01S)-H(01B)	110.3
H(01A)-C(01S)-H(01B)	108.5
O(11)-C(28)-H(28A)	109.9
O(11)-C(28)-H(28B)	109.9
O(11)-C(28)-C(29)	109.16
H(28A)-C(28)-H(28B)	108.3
C(29)-C(28)-H(28A)	109.9
C(29)-C(28)-H(28B)	109.9
N(2)-C(1)-H(1)	123.8
N(1)-C(1)-N(2)	112.56
N(1)-C(1)-H(1)	123.8
O(4)-C(4)-N(4)	121.36
O(4)-C(4)-C(2)	128.66
N(4)-C(4)-C(2)	110.16
C(7)-C(8)-H(8AA)	109.9
C(7)-C(8)-H(8AB)	109.9
C(7)-C(8)-H(8BC)	110.8
C(7)-C(8)-H(8BD)	110.8
H(8AA)-C(8)-H(8AB)	108.3
H(8BC)-C(8)-H(8BD)	108.8
O(6A)-C(8)-C(7)	109.07
O(6A)-C(8)-H(8AA)	109.9
O(6A)-C(8)-H(8AB)	109.9
O(6B)-C(8)-C(7)	104.95
O(6B)-C(8)-H(8BC)	110.8
O(6B)-C(8)-H(8BD)	110.8
N(3)-C(5)-N(4)	123.96
N(3)-C(5)-N(5)	120.26
N(5)-C(5)-N(4)	115.96
C(29)-O(12)-H(12)	109.5
O(7)-C(021)-H(02A)	109.7

O(7)-C(021)-H(02B)	109.7
O(7)-C(021)-C(022)	109.76
H(02A)-C(021)-H(02B)	108.2
C(022)-C(021)-H(02A)	109.7
C(022)-C(021)-H(02B)	109.7
O(8)-C(022)-C(021)	107.67
O(8)-C(022)-H(02C)	110.2
O(8)-C(022)-H(02D)	110.2
C(021)-C(022)-H(02C)	110.2
C(021)-C(022)-H(02D)	110.2
H(02C)-C(022)-H(02D)	108.5
N(12)-C(17)-N(11)	111.97
N(12)-C(17)-H(17)	124.1
N(11)-C(17)-H(17)	124.1
C(28)-C(29)-H(29A)	109.7
C(28)-C(29)-H(29B)	109.7
O(12)-C(29)-C(28)	109.97
O(12)-C(29)-H(29A)	109.7
O(12)-C(29)-H(29B)	109.7
H(29A)-C(29)-H(29B)	108.2
C(8)-O(6A)-H(6AA)	109.5
C(8)-O(6B)-H(6BA)	109.5

Table 30